Growth and Characterization of Cells Used to Design a Tissue Engineered Blood Vessel

Thesis submitted for the degree of

Doctor of Philosophy
in
Biochemical Engineering

by
Julia F. Markusen
BS MSc

The Advanced Centre for Biochemical Engineering
Department of Biochemical Engineering
University College London

June 2005

ProQuest LLC
789 East Eisenhower Parkway
P.O. Box 1346
Ann Arbor, MI 48106-1346

Abstract

This research characterized the cells used in the formation and growth of substitute arteries for use in treatments such as bypass surgery. Two cell types including immortalized rat smooth muscle cells (rSMCs) and adult human mesenchymal stem cells (hMSCs) were used to study this tissue engineered blood vessel system. Sodium alginate was used as the natural polymer to construct the tubular three-dimensional construct. Normally biologically inert, the alginate was modified to incorporate GRGDY peptides using carbodiiamide chemistry to provide cell adhesion sites for the cells.

The growth characteristics of the rSMCs and hMSCs in tissue flasks were established. Each cell source was assessed according to the viability post-thaw and at each passage, the cell yield and the glucose concentration in the spent medium. Following these measurements, the population doubling per day, the specific growth rate and the glucose consumption rate of the cells were calculated. Concurrently, the alginate was formed into sheets, beads or hollow tubes and the interaction of the cells with the alginate was studied. The biological activity of the alginate matrices was assessed by observing the cells' interaction with the matrices. Measurements such as viability of the cells post-immobilization into the alginate, cell growth and glucose consumption were made and compare to data for cell growth in tissue flasks. The survival and metabolic activity of the cells within the alginate matrices were also measured using the MTT (3-(4,5-dimethylthiazol-2-yl)-2,5-diphenyltetrazolium bromide) assay. Modifications were made to dissolve the cell/alginate matrix and incorporate a frozen storage step for analysis of time course samples.

Both the rSMCs and hMSCs readily attached and elongated when seeded onto the surface of alginate-GRGDY hydrogel sheets. However, only the hMSCs attached and elongation when immobilized within the alginate-GRGDY tubes and beads. Differentiation studies were conducted on the hMSCs immobilized within alginate-GRGDY beads using conditioned-medium (microfiltrate) from rSMC co-cultures. Expression of the hMSC surface markers SH2 and SH4 were lost after 6 days in co-culture. Immunohistological preparations of the beads confirmed the hMSCs expressed α-smooth muscle actin (ASMA). Control cultures of hMSCs in alginate-

GRGDY beads placed in unconditioned medium retained their expression of SH2 and SH4 and did not express ASMA. Using the MTT assay, the hMSCs were shown not to proliferate in unmodified alginate and alginate-GRGDY beads over the 2 week period examined.

Note to reviewers

This thesis is written in American English.

Acknowledgments

I would like to gratefully thank the individuals who assisted me during this research: Chris Mason and Martin Town at UCL Department of Biochemical Engineering for their clever alginate extrusion device and endless creativity; my principal supervisor, Professor Peter Dunnill, for his tissue engineering vision and wisdom and Dr. M. Susana Levy for her experimental guidance; Dr. Dearbhla Hull at St. Bartholomew and the London NHS Trust Hospital, Department of Histopathology for her assistance with the cytology and histology work; Andy Godfrey, Steve Elliman, Dr. Mark Clements, and Professor Chris Boshoff for their assistance with the human mesenchymal stem cell work and flow cytometry; Professor Ricky Wang, Cranfield University, BioMedical Centre for his collaboration on optical coherence tomography; Drs. Barry Buckland, John Aunins, Chuck Goochee, Michel Chartrain and Peter Salmon at Merck and Co., Inc. for their mentoring, support and sponsorship during this doctoral research; Ian Buchanan, Billy Doyle, Clive Osborne, and Julian Perfect for their technical assistance in the Advanced Centre for Biochemical Engineering (ACBE) and Engineering buildings.

On a more personal note I have to also acknowledge the support and friendship from my colleagues at Merck and UCL including Patrick McHugh, Fran Meacle, and Misti Ushio; the enthusiasm from the Tissue Engineering PhD newcomers Leda, Alfred, Garr and Spiros and master students Nurul and Ju-Wei; Barney Zoro for his tissue engineering conversations and fantastic trip to Cambridge; my dear polo friends especially Mary Dengler; the endless adventures with Ranna Patel; and the continual support and love from my parents, Tom and Mary, my sisters, Melisa and Tricia, and the rest of the family. Most of all I extend a very special thanks to my partner, Robert Miners, who has expanded my world to a new level and is the best possible outcome of this PhD experience.

Table of Contents

List of Figures

List of Tables

1. Introduction

In this age of biomedical discovery, it has become more of a potential reality that damaged or failing organs or tissue can be restored using replacements that are natural, synthetic or a combination of both. Although still in its infancy, tissue engineering has become a promising field (section 1.1). Advances in biomaterial science and successful delivery of bioactive substances, such as growth factors to develop tissue, have paved the way for viable prospects for tissue engineered matrices. Several companies have approved tissue engineered products in the marketplace, mostly serving as structural tissue substitutes including skin, cartilage and bone (section 1.2). However, more recently there has been a resurgence of companies focused in the cellular and metabolic sectors.

This research project was focused on vascular tissue engineering. The medical requirement for small diameter (<5-6mm) vascular grafts represents an unmet need in coronary and peripheral bypass surgeries. Currently surgeons must harvest vein or artery from other locations in the patient's body to replumb blocked arteries. The pathology of coronary heart disease and the corrective procedure for bypass surgery are described (section 1.3.1) with emphasis placed on the patency of the autografts currently being used. In addition the cellular composition and physical properties of native blood vessels are detailed (section 1.3.2). Although synthetic grafts have been developed and are in surgical use for larger diameter vessels with high flow; these materials are not suitable for low flow or small diameter sites (Teebken and Haverich, 2002). The synthetic and natural materials being investigated for use in tissue engineered vascular grafts and the approaches of different research groups are discussed (section 1.4). Cell-seeded vascular grafts that better mimic native vessels have met with some preliminary success (Mitchell and Niklason, 2003). The types of cells available for use in a tissue engineered blood vessel (TEBV) are discussed (section 1.5). In addition, bioactive substances such as adhesion molecules or growth factors that can be incorporated into the TEBV are reviewed (section 1.6). Finally in the context of this overview, the research plans for this doctoral thesis are described and include the materials, bioactive substances and cells selected for investigation (section 1.7).

1.1 The nature of tissue engineering

Historically, medical treatments for damaged or failing organs or tissue have included transplantation, surgical repair, artificial prostheses, mechanical devices or drug therapy (Persidis, 1999). However, many limitations exist in these options due to the lack of availability of donor organs, advanced progression of the disease state, and lack of compliance of artificial prostheses to allow growth. Tissue engineering has become a promising solution as a component of regenerative medicine; that is, using living cell substitutes to restore or improve lost tissue function or structure (Ross, 1998; Niklason and Langer, 2001).

One approach to tissue engineering is simple in that it just includes injecting a bioactive substance, such as a growth factor, into the damaged tissue or organ. That substance recruits the patient's own cells to migrate into the desired area, and encourages proliferation or differentiation to reform new healthy tissue. Delivery of the substance can be time-released. A slightly more complex approach is delivery of live cells that produce the desired bioactive product. In this cell therapy approach, the cells could remain isolated from the patient if there is incompatibility issues; or they could repopulate the diseased tissue or failing organ if there is not. The most complex and challenging approach involves the patient receiving a three-dimensional structure that may contain a combination of cells, scaffold or support material, and bioactive substances. The cells can be obtained from the patient's own cells (autologous) or from a donor source (allogeneic). The scaffold can be composed of natural or artificial materials, and be biodegradable or non-biodegradable. The bioactive substances can be growth factors, hormones, peptide sequences or protein coatings to promote cell attachment, migration and/or proliferation. Then the entire 3-D structure is transplanted into the damaged site where the cells proliferate and/or the patient's cells are recruited and organized into new tissue. As the tissue matures, the scaffold material can degrade, leaving only tissue (Persidis, 1999; Vacanti and Langer 1999; Niklason and Langer, 2001; Griffith and Naughton, 2002).

1.2 The current status of tissue engineering/cell therapies

Tissue engineering applications already exist for angiogenesis stimulating molecules for production of blood vessels from existing cells (Laham, 1999; Francis, 2001; Rasmussen, 2002), and for creation of structural tissue such as skin, bone and cartilage (Brittberg, 1994; Wilkins, 1994; Howell, 1995). Success in these areas has stemmed from advances in biomaterials and development of tissue via delivery of bioactive substances such as growth factors. A variety of methods can be used for delivery of the bioactive substances to the target tissue. One method is using controlled delivery using transdermal patches or injectable, biodegradable hydrogels or polymers with distinct release kinetics (Laham, 1999; Richardson, 2001; Perets, 2003). An alternative method of delivery is introducing genes coded for these substances in the form of plasmid DNA or using viral vectors (Wright, 2001; Rasmussen, 2002). Both delivery methods result in transient expression of the substance; however the gene delivery approach may result in longer term expression. These substances can also be incorporated within the pre-formed scaffold material which will help promote tissue growth at the same time as the scaffold material degrades (Simmons, 2004). In late 2002, Curis (previously Creative Biomolecules, Cambridge, MA) partnered with J&J Ortho Biotech to conduct human clinical studies on their bone morphogenic protein (BMP-7) product (www.curis.com). A number of proof-of-concept studies using virus-based or plasmid-based gene delivery of vascular endothelial growth factor (VEGF) or fibroblast growth factor (FGF) have been successfully conducted for treatment of coronary artery disease (CAD) or peripheral vascular disease (PVD) (Laham, 1999; Rasmussen, 2002).

Initially most regenerative scaffolds were produced from components of the natural extracellular matrix (ECM) or from a synthetic polymer material and have focused on the structural area of the market in skin-equivalents (Mooney and Mikos, 1997; Persidis, 1999; Vacanti and Langer, 1999). Decellularized allogeneic (same species) and xenogeneic (different species) tissues as well as purified matrix proteins, such as collagen and glycosaminoglycans, have been used. Some successful approaches use decellularized tissue including LifeCell (The Woodlands, Texas, USA) with their product, AlloDerm®, which is a decellularized human dermal tissue for skin replacement (www.lifecell.com). Medtronics (Minneapolis, Minnestota, USA) and

Edwards Lifesciences LLC (Irvine, California, USA) have FDA approval for decellularized porcine heart valves (www.medtronic.com; www.edwardslifesciences.com; Persidis, 1999). More recently OsteoBiologics, Inc. (San Antonio, Texas, USA) obtained 510(k) clearance from the FDA in July, 2003 to license PolyGraft™ BGS, a porous scaffold as a bone graft substitute. It consists of a patented blend of polylactide-co-glycolide, calcium sulfate and polyglycolide fibers, making it the first polymeric bone void filler to be cleared by the FDA (www.obi.com).

Greater success in promoting structural tissue development was achieved by seeding scaffold material (usually synthetic polymers or collagen) with cultured cells. In May 1998, Apligraf™ (Organogenesis, Canton, Massachusetts, USA) was the first 'living' tissue engineered product to obtain FDA approval for treatment of venous leg ulcers. Human allogeneic dermal cells (fibroblasts) and epidermal cells (keratinocytes) were seeded onto a bovine collagen (Type 1) matrix which developed in 20 days into a viable skin construct (Wilkins, 1994; www.apligraf.com). Similarly Dermagraft® was Advanced Tissue Sciences' (La Jolla, California, USA) skin replacement consisting of living human dermal fibroblasts on a bioabsorbable scaffold for skin ulcers. Dermagraft® was an improvement over their first product, TransCyte®, which was the first human based temporary skin substitute for treatment of burns to be approved by the FDA in 1997 which consisted of a human dermal with synthetic epidermal layer as an alternative to cadaver skin (www.dermagraft.com; http://wound.smith-nephew.com; Persidis, 1999).

For other structural tissue, Genzyme Biosurgery (Cambridge, Massachusetts, USA) received FDA approval for Carticel®, which was the first product which used patient's own (autologous) chondrocytes to replace cartilage in traumatic knee-cartilage damage (www.carticel.com; Mooney and Mikos, 1997; Persidis, 1999). Biotissue Technologies GmbH (Freiburg, Germany) have obtained a German commercial license for 5 products consisting of three-dimensional grafts seeded with cultured autologous cells. BioSeed®-Oral Bone, approved in 2001, utilizes autologous periosteum cells removed from the patient's jaw, which are cultivated *in vitro* in autologous blood serum for ca. 7 ½ weeks and seeded onto a 3-D matrix for

strengthening and replacing missing jawbone material. They have similar autologous products for chondrocytes cultured 3-6 weeks in autologous blood serum, seeded onto a resorbable 'fleece' and placed into the cartilage defect site which was approved in 2001. Finally their product for skin cells (keratinocytes) cultured 2-3 weeks *in vitro*, mixed within a fibrin adhesive gel and applied to leg ulcers, was approved in 1999 (www.biotissue-tec.com).

The field of dentistry also has effectively integrated the advancements in biomaterials, gene therapy, and tissue engineering. Growth factors (GF) have promoted periodontal tissue regeneration and alveolar bone repair in the oral cavity in varying degrees (Giannobile, 1996). Future studies require longer term GF release by refining the methods of delivery. Rutherford (2002) demonstrated formation of bone *in vivo* using porous biodegradable scaffolds (Matrigel and rat-tail collagen) implanted with dermal fibroblasts transduced with bone morphogenesis protein (BMP)-7 *ex vivo* using a recombinant adenovirus (AdCMVBMP). Rutherford is now CSO of Dentigenix Inc. (Seattle, Washington, USA) which has projects in development that treat and repair progressive destruction of tooth enamel and dentin by encouraging remineralization (www.dentigenix.com).

In 2000, the first phase I human trial using autologous skeletal myoblasts transplantation into ischemic myocardium (heart muscle with decreased blood flow) was conducted. Although the trial was only 10 patients and had no control group, 60% of the cell-implanted scar areas showed systolic thickening (increase in apparent tracer activity during systolic contraction) (Menasche, 2003). Other similar clinical trials are underway.

The cellular sector of tissue engineering has progressed significantly due to stem cell technologies and therapeutic cloning advances. There are a number of small biotech companies in clinical development. Osiris Therapeutics (Baltimore, Maryland, USA) has entered clinical trials with several products using adult human mesenchymal stem cells (hMSCs). They are in Phase II development of allogeneic bone marrow or blood stem cell transplants to improve engraftment of blood cells after transplantation. They have completed a Phase I study for delivery of autologous hMSCs on a hydroxyapatite matrix into the jaw to promote new bone formation in preparation for

dental implants. They have also conducted large animal studies for delivery of hMSCs into damaged myocardium and for hMSCs suspended in hyaluronan into damaged meniscus of the knee (www.osiristx.com). StemCells Inc. (Palto Alto, California, USA) have succeeded in identifying and sorting neural stem cells using surface markers (Uchida, 2000), and are in preclinical development of neural stem cell transplantation into the brain to treat neurological disorders such as Parkinson's and Alzheimer's disease (www.stemcellsinc.com).

Advances in the tissue engineering field also have offered great potential for drug screening and toxicity testing for consumer health products and pharmaceutical products. MatTek Corporation (Ashland, Massachusetts, USA) has three product lines for *in vitro* means of assessing dermal irritancy and corrosivity. EpiDerm™, is a skin model which is derived from normal, human derived epidermal keratinocytes which have been cultured to form a multi-layered, highly differentiated model of the human epidermis. Similarly, EpiOcular™ is a model for the cornea and EpiAirway™ uses tracheal/bronchial epithelial cells for a model for epithelial tissue of the respiratory tract (www.mattek.com). These products offer a promising alternative to animal testing (Persidis, 1999). Biopredic International (Rennes, France) has developed Liverbeads™, hepatocytes entrapped within an alginate matrix, which have shown suitability as a tool for toxicology testing (Vian, 2002).

At the end of 2002, 10 tissue-engineering products were in various stages of clinical trials; however 6 products had either failed or were abandoned. Two products, CytoTherapeutics' acute hepatic assist device and Circe's encapsulated cells for chronic pain, failed at Phase III efficacy because the trials were not powered to produce statistically significant end points (Lysaght and Hazlehurst, 2004). Financial challenges of development, manufacture, testing, distribution and poor market acceptance caused the industry leaders, Organogenesis and Advanced Tissue Sciences, to file for Chapter 11 and reorganize under new organizations (Novartis and Smith and Nephew, respectively) in late 2002. These tissue engineering companies held a large number of patents; however in order to convert these into revenue and profit streams, they needed to form alliances, such as marketing and distribution agreements, to enable them to realize the potential of their inventions (Pangarkar and

Hutmacher, 2003). Both companies suffered pressures created by slow regulatory approval, reduction in product pricing for coverage under US national insurance policies, competitors entering the market, and highly laborious and expensive manufacturing process prone to introduction of microbial contaminations (Stone, 2003). In order to be successful, new tissue engineering applications need to be designed to be highly automated and streamlined from platform technologies when feasible such that new applications can be addressed within the company's existing equipment and GMP facilities to decrease time to market (Mason, 2003a & 2003b; Naughton, 2002). Finally due to the failure of these companies in the structural sector of tissue engineering and the rapid emergence of stem cell technology and therapeutic cloning, there has been a dramatic shift in the specialization area of tissue engineering firms between 2000 and 2002. Growth in the cellular sector increased by 37%; whereas growth in the structural area decreased by 50%, and the metabolic area decreased by 33% (Lysaght and Hazlehurst, 2004).

1.3 Vascular tissue engineering

There are two main fields of research in vascular tissue engineering: one based upon cell seeding of synthetic polymers and the other based upon creating a completely biological scaffold. For either, the vascular graft must be biocompatible and have adequate mechanical strength, durability and compliance comparable to the existing vessel (Nerem, 2000; Teebken and Haverich, 2002). In addition the construct must have versatility, ease of use in terms of suturability and availability, and also have suitability of cost for health care management (Niklason and Langer, 2001; Mason, 2003b). Before discussing the current prospects for a tissue engineered blood vessel, a brief background is provided consisting of an introduction to coronary heart disease, an overview of the existing vascular autografts used for bypass surgery, and information relevant to blood vessel composition and important properties.

1.3.1 Coronary heart disease and bypass surgery

Advanced progression of arteriosclerosis leads to narrowing of the coronary arteries and weakening of the wall of the heart, the myocardium. A heart attack, or myocardial infraction, will eventually occur unless surgery is performed to bypass the blocked arteries. The surgeon uses existing vessels in the patient's body (autografts, e.g. the mammary arteries in the chest or the saphenous veins in the legs); however,

these vessels must be disease free and accessible (not removed from a previous surgery). The removal of the vessel adds additional complications to the surgery. The side branches of the vessel must be removed and stitched closed. Figure 1 shows the placement of the graft on the heart. Since over a half million coronary artery bypass graft (CABG) surgeries are performed in the United States alone, the potential benefit of an alternative vessel is enormous (Nerem and Seliktar, 2001). The saphenous vein (SV) remains the most commonly used conduit for CABG; however, the long term outcome of SV grafts shows limitations due to stenosis (narrowing of the graft) and subsequent occlusion (obstruction or closure) of the grafts (Davies and Hagen, 1995). After CABG surgery the SV is exposed to increased blood flow and pressure which is not the usual milieu of the veinous system. These changes trigger the SV grafts to remodel improperly following exposure to the arterial hemodynamic environment. In *ex vivo* studies mimicking this change, the production of matrix metalloproteinase decreased by 50% and cell proliferation was stimulated 220% to 750% - both conditions are undesirable consequences (Mavromatis, 2000). In addition, progression of atherosclerosis in SV grafts is the predominant cause of late graft closure after CABG. Only 60% of SV grafts are patent (i.e. unblocked) between 10-12 years after surgery. Of patent grafts, 45% show evidence of atherosclerosis with 70% of the vessels' lumen blocked 50% or greater (Bourassa, 1984). Internal mammary artery (IMA) grafts have been shown to be significantly better than SV grafts (Loop, 1986). At 10 years, 84% of IMA grafts were patent versus 53% of SV grafts (Grondin, 1984). However these IMAs have limited length and can only be used to bypass near the beginning (proximal end) of the coronary arteries. Surgery time is also longer due to the extra time needed remove them from the chest wall; therefore they cannot be used during emergency CABG. The radial artery has also been used with success, but their patency rates compared to SV grafts remain disputed (Khot, 2004; Zacharias, 2004).

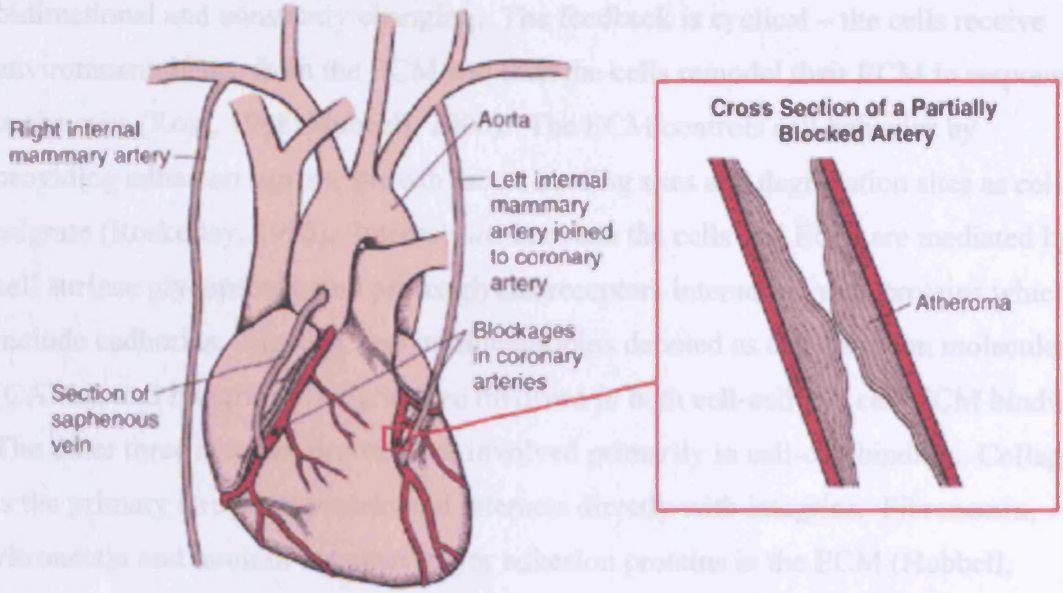

Figure 1. Schematic of the coronary artery bypass graft. Cholesterol buildup in the native coronary arteries eventually blocks the flow of blood causing the heart muscle to die. The bypass graft, usually saphenous vein from the leg, is sewn between the aorta and the coronary arteries beyond the blockage; or the internal mammary artery is joined to the coronary artery (from www.mercksource.com).

1.3.2 The nature of blood vessels

1.3.2.1 Cellular composition

Blood vessels are composed of concentric layers of three cell types: endothelial, smooth muscle and fibroblast that are schematically depicted in Figure 2. The innermost layer (intima) surrounding the central lumen, through which blood flows, is lined with endothelial cells (ECs) which are one cell layer thick. The center core of the vessel wall (media) consists of several layers of smooth muscle cells (SMCs), ca. 200μm thick, which provides the mechanical strength of the structure and the capability of the vessel to dilate or contract. The outer surface (adventitia) of the SMCs is covered by a layer of fibroblast cells that provide the connective tissue where nerve cells are also located (Nerem and Seliktar, 2001; Junqueira, 1998).

The extracellular matrix (ECM) that surrounds these cells consists of a complex network of proteins and glycoaminoglycans. The ECM organizes the cells in space, regulates the cells by providing environmental signals, and maintains the separate tissue space. The physical and chemical interactions between the cells and ECM are

bidirectional and constantly changing. The feedback is cyclical – the cells receive environmental cues from the ECM and then the cells remodel their ECM in response to the cues (Ross, 1998; Hubbell, 2000). The ECM controls cell behavior by providing adhesion signals, growth factor binding sites and degradation sites as cells migrate (Roskelley, 1995). Interactions between the cells and ECM are mediated by cell surface glycoprotein and proteoglycan receptors interacting with proteins which include cadherins, selectins, and immunoglobins denoted as cell adhesion molecules (CAMs), and integrins. Integrins are involved in both cell-cell and cell-ECM binding. The other three receptor proteins are involved primarily in cell-cell binding. Collagen is the primary structural protein and interacts directly with integrins. Fibronectin, vitronectin and laminin are other major adhesion proteins in the ECM (Hubbell, 2000). Elastin acts as a recoil protein that maintains the compliance of the vessel allowing it to stretch and then return to its original size with changes in pressure (Mitchell and Niklason, 2003).

1.3.2.2 Physical properties

Arterial pressure ranges up to 200mmHg; and native arteries have been shown to withstand a high rupture or burst pressure ≥2000mmHg (Nerem, 2000). Blood vessel cells are exposed to cyclical strain due to the fluctuation of blood pressure from the heart pumping blood through the body. In addition, the endothelial cells are exposed to shear stress due to the blood flow through the central lumen and must be non-thrombogenic (non-clotting) (Gooch, 1998). The ECs respond to increased or decreased blood flow by releasing factors (e.g. endostatin) which in turn cause the SMCs to contract or dilate. ECs also respond to flow by elongating and aligning parallel to the flow (Sato and Ohshima, 1994; Thoumine, 1995). The cells must be able to repair and replenish as needed (Nerem and Seliktar, 2001). In contrast, veins carry de-oxygenated blood back to the heart and as a result are from a correspondingly lower pressure system. Their cellular composition is the same as arteries, but the layers are thinner (Junqueira, 1998).

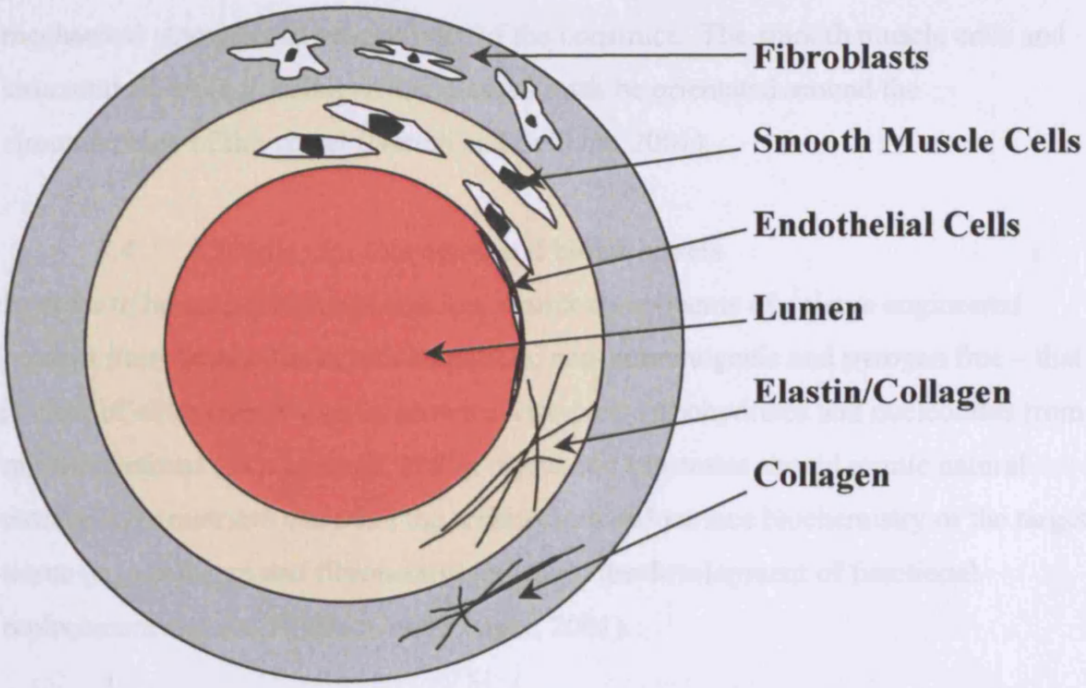

Figure 2. Composition of a blood vessel. The intima (inner layer) is composed of ECs, the media (center) is composed of SMCs, and the adventitia (outer layer) is composed of fibroblasts (adapted from Nerem and Seliktar, 2001).

Current CABG surgery has a reasonable success rate using autografts (e.g. SV and IMA), although long term patency (state of remaining unblocked) remains an issue. A suitable tissue engineered blood vessel (TEBV) would have to be proven to be a considerable improvement over the current option of autografts from vein and artery. It would have to be nearly 100% compliant to all of the physical and mechanical properties (e.g. strength, elasticity) of native vessel. It should be easy to prepare and suture by the surgeon and be of adequate length (ca. 6-12in/bypass). In addition, most CABG surgeries involve 2-4 arteries being bypassed. The replacement vessels must be free from contaminating microorganisms and must not be immunogenic since either would lead to thrombosis and/or inflammation which results in rejection (Mitchell and Niklason, 2003). The cells, in particular the endothelial cells (ECs), at minimum would need to be human leukocyte antigen (HLA) matched as is currently required for hematopoietic stem cell transplantation (HSCT) (Storb, 2003). HLA molecules are the alloantigens that trigger immune recognition and graft rejection in unmatched recipients (Parham, 1999). The ECs must be assembled in a confluent monolayer in order to prevent thrombosis. The cells must be viable and functional. In addition, the orientation of the cells and creation of ECM are critical for

mechanical strength and vasoactivity of the construct. The smooth muscle cells and structural fibers (e.g. collagen and elastin) must be orientated around the circumference of the vessel (Nerem and Seliktar, 2001).

1.4 Materials for bioengineered blood vessels

In order to be used for transplantation, matrix components of a tissue engineered product must be non-toxic, biocompatible, non-immunogenic and pyrogen free – that is clear of components such as proteins, complex carbohydrates and nucleotides from microorganisms (Skjak-Braek, 1989). Synthetic substrates should mimic natural extracellular matrices such that the architecture and surface biochemistry of the target tissue (e.g. collagen and fibronectin) enhances the development of functional replacement organs (Niklason and Langer, 2001).

Initial research to develop replacement vessels centered on synthetic materials such as Dacron™ or expanded polytetrafluoroethylene (ePTFE). These artificial materials have had success in humans when autologous vessels were not available for peripheral bypasses in large diameter (6-10mm) vessels and higher flow areas (above knee) (Tiwari, 2002b; Klinkert, 2004). However, when applied to low flow (below knee) or smaller diameter (3-4mm) vessels, thrombosis set in and closed the vessels off. Efforts were then focused to reduce these thrombotic effects by improving the surfaces of the synthetic polymers to permit seeding of autologous endothelial cells (ECs) (Deutsch, 1999). Despite these improvements, the EC-seeded synthetic grafts prohibit long-term adaption of a normal vascular system that permits a response to remodeling of cells and ECM (described in section 1.3.2.1). Therefore alternative approaches include the use of natural material such as collagen or biodegradable synthetic polymers such as PGA that permit the cells to remodel collagen and elastin as the original construct gradually decomposes (Nerem and Seliktar, 2001).

Most tissue-derived cells are anchorage dependent and require attachment to a surface for viability and growth. Therefore, the surface must promote cell adhesion, spreading, migration, and differentiated cell function (Saltzman, 2000). The surface chemistry of many polymers has been altered to improve these cellular functions.

1.4.1 Synthetic matrix materials

Polymers are made more suitable for cell attachment and growth by surface modification. Polystyrene (PS), which is commonly used for tissue flasks and microwells, can be modified to increase the number of charged groups at the surface. This is commonly done through treatment by radiofrequency plasma deposition or exposure to sulfuric acid (Ertel, 1990). The optimal surface for cell adhesion has an intermediate wettability and high surface free energy which allows cell adhesion proteins to adsorb to the surface. Alternatively, polymer surfaces are treated with purified protein solutions (such as fibronectin, collagen and other extracellular matrix (ECM) proteins) that permit cell adhesion (Ross, 1998). The more sophisticated polymer studies now incorporate smaller biologically active functional groups of the ECM that produce surfaces that are simpler and easier to characterize (Saltzman, 2000). The major cell binding peptide is arginine, glycine, and aspartic acid (RGD) which is the base amino acid sequence found in fibronectin, vitronectin, collagen and thrombospondin which only differ by a flanking residue. Another cell binding domain sequence is the laminin pentapeptide – tyrosine, isoleucine, glycine, serine, arginine (YIGSR) (Hubbell, 2000).

A variety of approaches are currently being used to develop compliant grafts for a tissue engineered blood vessel (TEBV). Many of these involve the fabrication of a tube using 1) non-degradable polymers such as polyethylene tetraphthlate (Dacron™), expanded polytetrafluoroethylene (ePTFE) (Nerem and Seliktar, 2001), MyoLink™ which is composed of poly(carbonate-urea)urethane (Tai, 2000 and Tiwari, 2002b); 2) biodegradable polymers including polyglycolic acid (PGA) (Niklason, 1999), poly(L-lactic acid) (PLA), poly(lactide-coglycolide) (PLGA), and a copolymer of lactic acid and ε-carprolactone [P(CL/LA)] (Shin'oka, 2001); and 3) photopolymerized hydrogels consisting of poly(ethylene oxide) PEG (Mann, 2001) and polyvinyl alcohol (PVA) (Schmedlen, 2002). Some of these polymers (PLA, PGA, PLGA) have been used as suture material for several decades since they are biodegradable (Saltzman, 2000). Many of these polymer constructs include surface treatments to improve hydrophilicity, porosity, and protein adsorption by addition of coatings (such as plasma or fibronectin) or adhesion factors (such as

RGD-containing peptides) to improve vascular cell attachment onto the surface of these scaffolds (Deutsch, 1999; Salacinski, 2000).

Dacron and PTFE are the most widely used synthetic polymers for peripheral bypass when acceptable autologous saphenous vein (SV) is not available because the patency of SV is still greater than PTFE. One survey of surgical cases showed SV was 81% patent at 2 years versus 69% for PTFE. At 5 years, patency was 69% versus 49%, respectively (Klinkert, 2004). Long term patency of the ePTFE femoropopliteal bypass graft (vessel located above or below the knee) was improved by clinical *in vitro* endothelialization. The 9-year patency rate was 65% for the 6mm endothelialized graft versus 16% for the control (non-treated) graft (Deutsch, 1999).

Despite markedly improved studies using endothelialized grafts, these synthetic materials are rigid and have been shown to have poorer compliance when used in low flow states such as below knee bypass and in vessels with <6mm in diameter (Tiwari, 2002b). MyoLink™ which is composed of poly(carbonate-urea)urethane (CPU) has demonstrated success in larger diameter vessels. It is being used worldwide as a peripheral arteriovenous fistula graft (abnormal channel between an artery and vein which bypasses the capillaries) and has shown patency for over 36 months in a dog aorta model. Its compliance was shown to be comparable to native artery; whereas Dacron and ePTFE have lower compliance and stiffness values differing significantly from artery (Tai, 2000). More recently, RGD and heparin were covalently immobilized onto the surface of MyoLink™ to help improve human umbilical vein endothelial cell (HUVEC) attachment and retention and to enhance anticoagulant properties of the graft under pulsatile flow as shown in *in vitro* studies (Tiwari, 2002a). In addition, sodium alginate was coated onto the surface of Dacron grafts to increase the imperviousness of the grafts and found to be equivalent to other sealants used including collagen, gelatin and albumin in a canine model (Lee, 1997). Prior to bankruptcy, Advance Tissue Sciences was developing a TEBV consisting of a polyurethane scaffold seeded with both SMCs and ECs because polyurethanes have the appropriate elastic properties and have been used in vascular applications (Ratcliffe, 2000). Finally a degradable, biocompatible, porous polyesterurethane

polymer, DegraPol®, has been tested for cartilage and bone (Yang, 2003) as well as in a porcine stent with good function over 3 months (Schob, 1997).

Niklason (1999) has developed a biodegradable PGA scaffold chemically modified with sodium hydroxide which caused increased hydrophilicity, absorption of serum proteins and SMC attachment. After seeding and 8 weeks of culture under pulsatile flow, the gross appearance of the vessels was similar to native arteries. The pulsatile flow was shown to increase collagen deposition by the SMCs. The grafts were shown to be patent in a swine model using autologous SMCs and ECs cultured under pulsatile flow *in vitro* and then implanted and monitored out to 4 weeks (Niklason, 1999).

Shin'oka (2001) successfully implanted a TEBV into a 4 year old Japanese girl with a totally occluded right intermediate pulmonary artery in 1999. Cells were obtained from a peripheral vein biopsy and expanded *in vitro* for eight weeks prior to seeding onto a copolymer of ε-caprolactone and lactic acid [P(CL/LA)] reinforced with woven polyglycolic acid (PGA). Ten days after seeding the graft was transplanted, and no postoperative complications occurred. Since this landmark operation, this procedure was successfully repeated on 22 patients using cells obtained from autologous bone marrow cells (BMCs) which were seeded onto the scaffold on the day of surgery – with no maturation *in vitro* (Matsumura, 2003a). This modified procedure was performed using a woven fabric reinforcement of polylactide acid (PLA) instead of PGA. Separate large animal studies using BMCs labeled with green fluorescence indicated that the BMCs enable the establishment of this graft as indicated by the expression of endothelial cell and smooth muscle cell markers, and the production of vascular endothelial growth factor (VEGF) and angiopoietin-1 by the cells (Matsumura, 2003b). Shin'oka and Matsumura's work represents the only human studies successfully performed with cell-seeded, biodegradable TEBVs.

Due to the harsh manufacturing conditions, these aforementioned polymer grafts are fabricated first, and then in a second step the cells are seeded onto the graft. Other polymers have been developed that form hydrogels that are "castable" during seeding such as the photodimerizable hydrophilic copolymer acryloyl-poly(ethylene glycol) PEG that has also incorporated a cell adhesive ligand KQAGDV (Lys, Gln, Ala, Gly,

Asp, Val). This hydrogel polymer was shown to support rat SMC growth (Mann, 2001). Some other synthetic hydrogels include: photopolymerized poly(ethylene glycol) di-[ethyl phosphatidyl (ethylene glycol) methacrylate] "PhosPEG-dMa" (Wang, D., 2003), photopolymerized polyvinyl alcohol (PVA) with peptide RGDS (Schmedlen, 2002), and photopolymerized N, N-dimethylacrylamide-acryloxy succinimide with peptide GGGRGDSP (Moghaddam and Matsuda, 1991). These synthetic hydrogels and natural hydrogels, such as chitosans (Chung, 2002) and sodium alginate (Rowley, 1999), have been shown to be compatible for cell association and growth; however they have not yet been studied for their capability to form a compliant TEBV.

Synthetic materials can be well-characterized and the manufacturing process can be tightly controlled; therefore the regulatory issues surrounding use and fabrication of synthetic materials are less troublesome than natural materials. Many polymers are already used in biomedical devices. Some synthetic materials do not break down nor have the ability to remodel, so determination of the long term patency of a tissue engineered product will be critical to determine if the application is suitable for human use. The degradation rate and the local effect of the by-products of biodegradable polymers must be well understood. Although deemed an early successful model for a TEBV candidate, the by-products of PGA have recently been reported to have undesirable effects on the SMCs during decomposition *in vitro*. Local areas containing residual polymer were found to contain SMCs with increased proliferation rate and dedifferentiated phenotype (Higgins, 2003).

1.4.2 Natural matrix materials

The use of a natural, biological material for developing a blood vessel has an advantage over use of an artificial matrix since the body can remodel the system. However, natural materials may be prone to immunological response if they are derived from animal proteins. In addition, there are substantial regulatory issues that need to be overcome surrounding the likelihood of transmission of adventitious agents from the material. Recombinantly produced or non-animal derived natural materials would be less contentious. Fibronectin-fibrinogen, collagen and sodium alginate are described in this section as possible TEBV materials. Finally the production of a

blood vessel from a cell-generated ECM matrix consisting of over confluent monolayers of SMCs and fibroblast cultures is described.

1.4.2.1 Fibronectin-fibrinogen

Fibronectin is a well-characterized cell adhesion protein. It is a natural extracellular matrix (ECM) molecule that has the ability to bind fibrin, gelatin and collagen, and is used to coat synthetic polymers to improve cell attachment. It is commercially available as a cryoprecipitated fraction of blood plasma. Fibronectin cable was produced at University College London and was previously investigated for use as a tissue repair aid. The cable was constructed from a solution of both fibronectin and fibrinogen (2:1 molar ratio). The solution was extruded into an acid bath (0.25M HCl, 2% $CaCl_2$) at room temperature to form cables. The cables were then washed with buffer and water and allowed to air dry. The basic material properties of the fibronectin/fibrinogen cable were extensively characterized by evaluating solubility curves, composition analysis using enzyme linked immunosorbent assay (ELISA), tensile strength, moisture absorption, stability in water, and solution viscosity. The cable was dried to promote cross-linking of the proteins to maintain stability. Further cross-linking and increased stability was achieved by gamma irradiation (Underwood, 1999).

The human plasma-derived fibronectin-fibrinogen cables were wet extruded with and without sodium alginate. Cables were prepared with solutions containing 140mg/mL total protein with 12.9mg/mL alginate (high protein) and 46mg/mL total protein with 47.6mg/mL alginate (high alginate) in a coagulation bath containing 0.25 M HCl, 2% $CaCl_2$ at a pH of <0.9. The cables had a suitable mechanical strength of 30kPa (225mmHg) needed for wound repair and nerve regeneration (Underwood, 2001). In addition, these multi-fiber cables had the ability to align human fibroblast cells which is important for restoration of normal connective tissue that is stronger and more flexible for wound repair (Harding, 2000). These cables had the ability to be wet spun at larger scale into hollow tubes for potential application for nerve guidance and vascular substitute. However the tubes made of wound fibers as on a bobbin of cotton came apart. Instead greater success was obtained when the tubes were extruded (Harding, 2002). However, because the fibronectin-fibrinogen was derived from

blood plasma, it is unlikely to be a viable matrix for a TEBV unless it can be produced recombinantly or derived from the patients own plasma (Bak, 2002).

1.4.2.2 Collagen

Another suitable natural approach to produce a TEBV utilizes collagen as the primary scaffold material. Collagen is one of the main ECM components of the native blood vessel. This "tissue-equivalent" approach refers to cells cultured within a collagen gel. The collagen is obtained from either acid-extracted or pepsin-digested type I collagen. The molecules self-assemble into a gel when physiological pH and temperature are restored (Tranquillo, 1999). Weinberg and Bell (1986) were the first to produce a totally biological TEBV. They constructed the vessel by combining individual collagen gel layers seeded with fibroblast, smooth muscle and endothelial cells. These constructs were structurally weak and could only withstand a burst pressure of less than 10mmHg without the use of a Dacron™ support sleeve to withstand physiological pressures (Weinberg and Bell, 1986). The rupture pressure of these vessels was increased from 50 to 100mmHg by increasing the concentration of collagen from 0.625mg of collagen per mL of solution to 1.25 or 2.5mg of collagen per mL of solution (Hirai, 1994). The collagen gel contructs were also strengthened by adding elevated levels of glucose or 30mM ribose to the growth medium. These agents cause glycation of the collagen matrix and increased the circumferential tensile modulus from 63 to 1025 kPa (473 to 7688 mmHg) (Girton, 2000). Finally, the strength of the collagen constructs was also improved by using dynamic mechanical stimulation (cyclic strain) to induce cell-mediated remodeling of the collagen gel scaffold. After eight days of exposure to dynamic stimulation (cyclic strain at 1 hertz), collagen constructs containing SMCs exhibited a modulus increase from 68 to 142 kPa (510 to 1065 mmHg) (Seliktar, 2000).

Another method utilizing collagen as the scaffold material begins with actual human or animal (e.g. porcine) vascular grafts. These grafts are decellularized and deproteinized without disrupting the native architecture of the collagen/elastin extracellular matrix. Since this material is devoid of foreign cells, proteins, lipids and nucleic acids, the construct is believed to be non-immunogenic. These acellular grafts rely on recruitment of autologous endothelial cells to seed the intimal (inner) surface after implantation and have shown some success in animal models (Nerem and

Seliktar, 2001). Dahl improved the decellularization method for native and engineered arteries that maximized cellular elimination, without greatly compromising mechanical integrity (Dahl, 2003). Rolled human acellular dermal matrix was also investigated as a small-diameter vascular graft; however, these grafts experienced false aneurysms (sac-like widening) along the longitudinal suture line made to join the seam of the rolled dermal matrix (Inoue, 1996). Another acellular collagen graft approach utilized rolled small intestinal submucosa (SIS). The SIS is a cell-free 100μm thick collagen layer derived from the small intestine. The burst pressure of 5.5mm diameter SIS averaged 3517mmHg (Hiles, 1995; Roeder, 1999). Another group used an alternative approach by wrapping porcine SIS around a mandrel to create a two-layer tube. Bovine type I collagen was deposited on the luminal (inner) surface and the entire graft was crosslinked; however a burst pressure of only 931+/-284mmHg was achieved (Huynh, 1999).

Materials such as collagen and fibronectin are animal proteins/materials usually derived from human, porcine or bovine sources. The largest risk involved in using animal-derived materials is the transmission of infectious agents to the recipient. Many infectious agents including bacteria and viruses are detectible and can be removed or inactivated. However, transmissible spongiform encephalopathies (TSE) are fatal human and animal neurological diseases that to-date have no early detection tests (Dormont, 2002). TSE agents are spread through bone and meat meal from infected animals. Bovine spongiform encephalopathy (BSE), also known as mad cow disease, is spread in cattle and is believed to have crossed species and infected humans who develop new variant Creutzfeldt-Jakob disease. Infected individuals and cattle have a long incubation period during which no detectable symptoms appear (Stecklow, 2001). Due to this predicament, and the fact that infection and pathogenicity is still not completely understood, animal-derived materials are significantly less desirable for a matrix material.

1.4.2.3 Sodium alginate

Sodium alginate is a natural water soluble copolymer of 1, 4-linked β-D-mannuronic (M) and α-L-guluronic (G) acids derived from kelp (brown seaweed). The ratio of the M and G polysaccharides and their sequential arrangement (e.g. in series of M or

G units or alternating MG) depends upon the source of the alginate which is harvested from different geographical locations and from whole plants or from individual sections – the stipe, blades, or leaves. Adjacent blocks of G subunits can be cross linked to form a 3-D hydrogel using divalent cations. A solution of calcium chloride is most commonly used to donate the calcium ions which compete for the sodium ion position on the carboxylic acid groups of adjacent blocks of G subunits. The gel formation can be reversed by the addition of excess sodium ions (Martinsen, 1989) or chelators of divalent cations such as citrate or EDTA. Figure 3 shows the molecular structure of these subunits and the formation of a hydrogel from an alginate solution using calcium ions. The ratio of M and G residues determines the alginate hydrogel strength. High G alginates produce gels with a strong, rigid structure due to the tightly nested molecular formation as shown in Figure 3.B; whereas high M alginates produce gels with less rigid gel structure (Constantinidis, 1999).

The mechanical and swelling properties of sodium alginate gels depend upon the monomeric composition, block-structure, molecular size and concentration of polymer and calcium ions. Nuclear Magnetic Resonance (NMR) spectroscopy can be used to determine the length of the G-blocks (repeating guluronic residues). Gel strength increases with increasing alginate concentration (e.g. 0.5 to 4% w/v) and with increasing proportion of G-blocks (Martinsen, 1989).

Upon cross linking, alginate gels shrink which causes an increased concentration of alginate in the gel due to loss of water relative to the concentration in the original alginate solution. Volume reduction and strength are dependent upon the type of alginate, but gel strength and volume reduction are independent of $CaCl_2$ concentration above a concentration of 0.02M (Smidsrod and Haug, 1972).

A

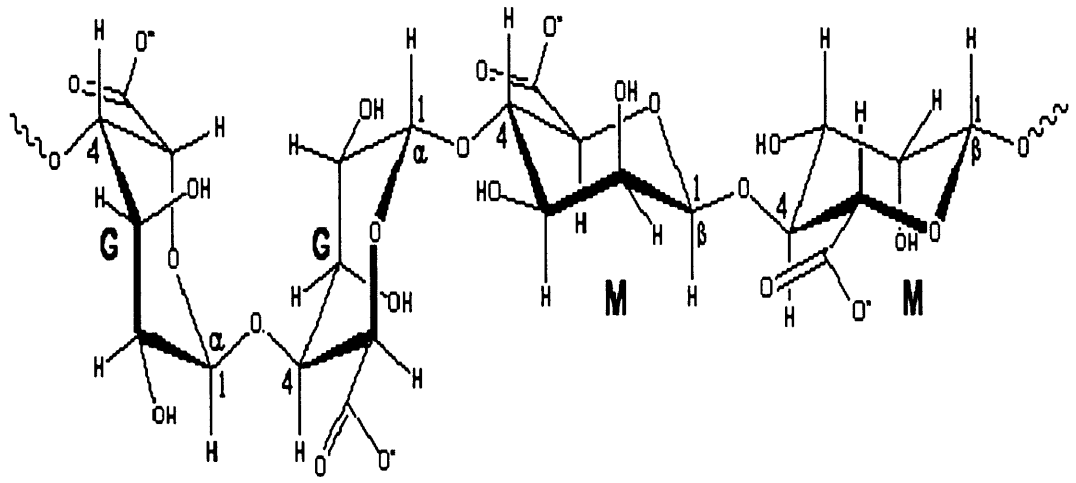

B

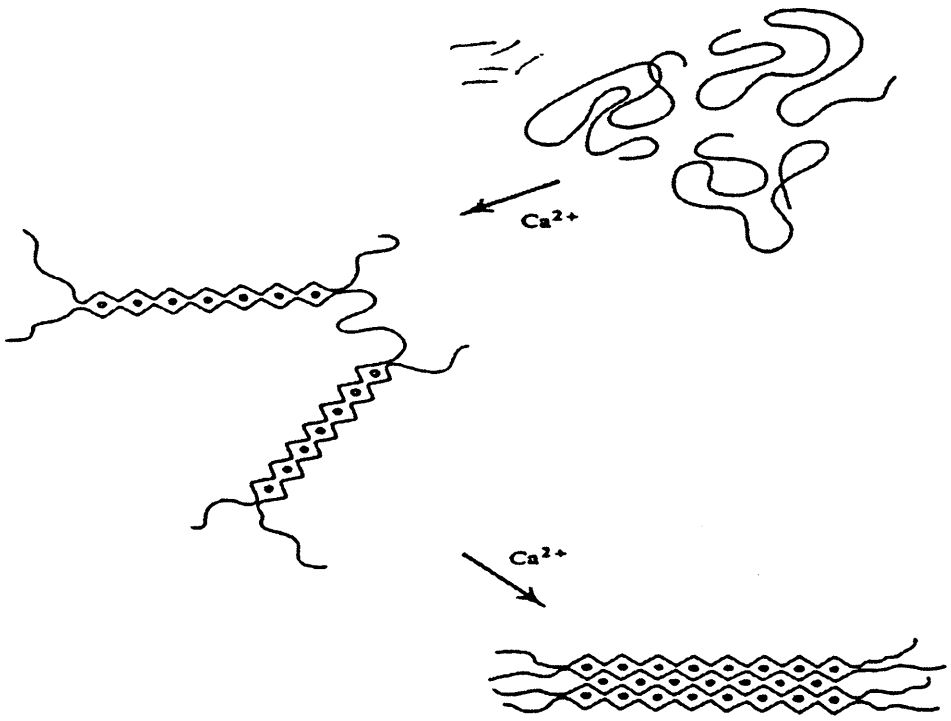

Figure 3. Molecular structure of alginate. (A) Repeat units of guluronic acid (G) and mannuronic acid (M). Sodium alginate would have sodium ions (Na+) associated with the carboxylic acid groups (COO-). (B) Polymerization of alginate. The poly-G chains initially in solution form nested structures in the presence of divalent ions such as calcium to form the hydrogel structure.

Gel strength is also dependent upon the molecular weight of the alginate. The molecular weight of alginate is determined from the viscosity of the alginate using the Mark Houwink Equation: $[\eta] = K * M^a$ where a = 1 and $K = 2x10^{-5}$ (Smidsrod and Haug, 1972). Gels with low molecular weight (low viscosity) do not form gels. Gels with a molecular weight below $2.4x10^5$Da, exhibit an increase in strength with increasing molecular weight. However, gel strength is independent of molecular weight for alginates with molecular weights above $2.4x10^5$Da. This characteristic is independent of the alginate concentration (Martinsen, 1989).

Heavy metals and polyphenols are present in alginate in various amounts according to the alginate source and species. The phenolic compounds can be detected using florescence spectroscopy. These contaminants can be reduced by selection of alginate material with low initial polyphenols or by their removal from the alginate by various purification methods. Some of these purification steps include treatment with H_2O_2 or another bleaching process such as sodium chlorite ($NaClO_2$); followed by dialysis to remove low molecular weight constituents; extraction with organic solvents, such as acetone or ethanol; adsorption chromatography through polyamide beads or granulated activated carbon; and filtration through a 0.45 μm membrane filter (Skjak-Braek, 1989).

The decomposition of sodium alginate has been studied in several animal models, but the degradation has varied based upon size, composition, method of matrix formation and application. Iannuccelli (1996) studied the release of an antibiotic during degradation of sodium alginate spheres cross linked with calcium and implanted in rats. In the first 12 hours the beads swelled approximately 2.5 fold, some cross linking bonds were cleaved at the surface and ~10% mass was lost. From 12 hours to 3 days, the mass reduced by 40% due to further hydrogel dissolution due to calcium ion displacement. The hydrogel was completely dissolved by 8-10 days (Iannuccelli, 1996). Matthews (1995) found the alginate dressing Kaltostat® created a foreign body reaction (i.e. inflammation, macrophage infiltration and fibrous tissue formation) when implanted between the bone and periosteum in the jaw of a dog and persisted out to 24 weeks after implantation (Matthew, 1995). The lack of biocompatibility in this last example likely elicited the dog's body to breakdown the

alginate. Mammals do not have indigenous enzymes to breakdown alginate *in vivo*. Enzymatic degradation of uronic acid subunits by β-elimination was demonstrated to be slow at physiological pH (Haug, 1963). In other *in vitro* studies, activated phagocytic cells were unable to degrade alginate that was derived from both seaweed and Pseudomonas aeruginosa bacteria (Simpson, 1993).

Alginate clearance from the body is another issue. Low molecular weight alginate (below 48,000Dalton) was demonstrated to be cleared by the kidneys and excreted in the urine using radioiodination labeling (Al-Shamkhani and Duncan, 1995). The high molecular weight components of alginate can be reduced by sterilization methods such as membrane filtration (Schneider, 2003), heat (Vandenbossche and Remon, 1993) and gamma irradiation (Alsberg, 2003). Gamma irradiation of alginate to create molecular weight components below 50kD has been demonstrated (Eiselt, 2000) and shown to have significant increase in alginate degradation rate in mice studies as compared to non-irradiated (higher molecular weight) alginate (Alsberg, 2003).

The biocompatibility of alginate has been widely studied in animal models. The reasons for immunogenicity of alginate implants have been widely disputed. Purification of commercial alginates reduces the total amount of impurities (e.g. polyphenols, endotoxins and protein) and has the greatest impact on whether the implants invoke an immune response (Klock, 1994; Zimmerman, 2000; Orive, 2002). From more recent studies, it is less clear whether chemical composition (e.g. high G, high M or molecular weight) has an impact (Orive, 2002; Schneider, 2003; vanHoogmoed, 2003). There are some studies demonstrating that low molecular weight alginate elicited a much stronger fibrotic response compared to higher molecular weight (Schneider, 2003). An ultra-pure alginate, Pronova™ MV (Pronova Biomedical, Oslo, Norway), was shown to support tissue and vascular ingrowth with minimal inflammatory response and capsule formation surrounding the implants when injected in the subcutaneous space of adult sheep (Halberstadt, 2002).

The easiest method of hydrogel formation using alginate is to add drop wise into a solution of $CaCl_2$ (1-2%v/v) forming spherical beads. A solution of $BaCl_2$ can also be

used (Zheng, 2003). The outside shell of the bead gels instantaneously, but the remainder takes several minutes. Others have made hydrogels by adding calcium sulfate ($CaSO_4$) to the alginate solution and pouring into molds (Rowley, 1999; Kong, 2003) which gel in 30-45 minutes. These techniques form a hydrogel with a closed pore structure which has been used extensively in cell therapy applications (DeVos, 1997; Constantinidis, 1999; Read, 2001). Often the alginate beads are coated with poly L-lysine (PLL) to further increase the stability of the bead (Joki, 2001). Several groups have modified the alginate hydrogel formation to produce larger, open pore matrix. Mooney's group, then at the University of Michigan now at Harvard, include sodium bicarbonate in the alginate mixture to create a foam, then form beads in $CaCl_2$ solution with acetic acid. Finally the beads are exposed to vacuum to open the pores (Eiselt, 2000). Cohen's group at the Ben-Gurion University produces porous scaffolds by freeze drying (Dar, 2002; Zmora, 2002) to create an open pore structure which also allows inclusion of drugs or proteins in the matrix (Perets, 2003). Cells are then seeded onto the surface of these alginate matrices.

Alginate hydrogels have been used successfully to encapsulate enzymes, secretory (e.g. pancreatic islet) cells (DeVos, 1997; Mullen, 2000), and transformed producer-cell lines such as transformed β-cells for secretion of insulin for treatment of diabetes (Constantinidis, 1999), delivery of recombinant proteins for cancer therapy such as tumour inhibitors (Joki, 2001; Read, 2001; Zheng, 2003) and for neuron regeneration (Tobias, 2001; Wu, 2002). In applications that require anchorage-dependent cell cultures, hydrogels have been chemically modified to covalently attach cell adhesion molecules. Some examples of cells cultured with peptide-modified alginate hydrogels have included osteoblasts on alginate-GGGGRGDY ($(Gly)_4$-Arg-Gly-Asp-Tyr) (Kong, 2003), mouse skeletal myoblasts on alginate-GRGDY (Gly-Arg-Gly-Asp-Tyr) (Rowley, 1999) and alginate-G_4RGDY (Rowley, 2002). However, others have found that alginate hydrogels without peptide motifs were suitable constructs for chondrocytes (Atala, 1994; Wong, 2001), myocytes (Dar, 2002) and rat bone marrow cells (Wang, L. 2003).

Data for retention of cell function and differentiation have been reported using alginate as a matrix. Chondrocytes have been shown to maintain a stable

differentiated phenotype when cultured in alginate as compared to 2-D cultures (Hauselmann, 1994; Lee, 2003); and liver cells in alginate secreted as much protein (e.g. albumin, fibrinogen, prothrombin) as in whole liver (Selden, 1998). Primary bovine chondrocytes entrapped in alginate were shown to synthesize extracellular matrix proteins (Wong, M., 2001). Bone marrow cells have been shown to proliferate on the surface of unmodified alginate and express osteoblast associated markers (Wang, L., 2003). However, rat neonatal cardiac cells were shown not to proliferate entrapped in unmodified alginate scaffolds despite retaining some spontaneous contraction for 2 weeks (Dar, 2002). Similar lack of growth was shown for entrapped human MSCs in alginate despite expression of differentiation markers for chondrocytes (Ma, 2003).

Although showing promise for structural tissues such as soft tissue, cartilage, myocardium, bone and liver; as of yet, no one has demonstrated that alginate has properties suitable for a TEBV. Natural, non-animal derived matrices are more desirable from a regulatory standpoint. Plant derived materials, such as alginate, are promising because they do not harbor human pathogens. However they still have natural mitogenic and cytotoxic impurities, as well as bacterial compounds of animal and human origin that need to be removed (Zimmermann, 2001).

1.4.3 Cell 'self-generated' matrix

An unconventional technique to develop a TEBV was developed by L'Heureux (1998) and requires no starting matrix material at all. Using this approach, human smooth muscle cells (SMCs) and fibroblast cells were grown independently to over confluence in culture vessels to form multilayers of cells and ECM. A tubular construct was fabricated by first placing a tubular acellular inner membrane (IM) produced by fibroblast cells over a perforated tubular mandrel, then rolling a sheet of SMCs over the IM and allowing the SMCs to mature for 1 week. Thereafter a sheet of fibroblast cells was rolled over top of the SMCs and allowed to mature for 7 weeks during which the cells (particularly the fibroblast cells) reorganize their ECM to orientate around the circumference of the tube. These constructs exhibited a burst pressure over 2000mmHg. Finally, endothelial cells were seeded onto the luminal surface of the vessel to form a confluent monolayer (L'Heureux, 1998). The entire maturation took over 3 months plus an additional month for the initial cell isolation

and expansion. Un-endothelialized human TEBVs created by this method were implanted into a canine femur model with 50% patency (L'Heureux, 1998). Subsequently, these TEBVs were characterized to have contractile and relaxation responses, cyclic nucleotide sensitivity and calcium ion handling mechanisms (stimulated by antagonists) comparable to normal vessel (L'Heureux, 2001). Although the fabrication process appears to be cumbersome; this method has definite potential as a TEBV. Cytograft Tissue Engineering, Inc. (Novato, CA, USA) was established to develop this approach and to bring forward this TEBV into clinical trials (www.cytograft.com).

1.4.4 Modification of materials for biocompatibility

A large number of ECM proteins (fibronectin, collagen, vitronectin, thrombospondin, tenascin, laminin and entactin) contain the RGD sequence (Saltzman, 2000). In order to simplify and improve cell binding to synthetic polymers, RGD peptides have been immobilized onto synthetic polymers including ePTFE, poly(carbonate-urea) urethane (Tai, 2000; Tiwari, 2002b), PEG (Mann, 2001), PVA (Schmedlen, 2002), PLA/PLGA (Eid, 2001; Yang, X., 2001) as described in section 1.4.1.

Alginate constructs have successfully incorporated cell adhesive ligand polypeptides (e.g. RGD) and have been used to grow adherent cells including pre-adipocytes for reconstruction of soft tissue defects caused by trauma or cancer (Halberstadt, 2002) and myoblasts which are precursors to skeletal muscle (Rowley, 1999 and 2002) as previously described in section 1.4.2.3.

In addition to surface chemistry, the overall micro-architecture of the matrix is critical. For building a solid organ, enhancing vascularization consisting of capillary networks will be essential for adequate mass transfer characteristics. Some approaches that have been utilized include altering pore size and microstructure or inclusion of growth factors (Nikalson and Langer, 2001; Leor, 2000; Perets, 2003).

Finally for long term biocompatibility, the degradation of the matrix needs to be considered. The rate of degradation will need to be established, what the degradation products are and where they end up (i.e. remain at implantation site, circulate into the blood stream or passed through the kidneys). For example large molecular weight

alginate (>48kD) is known not to be cleared by the kidneys (Al-Shamkhani and Duncan, 1995). Another more recent study found that degradation of synthetic PGA polymer graft *in vitro* resulted in localized areas of high acidity which caused undesirable de-differentiation of the SMCs (Higgens, 2003).

1.5 Cell selection for a tissue engineered blood vessel (TEBV)

The source of the cells used for implantation will be determined by whether the clinical procedure is elective or emergency. The urgency or lack of urgency will determine how the cells are obtained, cultivated, and manipulated (i.e. whether a saphenous vein or internal mammary artery would have to be used or a TEBV could be grown). For example, nerve repair must occur within several hours/days from the initial damage in order to be successful. Therefore stem cells or pre-cultured cells must be utilized. The type of cell selected for repair must address the proliferation requirements (and possible limitations) for expansion of large numbers in culture. Currently, a few cell types such as keratinocytes, fibroblasts, chondrocytes, and myoblasts can be expanded in sufficient quantity in culture (Young, 1997; Terskikh and Vasiliev, 1999). Embryonic and most adult stems cells are also capable of being expanded to sufficient number *in vitro* (Devine 2001; Zandstra and Nagy, 2001; Gepstein, 2002).

1.5.1 Autologous, allogeneic and xenogeneic cells

Autologous (recipient's own) cells are harvested from a tissue biopsy or blood sample, grown in culture and then reintroduced into the original donor. The use of autologous cells obviates the problem of host's immune rejection. Cultured autologous cells were the first clinical application of cellular tissue engineering. Autologous keratinocytes were grown in culture and grafted onto burn victims (Gallico, 1984). Autologous cultured chondrocyte transplantation was introduced in 1987 and has resulted in good to excellent long term (2-9 years) clinical results (Peterson, 2000). As mentioned above, autologous cells could be used for implants prepared in advance of the procedure. However, the time required to harvest the cells, expand the cells in culture, construct the implant, and release the final product back to the patient could limit the feasibility of using *ex vivo* cell therapies unless a validated quality assurance program is in place (Mayhew, 1998). Most fully differentiated cell types have a limited number of expansions in culture and may never grow to

sufficient quantity to seed a tissue engineered matrix (Seruya, 2004). Reagents and methods used in the culture of cells for cell/tissue therapies need to be screened and validated so that the cell population is not altered and adventitious agents are not introduced (Louet, 2004).

Autologous replacement of tissue function can also be achieved by providing an appropriate scaffold that fosters cell migration and proliferation. Once the scaffold is implanted, cells are recruited onto the surface and ultimately replace the implanted matrix components with new, host-derived, extracellular matrix. This approach has been taken for nerve regeneration because autologous cells are limited (Yu and Bellamkonda, 2003). The scaffolds can contain bioactive factors that can stimulate chemotaxis and cell differentiation (Young, 1997).

Autologous cells required for blood vessel repair could be isolated from the patient's own body, if the cell isolation and cultivation procedure is performed in advance as is currently done for autologous chondrocyte transplantation (Brittberg, 1994). Shin'oka (2001) successfully implanted an autologous TEBV into a 4 year old Japanese girl. The cells had been expanded *in vitro* for eight weeks prior to seeding onto the polymer matrix and then matured for a further ten days before transplantation. More recently autologous bone marrow cells (BMCs) were seeded onto a TEBV scaffold on the day of surgery in 22 human patients– with no maturation *in vitro* (Matsumura, 2003a).

Tissue availability, inherent variability and limitations on expansion in culture are the major drawbacks to the use of autologous cells. The use of allogeneic cells (cells derived from a different source within same animal species) permits the cells to be cultured and cryopreserved in sufficient quantity ready for immediate use. Allogeneic cells can be well characterized and allow development of a reproducible and consistent product. In addition, if cell lines are created, the cells can be screened for adventitious agents, abnormal karyotype, tumorigenicity, and phenotypic changes well beyond their use level (Wilkins, 1994).

One disadvantage of allogeneic cells is that they may be immunogenic to the host in which they are implanted. Allograft rejection is primarily a T cell mediated immune

response. Leukocytes and endothelial cells are strongly allostimulatory; whereas, keratinocytes, smooth muscle cells, and fibroblasts do not stimulate naïve T cells and are less allostimulatory (Young, 1997). There have been successful approaches to using allogeneic cells in tissue engineering. Allogeneic cells (e.g. keratinocytes and fibroblasts) have been used for skin replacement and wound healing in FDA approved skin substitutes such as Apligraf and Dermagraft. Bone marrow transplantations using allogeneic bone marrow cells have been successful since the 1970s and have advanced considerably in the 1990s due to several developments including improvement in histocompatibility typing technology (Storb, 2003). However the recipients (usually cancer patients) have undergone extensive chemotherapy and radiation treatment prior to transplantation and also have to be on anti-rejection/immunosuppression therapy since as many as 50% acutely suffer from Graft vs. Host Disease (GVHD) (Storb, 2003; www.osiristx.com). The major histocompatibility complex (MHC) proteins on the cells' surface play a major role in immune response. Resting T-cells are activated by the expression of antigens on the surface of antigen-presenting cells (Geppert and Lipsky, 1985). Techniques are currently being tested to both knock out expression of these proteins on the cells' surface (Hunt, 1998) and transfer the donor's MHC antigens to the transplant recipient using gene therapy (Wong and Wood, 2004).

Xenogeneic cells (cells derived from a different animal species, such as porcine) have been used to generate tissue. New technology including cell encapsulation, immune protection, extracorporeal systems, and genetic manipulation is being developed to enable the use of xenogeneic tissue. The use of xenogeneic cells requires additional safety assessment so that pathogenic viruses and prions are not introduced into the human population (Young, 1997; Dormont, 2002). Alginate beads containing xenogeneic (porcine) pancreatic islets and cross linked with barium ions have shown success in long-term immunoisolated transplantation studies in animal and human hypoparathyroidism (Zimmermann, 2000). However, it is extremely unlikely that xenogeneic cells would be used for a TEBV since the cells could not remain isolated.

1.5.2 Stem cells

Embryonic stem cells are pluripotent and can mature into virtually any cell type in the body. If the differentiation of human embryonic stem cells in culture could be well-

controlled and characterized, the resulting cells could be used to help repair human tissue. Human embryonic stem cells can be cultured by isolating a blastocyst, removing the outer cell wall, placing into culture with a layer of mouse feeder cells, and adding selected differentiation factors after colonies of embryonic stem cells have been formed (Pederson, 1997). This field is just beginning to be understood and obviously has many scientific challenges and ethical issues that need to be addressed prior to the feasibility of use for a repair aid. Researchers have already identified precursor cells that will preferentially differentiate into vascular endothelial or vascular SMCs (Carmeliet, 2000).

1.5.2.1 Adult stem cells

Adult stem cells are responsible for maintaining homeostasis of body tissue by continually replacing cells during normal physiological turnover. Many tissue-specific stem cells have been identified in skin (basal cells), muscle, liver, gastrointestinal tissue (intestinal crypt cells), bone marrow/whole blood and the brain (central nervous system stem cells). Initially adult stem cells were thought to have restricted capacity to differentiate, so-called 'committed-progenitors'. However, recently many more primitive progenitor stem cells have been acknowledged with long-term proliferation capacity and greater differentiation (multi-lineage) potential (Piscaglia, 2003).

Muscle-derived stem cells (satellite cells) have a great potential for autologous cell-mediated therapy. A muscle biopsy can be easily obtained from the patient without compromising the patient's health. The cells have capacity for *ex vivo* manipulation and expansion in culture, and can be used as a vehicle for gene therapy (Deasy, 2001; Wright, 2001). Human clinical trials have been successfully conducted using skeletal muscle satellite cells that were transplanted into cardiac muscle (Menasche, 2003); however, some groups have shown that these studies have not rigorously established expression of cardiac markers in cells originated from skeletal muscle (Reinecke, 2002). More recently adult stem cells from muscle have been shown to differentiate into SMCs (Seruya, 2004).

Human bone marrow is one of the most widely used sources of adult stem cells. Peripheral blood constantly regenerates from stem cells derived in bone marrow.

Bone marrow cells give rise to many cell types including hemopoietic and non-hemopoietic cell types. Mesenchymal stem cells (MSCs) derived from human adult bone marrow may provide a suitable source of autologous cells for cell and gene therapy (Prockop, 1997) and regeneration of tissue (Caplan and Bruder, 2001). MSCs are present in the bone marrow at about 1 in 100,000 cells (Galotto, 1999). Others have estimated from 1 in 10,000 to 1 in 100,000 (Deans and Moseley, 2000), or between 2-5 MSCs per 10^6 mononuclear cells (Koc and Lazarus, 2001). MSCs are selected in culture by adherence to tissue culture plastic (TCP) (Koc and Lazarus, 2001).

MSCs have been shown to differentiate *in vitro* into adipocytes, chondrocytes and osteoblasts (Pittenger, 1999), as well as myoblasts and myotubes (Wakitani, 1995). Recent studies have demonstrated the increased breadth of pluripotency of MSCs. By adding appropriate levels of growth factors *in vitro*, rat and mouse multipotent adult progenitor cell (MAPC) have been shown to differentiate into endothelium (mesoderm), neurons (ectoderm) and hepatocytes (endoderm) (Jiang, 2002). MAPCs have also been identified in human bone marrow cells which differentiate *in vitro* into myocytes (mesoderm), endothelium (visceral mesoderm), neurons (ectoderm) and hepatocytes (endoderm) (Reyes, 2001; Schwartz, 2002; Muguruma, 2003). Toma (2002) showed hMSCs differentiated into a cardiomyocyte phenotype in the adult murine heart. Although cell fusion could not be out-ruled as a contributing factor in this murine *in vivo* study, since bone marrow cells have recently been shown to adopt the phenotype of somatic cells by spontaneous cell fusion (Terada, 2002; Wang, X., 2003). Since these studies others have reported differentiation of hMSCs into cardiomyocyte phenotype *in vitro* (Xu, 2004).

Adult stem cells derived from human blood have also been shown to differentiate into SMCs (Simper, 2002). Circulating skeletal stem cells have been identified that are distinguishable from MSCs or stromal stem cells which have osteogenic and adipogenic potential (Kuznetsov, 2001).

The use of MSCs in tissue engineering and cell therapy applications has exploded in the last couple years, especially in the areas of bone and cartilage. Osiris Therapeutics is in Phase I clinical studies with their dental implants seeded with

MSCs, and were the first company with fast tract designation by the FDA for Prochymal, their adult stem cells for treatment of GVHD, after completion of Phase I studies in January 2005 (www.osiristx.com). As previously mentioned in section 1.4.1, BMCs have also been successful seeded onto vascular scaffolds of human patients (Matsumura, 2003a).

1.6 Selection of bioactive agents for a TEBV

The matrix and/or growth medium can be filled with cue materials to promote tissue regeneration. The cue materials can include support matrices (e.g. fibrin precursors, hyaluronic acid); bioactive agents such as simple molecules (e.g. ascorbic acid); insoluble ECM molecules such as laminin, fibronectin, or collagen (Hubbell, 2000; Saltzman, 2000); and soluble factors such as growth factors or hormones (Gooch, 1998). Chemicals can also be used to induce differentiation as has been shown using dexamethasone for triggering MSCs down an osteogenic pathway (Pittenger, 1999) and 5-azacytidine for differentiating MSCs into myocytes (Wakitani, 1995).

1.6.1 Adhesion molecules

Some polymers can be improved by just by coating the surface with ECM molecules (e.g. collagen, fibronectin). For example many tissue culture plates are treated with these molecules to improve cell binding. Bioactive polymers, polymer material enhanced through the incorporation of specific bioactive sequences, have been used for wound healing scaffolds. Short peptide sequences derived from cell binding regions of extracellular matrix proteins can be utilized to achieve biospecific adhesion of cells to biomaterials via integrins (a family of cell surface proteins that are involved in binding to extracellular matrix components) (Gooch, 1998). Some of these sequences include (see glossary for amino acid abbreviations):

a) RGD – fibronectin, collagen, fibrogen, laminin
b) YIGSR, IKVAV, LRE – laminin
c) REDV – fibronectin
d) DGEA – collagen
e) VTXG – thrombospondin
f) VGVAPG – elastin

Other bioactive substances have been used to achieve biospecific cell adhesion through immobilization of carbohydrate moieties such as N-acetylglucosamine and lactose, likewise immobilization of growth factors (EGF) and insulin. Several short peptide sequences derived from growth factors have been identified that can bind to the appropriate receptors. These have been used and may be advantageous over the intact proteins due to the denaturation and degradation that can occur with proteins (Sawhney, 1998).

1.6.2 Growth hormones and growth factors

Microencapsulated recombinant human growth hormone (rhGH) in PLGA was injected into rhesus monkeys and resulted in elevated serum levels of rhGH for more than one month. These data suggest that, in principle, any protein could be stabilized by forming a complex with zinc, atomizing, freezing and lyophilizing into a powder and encapsulating with a polymer in a methylene chloride solution since there is no water present during the encapsulation process that would promote chemical modification, denaturation and/or aggregation (Johnson, 1996).

Growth factors can stimulate or inhibit cell division, differentiation, and migration. They up- or down-regulate cellular processes such as gene expression, DNA and protein synthesis, and autocrine and paracrine factor release. Growth factors can interact with one another in an additive, cooperative, synergistic, or antagonistic manner. They can be added to the cell culture media *in vitro* to enhance cell proliferation. Alternatively, growth factors can be added either during manufacture of the scaffold or bound onto the scaffold after manufacture. Controlled delivery of growth factors can be examined using devices made from biodegradable polymers or gels incorporated with the desired growth factor (Johnson, 1996; Laham 1999; Richardson, 2001; Perets, 2003; Simmons, 2004). The growth factor can be strategically located on the scaffold, thereby creating a gradient to preferentially enhance cell attachment and/or direct cell migration (Gooch, 1998).

Potent mitogens (agents that induce cell division) for the two major cell types of large blood vessels, endothelial cells and smooth muscle cells, have been well characterized, they include:

a) basic fibroblast growth factor (bFGF) – both endothelial and smooth muscle

b) vascular endothelial cell growth factor (VEGF) – endothelial cells
c) platelet-derived growth factor (PDGF) – smooth muscle cells
d) epidermal growth factor (EGF) – smooth muscle cells
    i) heparin-binding EGF-like growth factor (HB-EGF)
    ii) betacellulin
e) endothelin-1 (ET-1) – smooth muscle cells

Each of these growth factors may up or down-regulate the production of others, and thus must first be studied individually. For tissue engineering, whether the cells are quiescent or activated, and whether they are in a two or three-dimensional culture will influence endogenous growth factor production and thus also the response to exogenously applied bioactive molecules. Endothelial and smooth muscle cells cultured together will respond differently to exogenous growth factors than will cultures of each cell type alone (Gooch, 1998).

A variety of these growth factors have been reported in the literature that directly affect differentiation of stem cells into SMCs. Yamashita (2000) found mouse embryonic precursors that gave rise to either endothelial cells using VEGF or to SMCs using PDGF-BB. However no evidence for such a growth factor driven differentiation events existed for adult humans until Simper (2002) demonstrated that smooth muscle progenitor cells exist in human blood. They isolated smooth muscle progenitor cells from peripheral blood samples and either maintained an endothelial cell phenotype using medium containing VEGF (10μg/mL) or differentiated the cells into SMCs by supplementing with PDGF-BB (50ng/mL). Subsequent to this research, Seruya (2004) used TGF-β1 (9μg/mL) to differentiate adult rat MSCs derived from leg muscle into smooth muscle cells (cells expressing α-smooth muscle actin (ASMA) and calponin).

1.6.3 Conditioned medium and co-cultures

In the absence of a definitive medium for differentiation of MSCs into SMCs, a feasible approach to perform differentiation studies was using conditioned medium. Potent mitogens and other non-mitogenic growth factors have been identified in vascular rSMC conditioned medium (Molloy, 1996; Pawlowski, 1997; Taylor, 1999). Therefore conditioned medium from fully differentiated rSMC cultures could

theoretically provide the necessary growth factors and biochemical cues to differentiate hMSCs into SMCs provided these molecules are conserved between species. Conditioned medium has been shown to be effective in cloning studies when cultures are below critical density (Takahashi and Okada, 1970). Researchers have studied the effect of soluble factors in conditioned (astrocyte) medium and co-cultures on the differentiation of neurons (Kilpatrick, 1993). Likewise many conflicting studies on EC-SMC interactions have been reported using co-cultures to investigate underlying pathology of arthrosclerosis which have reported that EC conditioned medium stimulated SMC growth (Schwartz, 1981; Vernon, 1997); while others have reported that EC conditioned medium or confluent co-cultures of ECs inhibited growth and delayed de-differentiation of SMCs in culture (Campbell and Campbell, 1986).

The use of feeder cells or co-cultures has been a common method for maintaining cell cultures. Undifferentiated human embryonic stem cells have been maintained on mouse embryonic fibroblast feeders (Thomson, 1998); although feeder-free growth is now possible (Xu, 2001). More recently, researchers have tested conditioned medium and co-cultures (in direct physical contact) to direct differentiation of MSCs (Rangappa, 2003). However cell fusion cannot be ruled out in these types of studies if co-cultures are in physical contact with the stem cells (Terada, 2002).

1.7 Planned research

The University College London Department of Biochemical Engineering group is interested in the formation of substitute arteries for use in treatments such as by-pass surgery. Sodium alginate was chosen as the polymer matrix since it is a natural, biodegradable polymer that sets rapidly within a solution of divalent ions. There is wide spread interest in alginate's use in tissue engineering (Atala, 1994; Hauselmann, 1994; Lee, 1997; Rowley, 1999; Eiselt, 2000; Alsberg, 2001; Dar, 2002; Halberstadt, 2002; Wu, 2002; Dvir-Ginzberg, 2003; Lee, 2003; Ma, 2003; Perets, 2003; Zimmerman and Eschenhagen, 2003; Wang, L., 2003; Kamil, 2004) and initial clinical studies have shown it to be safe (Hasse, 1997; Caldamone and Diamond, 2001). It was desirable to develop an engineering system to fabricate a tubular scaffold which provided initial 3-D form, encouraged cell attachment and proliferation using a process that achieved high initial cell viability after formation of

scaffold, provided the necessary bioactive molecules to encourage cell growth similar to *in vivo* conditions, and easily translated into a bioreactor system for automation.

In this project, in order to simplify the complexity of multiple cell types in a native blood vessel, only one cell type was investigated with the alginate scaffold. Either rat smooth muscle cells (rSMCs) or human mesenchymal stem cells (hMSCs) were homogeneously mixed with sodium alginate in normal-saline (n-saline, 0.9% w/v NaCl in distilled water, pH 7-7.4) and bioactive molecules (collagen or RGD containing peptides) prior to formation of the 3-D scaffold (bead, sheet or tube). A solution of divalent cations (e.g. $CaCl_2$) was used to cross link the alginate molecules to form a hydrogel containing the cells.

Tubes were fabricated using an extrusion process which allowed the cells to be immobilized within the scaffold. This technique allowed rapid formation of a tube with a 100-250μm cell/alginate wall thickness without necessitating a two step process involving tube formation and then cell seeding. The extrusion method was a type of reverse coating by which the cell/alginate hydrogel tube was formed on the inside surface of a hollow glass tube. The cells were mixed within the alginate prior to formation. After cross linking was completed using a solution of divalent cations, the tube was washed with culture medium to reduce the residual divalent cation concentration. The alginate/cell tube was matured within the hollow glass tube.

Because the availability of cells was severely limited (at the high concentrations being studied), beads were examined as a proxy for tubular artery constructs to produce significant amount of material on which to test multiple conditions. For example, 0.4mL of cell/alginate material could be used to form one tube or produce ca. 30 beads. Hydrogel sheets were initially studied because they permitted uncoupling of the cell seeding and hydrogel formation steps in order to study cell attachment and elongation without the cells immobilized within the alginate.

The sodium alginate from various commercial suppliers was chemically modified using carbodiiamide chemistry to incorporate GRGDY peptides onto the carboxylate moieties of the alginate's poly-guluronic acid backbone to provide cell adhesion sites. This modified alginate (alginate-GRGDY) was studied with cells comparatively

against the unmodified alginate. The method of derivatization of the alginate continuously evolved during the course of the research.

The general project goals of this research were to:

- determine conditions in which rSMCs and hMSCs were viable and proliferated in a natural matrix (e.g. alginate, collagen)
- characterize the growth of rSMCs and hMSCs incorporated into a 3-D scaffold and compare to 2-D growth in tissue flasks
- study the effect of biological cues (e.g. RGD peptide) on attachment, elongation and growth of the cells on the alginate scaffold
- examine differentiation of the hMSCs into SMCs using conditioned rSMC medium.

1.7.1 Characterization studies with alginate and rSMCs

So that numerous experiments could be performed with safe and consistent starting material, a cell line of rSMCs was established at UCL. A well characterized rat aortic smooth muscle cell line (ATCC cell line A7r5) (Kimes and Brandt, 1976) was used to complete the initial conceptualization and research. This immortalized clonal cell line was shown to maintain the biochemical, physiological and phenotypic characteristics of rSMCs *in vitro* (Kimes and Brandt, 1976) and provided a reliable supply for these studies. Cell culturing using this immortalized rSMC cell line was feasible for many passages; whereas, primary cell cultures derived from explants and other sources are usually limited (Hayflick, 1965). Hayflick showed fibroblasts (diploid cells) from fetal lung were capable of ~48 (35-63) doublings whereas fibroblasts from adult lung were only capable of ~20 (14-29) doublings (Hayflick, 1965). It was recognized that these immortalized cells would differ somewhat from primary sources; therefore later in the project, adult hMSCs derived from bone marrow cells were studied for this reason. This work is summarized in section 1.7.2 and 1.7.3.

The rSMCs were combined with sodium alginate in n-saline and then immediately formed into a hydrogel by cross linking the alginate molecules using a divalent cation solution such as $CaCl_2$. Three hydrogel forms were made – sheets, beads or tubes. Both unmodified sodium alginate and alginate-GRGDY were studied using rSMCs. Varying concentrations (e.g. 1X-50X) of the carbodiimide reagents were used to

determine the optimal concentration to allow cell attachment, elongation and networking within the alginate hydrogel while maintaining hydrogel integrity. Collagen containing matrices were also tested initially to study the effect of the cross linking solution concentration on the rSMCs. Characterization of these rSMC/alginate constructs included phase contrast microscopy, cell viability, proliferation and glucose metabolism studies.

1.7.2 Characterization studies with alginate and hMSCs

MSCs derived from human adult bone marrow provided a suitable source of primary cells for testing this cell/alginate system. HMSCs were isolated from bone marrow cells using a Ficoll gradient with prior approval from University College London Hospital ethics of human research committee. HMSCs were selected by their adherence to tissue culture flasks (Koc and Lazarus, 2001) and the cell population was confirmed using cell surface markers specific for MSCs (e.g. SH2+, SH4+ and CD34-) (Haynesworth, 1992). Frozen banks were produced to establish a consistent supply.

HMSCs were studied with both unmodified alginate and alginate-GRGDY hydrogels. Additional characterization was performed on these hMSC/alginate constructs including cytology and histology to examine overall cell morphology. A Live/Dead fluorescence assay was used to observe the hMSCs *in situ* in the beads. In addition, a modified MTT (3-(4,5-dimethylthiazol-2-yl)-2,5-diphenyltetrazolium bromide) assay was developed to examine cell proliferation/metabolism (Mosmann, 1983).

1.7.3 Differentiation experiments with hMSCs

MSCs have been shown to readily differentiate *in vitro* into adipocytes, chondrocytes and osteoblasts (Pittenger, 1999), as well as myoblasts and myotubes (Wakitani, 1995). Numerous *in vivo* studies have shown MSCs differentiate into cardiomyocytes (Toma, 2002), although cell fusion could not be ruled out for causing this (Terada, 2002). Therefore the first step toward production of an autologous tissue engineered blood vessel (TEBV) *in vitro* would be to differentiate the MSCs into SMCs. It was anticipated that conversion of MSCs to SMCs would be enhanced in a three-dimensional gel as was found with differentiation of MSCs to chondrocytes (Ma, 2003; Steinert, 2003). Chondrocytes have been shown to maintain a stable differentiated phenotype when cultured in alginate as compared to 2-D cultures

(Hauselmann, 1994; Lee, 2003). At the time of this research, a suitable differentiation medium was not published. Therefore, preliminary studies were conducted to examine differentiation of MSCs within alginate-GRGDY beads using conditioned rSMC medium and rSMC co-cultures.

Charbord (2000) and Remy-Martin (1999) proposed a sequential model of differentiation of MSCs to vascular-smooth muscle-like stromal cells from cytoskeletal and extracellular matrix protein expression in both mice and humans. The markers that appear sequentially in long term cultures of hMSCs were identified (Charbord, 2000) and are listed in Table 1. Remy-Martin and Charbord's model of stromal cell differentiation collaborates with Owens (1995) developmental studies performed on vascular SMCs.

Stage of Differentiation	Protein Marker Expressed
Early	Vimentin, laminin β1, fibronectin
Early-mid	EDa+ fibronectin, thrombospondin-1, ASMA
Mid	h-1 calponin, SM22α
Mid-late	h-caldesmon, metavinculin
Late	SM myosin heavy chain SM1

Table 1. Sequential expression of proteins in long term cultures of hMSCs (Charbord, 2000).

Immunohistochemistry was used to identify the presence of these cell-specific proteins (such as ASMA) in the cultures of MSC/alginate beads that were exposed to SMC conditioned medium as compared to control cultures. Additional characterization using fluorescence activated cell sorting (FACS) was used to monitor the change in MSC surface markers (e.g. SH2, SH4) during differentiation.

2. Materials and Methods

2.1. Methods of rat smooth muscle cell (rSMC) culture

Rat smooth muscle cells (rSMCs) were cultured in sterile, polystyrene tissue culture flasks (Corning Life Sciences, Corning, New York) which were treated to encourage cell attachment using a plasma charge which introduces a hydrophobic, negatively charged surface. The cell growth medium was Dulbecco's Modified Eagles Medium (DMEM) supplemented with 10% Fetal Bovine Serum (FBS), 2mM l-glutamine, 100U penicillin/mL and 100μL streptomycin/mL (all obtained from BioWhittaker Inc., Walkersville, Maryland, USA) and was used at 30mL/T150 flask or 0.2mL/cm^2. This supplemented cell growth medium will be referred to as "complete DMEM" for the remainder of this thesis.

2.1.1. Cell culture

2.1.1.1. Creation of frozen working cell bank

A cell bank of rSMCs was created at UCL to supply experimental material for this research. One vial of A7r5 rSMCs (American Type Culture Collection, Manassas, Virginia; product code CRL-1444; Kimes and Brandt, 1976) was obtained from ATCC and was planted into a vented 75cm^2 tissue flask (T75) containing 0.2mL/cm^2 growth medium. The culture was incubated at 37°C in a 10% CO_2 humidified incubator (Galaxy S, RS Biotech Laboratory Equipment Ltd., Irvine, Scotland). Two days after seeding, the spent medium was removed and fresh complete DMEM was added two days after seeding. Then on day 3, cells were trypsinized as per next section 2.1.1.2 and passaged into new flasks at a 1:2 to 1:3 split ratio (1 vessel into 2 or 3 new vessels). After 5 passages (6.7 population doublings) using this same procedure, the cells were trypsinized, counted using a hemacytometer, centrifuged at 100g for 10 minutes (Universal 32, Hettich-Zentrifugen, Tuttlingen, Germany) and resuspended to 2x10^{6}cells/mL in cryopreservation medium. The cryopreservation medium was DMEM containing 5% DMSO (Sigma Chemical Co., St. Louis, Missouri, USA), 29% FBS, 1.5mM l-glutamine, 73U penicillin/mL and 73μL streptomycin/mL. (Unless noted, all obtained from BioWhittaker.) Approximately 1mL of cell suspension was aliquoted into cryovials (Nalgene, Nalge Nunc International, Rochester, New York, USA) which then were frozen slowly in a insulated Styrofoam box in a –70°C freezer overnight. Then the cells were transferred to liquid nitrogen (< –150°C) for long term storage.

2.1.1.2. Cell passaging protocol in tissue flasks

A7r5 rSMCs derived from the UCL cell bank were thawed and seeded into 150cm^2 tissue flasks (T150) and passaged every 3-5 days at a split ratio of 1:3 (1 vessel into 3 new vessels). The cells were observed macro and microscopically for cell confluency (density), evidence of mitotic cells, pH/color of medium, amount of cell debris in medium, and other characteristics of the cells morphology (e.g. cells in stationary culture were more grainy in appearance due to increased ribosomes on the ER.).

During a typical passage, the spent medium was removed from the flask using a pipet. The spent medium from individual flasks was pooled together; samples were removed and frozen for later analysis for glucose and lactate concentration (section 2.3.6). Then the flask's cell growth surface was rinsed with 30mL (0.2mL/cm^2) of phosphate buffered saline, PBS, (BioWhittaker) to remove residual FBS proteins that will reduce trypsin activity. Next, 6mL (0.04mL/cm^2) of 0.25% trypsin/0.02% EDTA (Sigma) was added to each flask and spread evenly over the growth surface. After 5-7 minutes, the rSMCs were detached from the growth surface by tapping the flask against the palm of the hand. After completely dislodging the cells, 18mL (0.12mL/cm^2) of complete DMEM was immediately added to quench remaining trypsin activity. The cells were not exposed to trypsin longer than 15 minutes since trypsin is a nonspecific protease which will eventually permeate the cell membrane. The cell suspension from all individual flasks was pooled together and a sample was taken to determine cell density by counting the cells using a hemacytometer (section 2.5.2). Viability was assessed using trypan blue dye exclusion assay (section 2.5.3). To plant the next passage flasks, 8mL of the cell suspension were added to 22mL of fresh complete DMEM into each new T150 flask. Samples of the diluted cell suspension were removed for determination of initial glucose concentration and frozen for later analysis. Finally, the flasks were incubated at 37°C in a 10% CO_2 humidified incubator. Typical culture seeding densities were 5-9x10^{3}cells/cm^2 and final cell densities ranged from 1-1.7x10^{5}cells/mL or 1.5-3.0x10^{4}cells/cm^2 (1.3-2.0 population doublings per passage).

2.2. Methods of human mesenchymal stem cell (hMSC) culture

Adult human mesenchymal stem cells (hMSCs) were cultured in sterile, polystyrene tissue culture flasks (Corning) which were treated by the manufacturer for cell attachment using a plasma charge which creates a hydrophobic, negatively charged surface. The hMSC growth medium was MesenCult (Stem Cell Technologies, Inc., Vancouver, British Columbia, Canada) combined with Mesenchymal Stem Cell Stimulatory Supplements (Stem Cell Technologies), 100U penicillin/mL and 100μL streptomycin/mL (BioWhittaker) and 1ng/mL recombinant human fibroblast growth factor (rhFGF) (R&D Systems, Minneapolis, Minnesota, USA). This supplemented hMSC medium was used at 20mL/T150 flask or 0.13mL/cm^2 and will be referred to as "MSCCM" for the remainder of this thesis.

2.2.1. Isolation of hMSCs from bone marrow sample

Human MSCs were received from Dr. Chris Boshoff's lab at the Wolfson Institute of Biomedical Research, University College London. The use of human clinical samples had been approved by the joint UCL/University College London Hospital Ethics Committee of Human Research. The isolation procedure involved taking freshly harvested adult bone marrow and isolating the mononuclear cells in a Ficoll gradient. This procedure will be described using 7.5mL of sample, typically 5-10mL was used and the corresponding volumes adjusted for the specific volume used. First of all, the 7.5mL of bone marrow sample was filtered through a 40μm nylon cell strainer (Falcon, Bibby Sterilin, Stone, UK) and then rinsed with an equal volume (7.5mL) of Dulbecco's phosphate buffered saline without calcium and magnesium (DPBS, Biowhittaker). A 15mL aliquot of Ficoll (density 1.077g/mL, Histopaque-1077, Sigma) was added to a 50mL centrifuge tube (Corning) and the tube was held at a sharp, slanted angle to create a large surface area on the top of the liquid. Using a pipet, the DPBS/bone marrow sample was very carefully added to the edge of the 50mL tube such that the sample remained above the Ficoll surface. A counter-weight centrifuge tube was made with the same relative volumes of Ficoll and DPBS substituted for the bone marrow volume. The tubes were centrifuged (5810R Centrifuge, Eppendorf AG, Hamburg, Germany) at 652g for 30 minutes at room temperature (20°C) with no brake applied. This procedure fractionated most of the red blood cells to the bottom of the tube; whereas, the mononuclear cells remained at

the interface of the Ficoll liquid. Using a sterile plastic Pasteur pipet bulb (Fisher Scientific, Loughborough, UK), the mononuclear cells were carefully removed while trying not to disturb the Ficoll interface. Approximately 5-6mL was collected (maximum of 10mL) and placed into a 50mL centrifuge tube. The cells were rinsed with ca. 40mL of DPBS and then the tube was centrifuged at 290g for 8-10 minutes at room temperature with low brake setting. The supernatant was discarded and the cell pellet was gently resuspended with 5mL of MSCCM and added to a vented T75 flask (Corning, 75cm^2) or 10cm petri-dish (Corning, 55cm^2) containing 5mL MSCCM (total volume ca. 10mL). The flask or petri-dish was incubated at 37°C in a 5% CO_2 humidified incubator (HeraCell150, Kendro Laboratory Products GmbH, Langenselbold, Germany or Galaxy S, RS Biotech Laboratory Equipment Ltd., Irvine, Scotland) to allow the hMSCs to attach. After 2 days, the spent medium containing non-adherent cells was removed and fresh MSCCM was added. The hMSCs become visible within one week and within 2-3 weeks were ready for passaging. During this time, fresh MSCCM was added every 2-3 days. When the hMSCs were ca. 70-80% confluent, the cells were split into four new 10cm dishes or vented T75 flasks and labeled as passage 2 (P2). After 4-7 days, when the cells were 70-80% confluent; the cells were either frozen or passaged.

2.2.2. Cell culture

2.2.2.1. Creation of frozen working cell bank

A working cell bank of passage 4 (P4) hMSCs was created to supply experimental material for this research. P2 hMSCs were received from the Wolfson Institute in a vented 75cm^2 tissue flask containing MSCCM. This culture was about 50% confluent, so the spent medium was removed and 10mL of fresh MSCCM was added; then it was incubated at 37°C in a 5% CO_2 humidified incubator. The next day (day 6 in culture), the cells were passaged. The spent medium was removed and 10mL (0.13mL/cm^2) of DPBS was added to remove the residual proteins from the cell growth surface of the flask. The DPBS was discarded and 3mL of 0.25% trypsin/0.02% EDTA (Sigma) was added and rocked gently over the cell growth surface. The cells were allowed to detach and MSCCM was added after 6 minutes to quench the trypsin activity. A 0.5mL sample was removed for cell density determination (section 2.5.2) and then the remaining cell suspension was centrifuged at 160g for 5 minutes to remove the residual trypsin/EDTA. The supernatant was

discarded and the cell pellet was resuspended with 2mL of MSCCM. Then 1mL of cells was added to each of two new 150cm^2 tissue flasks (T150, Corning) containing 20mL of MSCCM; then the P3 cells were placed at 37°C in a 5% CO_2 humidified incubator.

The cells were refed with 20 mL MSCCM on day 2. On day 5 the cells were passaged. The spent medium was removed and 20mL of DPBS was added to rinse the flask. Then the DPBS was discarded and 6mL of trypsin/EDTA was added, the cells were allowed to detach and MSCCM was added after 5 minutes to quench the trypsin activity. A sample was removed for a cell count and then the cell suspension was centrifuged at 160g for 5 minutes. The supernatant was discarded and the cell pellet was resuspended with 9mL of MSCCM. Then 1mL of cells was added to each of nine new T150 flasks with 20mL of MSCCM; then the P4 cells were placed in at 37°C in a 5% CO_2 humidified incubator. The cells were refed with 20mL MSCCM on day 3 and then harvested on day 5. Seven flasks were used to make a P4 cell bank. The flasks were trypsinized identically to the previous passage and counted using a hemacytometer. After centrifuging the cells, the cell pellets were combined and resuspended in a total of 12.6mL in MSCCM. Then 3.2mL of freezing medium consisting of 75% fetal bovine serum (FBS, Biowhittaker) and 25% DMSO (Sigma) were added drop-wise to the cells such that the final cell concentration was 2.5x10^{6}cells/mL. The final concentrations in the freezing medium were 5% v/v DMSO and 15% v/v FBS. One mL aliquots of cell suspension were transferred into 16 cryo vials (Nalgene); and then the vials were placed into a styrofoam box in a -70°C freezer and allowed to freeze overnight. The next day the 16 vials were transferred to liquid nitrogen for long term storage at < -150°C.

Additional working banks of hMSCs were produced during this research project. The same procedures were used as described above. Some modifications included using a reduced centrifugation speed of 100g. A working bank of 17 vials of P8 cells was produced; and a bank of 25 vials of P7 cells was produced from frozen P4 cells from Steve Elliman, at the Wolfson Institute of Biomedical Research, University College London.

2.2.2.2. Cell passaging protocol in tissue flasks

Human MSCs derived from a UCL working cell bank were thawed and seeded ino 150 cm^2 tissue flasks (T150) and passaged every 3-5 days at a split ratio of 1:3 to 1:4 (1 flask into 3 or 4 new flasks). The cells were observed macro and microscopically for cell confluency (density), evidence of mitotic cells, pH/color of medium, amount of cell debris in medium, and other characteristics of the cells morphology.

During a typical tissue flask passage, the spent medium was removed from the flask using a pipet, samples were removed and frozen for analysis for glucose and lactate concentration using a YSI 2700 Select Biochemistry Analyzer (YSI (UK) Ltd, Analytical Technologies, Farnborough, UK; section 2.5.6). Then the flask's cell growth surface was rinsed with 20mL (0.13 mL/cm^2) of DPBS to remove residual FBS proteins that reduce trypsin activity. Next, 6mL (0.04 mL/cm^2) of 0.25% trypsin/0.02% EDTA was added to each flask and spread evenly over the growth surface. After 5-7 minutes, the hMSCs were detached from the growth surface by tapping the flask against the palm of the hand. After completely dislodging the cells, 12mL (0.08 mL/cm^2) of MSCCM was immediately added to quench remaining trypsin activity. The cells were not exposed to trypsin longer than 15 minutes since trypsin is a nonspecific protease which will eventually permeate the cell membrane. The cell suspension from all individual flasks was pooled together and a sample was taken to determine cell density by counting the cells using a hemacytometer (section 2.5.2). Viability was assessed using the trypan blue dye assay (section 2.5.3). To plant the next passage flasks, the cell suspension was transferred into 50mL centrifuge tubes and centrifuged at 100g for 5 minutes. The supernatant was discarded and the cell pellet was resuspended with 1mL of MSCCM for each T150 flask planted. The 1mL of the cell suspension was added to 20mL of fresh MSCCM medium into each new T150 flask. Samples of the diluted cell suspension were removed for determination of initial glucose and lactate concentration and frozen for later analysis. Finally, the flasks were incubated at 37°C in a 5% CO_2 humidified incubator. The hMSC cultures were also refed with fresh MSCCM after 2-3 days to prevent buildup of metabolic intermediates and waste products, and depletion of nutrients and growth factors in the medium.

The initial cell seeding density of the P4 frozen cells in tissue flasks was higher at P5 ($1.1+/-0.2x10^4$cells/cm^2) due to the concentration of the cells in the vial (ca. $2x10^6$cell/vial); however subsequent passages averaged a seeding density of $6.6+/-2.3x10^3$cells/cm^2. The remaining growth characteristics of the hMSCs are discussed in section 3.4.1.

2.2.2.3. Sterility of cultured hMSCs

During the project it was necessary to examine each component of the cell-matrix system to determine whether microorganisms/contaminants were being inadvertently introduced because cultures were maintained for several months. Most typical human (e.g. skin) and environmental microbes immediately overgrow the cultures and become visible either through a pH or turbidity change in the culture medium. However, low level or slow growing contaminants do not overwhelm the culture until several passages later, if ever. In addition, the growth medium is changed frequently in hMSCs cultures, every 2-4 days which also dilutes the microbes. Therefore, the spent medium was removed from ongoing cultures of hMSCs and placed into microwell plates to observe microscopically without the visual interference of cells on the surface of the plate. This allowed the presence of microbes to become visible microscopically at 400X magnification that would not be apparent in the regular cultures. As a negative control the MSCCM was also incubated with the spent medium. As a precautionary measure, the formulated MSCCM was also filtered through a 0.2μm cellulose acetate Nalgene filter flask to ensure sterility.

2.3. Preparation of matrix solutions

Initially matrix research focused on sodium alginate solutions based upon the widely established literature using alginate constructs in the cell therapy field (Constantinidis, 1999; Read, 1999; Mullen, 2000; Tobias, 2001) of which cells were of a secretory type (e.g. islet cells) or transformed producer-cell lines. These cells are capable of expansion in suspension cultures. Since this project was based upon attachment dependent cells (e.g. rSMCs and later hMSCs), work gradually progressed toward derivatization of alginate using the pentapeptide glycine-arginine-glycine-aspartic acid-tyrosine (GRGDY) based upon recent literature which showed improved cellular interaction with hydrogels that had been chemically modified to covalently attach cell adhesion molecules i.e. RGD-containing peptides (Rowley, 1999; Schmedlen, 2002; Chung, 2002). Concurrent to the preparation of derivatized alginate, some work was also performed using collagen matrices and combined collagen/alginate matrices using rSMCs to observe the effects of cross linking solutions. This section describes the preparation of sodium alginate, collagen and alginate-GRGDY matrices. The incorporation of cells within these matrices is described in section 2.4.

2.3.1. Sodium alginate matrix

Table 2 provides the list of sodium alginate manufacturers used in this research which included Fluka, ISP Alginates (Manugel), NovaMatrix (Pronova) and Sigma. The defining characteristics of the alginate such as the uronic acid content and molecular weight as measured by viscosity were provided by the manufacturer. Also included in the table are the studies in which the alginate was used. A variety of alginate types were selected to be evaluated due to the significant differences in hydrogel properties (e.g. porosity, strength) depending upon the monomeric composition, guluronic acid and mannuronic acid ratios and molecular weight (Martinsen, 1989 and 1992).

	Manufacturer and location	Uronic acid content	Molecular weight (viscosity)*	Cell studies in which used
Fluka (prod. 71238)	Fluka Chemie GmbH, Buchs, Switzerland	65-75% G	MW: 100-200 kg/mol; 1%: 100-200 mPa·s	rSMCs rSMCs+collagen hMSCs
Manugel© DMB (prod. 1131073)	ISP Alginates (UK) Ltd., Tadworth, UK and Koln, Germany	high G	'high' 1%: 200-400 mPa·s	rSMCs hMSCs MTT assays
Pronova™ MVG	Pronova Biomedical, Oslo, Norway (NovaMatrix)	73% G	MW: 231 kg/mol, 1%: 287 mPa·s	rSMCs
Pronova SLG 100 (prod. 28023206)	NovaMatrix FMC BioPolymer AS, Drammen, Norway	>60% G (67% G)	1%: >100 mPa·s (148 mPa·s)	rSMCs hMSCs MTT assays
Sigma (A-2033)	Sigma, St. Louis, Missouri	'primarily M'	'medium' 2%: 3500 mPa·s	rSMCs not derivatized
Sigma (A-2158)	Sigma, St. Louis, Missouri	'primarily M'	'low' 2%: 250 mPa·s	rSMCs
* Molecular weight/viscosity specifications provided from vendor literature or specific certificate of analysis (when available).				

Table 2. Types of sodium alginate investigated. Details were obtained from the manufacturer including the uronic acid content (G=guluronic acid, M=mannuronic acid), molecular weight as defined by apparent viscosity and the cell experiment(s) in which used.

To prepare a solution, the powdered alginate was weighed and added to water or saline solutions to concentrations ranging from 0.5-6% w/v alginate. Initially, cell culture grade water (BioWhittaker) was used to mix with the alginate. Then phosphate buffered saline (e.g. DPBS and PBS, BioWhittaker) and normal saline solution (n-saline, 0.9% w/v NaCl (Sigma) in cell culture grade water) were tested. The n-saline solution was adjusted to pH 7-7.4 using 0.1N NaOH using a 10-fold dilution of 1N NaOH (Sigma).

Since sodium alginate is water soluble, solutions with a concentration less than 2% w/v were homogeneous after mixing overnight on a platform roller (Roller Mixer

SRT2, Bibby Stuart Scientific, Stone, UK). Alternatively, the sodium alginate solutions were dissolved by autoclaving for ca. 22 minutes at 121°C (Omega Media, Prestige Medical, Blackburn, UK). Higher concentrations (2-6% w/v) had to be autoclaved to ensure a homogeneous mixture. This heat treatment not only served to completely dissolve the alginate, but also was intended to sterilize the solution.

An alternative method for sterilization of the alginate solution using filtration through a 0.22 or 0.1 micron membrane was also tried. Due to the high viscosity of the alginate solution, at least a 10-fold dilution of a 1% w/v alginate solution (to 0.1%) was required to effectively filter the solution. In addition, a slow flow rate (3mL/min) and large filtration surface area was required with a step-down series of filters ending in a sterilizing 0.22 or 0.1 micron membrane. Approximately 500mL of a 0.1% alginate solution (Manugel DMB, ISP Alginates) in water (pH 5.6) was filtered through a series of filters (CUNO Inc., Meriden, Connecticut) including a carbon zeta plus (catalog BC0030AR53SP, 27cm^2 disc capsule composed of cellulose fibers, activated charcoal and resin for binding), a zeta plus (BC0030A90SP, 27cm^2 disc capsule composed of cellulose fibers, diatomaceous earth and resin for binding), and then only ca. 250mL were filtered either through a 0.2μm filter (PSA020, 14cm^2 disc capsule with 0.65μm prefilter) or 0.1μm filter (PSA010, 14cm^2 disc capsule with 0.45μm prefilter). The filtrate was lyophilized and then reconstituted to 1/10th of its original volume to obtain 1% alginate.

The sterilization of the alginate by autoclaving for ca. 22 minutes at 121°C was one method used to sterilize the alginate prior to the discovery of thermophilic spores in the alginate which will be discussed in section 3.1.2. This problem led to the required sourcing of sterile alginate, Pronova SLG100 (NovaMatrix). Vials of sterile alginate were reconstituted as required with sterile filtered n-saline or buffer for derivatization of alginate-GRGDY as described in section 2.3.3.

2.3.1.1. Cross linking solution

Several formulations were examined for the cross linking solution. Calcium chloride (Sigma) was weighed and solutions between 0.1 to 2% w/v were prepared in distilled water, buffered saline (such as PBS and DPBS) and in n-saline to examine the best

solution for cross linking the alginate matrices. The pH of the $CaCl_2$ in n-saline solution was adjusted to 7-7.4 using 0.1N NaOH. All of the $CaCl_2$ formulations were sterile-filtered through a 0.22μm cellulose acetate membrane (Nalgene) or sterilized by autoclaving for ca. 22 minutes at 121°C. In addition, barium chloride (Riedel-de Haen AG, Seelze, Germany) was tested as a cross linking solution.

2.3.2. Collagen matrix

Rat SMCs are attachment dependent cells. In order to proliferate they need to physically attach to a binding site. Rat SMCs cultured in tissue flasks attach readily to the treated polystyrene surface; however, alginate has no attachment sites for cells. Collagen is the primary protein of tissue and is a component of the extracellular matrix that rSMCs naturally produce. Collagen has the role of organizing cells through association with other proteins. It also interacts directly with cell integrins (Hubbell, 2000); therefore, it should encourage cell attachment and/or proliferation. A series of experiments were conducted to characterize rSMC growth in a 3-D collagen matrix.

Rat tail collagen type 1 (First Link (UK) Ltd., Brierley Hill, UK; product no. 60-30-810) was supplied in a 0.6% acetic acid solution. The collagen was set by increasing the pH to ca. 7 using 1N NaOH. Therefore collagen scaffolds were fabricated without the requirement of a cross linking solution that alginate required. It was not known prior to these studies if the alginate or the high molar concentration of cross linking solution was detrimental to cell viability and proliferation. The collagen matrix was prepared by combining 400μL of collagen with 50μL of 10X Eagles Minimum Essential Medium (10X EMEM, BioWhittaker). The concentrated 10X EMEM was required to provide a suitable physiological environment for the cells and to indicate the pH of the collagen matrix (from the phenol red component). Due to the presence of phenol red in the 10X EMEM, the collagen matrix turned from yellow (acidic) to bright pink (alkaline) upon increasing the pH using NaOH. In order to determine the amount of base required to set the collagen, aliquots of 1N NaOH were placed into microwells ranging from 37.5μL to 50μL per well. Then 450μL of the collagen and EMEM were added to each well and mixed thoroughly. Cells were added as per section 2.4.2.2. In addition, alginate was added to the collagen matrix to determine

the effects of cross linking solution on cell viability and proliferation as described in section 2.4.2.3.

2.3.3. Derivatized alginate-GRGDY

Alginate hydrogels do not permit cell adhesion due to their hydrophilic properties. Mooney's lab at University of Michigan successfully incorporated the pentapeptide, GRGDY, onto the alginate polysaccharide backbone and reported improved cell attachment and proliferation for myoblasts, precursors to skeletal muscle cells (Rowley, 1999). In this research, sodium alginate was chemically modified in a similar manner using carbodiimide chemistry to incorporate GRGDY peptides that will be referred to in this thesis as alginate-GRGDY. A schematic is provided in Figure 4 of the methods used to prepare alginate-GRGDY during the course of this research. Three generalized processes (initial, intermediate and sterile) were used as research progressed. Detailed descriptions of each of these methods follow the figure.

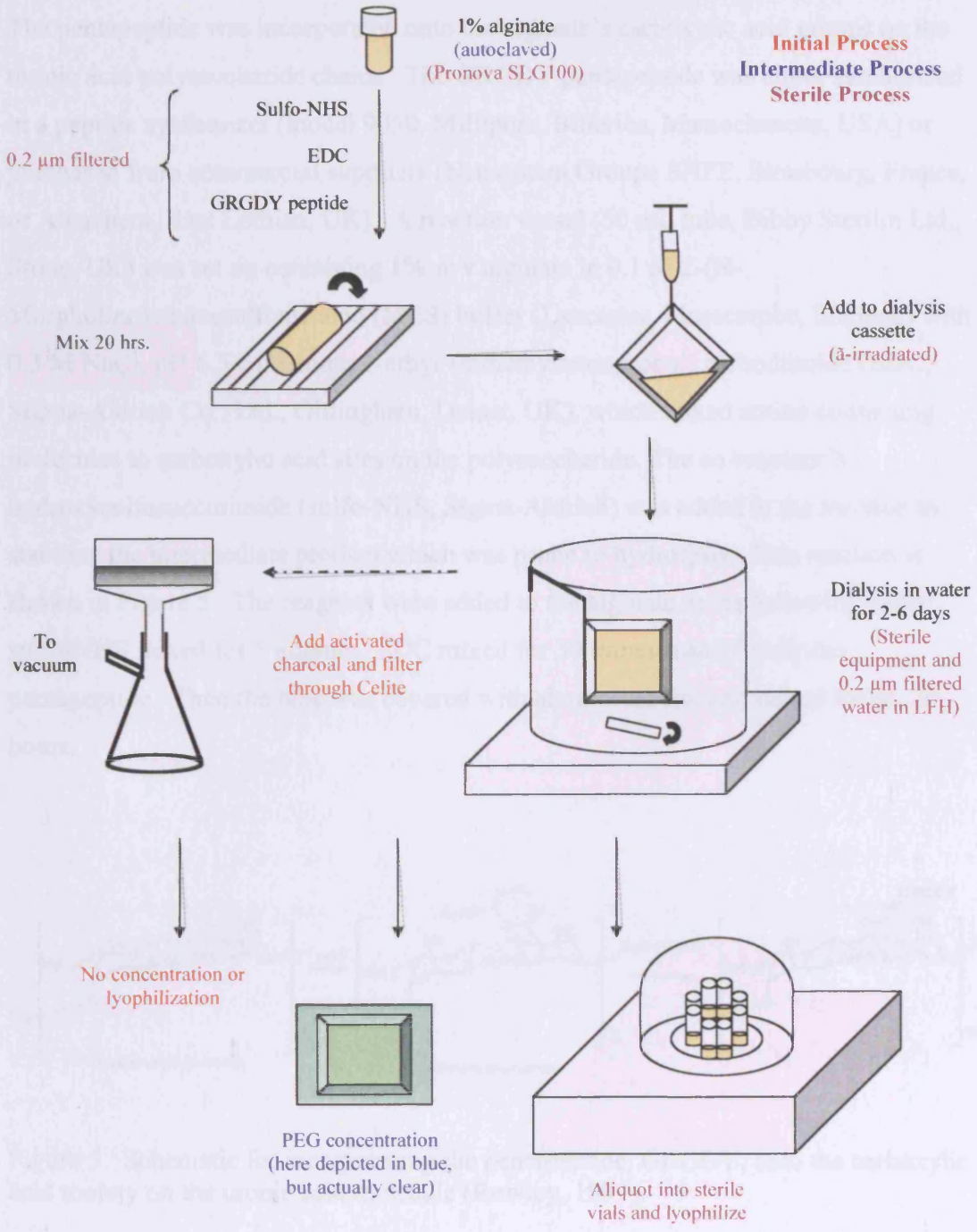

Figure 4. Schematic of alginate-GRGDY derivatization methods. Three generalized processes were utilized: initial, intermediate and sterile. Steps specific to the initial process in red text, intermediate process in blue text and sterile process in purple text.

The pentapeptide was incorporated onto the alginate's carboxylic acid groups on the uronic acid polysaccharide chains. The GRGDY pentapeptide was either synthesized in a peptide synthesizer (model 9050, Millipore, Billerica, Massachusetts, USA) or purchased from commercial suppliers (Neosystem Groupe SNPE, Strasbourg, France; or Albachem, East Lothian, UK). A reaction vessel (50 mL tube, Bibby Sterilin Ltd., Stone, UK) was set up containing 1% w/v alginate in 0.1 M 2-(N-Morpholino)ethanesulfonic acid (MES) buffer (Lancaster, Morecombe, England) with 0.3 M NaCl, pH 6.5 containing 1-ethyl-(dimethylaminpropyl) carbodiimide (EDC, Sigma-Aldrich Co., Ltd., Gillingham, Dorset, UK), which linked amino containing molecules to carboxylic acid sites on the polysaccharide. The co-reactant N-hydroxysulfosuccinimide (sulfo-NHS, Sigma-Aldrich) was added to the reaction to stabilize the intermediate product which was prone to hydrolysis. This reaction is shown in Figure 5. The reagents were added to the alginate in the following order: sulfo-NHS mixed for 5 minutes, EDC mixed for 30 minutes and finally the pentapeptide. Then the tube was covered with aluminium foil and mixed for ca. 20 hours.

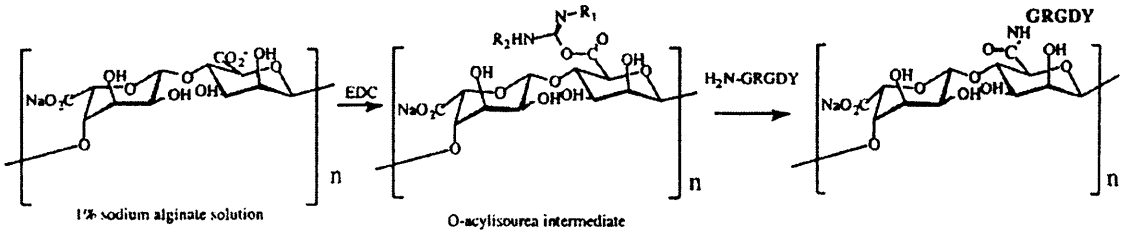

Figure 5. Schematic for incorporating the pentapeptide, GRGDY, onto the carboxylic acid moiety on the uronic acid molecule (Rowley, 1999).

All mixing steps occurred on a platform roller (Roller Mixer SRT2, Bibby Stuart Scientific, Stone, UK) at room temperature (ca. 20-26°C) during which it was protected from light by wrapping in foil.

2.3.3.1. Alginate treatment prior to reaction

For the 'initial process', the 1% w/v alginate was reconstituted with the MES/NaCl buffer, mixed overnight, then the sulfo-NHS, EDC and peptide reactants were added as previously described. During the 'intermediate process', the alginate in MES/NaCl buffer was autoclaved at 121°C for ca. 22 minutes in order to sterilize the contents prior to the reaction. This step reduced the molecular weight of the alginate since the high temperature tended to cleave the covalent C-O bonds (Leo, 1990; Vandenbossche and Remon, 1993; Wong, M. 2001). The 'sterile process' used only Pronova SLG100 alginate which was supplied as a sterile product. This alginate was reconstituted with sterile filtered MES/ NaCl buffer and mixed until visibly homogeneous; then the sterile filtered reactants were added as described in the next section.

2.3.3.2. Concentration of reactants

Rowley (1999) determined the concentration of reactants based upon the efficiency of peptide incorporation onto the uronic acid units of the alginate, which they estimated for 1mg of alginate to be 38μg of sulfo-NHS, 67μg of EDC and 1μg of peptide. Unfortunately, Rowley did not provide the number of uronic acid units per mg of their alginate; and they used a radioactive label to measure the amount of peptide incorporated into the alginate, which was not feasible to implement for this project. In addition, alginate manufacturers do not report the number of uronic acid units per mg of alginate which would be expected to be different according to the type of alginate and the processes used to manufacture and purify the alginate. Therefore, range finding experiments were necessary for this research to determine the concentration of reactants needed for this system.

The 'initial method' for alginate-GRGDY derivatization utilized large increments (e.g. 1X, 10X and 50X) for Rowley's reactant concentrations, where 1X was 1mg of alginate containing 38μg of sulfo-NHS, 67μg of EDC and 1μg of peptide; 10X was ten times the reactants for 1mg of alginate or 380μg of sulfo-NHS, 670μg of EDC and 10μg of peptide; and 50X was fifty times the reactants for 1mg of alginate or 1.9mg of sulfo-NHS, 3.35mg of EDC and 50μg of peptide. Since the viscosity of the alginate used in the 'intermediate method' was reduced due to autoclaving, lower concentrations of reactants were used for range finding (e.g. 1X, 3X, 9X and 27X).

Likewise the 'sterile method' utilized low viscosity, highly purified alginate such that the reactant concentrations tested were similar (e.g. 1X, 3X, 6X, 9X, 12X and 27X).

For range finding experiments, each reactant (sulfo-NHS, EDC and peptide) was weighed and dissolved in a small volume (ca. 0.5-1.0mL) of WFI (Biowhittaker). Then the desired concentration of reactant was added to the 1% w/v alginate (typical alginate volumes were 3-12mL) in the 50mL reaction vessel as described previously. The reactants for the 'sterile process' were filtered through 13mm syringe filters (0.2μm pore size) prior to addition to the reaction vessel. A low binding PVDF membrane (Durapore, Millex®-GV, Millipore Corp., Bedford, Massachusetts, USA) was used for the peptide and a PTFE membrane (Millex®-LG, Millipore) was used for the sulfo-NHS and EDC.

2.3.3.3. Dialysis

After the 20 hour reaction, the alginate-GRGDY was dialyzed for 2-6 days using dialysis cassettes (Slide-A-Lyzer®, Pierce, Rockford, Illinois) with a molecular weight cutoff (MWCO) of 3.5 or 10 kDaltons. The alginate was carefully injected into the pre-wetted dialysis cassettes using a 20mL leur-lock syringe with a 21 gauge needle (Becton Dickinson UK Ltd., Cowley, UK). Dialysis occurred in 5 liter beakers (Azlon, Bibby Sterilin Ltd., Stone, UK) with slow mixing (ca. 80-120 rpm) in a cold room (ca. 8-12°C) using ca. 4-5 liters of purified, autoclaved water that was changed twice per day at approximately 12 hour intervals. The beakers were covered with aluminum foil and lighting was kept to a minimum. For the 'sterile process', all aseptic operations were conducted inside a laminar floor hood (LFH) using sterilized equipment. Gamma-irradiated dialysis cassettes (Pierce) were used and the water for dialysis was filtered through a 0.2μm filter (Acropak 500 capsule, Pall, Ann Arbor, Michigan) immediately prior to use every 12 hours. Due to processing inside the LFH, the temperature during dialysis was considerably warmer (ca. 26-31°C).

2.3.3.4. Post-dialysis treatment

After dialysis for the 'initial process' only, the alginate-GRGDY was mixed with 0.5 g of activated charcoal (Sigma, C-9157) per gram of alginate to remove impurities on a platform roller for 5-30 minutes. Then the alginate/charcoal mixture was filtered

through a vacuum flask containing Celite® diatomaceous earth (Celite Corp, Lompoc, California) to remove the charcoal.

2.3.3.5. Concentration of alginate

During dialysis the alginate-GRGDY volume increased due to the influx of water into the dialysis cassette. Due to the increased water content, the resulting alginate concentration was much lower than the desired concentration of 1% to allow addition of the cell suspension. One solution to this problem was that the cells were resuspended in a very small volume of culture medium (e.g. 100μL) and then added to the alginate-GRGDY in order to make into hydrogels. This allowed the alginate-GRGDY to be used without having to lyophilize or concentrate. However the resulting hydrogels still had low strength and amorphous shape.

During the 'initial process' the alginate-GRGDY was snap frozen in liquid nitrogen in a glass flask and then lyophilized by attaching to a freeze drier chamber (Edwards Freeze Dryer Modulyo, Edwards High Vacuum, Crawley, UK) in order to increase the concentration of the alginate. However this technique was associated with decreased biological activity that was characterized by decreased cell binding or the cells' capacity to elongate. In addition, the biological activity seemed to decrease over storage in the liquid form.

During the 'intermediate method', polyethylene glycol (PEG) was used to concentrate the alginate-GRGDY after dialysis while it was still inside the dialysis cassette. Initially, solid PEG crystals were tried 8k MW (Sigma, P-2139) for 3.5kDa MWCO dialysis cassettes and 35k MW (Fluka Chemie, no. 94646) for 10kDa MWCO cassettes. The PEG absorbed water through the dialysis membrane over about 2-12 hours. During this concentration step, the weight of the alginate and dialysis cassette was monitored to target a final 1% alginate concentration at the completion of the step. Sterile Slide-A-Lyzer® concentrating solution (Pierce, identity of which was proprietary) was also used to concentrate the alginate in the dialysis cassette. Although supplied sterile, it was still difficult to use because it required excessive handling and non-aseptic manipulations as weighing was still required to target the final alginate concentration.

Due to the cumbersome PEG concentration step, lyophilization was revisited during preparation of the 'sterile process' as the method to concentrate the alginate-GRGDY. It had a great advantage for sterile processing due to decreased aseptic manipulations; however, the process was longer (2 days) and was previously associated with loss in biological activity. After dialysis the alginate-GRGDY was carefully removed from the swollen dialysis cassette using a 50 mL Luer-Lok syringe with a 21 gauge needle (Becton Dickinson). Air was injected into the cassette as the alginate was removed to prevent damage to the membrane. The alginate-GRGDY was subdivided into 75x25mm sterilized soda glass vials (Samco, LIG Supplies Ltd., March, UK). The vials were loaded onto a tube rack, loosely covered with sterilized aluminium foil, and then plunged into liquid nitrogen for 10 minutes. The rack was only submerged 1/3 of the way up the vial so nitrogen did not enter the vials. After the alginate was completely frozen, the rack and vials were placed onto the shelf of the pre-cooled (-60°C) freeze drier chamber (Edwards Freeze Dryer Modulyo), the foil was removed, and the cover containing a thin film of vacuum sealant (Dow Corning high vacuum grease, Dow Corning Corp, Midland, Michigan, USA) was placed over the chamber. The vacuum pump for the chamber was immediately turned on to prevent a temperature transition in the vials above -60°C. The alginate-GRGDY was allowed to freeze dry for ca. 2 days. The initial vacuum was ca. 0.2-0.4mbar, and after two days the vacuum pressure decreased to 0.6-0.8mbar which indicated the contents were dry. The alginate plug also appeared to be dry and slightly pulled away from the sides of the vial. The vacuum was shut off and the chamber was slowly vented through a 0.2μm PTFE filter (Midisart®2000, Sartorious AG, Goettingen, Germany). The cover of the chamber was removed and the vials were covered with sterilized foil and transferred to the LFH where they were covered with sterilized caps.

2.3.3.6. Alginate storage conditions

Liquid alginate-GRGDY or reconstituted alginate was stored in a refrigerator at ca. 6-12°C. The lyophilized alginate-GRGDY was stored in a freezer at ca. -10 to -15°C.

2.3.3.7. Sterility testing

During the 'initial' and 'intermediate' process, the alginate-GRGDY was produced using methods that were not designed to produce microbe-free product; for example, the charcoal adsorption and Celite filtration steps were not sterile steps. However, effort was made to progress to a process that would be free of microbial contamination when tested. During the 'sterile process', the alginate and all of the reactants were tested for sterility at each stage of the process so that every component and every process step could be tested to see if contamination was introduced. The samples tested included: MES/NaCl buffer, reconstituted Pronova SLG100 alginate in MES/NaCl buffer, filtered sulfo-NHS, filtered EDC and filtered peptide. Then the alginate-GRGDY was tested after the 20 hour reaction, after completion of dialysis and after lyophilization (post-reconstitution with n-saline). A sample aliquot (ca. 50-100μl) was added to 1mL of terrific broth (Sigma, T-0918) in a microplate (24 well) which was placed in a humidified incubator at 37°C. For each test, a control well of 1mL terrific broth was always included as a negative control. Terrific broth was made by combining 47.6g of powdered terrific broth with 8mL of glycerol (Sigma, G-5150) in 1 liter of water. After the solution was thoroughly mixed, the terrific broth was aliquoted into 100mL aliquots in glass bottles (Schott bottle, Fisher Scientific, Loughborough, UK) and autoclaved with loose caps at 121°C for 22 minutes. After removal from the autoclave, the caps were tightened and the terrific broth was stored at room temperature. The sterility samples were observed under a microscope for presence of microbes. Because the terrific broth contained lint/particulates, it was also filtered through a 33mm Millex®-GV syringe filter (0.2μm pore size) to clear particulates out of the samples for improved clarity of microscopic observation. The samples were observed microscopically every 2-4 days for at least 9-14 days.

2.4. General methods of cell-matrix construction

The creation of the cell-matrix three dimensional complexes are described in this section. For ease of explanation, general methods are provided. In preparation of the constructs, sodium alginate (various suppliers), derivatized alginate-GRGDY (various reactant levels) or collagen was used. The cells (rSMCs or hMSCs) were prepared for mixing with the matrix solution as described in section 2.4.1. The presence of cells, or even cell type, did not affect the basic methods of formation of the construct unless specifically noted. Three types of cell-matrix constructs were made during this research including sheets, tubes and beads. Figure 6 shows a schematic of these processes. The method of formation of each individual construct is described in each of the following sections: sheets (section 2.4.2), tubes (section 2.4.3) and beads (section 2.4.4). Specific experiments are also described which were used to evaluate hydrogel tubes by cutting into discs (section 2.4.3.1), to evaluate the effect of matrix components and cross linking solution (section 2.4.3.2) and to evaluate hydrogel tubes *in situ* (section 2.4.3.3).

2.4.1. Preparation of cells for mixing with matrix solution

Cells (either rSMCs or hMSCs) were harvested from tissue flask cultures using the same trypsinization protocol as used for cell passaging. After the trypsinized cell suspension was pooled together, a sample was removed for cell density determination using a hemacytometer. Then the cells were centrifuged in 50mL centrifuge tubes at 100-160g for 5-10 minutes. The supernatant was removed and discarded, and the cell pellet was resuspended using the selected culture medium (e.g. complete DMEM or MSCCM) to the desired concentration. The residual trypsin/EDTA present in the trypsinized cell suspension needed to be removed from the cell suspension because EDTA chelates divalent ions such as calcium, so it would dissolve the alginate hydrogel if it was added as part of the cell suspension. In cases of very small working volumes (e.g. 100-500μL) and/or high cell concentrations (>10^7cells/ml), the cells were often centrifuged twice to allow an intermediate resuspension of the cells in a larger volume (e.g. 5-7mL) of culture medium prior to being resuspended in a small volume and mixed homogeneously into the matrix solution. This was performed to further dilute the trypsin/EDTA residuals because the cell pellet comprised of the majority of the resuspended volume.

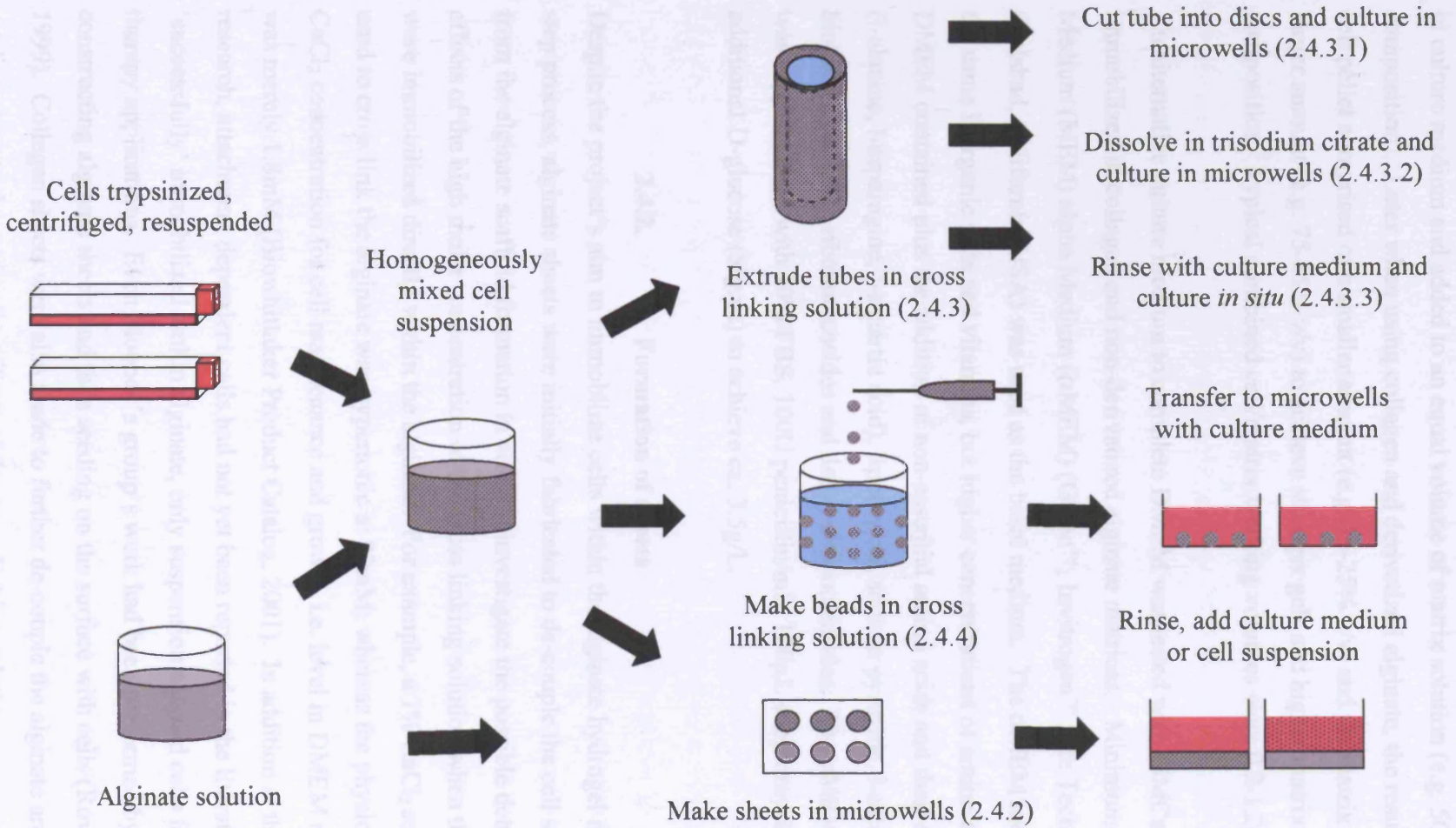

Figure 6. Schematic of cell-matrix construction. Cells were combined with alginate and formed into tubes, beads or sheets. The methods are described in each section (designated in parentheses). Color coding includes red (culture medium), grey (alginate), black dots (cells) and light blue (cross linking solution).

Initially when working with non-derivatized alginate, the cell pellet was resuspended in culture medium and added to an equal volume of matrix solution (e.g. 50% v/v composition). Later when using collagen and derivatized alginate, the resuspended cell pellet comprised of a smaller amount (e.g. 15-25% v/v) and the matrix solution a larger amount (e.g. 75-85% v/v) to achieve stronger gels and higher matrix composition. Typical combined cell/matrix working volumes were 0.2-1.2mL.

An alternative culture medium to complete DMEM was tested with rSMCs immobilized in collagen and non-derivatized alginate matrices. Minimum Essential Medium (MEM) alpha Medium (αMEM) (Gibco™, Invitrogen™ Life Technologies, Carlsbad, California, USA) was used as the basal medium. The αMEM medium had the same inorganic salts and vitamins, but higher concentrations of amino acids than DMEM contained plus the addition of non-essential amino acids and their derivatives (l-alanine, l-asparagine, l-aspartic acid), lipoic acid, sodium pyruvate, l-ascorbic acid, biotin, vitamin B_{12}, ribonucleosides and deoxyribonucleosides. The αMEM medium was supplemented with 10% FBS, 100U penicillin/mL, 100μL streptomycin/mL and additional D-glucose (Sigma) to achieve ca. 3.5g/L.

2.4.2. Formation of sheets

Despite the project's aim to immobilize cells within the alginate hydrogel in a one-step process, alginate sheets were initially fabricated to de-couple the cell seeding step from the alginate scaffold formation in order to investigate the possible detrimental effects of the high molar concentration of the cross linking solution when the cells were immobilized directly within the alginate. For example, a 1% $CaCl_2$ solution used to cross link the alginate was hypertonic at 90mM; whereas the physiological $CaCl_2$ concentration for cell maintenance and growth, i.e. level in DMEM medium, was merely 1.8mM (Biowhittaker Product Catalog, 2001). In addition at the start of research, attachment dependent cells had not yet been reported in the literature as 'successfully' immobilized within alginate, only suspension adapted cells for cell therapy applications. Even Mooney's group's work had been performed by constructing alginate sheets and then seeding on the surface with cells (Rowley, 1999). Collagen sheets were also made to further de-couple the alginate and cell seeding steps to determine the effects of the cross linking solution.

2.4.2.1. Alginate sheets

Alginate sheets were fabricated by spraying a fine mist of 40-50% w/v $CaCl_2$ solution onto 22mm diameter glass coverslips (BDH, VWR International Ltd., Poole, UK). The glass coverslips were first heated through an aluminum heat block using a propane blow torch. Then the coverslips were sprayed with a fine mist of $CaCl_2$ solution which immediately evaporated the solution into a powder on the surface of the coverslip. The coated coverslips were immediately placed inside a 12 well ($3.8cm^2$) microplate (Costar, Corning Life Sciences, Corning, New York); then 0.4-0.6mL of alginate solution (usually derivatized with GRGDY peptide) was added to each well. The calcium ions diffused into the alginate and formed a hydrogel sheet. After washing the hydrogel sheet extensively with sterile WFI (to reduce residual $CaCl_2$), culture medium (either complete DMEM or MSCCM) was added as a final rinse. The cell suspension (either rSMCs or hMSCs) was prepared by trypsinizing flasks, then centrifuging and resuspending the cells in culture medium to remove residual trypsin and EDTA present in the trypsinized cell suspension. Then the cell suspension was seeded into the microwells at $1.2x10^5$ to $3x10^5$cells/well ($3x10^4$ to $8x10^4$cells/cm^2) containing the alginate hydrogels with 2mL of medium/well (0.5 mL/cm^2). Then the plate was placed at 37°C in a humidified incubator containing 5-10%CO_2 depending upon the culture media selection. The cells were observed microscopically over several days to see if the cells attached and elongated on the surface of the hydrogel. Experiments were also performed where cells were mixed directly within the alginate as described in section 2.4.1. In this case, after formation of the sheet the cell/alginate hydrogels were rinsed with culture medium (either complete DMEM or MSCCM) instead of WFI to maintain balanced physiological conditions (osmolarity/pH) for the cells.

2.4.2.2. Collagen sheets

Several formulations of rat tail collagen were prepared by adding 10X EMEM and graduated amounts (37.5-50μL) of 1N NaOH to the collagen as per methods described in section 2.3.2. Each formulation was made in the well of a microplate (24 well, Corning). Rat SMCs were trypsinized, centrifuged and resuspended by gentle pipetting in complete αMEM medium. Then 50μL aliquots of rSMCs were added to each well. The cells were mixed throughout the collagen matrix in each microwell and then the collagen was allowed to set at 37°C for 10 minutes. Then 1mL of complete αMEM medium was added to each well. All of the microwells were incubated at 37°C/10% CO_2. The final concentrations in the matrices were: 73-74% v/v rat-tail collagen type 1(final concentration ca.1.6mg/mL), 9% v/v 10X EMEM, 7-9% v/v 1N NaOH, and 9% v/v rSMCs resuspended in complete αMEM medium.

In this experiment the αMEM medium was supplemented with 10% FBS, 60U penicillin/mL, 60μL streptomycin/mL (all obtained from Biowhittaker) and additional glucose to a final concentration of 3.3g/L. The final SMC concentration in the collagen matrix was $1x10^6$cells/mL with 0.5 mL in each microwell or $5x10^5$cells/well.

Control cells were seeded directly into microwells (24 well, 1.9cm^2) with no matrix at $9.6x10^3$cells/well ($5x10^3$cells/cm^2). The amount of complete αMEM medium used in each microwell was 1mL (0.5mL/cm^2).

At each time interval, the matrix was observed macroscopically to determine the extent of matrix shrinkage, and microscopically to determine if the cells were associated with the matrix. The spent medium was removed from one well and measured to determine losses due to evaporation. At the conclusion of the experiment, the glucose concentration in the spent medium was determined using the YSI bioanalyzer.

2.4.2.3. Collagen and alginate sheets

Once cell growth was observed in the collagen matrix, the next step was to examine the effect of cell proliferation in collagen and alginate matrices when cross linking solutions were introduced. A scaffold containing both collagen (1.25 mg/mL) and 1% alginate was constructed and different cross linking solutions ($CaCl_2$ or $BaCl_2$) at concentrations between 0.1 to 1% were tested. 1% cross linking solutions were prepared by combining 0.5g of $CaCl_2$ or $BaCl_2$ with 50mL of n-saline solution. Then 0.5% and 0.1% solutions were prepared by combining 10mL of 1% solution with 10mL of n-saline, and 2mL of 1% solution with 18mL of n-saline, respectively. The pH of the solutions was adjusted between 7.0 to 7.4 using 0.1N NaOH. The final molar concentrations were calculated as 48, 24 and 4.8mM $BaCl_2$ and 90, 45 and 9mM $CaCl_2$ for the 1.0, 0.5 and 0.1% solutions respectively. In addition, both complete medium and n-saline solution were used as control conditions to the cross linking solutions. These media contain 1.6mM and 0mM $CaCl_2$, respectively.

The collagen/alginate matrix was prepared by combining in sequential order: 58% v/v rat-tail collagen (final concentration 1.25mg/mL), 7.2% v/v 10X EMEM, 24.2% v/v of 4% alginate (final concentration 1%), 6.4% v/v 1N NaOH, and 4.2% v/v SMCs resuspended in complete medium. Rat SMCs were trypsinized, centrifuged, resuspended with complete DMEM medium according to section 2.4.1, and added to this homogeneous mixture. Then 0.3mL of cells/matrix solution was aliquoted into each microwell. The final rSMC concentration in the matrix was $4.2x10^5$cell/mL with 0.3mL aliquoted into each microwell or $1.26x10^5$cells/well.

The collagen in each microwell was allowed to set at 37°C for 10 minutes then 1mL of cross linking solution (0 to 1%) was added to each individual microwell for ca. 10 minutes. After the cross linking solution was carefully removed, 1mL of complete medium was added for ca. 10 minutes, removed and replaced with 1mL of complete medium. Control matrices were set up using the identical conditions using n-saline or complete DMEM medium instead of the cross linking solution. In addition, control cells with no matrix were seeded directly into microwells at $1.26x10^5$cells/well ($6.63x10^4$cells/cm^2). Collagen/alginate matrices with no cells were also set up to measure the decrease in glucose due to degradation at 37°C. All of the microwells

were incubated at 37°C/10% CO_2 and removed after 1, 3, 5, 7, 10 and 13 days. The matrix was observed macroscopically to determine the extent of matrix shrinkage and microscopically to determine if the cells elongated within the matrix. At each time interval, the spent medium was removed from one well and measured to determine losses due to evaporation. At the conclusion of the experiment, the glucose concentrations in the spent medium were determined using the YSI bioanalyzer.

2.4.3. Extrusion of alginate tubes

Alginate tubes were fabricated using a single step extrusion/cell immobilization process which allowed rapid formation of a tube under 'cell-friendly' process conditions thereby eliminating the traditional two step tube formation and cell seeding process that were required for many synthetic polymers such as PTFE, PGA or PLGA.

The extrusion method was developed by Mason and Town (2002) and was a type of reverse coating by which a hydrogel tube was formed on the inside surface of a glass tube. As shown in Figure 7, the device consisted of a dual injection chamber – one for the cell and alginate mixture and one for the $CaCl_2$ solution. First, the cells were trypsinized and centrifuged according to section 2.4.1. The cell pellet was resuspended to the desired cell concentration and combined with the alginate solution, mixed and injected into the bottom of a hollow glass tube using a 1mL syringe (Becton Dickinson). The cell/alginate mixture (ca. 0.3-0.4mL – minus volume held up in the syringe and device port) filled the space surrounding a small float that was positioned inside the glass tube directly above the inlet port in which 0.5 - 2% $CaCl_2$ solution was injected. Then as the $CaCl_2$ was rapidly injected (100mL/min) into the tube device using a 50mL glass syringe (Samco) and syringe driver (Harvard Apparatus PHD2000, Holliston, Massachusetts, USA), the displacement of the $CaCl_2$ fluid propelled the float upward through the alginate, leaving a thin coating of alginate and cells (100-200μm) on the inner surface of the glass tube which immediately cross linked the alginate molecules forming a hydrogel tube of alginate and cells. A time lapse schematic of the tube formation is shown in Figure 8.

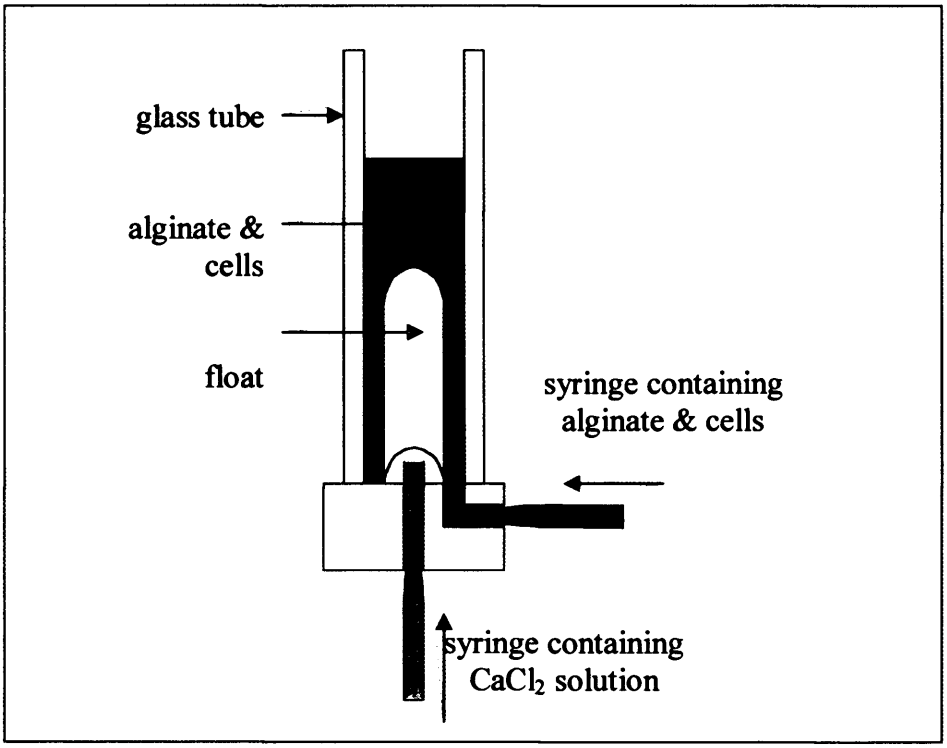

Figure 7. Hydrogel tube extrusion device. The alginate and cell mixture (grey) was injected into the hollow glass tube through the side port and $CaCl_2$ (light purple) was used to propel the float upward through the center port using a syringe driver (Mason, 2005).

After cross linking was completed (ca. 5-15 minutes), culture medium was injected into the tube to reduce the residual $CaCl_2$ concentration. The cell/alginate tube was either matured within the glass tube in a 37°C incubator containing 5-10% CO_2 as described in section 2.4.3.3 or the cell/alginate tube was dissolved using trisodium citrate for further analysis as described in section 2.4.3.2. The tubes fabricated using this technique were approximately 4mm in diameter, 100-200μm in wall thickness and typically 6-12cm in length. The tube wall thickness was varied by changing the size (diameter) of the float from 3.6-3.8mm. Smaller diameter floats produced thicker wall tubes. In addition the shape of the float was changed from bullet-shaped to spherical which provided better stability of movement as the cross linking solution was injected.

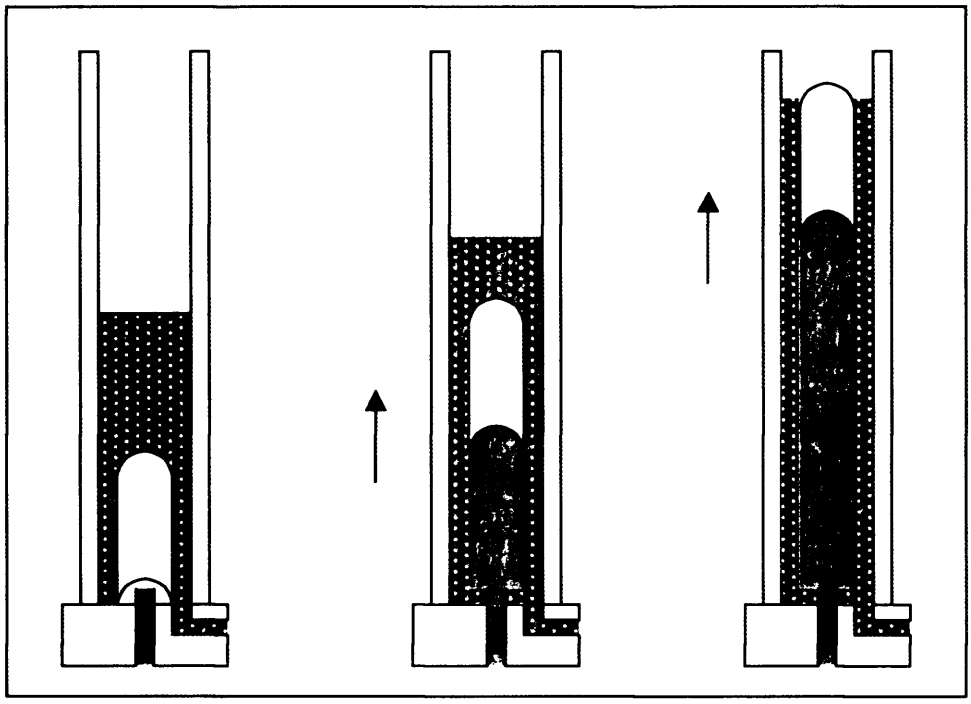

Figure 8. Time lapse of hydrogel tube formation. Alginate and cells (grey) coated the wall of the glass tube as the $CaCl_2$ solution (light purple) filled the space cleared by the float as the solution was driven upward into the glass tube through the center port (Mason, 2005).

Originally an alternative technique (pneumatic, piston driven tube-forming device) was used to fabricate 9mm diameter x 14cm length tubes during initial alginate experiments (Mason, 2005). Alginate and cells were filled into the top of the glass tube above a PTFE piston on a threaded rod. As the rod was pulled downward using a pneumatic drive, the PTFE piston was lowered causing the viscous cell/alginate mixture to leave a thin coating on the wall of the glass tube. The resulting cavity above the PTFE piston and cell/alginate mixture was simultaneously filled with a $CaCl_2$ solution at the top of the glass tube. (Diagram not shown.) These cell/alginate tubes were carefully removed and cut into disc sections for further analysis as described in section 2.4.3.1. This downward pneumatic, piston driven tube extrusion device was replaced by the upward syringe driven tube extrusion device shown in Figures 7 and 8 to make 4mm diameter tubes.

2.4.3.1. Evaluation of alginate discs

Cultures of rSMCs were trypsinized, centrifuged at 100g for 10 minutes, resuspended in n-saline and homogeneously mixed into non-derivatized alginate (3% Fluka) in n-saline to a final concentration of 2.7% alginate and $1x10^6$ viable cells/mL. A tube

(9mm diameter x 14cm length x 0.25mm wall thickness) was extruded by the reverse coating technique using a glass tube and pneumatic piston device described in section 2.4.3. 0.5% $CaCl_2$ in water was used to cross link the alginate molecules to form a hydrogel. The cell/alginate tube was removed from the glass tube and placed into a petri dish containing complete DMEM to dilute residual $CaCl_2$. Then using a device similar to a cookie cutter, 7mm diameter discs were stamped through both sides of the tube as it lay flat in the dish. The individual discs were cultured in 24 well ($1.9cm^2$) microwell plates (Costar, Corning Life Sciences, Corning, New York) with 1mL of complete DMEM. This process was detailed in Figure 6, section 2.4.1. The number of cells in a 7mm diameter alginate disc was estimated to be ca. $9.6x10^3$ given the cell concentration of $1x10^6$cells/mL and the volume of a disc ($\Pi r^2 h$), where h was estimated to be 0.25mm (tube wall thickness) and mm^3 was converted to mL by multiplying by 0.001 the standard units conversion. Control cells were also cultured in T25 flasks ($25cm^2$) at $9.6x10^3$cells/flask ($4x10^2$cells/cm^2) and in microwell plates ($1.9cm^2$) at $9.6x10^3$cells/well ($5x10^3$cells/cm^2). The amount of complete DMEM used in each microwell was 1mL and 5mL in the T25 flask, which were 0.5mL/cm^2 and 0.2mL/cm^2 respectively. Cells were incubated in a 37°C humidified incubator containing 10% CO_2 / 90% air.

Control cells in the T25 flasks were trypsinized daily. Cells in alginate discs were released from alginate hydrogel by addition of 0.1M trisodium citrate solution (section 2.5.5). In all cases, total cell density was determined using a hemacytometer (section 2.5.2). Viability was assessed using trypan blue dye exclusion assay (section 2.5.3). Spent medium samples were removed from all culture vessels and analyzed for glucose using the YSI bioanalyzer (section 2.5.6). The results from this experiment are described in section 3.3.2.2.

2.4.3.2. Evaluation of matrix components and cross linking solution

An experiment was conduction in which rSMCs were mixed with non-derivatized alginate, extruded into 4mm tubes and cross linked using $CaCl_2$ solution. After rinsing the tubes with complete DMEM or n-saline, the rSMCs were released from the alginate hydrogel using trisodium citrate solution. Then the cells were seeded into

microwells and monitored for glucose consumption. This approach was used to determine any significant detrimental effect of scaffold components (e.g. cross linking solution) or process steps. In addition control cultures of rSMCs were prepared which examined the elimination of each component/step from the tube fabrication.

In detail, rSMCs were trypsinized, centrifuged, resuspended in complete DMEM as described in section 2.4.1. Equal volumes of resuspended cells and non-derivatized alginate (2% Fluka, in n-saline, pH7.2) were mixed at a concentration of $2x10^6$cells/mL. Four tubes (4 mm in diameter, 100-200μm in wall thickness and 12cm in length) were extruded within glass tubes and cross linked in 1% $CaCl_2$ in n-saline, pH 7.2, for 15 minutes. After exposure to $CaCl_2$, the tubes were rinsed with either complete DMEM (1.5, 12.5 or 125mL) or n-saline (1.5mL) to reduce residual $CaCl_2$. These volumes were delivered over a 1, 2 and 15 minute time period for the 1.5, 12.5 and 125mL volumes respectively using a syringe driver. Rinse volumes greater than 1.5mL were not possible using n-saline because the alginate tubes completely dissolved. After rinsing, 0.1M trisodium citrate solution was added to the glass tube to dissolve the alginate tubes. After the tube was visibly dissolved, a cell count and viability assessment using trypan blue dye exclusion was performed on the resulting cell suspensions. The cells were then mixed in complete DMEM and seeded at 1mL/well into microwells and incubated in a 37°C humidified incubator containing 10% CO_2 / 90% air.

Likewise, control cultures of rSMCs were set up to examine the serial elimination of each scaffold component or process step used in tube fabrication as shown in Table 3. Complete DMEM was substituted for each component eliminated so that the sample was manipulated in a similar manner, but without the effect of that component. The components/steps that were serially eliminated included exposure to $CaCl_2$, addition to trisodium citrate, addition to alginate, and centrifugation of the cells. Trisodium citrate was not a scaffold component; however, in this study it was used to release the cells from the alginate hydrogel and therefore it was important to determine if its inclusion resulted in any detrimental effect to the cells.

	cells centrifuged	added to alginate	added to trisodium citrate	exposed to $CaCl_2$
Tubes fabricated, rinsed and released with sodium citrate	+	+	+	+
Control, No $CaCl_2$ exposure	+	+	+	-
Control, No $CaCl_2$ & sodium citrate	+	+	-	-
Control, No $CaCl_2$, sodium citrate, alginate	+	-	-	-
Control, No $CaCl_2$, sodium citrate, alginate, centrif.	-	-	-	-

Table 3. Conditions examined to evaluation the matrix components and cross linking solution on rSMC growth. Tubes were extruded and cross linked with CaCl2, rinsed, then the rSMCs were released using trisodium citrate. Control conditions were created that serially eliminated each component or step of the tube fabrication. (The + symbol indicates step/component was utilized, the – symbol indicates step/component was not utilized)

The rSMCs released from the tubes were seeded into the microwells between $0.74x10^3 - 1.7x10^3$cells/cm^2. The number of rSMCs released from the tubes rinsed with complete DMEM and n-saline was determined because the rinse using n-saline dissolved the alginate tubes. The control rSMCs were theoretically seeded at ca. $5.3x10^3$cells/cm^2 (see Table 4); however, a cell count was not performed following manipulation of the control cultures through their process steps so a lower density was likely due to losses. The volume of rSMCs added to each well was not adjusted for the actual cell count; therefore, there was as much as a 7.5 fold difference between the theoretical seeding densities for the control cells and the actual density of the rSMCs in each tube group. The seeding density difference did not appear to be significant as described in the results in section 3.3.2.3.

Alginate tube rinse condition	Viability (%)	Seeding density ($x10^3$ cells/cm^2)
1.5 mL complete	92	1.4
1.5 mL n-saline	85	0.74
12.5 mL complete	89	1.7
125 mL complete	87	1.3
control cells	96*	5.3 (theoretical)
* = after trypsinization		

Table 4. Viability and seeding density for rSMCs released from alginate tubes. The viability for the conditions was similar; however, the control cell's viability appeared to be highest as measured after trypsinization, not after manipulation through the process steps. The seeding densities were similar for the tube conditions, whereas the density for the control cells theoretically was greater. The actual cell density of the control cells was not determined after manipulation, but the actual seeding density was likely to be lower.

2.4.3.3. Evaluation of tubes *in situ*

Cells (rSMCs or hMSCs) were mixed into alginate-GRGDY and extruded into 4mm diameter alginate tubes as described in section 2.4.3. The tubes were cross linked using a 1% $CaCl_2$ solution in n-saline. The cell/alginate tubes were washed with culture medium and incubated in the glass tubes filled with culture medium (e.g. complete DMEM or MSCCM). Fresh medium was added regularly (e.g. twice a day, daily or every two days) using a 5-10mL syringe (Becton Dickinson). Micrographs of these constructs were taken, and the spent medium was analyzed to see if glucose consumption and lactate production were similar to cells grown in tissue flasks. Results are shown in section 3.3.5.2 for rSMCs and in section 3.4.2.4 for hMSCs.

2.4.4. Formation of alginate beads

Both rSMCs and hMSCs were immobilized in alginate (or alginate-GRGDY) beads. Beads were fabricated because it was an easier and more rapid method to produce high numbers of multiple individual units to evaluate at micro-scale level the cell growth and viability as compared to fabricating multiple tubes and/or cutting tubes into sections for evaluation. These processes were outlined in section 2.4.1, Figure 6.

Cells from tissue flask cultures were trypsinized, centrifuged and resuspended in culture medium as described in section 2.4.1, and homogeneously mixed with alginate

or derivatized alginate to final concentrations ranging from 0.5-3% alginate and $1x10^6$ – $2x10^7$viable cells/mL. After mixing the cell/alginate mixture was drawn into a 1mL syringe; and beads were fabricated by very slowly syringing the mixture through a sterile 0.1mm diameter blunt needle and forming small droplets that dripped into a 0.5-2% $CaCl_2$ solution used to cross link the alginate molecules to form spherical shaped hydrogel beads (see section 2.4.1, Figure 6). The beads were left in the $CaCl_2$ solution for 5-20 minutes, then the $CaCl_2$ solution was decanted or the entire contents were poured into a metal strainer to collect the beads. The beads were transferred into a Petri dish and culture medium was added to rinse the beads to reduce the residual $CaCl_2$ levels. The beads were transferred into microwells containing culture medium using a 25mL pipet and cultured in a humidified 37°C incubator containing 5-10% CO_2. The size of the beads produced by this manual method was estimated to be ca. 2-2.5 mm in diameter.

2.5. Methods of cell and matrix characterization

2.5.1. Visualization of cell growth using light microscopy

Cells grown in tissue flasks were observed using 100-400X magnification on an inverted light microscope. The cells were observed for degree of confluency (cell density), presence of mitotic cells which indicated cultures were in exponential growth phase, and amount of cellular debris in the spent medium which indicated cell death. As the age of the culture increased, the cells became more densely packed in the flask. For optimal detachment as single cells, the cultures were trypsinized when ca. 80-90% confluent. In addition the pH of the spent medium indicated a healthy culture if it was orange/red in color due to release of CO_2 from respiring cells and buildup of metabolic waste products such as ammonia. Cultures that were red/purple indicated lower cell density or possibly poor cell growth. The medium from cultures that were contaminated with microorganisms was turbid or more yellow (acidic) in color.

Cells seeded onto the surface or within the alginate or collagen constructs were also observed in this same manner. In addition the morphology of the cells could be observed to determine whether the cells were rounded, or elongated and networked together.

2.5.2. Cell enumeration using hemacytometer

The density of the cell suspension was determined using a hemacytometer. After trypsinization and quenching with complete medium, a small sample ca. 0.5mL was removed to determine the cell density. 100μL of cell suspension was typically added to 100μL of trypan blue dye (Biowhittaker) and mixed homogeneously using a micropipet. Then ca. 20μL of sample was injected onto the hemacytometer under a cover slip. Cells were counted in the grid that was etched onto the surface of the hemacytometer. The cell count was repeated for a total of 3-4 replicates and averaged. The total number of cells/mL was determined by multiplying the total cells counted in 10 squares by 1000 times the trypan blue dilution factor (usually 2) as shown below. The multiplication factor of 1000 was obtained from the volume of

$1mm^3$ contained in the counting grid (10 squares x 1mm x 1mm x 0.1mm) and converted to mL ($1mm^3$ = 0.001mL) for the original sample.

Avg. no. of cells in 10 squares x 1000 x Dilution factor (2) = Number of cells/mL

(equation 2.1)

Accuracy of the cell count was dependent upon the homogeneity of the cell suspension. Suspensions that were aggregated produced lower results than actual numbers. Therefore this operation was dependent upon the age of the culture, effective trypsinization and the operator's technique. If possible between 100-300 cells were counted for each replicate so that the numbers were not prone to increased statistical error due to small sample size.

2.5.3. Cell viability using trypan blue dye exclusion

Viability was assessed using the trypan blue dye exclusion assay. Trypan blue is a small molecular weight dye that stains the cytoplasm of cells. Equal volumes of trypan blue stain and cell suspension were added together. Live cells had an intact cell membrane which excluded the dye. Dead cells had a permeable membrane that allowed the dye to enter the cell, thus dead cells appeared blue. The microscopic evaluation was completed within 15 minutes after dye addition because trypan blue dye will eventually permeate live cells. The viability of the cell suspension was determined by the equation:

$$\text{Percentage of viable cells} = \frac{\text{Number of live cells (unstained)}}{\text{Total number of cells (unstained + stained)}} x\,100$$

(equation 2.2)

2.5.4. Calculation of cell growth rates

Adherent cells grown in tissue culture exhibit a characteristic growth cycle that includes a lag phase in which the cells adjust to the culture conditions, an exponential growth phase in which the cells proliferate rapidly, a stationary phase in which cell growth diminishes, and a death phase in which metabolic by-products build up and become toxic to the cells inhibiting further growth and/or essential nutrients are depleted in the culture medium. (Doran, 1995) Cells seeded below an optimal

density ($<10^3$ cells/cm^2) typically experienced a longer lag phase due to insufficient release of growth factors into the culture medium. Once the cells have assimilated to the culture conditions, growth commences. Mammalian cells have a relatively long growth cycle. A7r5 rSMCs have a population doubling time of ca. two days in tissue flasks. The growth of cells in the flasks (closed system) can be described as $dX/dt = \mu X$, which when integrated with initial conditions of $X = X_0$ at $t=0$, becomes $X = X_0 \exp(\mu t)$. For the time required for the cell population to double, T_d, the cell population increases from X_0 to $2X_0$. Thus the equation becomes $2X_0 = X_0 \exp(\mu T_d)$ which when reduced after taking the natural logarithm of both sides becomes $T_d = \ln(2) / \mu$ (Doran, 1995; Butler, 2004).

The aim of this research was to characterize the growth rate of the A7r5 rSMCs, and later the hMSCs, in tissue culture vessels. Extensive growth kinetics studies were conducted for the rSMCs over 20 consecutive passages (more than 34 population doublings) to measure growth rates of these cells. The cells were cultured in T150 flasks as outlined in section 2.1.1.2. Studies were also repeated using hMSCs over 10-12 consecutive passages as per section 2.2.2.2. The initial and final cell densities (X_0 and X) were determined by trypsinization and cell count using a hemacytometer. Then the population doubling level (PDL) was calculated to be:

$$PDL = \log_{10}(X/X_0) / \log_{10}(2) \qquad \text{(equation 2.3)}$$

The doubling time (T_d, hours) of the cells was calculated from the total length of culture (T, hours) and the equation:

$$T_d = T / PDL \qquad \text{(equation 2.4)}$$

Then the growth rate ($hours^{-1}$) was calculated directly from the equation (Doran, 1995; Butler, 2004):

$$\mu = \ln(2) / T_d \qquad \text{(equation 2.5)}$$

or combining with equation (1) and (2):

$$\mu = 2.3 * \log_{10}(X/X_0) / T \qquad \text{(equation 2.6)}$$

Variations of the growth rate were calculated by multiplying μ by 24 hours/day to obtain PD/day. Alternatively, the growth rate of the cells (cells/cm^2/hour) was estimated from the slope of the line plotted for the increase from initial seeding density to final density (cells/cm^2) plotted versus time (hours).

Two detailed growth studies using rSMCs were performed in T25 flasks with daily cell count, viability assessment and measurement of glucose concentration in the spent medium. Cells were seeded in T25 flasks at two densities, $5.1x10^3$ and $4.0x10^2$cells/cm^2. Two seeding densities were selected for the T25 flasks to determine possible differences in growth rate and glucose consumption. Additionally, 24 well microwell plates were seeded at $5.1x10^3$ and $4.8x10^3$cells/cm^2. Cell counts were not performed for microwell cultures, since the rSMCs could not be effectively trypsinized and detached from the surface without the contents spilling out. The rSMCs adhered too strongly to the microwell surface. Only spent medium samples for glucose concentration were removed for analysis from the microwells.

T25 flasks have a surface area of 25cm^2 and 24 well plates have a surface area of 1.9cm^2. The amount of growth medium was 5mL (0.2mL/cm^2) and 1mL (0. 53mL/cm^2) respectively. The microwell volume was significantly affected by evaporation during incubation at 37°C for the culture length; therefore, this larger medium volume was selected and the actual volume of the medium at each time point was used as a correction factor during glucose consumption analysis as described in section 3.3.2.2. The results obtained from the rSMCs growth studies are discussed in section 3.3.1.1 and from the hMSCs in section 3.4.1.1.

2.5.5. Release of cells from matrix using trisodium citrate solution

Trisodium citrate was used to release the cells from the alginate hydrogel by reversing the cross linking of the alginate molecules (Read, 2001). Citrate is a chelator of calcium ions; therefore, the calcium ions dissociate from the alginate hydrogel. After release, the cells were assessed for viability using trypan blue dye. Control experiments using rSMCs were performed to determine the effect of trisodium citrate solution on cell viability over a time period typically required to perform analysis on a matrix. If the rSMCs exposed to the trisodium citrate solution do not exhibit an

overall lower cell viability nor a decrease in cell viability over the time period examined as compared to the control cells; then this method could be used to access cell viability.

A 0.1M trisodium citrate solution was prepared in complete DMEM. In the first study, rSMCs were trypsinized, centrifuged at 100g for 10 minutes, resuspended in PBS, and added to 4 fold volume of trisodium citrate solution to a final cell concentration of $7x10^4$cells/mL. Control rSMCs were treated identically except added to 4 fold volume of complete DMEM. This is the appropriate control since the trisodium citrate solution was prepared in complete DMEM. The second study was performed identically to the first, except rSMCs were added to a 9 fold volume of trisodium citrate solution and control cells were added to a 9 fold volume of complete medium to a final cell concentration of $1x10^5$cells/mL. In both studies, the rSMCs were added to an equal volume of trypan blue dye and assessed for viability over a time course. These results are discussed in section 3.3.2.1.

2.5.6. Metabolite analysis of spent medium using biochemical analyzer

The YSI 2700 Select Biochemistry Analyser (YSI (UK) Ltd., Analytical Technologies, Farnborough, United Kingdom) utilized an immobilized enzyme reaction on a membrane to measure the amount of substrate in a sample. The substrate (e.g. glucose or lactate) was catalyzed using oxidase to produce hydrogen peroxide, H_2O_2, which was then oxidized at the platinum anode to produce electrons (Figure 9.A). The membrane consisted of three layers including an outer polycarbonate membrane which excluded large molecules, cells, and debris; a middle membrane containing the immobilized enzyme; and an inner cellulose acetate membrane that only permitted chemical compounds, such as H_2O_2, with molecular weights below 200 to pass through (Figure 9.B). When a sample was injected into the buffer-filled sample chamber, the substrate diffused through the polycarbonate membrane where it was catalyzed to H_2O_2 (reaction 1). The H_2O_2 then passed through the cellulose acetate membrane and was oxidized to yield electrons (reaction 2).

A

Reaction 1:

$$\text{Glucose} + O_2 \xrightarrow[\text{Glucose oxidase}]{} H_2O_2 + \text{D-Glucono-}\delta\text{-Lactone}$$

$$\text{L-Lactate} + O_2 \xrightarrow[\text{L-lactate oxidase}]{} H_2O_2 + \text{Pyruvate}$$

Reaction 2:

$$H_2O_2 \xrightarrow[\text{Platinum anode}]{} 2H^+ + O_2 + 2e^-$$

B

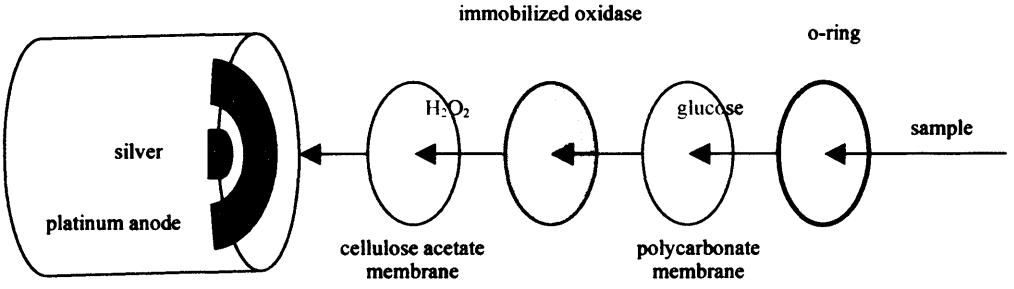

C

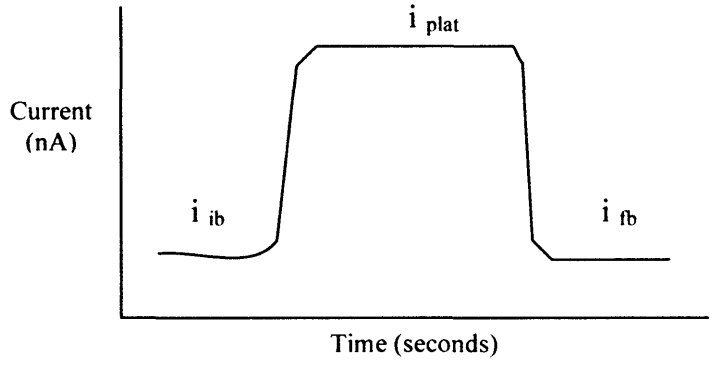

Figure 9. Operation of YSI bioanalyzer. (A) Enzymatic and electrochemical reactions. (B) Sensor probe and membranes. (C) Typical sensor response, where i_{ib} = initial baseline current, i_{plat} = plateau (steady state) current, i_{fb} = final baseline current. (adapted from YSI 2700 Select Biochemistry Analyzer User's Manual)

When the H_2O_2 reaction reached a dynamic equilibrium, a steady state electrical current was produced that was proportional to the concentration of the substrate. The resultant current was used to calculate the actual concentration of the substrate in the sample. The sensors' response or output current was measured against a calibration standard of known substrate concentration. In addition after every sample and calibration, a baseline current was measured. If a shift was detected, the pump continued to flush buffer through the sample chamber until the current stabilized (Figure 9.C).

Samples of the spent medium from both rSMC and hMSC cultures were removed and frozen in ca. 1mL volumes. At the completion of a study, the samples were removed from storage, thawed and analyzed on the YSI bioanlayzer.

2.5.6.1. Using glucose consumption to monitor cell growth

Glucose is utilized by cells as an energy source. The rate at which glucose is consumed in a culture can be used as an indication of cell proliferation (Ozturk, 1997). Culture conditions can affect the glucose consumption of a population of cells. If culture conditions are standardized by maintaining control over the composition and volume of medium, the gas exchange (O_2, CO_2), the age and type of cells, the seeding density, and the culture length; then it is possible to use glucose consumption as an indication of cell proliferation.

The glucose consumption in tissue flasks was calculated by measuring the glucose concentration in the medium at initial seeding and then just prior to trypsinization. Then the rate was determined by dividing the amount of glucose consumed by the time integral of the change in cell density. The cell densities were determined by trypsinization and cell count using a hemacytometer. The final formula used was:

$$GCR = \frac{G_c V}{\int_0^t X_s ds} = \frac{G_c V}{[A\exp(kt) - A]t/2} = \frac{G_c V}{(X_t - X_0)T/2} \quad \text{(equation 2.7)}$$

where GCR = glucose consumption rate (g/cell/hour), G_c = glucose consumed during culture period (g/L), V = volume of growth medium (L/cm^2), and the time integral of the change in cell density, X_s, for the culture length (hr cells/cm^2).

An exponential curve was fit to the cell growth data, and then the change in cell density between two time points (t=0 and t=t) was calculated using $X_0 = A$ and $X_t = Aexp(kt)$, where A = the initial seeding density and k equals the growth rate constant. The time integral was further simplified to $(X_t - X_0)T/2$ for estimating when only two data points for a cell passage existed, where X_s = cell density (cells/cm^2) and T = total culture time (hours). The cells were passaged during exponential growth phase so the estimates would be more reliable.

Ultimately, glucose consumption was used to monitor the cell growth of the cells when direct cell density measurements were not possible when cultures were grown in microwells or in alginate scaffolds. In these cases, glucose data in g/L were plotted over the desired culture period in hours; and then a linear curve was fit to the data. The final glucose consumption rate (g/hr) was determined from the slope of the curve over the culture period (g/L/hr) multiplied by the volume of the growth medium (L) in the culture vessel.

2.5.6.2. Using lactate production to monitor cell growth

Lactate is a by-product of glutamine metabolism. The lactate levels in the spent medium were measured using the YSI bioanalyzer. Lactate data in g/L were plotted over the desired culture period in hours and then a linear curve was fit to the data. The final lactate production rate (g/hr) was determined from the slope of the curve over the culture period (g/L/hr) multiplied by the volume of the growth medium (L) in the culture vessel.

In addition, the metabolic state of the cells was monitored using the 'respiratory quotient' which was the ratio of the amount of lactate produced over the amount of glucose consumed.

Respiratory quotient = L_p / G_c (equation 2.8)

Where L_p = lactate produced during culture period (g/L),and G_c = glucose consumed during culture period (g/L).

If the respiratory quotient was 1, the cells were metabolizing aerobically. A ratio of 2 indicated anaerobic metabolism, and a value in between 1 and 2 indicated something intermediary (Carrier, 1999).

2.5.7. Live/dead assay using fluorescence microscopy

Another technique used to determine cell viability employed two fluorescent dyes – calcein AM and ethidium homodimer (EthD-1) which were supplied as a Live/Dead kit (Molecular Probes, Eugene, Oregon, USA). Calcein AM diffuses into the cell and was converted by intracellular esterase activity into a polyanionic, fluorescent molecule. Since live cells have an intact membrane, this fluorescent molecule was retained inside the cell cytoplasm. EthD-1 was a highly charged (polyionic) fluorescent molecule which diffused into dead cells which have a permeable membrane and then bonded to the nucleic acids. Upon binding EthD-1 undergoes a 40-fold increase in fluorescence. The optimal concentration of calcein AM required for this assay was determined by simultaneously evaluating live cell samples which exhibited high green fluorescence, while exhibiting negligible green fluorescence in dead cell samples. The saturating concentration of EthD-1 required for this assay was determined by observing dead cell samples with increasing concentrations of EthD-1 until maximum fluorescence was observed with minimal red background (excess dye) in the sample. Samples were prepared for evaluation by harvesting rSMCs from tissue flasks using trypsin/EDTA and then centrifuging at 100g for 10 minutes. The supernatant was removed and discarded without disturbing the cell pellet. The cell pellet was resuspended in PBS or DPBS since the phenol red in DMEM interfered with the fluorescence signal. Approximately $1x10^6$cells were resuspended in 333µL of PBS, and then 333µL each of 4µM EthD-1 and 2µM calcein AM was added. The sample was allowed to incubate at room temperature for 45 minutes to 1 hour prior to evaluation using rSMCs. For the hMSCs, 30 minutes at 37°C was sufficient for optimal viewing without the alginate bead/background becoming excessively stained. The samples were observed on a fluorescence microscope with optimal excitation/emission wavelengths of ca. 495/515nm for calcein AM and 495/635nm for EthD-1.

2.5.8. Cytology and histology preparation

Cytology preparations were made from hMSCs that were grown in microwells. The hMSCs were scrapped from the microwell surface with a metal spatula and smeared onto a glass microscope slide (SuperFrost Plus, Menzel-Glaser, Germany). After the slide was allowed to air dry for 20 minutes, the cells were fixed in high grade acetone at room temperature for 10 minutes. Then the slide was allowed to air dry so the acetone evaporated, and the slide was stored frozen at -20°C until analysis. The slides were exposed to hematoxylin to stain the cells' nuclei blue and to the specific monoclonal antibody for α -smooth muscle actin (ASMA, Dako UK Ltd., Ely, UK) using the biotin avidin complex method to assess the presence of these specific cell proteins in the cytoplasm. ASMA is an indicator for smooth muscle cells.

Histologic preparations were made of the hMSC/alginate beads by fixing in 10% formaldehyde saline solution (formal saline) at room temperature. Early preparations were performed by smearing/spreading the bead across the surface of a glass slide prior to perfecting the techniques needed to prepare microsections embedded in paraffin wax due to the fragile nature of bead and its translucent appearance within the paraffin block. In order to locate the beads, they were marked with histological marking ink, placed in biopsy capsules and cassettes (Surgipath Europe Ltd., Peterborough, UK) and underwent standard histopathologic processing in formalin, industrial methylated spirits, xylene and paraffin wax in a Leica ASP 300 processor (Leica Microsystems (UK) Ltd., Milton Keynes, UK). The beads were embedded in paraffin wax and sliced into 3 micron sections on a rotary microtome. Sections were dewaxed and stained with hematoxylin and eosin (H&E) for overall morphology immediately after cutting. Eosin stained the cells' cytoplasm pink; and hematoxylin stained the nuclei blue. Slides that were prepared for immunohistochemistry were first pressure cooked for 4 hours. This procedure was performed as an antigen retrieval step for the cell proteins that became crosslinked during histological processing. Due to non-specific binding (see results section 3.6.1), a biotin blocker (Dako) was applied to the samples. Then the monoclonal antibody with the biotin avidin complex was left on the slide overnight. The next day the slide was washed, allowed to dry, covered with a glass coverslip and sealed. The immuno-slides were also counter stained with hematoxylin to clarify the cells' nuclei. A positive result

using monoclonal antibodies specific for the cell cytoplasmic protein, ASMA, was indicated by brown cytoplasmic staining around the cell nucleus.

2.5.9. Fluorescence activated cell sorting (FACS)

During differentiation studies, ca. 5 hMSC/alginate beads were washed twice with 1mL DPBS then the beads were dissociated into a single cell suspension by adding 200μL of 0.1M trisodium citrate and 200μL of 0.25% trypsin/0.02% EDTA to the beads containing 200μL DPBS for ca. 30minutes and then gently micropipetting until the bead was completely dispersed. Then 400μL of complete medium was added to quench the trypsin activity. One bead was dissolved per antibody tested, including a bead for the 'empty' control (containing no antibody). The dissociated cell suspension was centrifuged at 1200rpm (160g) for 5 minutes, the supernatant was poured off, the pellet was resuspended with 500μL DPBS and 100μL was aliquoted into individual tubes (1/antibody tested + empty control). A dilution of 1:100 was made of each antibody in DPBS and then 100μL of antibody solution was added to the individual 100μL of cell suspension for a final 1:200 dilution level (one antibody per tube). DPBS was added to the empty control sample. The samples were vortexed and incubated in the refrigerator for 1 hour. Then the tubes were centrifuged at 160g for 5 minutes, the supernatant was poured off and the pellets were resuspended with 100-200μL of DPBS. If a secondary polyclonal with a fluorescent tag was needed for conjugation to the primary antibody, a second dilution series with 100μL of diluted antibody with fluorescent tag in DPBS (1:100) was added to the 100μL of cell suspension sample resuspended in DPBS (final 1:200) which was already exposed to the primary antibody and incubated in the refrigerator for 1 hour. The primary monoclonal antibodies used were CBL555 anti-human CD34 type III (Cymbus Biotechnology Ltd., Chandlers Ford, UK) and anti-mouse smooth muscle cell actin (Ab-2) (Oncogene Research Products, Boston, Massachusetts, USA). These antibodies were conjugated to secondary anti-mouse immunoglobulins/Rhodophyta-phycoerythrin (RPE) Goat F(ab) (DAKO A/S, Copenhagen, Denmark). The SH2 (endoglin) and SH4 monoclonals (gift from StemCell Technologies) were already conjugated to fluorescein isothiocyanate (FITC). After the cells were labeled with the fluorescent tag, the individual samples were immediately run through a FACS machine (Beckman Dickinson FACSCalibur, BD Biosciences, San Jose, California, USA) which produced graphical outputs showing the distribution of the cells.

Each cell was designated by a dot on the graph. The gated region of the graph was selected using an empty sample from the distribution of the cells on the graph of side scatter (SSC-H) vs. forward scatter (FSC-H). The gate was selected for the desired cell population which excluded cellular debris and cell aggregates. Examples of the designated gated area are shown in the Appendices, section 6.2.4.

Cells within the gated region on the graph of RPE tag (FL2-H) versus FITC tag (FL1-H) were negative for the fluorescent tag and hence the surface marker. Cells that expressed the surface marker, and hence were positive for the antibody with fluorescent tag, fell outside the gated region (in R2). The FACS results were used to monitor the change in hMSC surface markers after being immobilized within the alginate-GRGDY beads and cultured in either DMEM (control medium) or in CDMEM with rSMC co-cultures. These studies are described in section 3.6.

2.5.10. pH measurements

PH measurements were made using a standard pH meter and electrode (Hanna Instruments Inc., Woonsocket, Rhode Island, USA). A two point calibration using pH 7.0 and pH 4.0 standards was performed prior to analysis to ensure the probe was operating properly.

2.5.11. Viscosity measurements

The alginate solution viscosity had a strong dependence on alginate concentration. Only alginate concentrations around 0.5-3% were considered for matrix studies with cells. Viscosity measurements were taken using a cone and plate rheometer (LVDV-II+, Brookfield, Massachusetts, USA) with a 1mL working volume which had been calibrated using a silicone oil standard (RT1000, Cannon Instrument Co., State College, Pennsylvania, USA). Water in a room temperature water bath was circulated through the device jacket in order to maintain a constant temperature during measurements since viscosity is temperature dependent. The viscosity was measured at several shear stress rates (altered by changing the number of revolutions per minute). For simplicity, the alginate solutions were assumed to behave as a Newtonian liquid so that the formula for viscosity was calculated as:

$\eta = \tau / \gamma$ (equation 2.9)

where η = Newtonian viscosity (Ns/m^2), τ = shear stress (N/m^2) and γ = shear rate (1/s)
(Coulson and Richardson, 1996).

The molecular weight of alginate can be determined from the viscosity of the alginate using the Mark Houwink Equation:

$\eta = K * M^a$ (equation 2.10)

where M = molecular weight, and constants a = 1 and $K = 2x10^{-5}$ (Smidsrod, 1972).

The determination of molecular weight of the alginate is important for characterization of the matrix solution, since the length of the polymer chains has important implications for the hydrogel strength and structure – such as porosity and dissolution characteristics as described in section 1.4.2.3 (Martinsen, 1989; Leo, 1990). Alginate treatments such as heat sterilization and filtration greatly affect the molecular weight of the alginate (Leo, 1990, Vandenbossche and Remon, 1993).

2.5.12. Statistical analysis

Statistical analysis was performed using the single factor analysis of variance (ANOVA) program from Microsoft Excel 2002. The single factor ANOVA analysis tool performed a simple analysis of variance, testing the hypothesis that the means from two or more samples were equal (drawn from populations with the same mean). This technique expands on the tests for two means, such as the t-test. Analysis of the groups of data that produced a p-value >0.05 indicated that the means were not statistically different (to the 95% confidence level); whereas a p-value <0.05 indicated one or more of the samples did not have the same mean.

2.6. Cell proliferation assays

Quantitation of cell growth of attachment dependent cells is usually performed by the cell count method that involves cell harvesting using trypsinization, staining and enumeration using a hemacytometer and microscope (section 2.3.2). This method is labor intensive, time consuming and results can be dependent upon the operator. In addition, cell cultures that are post-confluent tend to be densely packed and aggregated which tends to produce inaccurate results due to cell clumping (Lombarts,

1992). Release of cells from matrices and quantification using the cell count method can be inaccurate for the same reasons, in addition, the cells can be lysed during their release from the matrix. Therefore, an intact cell component-based protocol was preferred to monitor cell proliferation. Two assays were investigated during this research: CyQuant assay for nucleic acid quantification and MTT (3-(4,5-dimethylthiazol-2-yl)-2,5-diphenyltetrazolium bromide) assay for mitochondrial dehydrogenase activity. These assays were investigated during the research project. The CyQuant assay was tested with the earlier rSMC studies and the MTT assay was tested with subsequent research on hMSCs.

2.6.1. CyQuant assay

This assay uses a fluorescent dye, CyQuant® (Molecular Probes, Eugene, Oregon, USA; product no. C-7026), which binds to nucleic acids giving a signal that is proportional to the cell number (Jones, 2001). The assay was performed in 96 well microplates (Costar, Corning Life Sciences, Corning, New York, USA; product no. 3603) and analyzed on a fluorometer (Fluorocount, Packard BioSciences, Perkin Elmer™ Life Sciences, Boston, Massachusetts, USA). The cell samples were frozen and stored at –20°C for up to four weeks before quantitation. Upon thawing, lysis buffer was added to the cell sample to make the nucleic acids accessible to the stain. The quantity and ratio of RNA and DNA in cell cultures can vary based upon cell type and culture conditions; therefore ribonuclease (RNAse) (Sigma) was also added to the cell samples to eliminate contributions of RNA to the results.

2.6.1.1. Preparation of cell number standard

A reference standard for A7r5 rat SMCs was required for converting sample fluorescence values into cell numbers by diluting a known quantity of cells to concentrations between 50 to $1x10^5$cells/well. The cell number standard was prepared by trypsinizing flasks of rSMCs and performing a cell count using a hemacytometer. The cells were dispensed into aliquots (ca. $1\text{-}2x10^5$cells/tube) for individual assays and then centrifuged at 200g for 5 minutes. The supernatant was removed without disturbing the cell pellet and discarded. The cell pellet was frozen and stored until needed for assays. On the day of analysis, one or more tubes were removed and thawed. 1X cell lysis buffer (Molecular Probes, #3603, component B) was prepared

and added to each cell pellet and mixed by pipetting and vortexing. RNAse was also added at this point to samples in which only nucleic acid contributions from DNA were desired. RNAse was added to the cell sample at a concentration of ca.1.35Kunitz units/mL. After ca. 1 hour, the individual tubes were combined and 2X CyQuant®GR dye (Molecular Probes, #3603, component A) in 1X cell lysis buffer was added to the sample. This achieved a final concentration of 1X CyQuant dye in 1X cell lysis buffer. Then dilutions were made to achieve a standard curve between 50 to $1x10^5$cells/well. Similarly, twice the concentration of dye (2X) was used to prepare cell number standards with 1X cell concentration to determine the robustness of the assay.

2.6.1.2. Preparation of DNA standard curve

A sample of bacteriophage λ DNA (Molecular Probes, product no. C-7026) was used to prepare a standard curve for DNA content. This curve was used to calibrate the assay for samples analyzed on the Fluorocount on separate days due to variation in the fluorescent signal intensity which is instrument dependent. Dilutions were prepared in 1X cell lysis buffer from 100μg/mL DNA sample to cover the range between 0 – 1000ng/mL of DNA. Additional dilutions with twice the CyQuant dye concentration were prepared in 1X cell lysis buffer to cover the range between 0 – 2000ng/mL of DNA.

2.6.1.3. Analysis on fluorometer

Microplates were loaded into the Fluorocount and 3-5 independent readings were taken of each plate using 405nm excitation and 530nm emission filters. The gain was set to the well with the highest DNA concentration (in the DNA standard curve). The gain was held constant at 1 and the PMT (voltage) was set to 800 and 900. The higher PMT setting results in a higher sensitivity of the fluorescence reading. Samples were analyzed at two PMT (voltage) readings to ensure all wells could be read by the fluorometer so that readings at the same PMT setting from different experiments could be compared. All readings were subtracted from the background fluorescence (reading from the control well that did not contain any cells).

2.6.1.4. Interference of assay components with fluorescence results

A set of typical rSMC standard curves is shown in the Appendices, section 6.1.2.1, Figure 69. The assay was linear up to 56,000cells/well when treated with RNAse. However, the standard curve slope increased ca. 47% when the CyQuant dye concentration was doubled. A set of typical DNA standard curves is shown in the Appendices, Figure 70. The assay was linear for both dye concentrations; however the standard curve slope increased ca. 38% when the CyQuant dye concentration was doubled. This was not expected and may have been due to additional binding of the dye to the DNA or higher background interference with the higher dye concentration. However a similar increase in fluorescence was observed in both the DNA and rSMC standard curves. Before this issue was resolved, the assay was tested to see if the alginate matrix components interfered with the fluorescence results. Tubes containing rSMC reference standard (as described in section 2.6.1.1) were thawed and treated with RNAse and added to CyQuant dye to a final 1XCyQuant dye concentration in 1X cell lysis buffer. Three cell concentrations (4.2×10^3, 8.4×10^3 and 16.8×10^3cells/well) were transferred into a 96 well plate. Then either a dissolved alginate solution or control solution (n-saline and PBS) were added to each individual wells at 0, 5, 20 and 80µL per well. The wells were thoroughly mixed with a micropipette and measured on the fluorometer at 900 PMT. As shown in the Appendices, section 6.1.2.1, Figure 71, the fluorescence signal increased considerably as the volume of alginate solution increased indicating the alginate or other components of the solution significantly altered the binding affinity of fluorescence dye to the cellular DNA as compared to the control solution at the same cell concentrations. The cell standard consisted of 0µL volume of solution and is shown in the Appendices, Figure 69. It conformed well to the previous standard using 1X dye concentration. Due to the interference of the alginate solution with the fluoroprobe's binding affinity to the cellular DNA, the CyQuant® assay was deemed unacceptable for use as a proliferation assay for this application.

2.6.2. MTT assay

A modified MTT assay (Mosmann, 1983) was performed in 96 well microplates (Sarstedt Inc., Newton, North Carolina, USA). Three methods of cell preparation

were used based upon whether the hMSCs were in a cell suspension, if they were immobilized in alginate beads or if they were adherent cultures in microplates. Details described below are the finalized assay method. The results used to construct these methods are described in detail in section 3.5.3. In addition the method used to determine whether alginate interfered with MTT absorbance is described section 2.6.2.8. Overviews for the steps of each assay are provided in the Appendices, section 6.1.1.

2.6.2.1. Preparation of cell number standard

Flasks of hMSCs were trypsinized as per usual protocol and a 0.4mL sample was removed for a cell count using a hemacytometer to determine the cell concentration as per section 2.5.2. The cells were centrifuged, supernatant removed and pellet resuspended to $2x10^6$viable cells/mL using Dulbecco's phosphate buffered saline with 1g/L D-glucose and 36mg/L sodium pyruvate (DPBSG, Biowhittaker, Cambrex, Verviers, Belgium). A 20μL aliquot of this cell suspension was added to 80μL of DPBSG to perform an additional cell count to confirm the actual cell concentration in the resuspended pellet. A serial dilution of the cell suspension was performed in a 96 well microplate with volumes of DPBSG added to equalize the volume in all of the wells to 100μL total volume. The dilutions were performed in duplicate with cell concentrations per well shown in Table 5. This dilution series created a cell standard curve. MTT solution was added as described in section 2.6.2.4.

Volume of cells (μL)	Volume of DPBSG (μL)	Number of viable cells/well ($x10^4$)
100	0	20
75	25	15
50	50	10
25	75	5
12	88	2.4
In separate vial add 60μL of cells to 440μL of DPBSG then continue dilutions below		
50	50	1.2
30	70	0.72
10	90	0.24
0	100	0

Table 5. Dilutions performed for MTT cell standard.

2.6.2.2. Preparation of standard of hMSCs immobilized in alginate beads

At each time point, cell/alginate beads were removed from culture using a 25 mL pipet and placed in 10cm petri dish (Sterilin, Bibby Sterilin, Stone, UK) containing DPBSG. This wash step was used to remove residual culture medium containing phenol red that would interfere with the absorbance reading. Then the cell/alginate beads were transferred into a 96 well microplate using a 25mL pipet. Duplicate serial dilutions of beads were made to assess the linearity of each MTT assay, such that the wells contained 0 (for a background blank), 1, 2 and 3 beads as shown in Table 6. This dilution series created a cell standard curve for the cells immobilized in the beads, since the number of cells/well would be a multiple of the number of beads. The number of cells/well was determined from dissolving additional beads and performing a hemacytometer count as described in the next section. Then, as needed, the volume of DPBSG was adjusted to 100μL/well using a micropipet. MTT solution was added as described in section 2.6.2.4.

Number of beads per well	Volume of DPBSG (μL)	Total (average) number of cells/well
0	100	0
1	100	1X
2	100	2X
3	100	3X

Table 6. Dilutions performed for MTT assay with alginate beads. The total number of cells/well was determined for each experiment by dissolving additional beads and performing a hemacytometer count. The average number of cells/bead, denoted as 1X, was multiplied by 2 (2X) and by 3 (3X) to calculate the remaining total number of cells/well.

2.6.2.3. Determination of cell concentration in alginate beads

The cell concentration of the beads was determined separately by dissolving of 1-3 beads in 100μL of 0.3M trisodium citrate (Sigma) and 100μL of trypsin/EDTA or 10μL of 10X trypsin/EDTA in saline (BioWhittaker) for at least 15 minutes. Then the beads were dispersed into a single cell suspension using a 200μL micropipet. The total volume of the sample was measured using a 1-2 mL pipet, an aliquot was removed and a cell count was performed using a hemacytometer (section 2.5.2) and viability assessed using the trypan blue dye exclusion assay (section 2.5.3). The total

cell concentration was calculated by multiplying the cell concentration per mL by the total volume. The average cell concentration per bead was calculated by dividing the total cell concentration by the number of beads dissolved which varied by experiment depending upon the size of the bead and the original concentration of cells immobilized in the bead.

2.6.2.4. Addition and incubation of MTT solution

A 10μL aliquot of 5 mg/mL MTT (Molecular Probes or Sigma) dissolved in DPBSG was added to each sample well and incubated for 3 hours (range of 1-3 hours used) at 37°C in a humidified, 5% CO_2 incubator (Galaxy S, RS Biotech, United Kingdom). Plastic film was used to cover the plate to minimize evaporation during incubation. The water soluble MTT salt diffused into the hMSCs (through the alginate hydrogel if present) and mitochondrial dehydrogenase activity converted the salt into an insoluble formazan product. After the 3 hours (range of 1-3 hours used), 40μL of 0.3 M trisodium citrate in distilled water (BioWhittaker) was added to dissolve the alginate within the bead. No mixing of the cell suspension was performed in order to reduce loss of cells adhering to the pipet inner surface. After 1 additional hour at 37°C (total of 4 hours - range of 2-4 hours used), the microplate was centrifuged (5810R, Eppendorf AG, Hamburg, Germany) at 100g for 5 minutes, the supernatant was carefully removed with a micropipet without disturbing the pellet/cells until an 'O' appeared in the bottom of the well. This procedure eliminated any volume inconsistencies that may have arisen from the initial DPBSG or alginate beads. In addition, the removal of the supernatant eliminated the majority of the alginate solution from the well. Due to the pronounced color change of the yellow MTT solution to purple formazan product, the supernatant in the pipet tip could be easily observed not to contain sample when removing the supernatant.

For hMSC cell standards that did not contain alginate (so theoretically did not need the addition of trisodium citrate), this procedure was followed to mimic the contents of the residuals (except alginate) in the wells containing beads.

2.6.2.5. Dissolution of formazan product

After the supernatant was removed, the dissolution procedure continued immediately or the plate containing the cell pellets was wrapped in foil and frozen. Freezing and

storage of the plates at -70°C allowed a time course study to be performed; then all plates could be completed (e.g. dissolved and read) on the same day. Plates from each time point, if frozen, were thawed and each well with cell pellet or bead(s) was reconstituted with 70µL DPBSG. The plate was tapped gently to distribute the pellet and DPBSG. For experiments with alginate-GRGDY beads, instead of 70µL of DPBSG, 50µL of DPBSG and 20µL of 10X trypsin/EDTA in saline were added to dissolve cell-to-cell networking within the bead. Addition of 10X trypsin/EDTA was critical to achieve a homogeneous suspension. Plates containing DPBSG/trypsin/EDTA were incubated wrapped with film for ca. 30 minutes at room temperature; then the bead(s) was thoroughly resuspended into a single cell suspension using a micropipet. Plates not requiring trypsin/EDTA (e.g. those without alginate-GRGDY beads) were processed to the next step immediately and did not require incubation nor mixing to homogenize the sample. Finally 100µL of a solution of isopropanol (Sigma) with 0.1N HCl (Fluka) was added to all samples to permeablize the cells and dissolve the formazan product. The plate(s) was covered with film and incubated at room temperature for 20 minutes. Then each well was mixed thoroughly with a separate micropipet and incubated at room temperature for another 20 minutes. Then each sample was mixed again after a total of 40 minutes.

2.6.2.6. Analysis of data

Within a maximum of one hour from the time of isopropanol/HCl addition, the 96 microwell plates were read on a spectrophotometer (Packard Bioscience Spectracount™, Packard-Becker BV, Groningen, Netherlands) at an absorbance reading of 600nm. In some cases these data were subtracted from the background absorbance at 670nm.

The majority of researchers using isopropanol to dissolve the formazan product measured absorbance at 570nm with background subtraction (reference wavelength) at 630nm (Mosmann, 1983; Wang, D., 2003; Yang, 2003). Carrier (1999) read the plates at 620nm. Zund (1999) used 550nm blanked with isopropanol solution (MTT solution was removed prior to dissolution with isopropanol and 10% formic acid). The closest filter available on the Packard Bioscience microplate spectrophotometer to 570nm was 600nm; therefore, this wavelength was used. As demonstrated in section 3.5.1, this difference did not affect the results of the assay.

The complete assay protocols are summarized in the Appendices, section 6.1.1.1 for the cell number standard and section 6.1.1.2 for the cell number using alginate beads. For experiments with simultaneous MTT absorbance measurement and cell count with hemacytometer using trypan blue, the absorbance could be plotted using the actual viable cell count.

2.6.2.7. Adherent cell assays

All of the adherent cell assays were performed in 24 well microplates (Corning) to evaluate cell growth of hMSCs over a time course. The spent medium was removed from the well, and 300μL of DPBSG was added to the well. Then 30μL of 5mg/mL MTT solution was added. After the plate was incubated for 1-3 hours (3 hours required for high cell densities) at 37°C, 120μL of 0.3 M trisodium citrate was added to the well. Although there was no alginate in these samples, trisodium citrate was added to reflect the same procedure used for dissolution of alginate beads. After an additional hour of incubation (2-4 hours total), the entire MTT solution was removed from the microwell. Centrifugation was not necessary since the cells were adherent to the microwell. At this point the plate was frozen and stored at -70°C, or the assay was continued immediately to the dissolution step. For dissolution, the plates were thawed (if frozen) and 210μL of DPBSG and 300μL of isopropanol/0.1N HCl were added to each well. The plates were then incubated at room temperature covered with film. After 20 minutes, the contents of the well were mixed with separate micropipets to release the formazan, and returned for a further 20 minutes of incubation. After a total of 40 minutes dissolution and an additional mixing step, a 100μL sample was removed and read on the spectrophotometer in a 96 well microplate. These results were correlated to data obtained using the 96 well format by multiplying the absorbance results by a factor of 3.0 (3 times the volume of DPBSG and isopropanol/HCl were added to the 24 well microplate compared to the 96 well microplate). Since the 24-well plates used three times the amount of isopropanol/HCl for dissolution than the 96 well plates, a much higher concentration of cells (e.g. formazan product) could be dissolved. The complete adherent cell assay protocol is summarized in the Appendices, section 6.1.1.3.

2.6.2.8. Interference of alginate with MTT absorbance

In order to determine if residual alginate or assay residuals (e.g. trisodium citrate) interfered with the MTT assay, alginate beads without cells were made by mixing 25% v/v MSCCM with 75% v/v of 1% alginate (Pronova SLG100) and adding drop-wise through a syringe with blunt needle (0.1mm diameter) into a solution of 1% $CaCl_2$ in n-saline and letting cross link for 15 minutes. The alginate beads were collected by pouring through a sterile metal strainer, and then washed with DPBSG. Using this manual procedure, the alginate beads were approximately 2-2.5mm in diameter.

For this experiment, the wells of a 96 well microplate were loaded with 12µl of cell suspension (producing $2.05x10^4$cells/well) and an increasing amount of alginate (number of alginate beads) per well. The alginate beads did not have cells immobilized within them, so the cell concentration of the well was constant for each well. The number of alginate beads, volume of DPBSG and cell suspension added to each well is shown in Table 7. The cell suspension of hMSCs was prepared as per section 2.6.2.1; however, the same volume of cells (12µL) was added to each well to produce the same number of cells/well. The MTT assay was carried out with dissolution of the beads using trisodium citrate (but no trypsin/EDTA) according to procedure detailed in section 2.6.2.4 and 2.6.2.5. This assay was performed without freezing the plate. Although the supernatant from each well was removed after centrifugation as detailed in section 2.6.2.4; the residual volume/well would still contain an increasing concentration of alginate as the number of beads/well increased.

Number of beads per well	Volume of DPBSG (µL)	Volume of cells (µL)	Total number of cells/well ($x10^4$)
0	100	0	0
0	88	12	2.05
1	88	12	2.05
2	88	12	2.05
3	88	12	2.05
4	88	12	2.05

Table 7. Concentration of cells and number of beads used for the alginate interference test for the MTT assay. The same concentration of cells was used per well; whereas an increasing number of alginate beads (without cells) were added to each well.

The absorbance readings varied between 0.2 and 0.3 for all the conditions 0, 1, 2, 3, and 4 beads per well. A graph of these results is shown in the Appendices section 6.1.2.2, Figure 72. The absorbance values were not greatly effected by the increased level of alginate per well. Single factor ANOVA (analysis of variance) statistical comparison indicated that the results were statistically different ($p=0.0000$) among the 5 samples; however, the statistical difference between the absorbance readings for 0 and 4 beads was not significant ($p=0.4023$) and between the absorbance readings for 2 and 3 beads ($p=0.5021$). The variability of the data seems to be due to well-to-well variability (Wan, 1994), rather than a true effect of the presence of alginate or an increasing concentration of alginate. More replicates would have been useful to help confirm this. Despite this shortcoming, the results were significantly better than the CyQuant assay; therefore, the MTT assay was deemed acceptable for further work.

2.7. Methods for differentiating hMSCs

HMSCs were immobilized in alginate-GRGDY beads for conducting differentiation studies as described in section 2.7.1. The preparation of the rSMCs cultures for the differentiation studies is described in section 2.7.2 and 2.7.3. In addition, a media differentiation study was conducted with hMSCs grown long term in microwell plates as described in section 2.7.4 to establish a base-line for α-smooth muscle actin (ASMA) protein expression for cultured hMSCs using the biotin avidin complex method as described in section 2.5.8. ASMA is a sensitive indicator for smooth muscle cells.

2.7.1. Preparation of hMSCs immobilized in alginate beads

Sodium alginate was derivatized to incorporate GRGDY peptides for cell attachment as described in section 2.3.3. The alginate was dialyzed for 2-6 days in water using dialysis cassettes, treated with activated charcoal, filtered through Celite and then concentrated either by PEG treatment or by lyophilization as described in section 2.3.3.5.

Cultures of hMSCs were trypsinized, centrifuged twice to remove residual trypsin and EDTA, and mixed homogeneously into the alginate-GRGDY solution at $5x10^6$ to $2x10^7$cells/mL as described in section 2.4.1. Hydrogel beads of 2-2.5mm diameter

were produced as described in section 2.4.4. The beads were collected in 1% $CaCl_2$ in n-saline solution for 10-15 minutes and rinsed with MSCCM. For differentiation studies, the beads were transferred into Millicell-CM culture plate inserts (Millipore Corp., Bedford, Massachusetts, USA) and cultured in 24-well microplates (Corning) containing ca. 1mL of MSCCM and incubated at 37°C in a 5% CO_2 humidified incubator.

2.7.2. Preparation of rSMC co-cultures and conditioned medium

RSMCs were cultured in tissue flasks as previously described in section 2.1.1.2. Due to the presence of residual trypsin/EDTA in the medium during passaging, flasks used for differentiation studies were refed with 20mL (0.13 mL/cm^2) of fresh DMEM after the cells had adhered to the flask surface, typically one day after passaging. The conditioned DMEM medium (CDMEM) from ca. 2-6 day old cultures of rSMCs was collected and centrifuged at 200g for 5 minutes to remove all cell debris and residual cells from the medium. The supernatant was removed and the CDMEM was stored in the refrigerator until needed. The CDMEM was not stored for longer than ca. 1 week prior to use in the differentiation studies since the stability of its components had not been determined. Co-cultures of rSMCs were prepared for differentiation studies from ongoing flask cultures. The rSMCs were trypsinized as described in section 2.1.1.2 and seeded at $5x10^3$cells/cm^2 into 24 or 12-well microplates containing 1mL or 2-3mL of complete DMEM per well respectively, and incubated at 37°C in a 10% CO_2 humidified incubator.

2.7.3. Differentiation of hMSCs using CDMEM and rSMC co-cultures

After ca. 1-3 days, the Millicell inserts containing the hMSC/alginate beads (as described in section 2.7.1) were transferred into the 24 or 12-well microplates containing the rSMCs. First of all, the inserts were removed from their individual wells using sterile tweezers, and the MSCCM was carefully removed from inside the insert without disturbing the hMSC/alginate beads. Concurrently, the spent medium was removed from the microwells containing the rSMC co-cultures. Then the inserts containing the hMSC/alginate beads were placed into the microwells containing the

rSMC co-cultures (1 insert per well). The Millicell insert and microwell were carefully filled with the supernatant from CDMEM as prepared in section 2.7.2. The culture plate inserts contained a 0.4μm membrane, which acted as a physical barrier to the rSMCs such that they could not come into direct contact with the hMSC/alginate beads. However, the membrane allowed molecules to diffuse through. Beads were removed from culture at approximately three day intervals and analyzed for changes in the cell characteristics using fluorescent activated cell sorting (FACS) as described in 2.5.9 and immunohistochemistry as described in section 2.5.8. Similarly, inserts containing hMSC/alginate beads were also transferred into microwells containing complete DMEM (not conditioned in rSMCs) for control cultures. These control beads were removed and analyzed at the same time intervals as the beads that were cultured in the CDMEM and rSMC co-cultures.

2.7.4. Media differentiation studies of hMSCs in microwells

Since long term cultures of hMSCs have been characterized as 'smooth muscle cell-like' (Charbord, 2000; Dennis and Charbord, 2002; Kadner, 2002) and because there are undefined components in the FBS used in the culture medium, a base-line study was performed to determine levels of ASMA staining in cultured hMSCs. Cultures of P5 hMSCs were trypsinized from the P4 JM cell bank, seeded into12-well microplates ($3.8cm^2$) at a density of $5x10^3$cells/cm^2 with 2mL of MSCCM per well, and incubated at 37°C in a 5% CO_2 humidified incubator. After five days when the cells were ca. 90-100% confluent, the spent medium from each well was removed and replaced with MSCCM, complete DMEM or rSMC conditioned DMEM (CDMEM) as described in section 2.7.2. For this study the CDMEM was obtained from centrifuged supernatant from conditioned medium from P6-P8 rSMCs after 2-4 days in culture. The culture medium for each condition was replaced every 3 days, and the length of storage of the CDMEM at 6°C was between 1-5 days prior to use since the stability of the conditioned medium was not known. At time points on days 3, 6 and 9, the cell layer was scraped with a metal spatula, smeared onto a glass slide and fixed in acetone as described in section 2.5.8. The slide was allowed to air dry and then was stored at -20°C until analysis. The slides were exposed to hematoxylin to stain the cells' nuclei and to the specific monoclonal antibody stain for ASMA to assess the presence of these specific cell proteins.

3. Results

The results for sodium alginate formulation and incorporation of the pentapeptide Gly-Arg-Gly-Asp-Tyr onto alginate polymer (alginate-GRGDY) are discussed in sections 3.1 and 3.2 respectively. These sections are focused on the process results which are independent, although closely linked, to the results obtained using cells. The incorporation and characterization of rat smooth muscle cells (rSMCs) with the alginate and collagen matrices are discussed in section 3.3. Results obtained using human mesenchymal stem cells (hMSCs) and alginate matrices are described in section 3.4. The MTT (3-(4,5-dimethylthiazol-2-yl)-2,5-diphenyltetrazolium bromide) assay results for cell proliferation are discussed in section 3.5. Finally the results from differentiation studies using hMSCs in alginate-GRGDY beads are provided in section 3.6.

3.1. Alginate formulation

Alginate concentrations ranging from 0.5-6% w/v were examined. Initially, WFI for cell culture applications was used to mix with the alginate. However, low cell viability and cell lysis were observed upon mixing due to the non-physiological conditions (e.g. low pH and osmolarity) especially in the high viscosity alginates. Then the alginate was reconstituted in buffered saline solutions (e.g. DPBS and PBS) since they were buffered and isotonic. However when 1% $CaCl_2$ solution (ca. 90mM) was added to cross link the alginate, the PBS caused insoluble calcium phosphate (i.e. $CaHPO_4$) precipitates to form which were undesirable as explained in the next section on cross linking solution. Finally normal saline (n-saline, 0.9% NaCl in WFI, pH 7-7.4) was selected because it was the best alternative, although the pH was unstable because it was not buffered. When the alginate in n-saline was mixed with an equal volume of cells resuspended in complete DMEM medium, the pH was stable at ca. 7.6.

The alginate solutions were mixed overnight or autoclaved (121°C for ca. 22 minutes) to aid dissolution. Higher alginate concentrations (2-6% w/v) had to be autoclaved to ensure a homogeneous mixture. Viscosity studies showed that heat treatment significantly reduced the high molecular weight components of the alginate (Leo, 1990; Vandenbossche and Remon, 1993; Zoro, 2005) resulting in lower equilibrium modulus (Wong, M., 2001). Zoro showed the effect of autoclaving on the viscosity of

Fluka alginate in n-saline solution for concentrations between 0 and 2% (Table 8). The 1% solution viscosity was reduced from 109 to 13mPa·s after autoclaving, which was calculated to be a molecular weight change of 151 to 66kDa (Zoro, 2005). Similarly, this research showed that the viscosity of 1% w/v Manugel was reduced from 200 to 5mPa·s after autoclaving. Because the sterilization cycle length (including warm up, sterilization, and cool down) would vary considerably depending upon the size of autoclave and load, this process step would require careful standardization for a marketed product. Considerable validation of this process would need to be performed to understand the impact on the final matrix's strength, porosity, and decomposition. This heat treatment was also intended to sterilize the alginate solution. In actuality thermophilic bacillus spores were found to be prevalent, as discussed in section 3.1.2., which were resistant to these autoclaving conditions. This problem led to the sourcing of sterile alginate, Pronova SLG100, from NovaMatrix to avoid diversion from the main target.

Fluka in n-saline	Not autoclaved	Autoclaved
0% alginate viscosity (mPa·sec)	1.2	1.2
0.5% alginate viscosity (mPa·sec)	20	3.5
1.0% alginate viscosity (mPa·sec)	109	13
1.5% alginate viscosity (mPa·sec)	472	44
2.0% alginate viscosity (mPa·sec)	1360	154
Molecular weight (kDa)	151	66

Table 8. Comparison of the viscosity and molecular weight of Fluka alginate in n-saline that was autoclaved (Zoro, 2005).

Filtration through a step-down series of Cuno Inc. filters as described in section 2.3.1 ending a 0.2 or 0.1μm membrane was an alternative method for sterilization; however this method was not desirable. Due to the high viscosity of the 1% w/v alginate solution, a 0.1% w/v alginate solution was required to effectively filter the solution. In addition, a low flow rate (3mL/min) using a large filtration surface area (27cm^2) was required to process only ca. 250mL of 0.1% alginate solution through the 0.2μm filter step prior to fouling of the filter which was associated with an increased pressure differential of 2.3bar across the membrane because the high molecular weight polysaccharide chains were retained by the filter. The filter rating was 77 psig (5.3

bar). Only the low molecular weight components and water passed through the membrane. The resulting alginate filtrate had to be lyophilized to dryness to return to the desired 1% concentration. In addition, the solution was still found to have thermophilic spores even after passing through the 0.1μm filter. This was most likely due to the high pressure causing the pores of the filter to deform and thereby allowing the small bacillus spores to pass through. Bacillus *subtilis* endospores range in size down to ca. 0.38 microns in diameter (Katz, 2005).

3.1.1.1. **Cross linking solution**

Several formulations were examined for the calcium chloride cross linking solution. Initially the calcium chloride was just dissolved in WFI for cell culture applications. Calcium chloride could not be added to a buffered phosphate saline solution, such as PBS, because when combined a calcium phosphate precipitate formed. Therefore the final cross linking formulation selected was calcium chloride in n-saline for the reasons described above for the alginate solution. The pH of the $CaCl_2$ in n-saline solution was adjusted between 7 to 7.4 using 0.1N NaOH. All of the $CaCl_2$ formulations were sterile filtered through a 0.2μm cellulose acetate membrane (Nalgene) or autoclaved for 22 minutes at 121°C. Barium chloride was also investigated as a potential cross linking solution. This experiment is described in section 3.3.4.

Cells are known to be sensitive to calcium levels, particularly muscle cells which contract and dilate during stimulus. In addition, calcium levels could adversely affect cell receptors, such as cadherins, which are transmembrane, calcium dependent glycoproteins that mediate cell-cell interaction by binding homophilically (by adhering to the same cell surface adhesion protein) with adjacent cells (Kukreti, 1998). Calcium ions are essential in stabilizing the active conformation of the cadherins. Another family of cell adhesion receptors, selectin, is completely dependent on the conformational changes associated with filling of two Ca^{2+} binding sites. Binding is also sensitive to pH which must be maintained near physiological levels (Kukreti, 1998).

The physiological $CaCl_2$ concentration for cells, which is present in DMEM medium, is 1.8mM. The concentrations used to cross link the alginate are considerably higher

and may be toxic to cells such as rSMCs. The molar concentrations of $CaCl_2$ were calculated to be 180, 90, 45, and 9mM for 2%, 1%, 0.5%, and 0.1% solutions respectively. Due to the high molarity of the $CaCl_2$ solutions needed to cross link the alginate molecules, the lowest concentration that was found to reproducibly work was 0.5%. 1-2 % $CaCl_2$ was found to work as well as a 0.5% solution, typically a 1% concentration was used. These results corresponded well with Martinsen (1989) who showed gel strength and volume reduction were independent of $CaCl_2$ concentration above 20mM. Section 3.3.2.3 describes an experiment conducted to determine if the transient exposure to $CaCl_2$ was toxic to rSMCs.

3.1.2. Sterility issues with alginate

During culturing in MSCCM, the alginate-GRGDY beads with entrapped hMSCs were observed turning white (or black, microscopically due to loss of light transmission) when the alginate was autoclaved beginning with the 'intermediate' alginate-GRGDY process (section 2.3.3, Figure 4). The potential source of the contamination was investigated by sterility testing of all components of the derivatization process (as described in section 2.3.3.7) and the cell cultures (section 2.2.2.3). From the sterility tests performed, microorganisms were observed in the alginate samples despite having undergone autoclaving. Therefore, all of the conditions for autoclaving were monitored. The autoclaves were serviced and calibrated routinely. Correct temperature, pressure and sterilization length were verified using the 3M Electronic Test System device (3M Health Care Ltd., Loughborough, UK); and indicator ampoules containing Bacillus stearothermophilus spores (Sterikon plus Bioindicator, Merck KGaA, Darmstadt, Germany) were used to verify kill of heat resistant microorganisms. The autoclaves were found to be functioning properly. It was hypothesized that the high viscosity of the alginate could be protecting the microorganisms from thermal inactivation. Therefore 1%, 0.1% and 0.01% alginate solutions in water were prepared and autoclaved with a control (water, no alginate). All samples were placed in terrific broth or in DMEM and incubated overnight at 37°C. All samples except the control were positive for microbes (under microscope 60X magnification). A sample from the 1% autoclaved alginate was re-combined with terrific broth to make a 0.1% alginate solution and was autoclaved again. This sample was then added to new DMEM or terrific broth and incubated at

37°C. The re-autoclaved samples contained a few microorganisms (observed microscopically under 60X magnification).

Samples of the autoclaved 1% (Manugel DMB) alginate in water were submitted to Dr. Michael Wren at University College London Hospital for identification. The actively growing microbes were recovered from the alginate solution by plating on agar media plates using standard microbiological techniques. Then the microbes were dehydrated by graded series of ethanol to cause sporulation. Then the new solution of spores (not in the presence of alginate) was autoclaved again to see if the spores were truly thermophilic and not due to inadequate sterilization caused by the alginate's high viscosity or other protective effects. Tubes of the autoclaved spores were incubated in a 37°C incubator and 60°C water bath with control ampoules of thermophilic spores (Sterikon). Live bacillus cultures were microscopically observed from the autoclaved spores the second time through the autoclaving process. Finally, the microbes from the original alginate sample were identified by the Central Public Health Laboratory (Colindale, London, UK) as Bacillus *licheniformis*. Other commercial alginate sources in the lab were autoclaved from Pronova test kit (MVG, LVG, LVM, MVM); and were also observed to contain microbes after autoclaving; although the microbes were not specifically identified as was done for the Manugel DMB alginate.

Interestingly, other groups have studied immobilized spores (Bacillus subtilis and Bacillus stearothermophilus) in alginate beads as bioindicators in the validation of thermal sterilization processes (Serp, 2002). Therefore the protective effect of alginate from thermal inactivation of thermophiles has been studied. Bacillus *licheniformis* has been isolated from marine alga (Yan, 2003), but no previous reports were found from isolation in alginate. Bacillus *licheniformis* was isolated from milk powder from 18 different countries (Ruckert, 2004). Although believed to be non-pathogenic, Bacillus *licheniformis* has been shown to be cytotoxic to McCoy mouse cells (Lindsay, 2000), and harmful when injected into pregnant cows (Agerholm, 1999) and immunodepressed mice (Agerholm, 1997). There have been five cases reported of Bacillus *licheniformis* infection in patients with cancer and central venous catheters (Blue, 1995). Given these reports, clearance of this microorganism from alginate is absolutely essential to its future use as an implantable tissue engineering matrix. The variability of its removal using different purification processes may be

one of the reasons why alginate implants have elicited varied immune responses in animal studies (Klock, 1994; Zimmerman, 2000; Orive, 2002).

3.2. Derivatization of alginate-GRGDY

This section summarizes the general physical results for derivatization of alginate with GRGDY peptides. Results from studies conducted with rSMCs and hMSCs for bioactivity (cell association) and characterization are provided in sections 3.3 and 3.4. A description of the three derivatization methods used to prepare alginate-GRGDY during the course of this research was provided in the Materials and Methods section 2.3.3 and summarized in Figure 4. A synopsis of these processes is provided in Table 9. The range of reactant's concentration used in the alginate-GRGDY derivatization were increments (e.g. 1X, 10X and 50X) of Rowley's (1999) reactant concentrations, where 1X was 1mg of alginate containing 38μg of sulfo-NHS, 67μg of EDC and 1μg of peptide; 10X was ten times the reactants and 50X was fifty times the reactants (section 2.3.3.2).

	Alginate treatment	Concentration of reactants	Dialysis	Treatment post-dialysis	Concentration
Method 1: Initial process	none	1X, 10X, 50X	3.5 kDa cassette	Activated charcoal and Celite filtration	None or lyophilization tried
Method 2: Intermediate process	Autoclaved	1X, 3X, 9X, 27X, 35X	3.5 or 10 kDa cassette	None	PEG (solid and liquid)
Method 3: Sterile process	Sterile (Pronova SLG100)	1X, 3X, 6X, 9X, 12X, 27X 0.2μm filtered reactants	gamma-irradiated cassettes, 0.2μm filtered water in LFH	None	Lyophilization

Table 9. Summary of the three methods used to produce alginate-GRGDY. The 'initial process' was tested using 1X, 10X and 50X reactants (e.g. sulfo-NHS, EDC and peptide) and after dialysis was treated with activated charcoal and filtered through Celite. The 'intermediate process' used autoclaved alginate which was tested using 1X-35X reactants and the post-dialysis alginate was concentrated using polyethylene glycol (PEG). The 'sterile process' utilized sterile Pronova SLG100 alginate using 1X-27X reagents that were filtered prior to use. Aseptic operations were conducted in a laminar floor hood (LFH) using sterilized equipment, 0.2μm filtered water for dialysis, and the post-dialyzed alginate was lyophilized.

3.2.1. Effect of alginate source/treatment on reactant concentration

As described in the methods section 2.3.3, the 'initial process' used 1% alginate in MES/NaCl buffer which was made by reconstituting the alginate overnight without autoclaving. These solutions were the most viscous and required the highest reactant concentrations (50X) to achieve cellular interaction. This cellular interaction was evident by the elongation of the cells from the initial spherical shape obtained after trypsinization and immobilization in the alginate hydrogel. The 1X and 10X concentrations had little or no cellular interaction. These results are discussed for rSMCs in section 3.3 and for hMCSs in section 3.4. The 50X concentration was needed for high guluronic acid containing alginates (Fluka, Manugel, Pronova). During the 'intermediate process', the 1% alginate in MES/NaCl buffer was autoclaved and immediately the effective concentration of reactants decreased to 27-35X because the 50X beads did not maintain shape and completely dissociated within 1 day after immobilization. This was most likely due to the lower gel strength after sterilization due to the decrease in the high molecular weight components (Leo, 1990; Vandenbossche and Remon, 1993; Wong, M., 2001). In addition, the 50X reactants incorporated many more GRGDY peptides onto the guluronic acid subunits, thereby not permitting enough calcium binding sites to hold the polysaccharide chains together. Thus the hydrogel dissociated very rapidly. Figure 10 shows the calcium binding sites between adjacent G subunit blocks which would be blocked by the presence of a GRGDY peptide within the binding domain. Finally, the 'sterile process' used highly purified, sterile alginate (Pronova SLG100) which was higher in viscosity (ca. 148mPa·s) than autoclaved Manugel (ca. 5mPa·s). For this process, the 27X reactants were too high, possibly due to its higher purity, and hydrogel beads dissociated within 1 day of formation. Therefore 9-12X reactants were determined to be optimal.

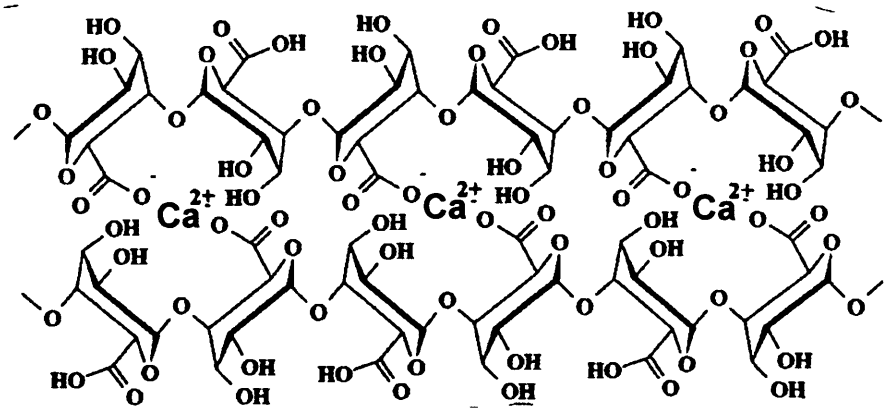

Figure 10. Schematic showing the calcium (Ca^{2+}) binding site with the carboxylic acid groups (COO-) on adjacent guluronic acid molecules. This is the same site on which the GRGDY peptide was attached. (adapted from Llanes, 2000)

3.2.2. Other factors influencing reactant amounts

As described in the previous section, the alginate source and treatment affected the concentration of the reactants. However, large batch variability of EDC was also detected when the EDC batch was changed from Sigma lot number S08123-262 to S14736-023. As a result, the effective concentration of reactants decreased from 27-35X to 9X. In addition, the temperature used for the carbodiimide reaction was found to affect the reaction, as would be expected due to changes in reaction rates and molecular mixing. Temperature control of the steps would be beneficial since the room temperature ranged between 20-26°C. In addition the temperature during dialysis varied from cold (6-10°C) during the initial process to very warm (26-31°C) in the hood during the sterile process. The diffusion of molecules across the dialysis membrane would certainly be affected by temperature.

3.2.3. Dialysis length

During this research the length of dialysis in water varied from 2 to 6 days. Initially a 2 day dialysis length was frequently used for speed of operation. In addition the dialysis cassette membrane expanded considerably within the first 48 hours, and there was concern that the cassette would burst if dialysis continued for a longer length. A 2 day dialysis length for the 'initial process' was probably sufficient because of the subsequent charcoal absorption step. However, later in the 'intermediate process' it became evident that 2 days of dialysis was insufficient. It was observed that the

hydrogels (i.e. beads) would swell within 24 hours after formation. The outer shell of the bead was still intact however the inner contents of the beads appeared to spill out due to the influx of water into the bead. Therefore dialysis was returned to a minimum of 5 days during the 'sterile process'.

3.2.4. Charcoal absorption and diamentacous earth (Celite) filtration

Activated charcoal absorption provided an advantageous step to remove heavy metals and polyphenols from commercial alginate (Skjåk-Bræk, 1989) and other cell-toxic residuals, such as EDC, leftover from the carbodiimide reaction. However, this absorption process was not suited for sterile operations that are mandatory for cell culture applications. In addition, the Celite filtration times were very long (5-8 hours) due to the high viscosity and the high molecular weight components (long chain polysaccharides) that were retained in the Celite film layer. As a result the alginate-GRGDY filtrate, although biologically active, had a very low alginate concentration (i.e. water-like consistency) and evidently consisted of primarily small chain polysaccharides (i.e. low molecular weight) causing the cell/alginate beads to be amorphous, often pancake or donut shaped, after cross linking in $CaCl_2$.

3.2.5. PEG concentration

As discussed earlier, dialysis caused the alginate to have an increase in water content due to influx of water into the dialysis cassette. During the 'intermediate process', solid PEG crystals (8K and 35K MW) were used to concentrate the alginate-GRGDY after dialysis while still inside the dialysis cassettes. This method was non-sterile, messy, and cumbersome because the PEG had to be carefully scraped off the membrane surface in order to monitor the volume/weight change of the alginate-GRGDY. In addition, the water diffusion across the membrane did not decrease consistently at the same rate (mL/hr) possibly due to the variable change in membrane pore size due to stretching of membrane from influx of water. Thus the concentration step required hourly monitoring. Using the liquid Pierce concentrating solution was slightly easier than the solid PEG; however it still had the problem associated with monitoring the decrease in volume. Although the concentrating solution was provided sterile, it was impossible to handle the dialysis cassettes in a sterile manner for multiple weighing.

3.2.6. Lyophilization

During the 'initial process', lyophilization was associated with decreased biological activity such that the cells did not elongate within the alginate-GRGDY hydrogel post-lyophilized to the same extent as within the hydrogel prior to lyophilization. This was most likely because the alginate-GRGDY did not freeze-dry properly. Phase change alters the pH and moisture that can damage peptides (Wu, 2000; Baffi and Garnick, 1992; Volkin and Klibanov, 1992). The lyophilization unit was shared with multiple users which frequently resulted in the removal of the alginate-GRGDY from the unit prior to completion of the drying process. If material was removed during the cycle or prior to complete drying; any remaining frozen water crystals would melt due to the loss of vacuum and/or increase in temperature above the glass transition temperature. Even if refrozen, the water becomes bound to the dried material resulting in higher final moisture content and decreased stability of the peptide in the alginate cake. Therefore during the 'intermediate process', the use of PEG was investigated to concentrate the alginate-GRGDY as described in previous section 3.2.5. However, due to the disadvantages with using PEG, lyophilization was revisited for aseptic improvements during the final 'sterile process'. Once a dedicated lyophilizer was used and a strict 2 day minimum cycle length was followed, the biological activity of the lyophilized alginate-GRGDY seemed to improve. In addition, a more reliable alginate concentration could be achieved upon reconstitution, and aseptic operations such as transfer of alginate after dialysis into sterilized vials for freeze drying were possible to maintain sterility.

3.2.7. Reconstitution of alginate-GRGDY

Lyophilized alginate-GRGDY was typically reconstituted with n-saline (0.9% NaCl) to achieve a final 1% alginate concentration so that it was isotonic for subsequent addition to the cell suspension. Reconstitution of lyophilized alginate-GRGDY using n-saline was not a problem for alginate that was only dialyzed for 2 days. However after 5 days of dialysis, the sterile (Pronova SLG100) alginate-GRGDY would not reconstitute using n-saline. Apparently the extensive dialysis with water removed the majority of the sodium ions resulting in protonation of the carboxyl groups on the non-GRGDY-derivatized alginate polysaccharides turning it into alginic acid which is

insoluble in water (Doumeche, 2004). However, alginic acid can be solubilized by adding sodium carbonate (Na_2CO_3), sodium hydroxide (NaOH) or trisodium phosphate $Na_3PO_4 12H_20$) (www.fao.org/docrep/W6355E/w6355e04.htm). In this system, phosphate and carbonate were not desirable. Therefore the sterile (Pronova SLG100) alginate-GRGDY dialyzed for 5 days was solubilized by adding ca. 22.5-35μL of 1N NaOH (Sigma) to 0.75-1mL of n-saline (not pH adjusted) in each vial. Less NaOH, if any, was needed to reconstitute the alginate-GRGDY that underwent a shorter dialysis length. The pH was measured to be 8.5 for 2-day dialyzed alginate-GRGDY reconstituted with 13μL 1N NaOH per mL of n-saline. However the pH was 4.0 for 5-day dialyzed alginate-GRGDY reconstituted with 22.5μL 1N NaOH per mL of n-saline. These results were extremely variable due to the difference in dialysis length. However, the readings were taken using minimal sample volume to cover the electrode; therefore future readings will be performed with a micro-electrode. In addition the viscosity of the reconstituted 1% alginate-GRGDY was measured using a cone and plate rheometer and found to range between 29 to 56mPa·s. In addition a sample containing 0.75% w/v alginate-GRGDY containing $9x10^6$hMSCs/mL was measured to be 33mPa·s. The original (underivatized) Pronova SLG100 was measured to be 60mPa·s when reconstituted to 0.75% w/v in culture medium with no cells.

3.2.8. Sterility of alginate-GRGDY

Reactants used in the carbodiimide chemistry were tested for sterility using terrific broth as described in section 2.3.3.7. Prior to the introduction of 0.2μm filtration it was found that the GRGDY peptide contained low levels of microbes. In addition the pharmaceutical grade alginates were found to contain the thermophilic bacillus spore, B.*licheniformis* (section 3.1.2). All of the other components including the sulfo-NHS, EDC and the Pronova SLG100 alginate appeared to be free from microbial contamination. However 0.2μm filtration was still performed on the sulfo-NHS and EDC because it was possible that there were still microbes present, but unable to grow under the conditions of the sterility test. The EDC caused precipitates to form in the terrific broth, but did not affect the testing and observations. After ensuring sterile components and equipment throughout the process, samples from the various process steps were found free from microbial contamination including: post 20 hour reaction,

post dialysis using 0.2μm filtered water and gamma-irradiated dialysis cassettes, and post lyophilization and reconstitution. Samples were maintained and observed out to 2 weeks to confirm sterility.

3.2.9. Summary

Sodium alginate was selected as the matrix for this research project based upon the success of alginate hydrogels in the cell therapy field and the initial success reported growing anchorage dependent cells on the surface of hydrogels by incorporating RGD containing peptides onto the polymer backbones. In addition, a variety of hydrogel shapes (e.g. sheets, tubes and beads) could be easily fabricated using solutions of divalent cations such as $CaCl_2$. Sodium alginate solutions were prepared using a variety of commercial sources with different properties including composition of mannuronic and guluronic subunits and molecular weights (viscosities). Autoclaving was used as a method of sterilization; however it was associated with a severe decrease in viscosity (i.e. 1% solution - 200mPa·s reduced to 5mPa·s). Sterile filtration was performed using a 0.1% alginate solution through a series of Cuno Inc. filters down to 0.1μm pore size with low volume throughput. Both sterilization methods were found to be unacceptable for elimination of microbes. The thermophilic bacillus spore, B.*licheniformis*, was found to be contained in several of the commercial alginate suppliers. Sterile Pronova SLG100 alginate was procured and found to be free from these microbes. The cross linking solution used for the majority of the experiments was 1% $CaCl_2$ in n-saline pH 7-7.4, despite its high molarity (90mM) compared to physiological conditions (ca. 2mM). Carbodiimide chemistry was used to incorporate GRGDY peptide onto the alginate polysaccharide polymer. A progression of three derivatization processes was used during the course of the project culminating in a final sterile preparation. The amount of reactants (e.g. sulfo-NHS, EDC and peptide) added to the alginate was varied between 1X and 50X, where 1X was 1mg of alginate containing 38μg of sulfo-NHS, 67μg of EDC and 1μg of peptide; and 50X was fifty times the reactants per 1mg of alginate. The concentration of reactants was determined to be dependent upon the alginate type and treatment. Lower viscosity (molecular weight) and higher purity alginates needed lower concentrations of reactants probably due to better mixing and less impurities. Other factors such as EDC batch heterogeneity, reaction and dialysis temperature, and mixing could be attributed to further variability of the process. Hydrogels produced

with too many peptides incorporated into the guluronic polysaccharide chains dissociated within 1 day of formation most likely due to decreased gel strength, interference with calcium ion binding sites, or influx of water into the hydrogel due to residual levels of reactants remaining after a short (e.g. 2 days) dialysis step. At least 5 days of dialysis were deemed necessary to reduce the levels of residual reactants. However the excessive dialysis also rendered the sodium alginate into alginic acid; therefore NaOH was added upon reconstitution with n-saline to solubilize the alginate-GRGDY after lyophilization.

3.3. The characterization of rSMCs in tissue flasks and 3-D matrices

In order to understand and characterize rSMC growth within alginate hydrogels, the growth characteristics of rSMCs in tissue flasks needed to be established. RSMCs were obtained from an immortalized rat cell line, A7r5, from American Type culture collection. These cells have been well characterized (Kimes and Brandt, 1976). A frozen working cell bank was established for experiments conducted in this research project as described in section 2.1.1.1. The viability of the rSMCs post-thaw was 79 +/- 7% (n=11). The rSMCs were assessed according to its percent viability at each passage, the doubling time (hr), the population doubling per day (PD/day), and the glucose consumption rate (g/cell/hr). The cell concentration was measured using a hemacytometer, viability using trypan blue dye and the glucose and lactate concentrations in the culture medium using the YSI bioanalyzer. Following these measurements, the specific growth rate, glucose consumption rate (GCR) and respiratory quotient were calculated.

RSMCs were immobilized within alginate, collagen and alginate-GRGDY matrices, and the interaction of the rSMCs with the matrices was studied. These studies helped to concurrently establish the alginate-GRGDY derivatization process. The biological activity of the alginate and collagen matrices was assessed by observing the cells' interaction with the matrices, such as the change in morphology. The cells remained rounded (spherical) indicating no interaction, or the cells elongated indicating association with the matrix.

During preparation and culturing of 3-dimensional hydrogels, measurements such as viability of the cells post-immobilization into the alginate, cell density and glucose consumption were taken and compared to data for rSMC in 2-dimensional (tissue flasks) environments.

3.3.1. Growth of rSMC in tissue culture plastic

RSMCs were passaged according to section 2.1.1.2 and data such as the number of cells harvested per flask and viability were collected. These results were used to calculate the growth rate and doubling time of the rSMCs. In addition, samples of the spent medium were collected so that glucose and lactate measurements could be obtained using the YSI bioanalyzer as described later in this section. The average viability of the rSMCs during passaging was 97 +/- 2% (n=88). During trypsinization, the rSMCs adhered to the tissue culture plastic very strongly. Therefore the flasks were tapped firmly against the palm of the hand to release the cells from the plastic after being exposed to the trypsin/EDTA for about 5-6 minutes. Trypsinization was not possible in microwell plates because the cells adhered too strongly; and the cells could not be released by tapping due to medium spillage out of the microwells.

3.3.1.1. Growth rate of rSMCs

A7r5 rSMCs had a population doubling time of ca. two days in tissue flasks. Figure 11 shows graphs of three separate experiments examining the population doubling level (PDL) increase for rSMCs grown in T150 flasks over multiple passages (P1-P23). The PDL level was calculated by taking the logarithm of the population increase (the total number of cells harvested/cm^2 divided by the number of viable cells planted/cm^2) and dividing by the logarithm of 2 as described in section 2.5.4, equation 2.3 (Doran, 1995; Butler, 2004). The slopes of the linear approximations averaged 0.019 ± 0.0008 PD/hr. These lines were fit through zero. The inverse of the slope of the line was the doubling time, t_d, which averaged 53 ± 2 hours. The growth rate, μ, was calculated as the natural logarithm of 2 divided by the doubling time as described in section 2.5.4, equation 2.5 (Doran, 1995; Butler, 2004) and multiplied by 24 (to convert hours to days) which averaged 0.31 ± 0.01 day^{-1}.

A

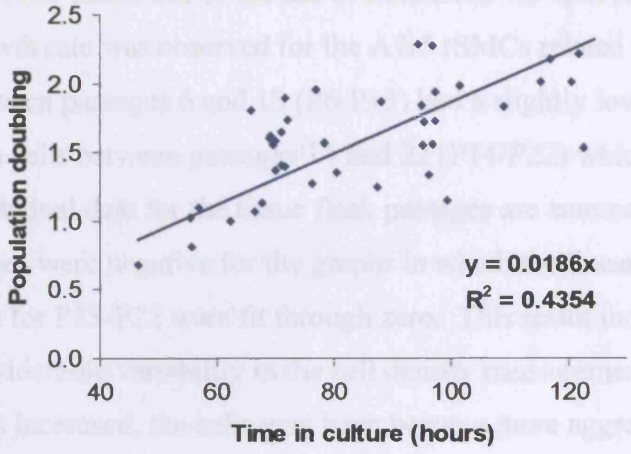

B

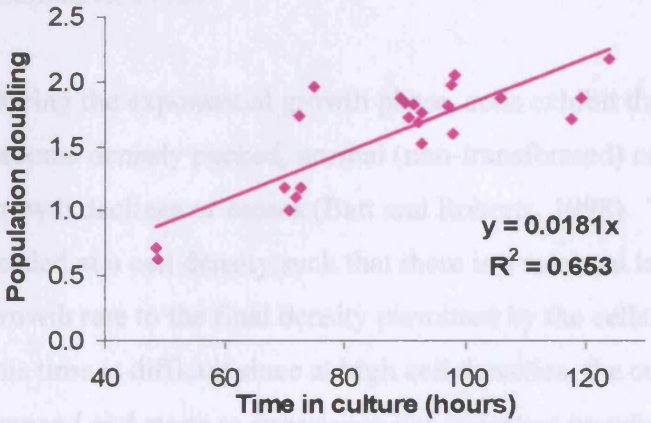

C

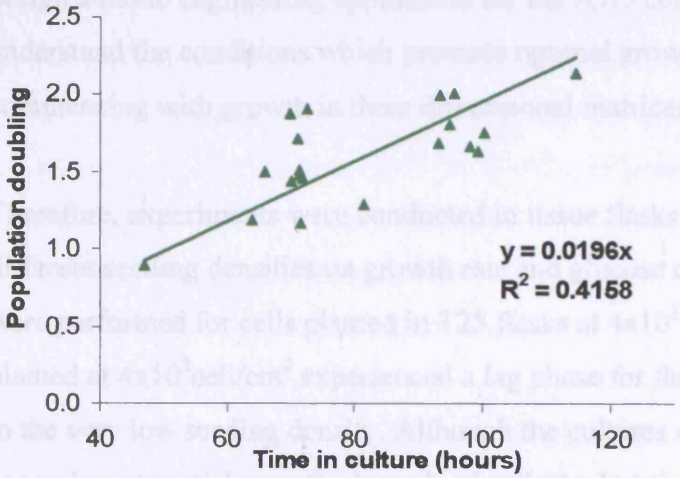

Figure 11. Population doubling level (PDL) increase for rSMCs grown in T150 flasks for three cell expansions. (A) Original vial from ATCC. (B) and (C) Two cell expansions from the frozen working cell bank made from original vial. The inverse of the slopes of these linear approximations was the doubling time of the cells 53 +/- 2 hours.

The initial seeding density was not tightly controlled during the routine passaging of the T150 flasks due to the use of a standard 1:3 split ratio. A very slight difference in growth rate was observed for the A7r5 rSMCs related to passage number. Cells between passages 6 and 13 (P6-P13) had a slightly lower growth rate of 0.30 day^{-1} than cells between passages 14 and 22 (P14-P22) which was 0.33 day^{-1}. The individual data for the tissue flask passages are summarized in Table 10. The R^2 values were negative for the graphs in which the linear estimate for the growth rate data for P13-P22 were fit through zero. This result indicated that there was considerable variability in the cell density measurement. As the passage level of the cells increased, the cells may have become more aggregated upon trypsinization which led to greater inaccuracy in the cell density at later time points in culture (Lombarts, 1992).

During the exponential growth phase, cells exhibit their highest growth rate. As they become densely packed, normal (non-transformed) cells become contact inhibited and growth declines or ceases (Batt and Roberts, 1998). The optimal culture processes are seeded at a cell density such that there is a minimal lag phase, ensuring a maximum growth rate to the final density permitted by the cells. Maintaining the cells beyond this time is difficult since at high cell densities, the culture has a high nutritional demand and starts to experience gas and mass transfer limitations. All *in vitro* mammalian cell cultures exhibit a decline in growth and eventual death. In order to design a tissue engineering application for the A7r5 cells, it was essential to understand the conditions which promote optimal growth in tissue flasks prior to commencing with growth in three dimensional matrices.

Therefore, experiments were conducted in tissue flasks to determine the effects of different seeding densities on growth rate and glucose consumption. Daily cell counts were performed for cells planted in T25 flasks at $4x10^2$ and $5x10^3$cell/cm^2. The cells planted at $4x10^2$cell/cm^2 experienced a lag phase for the first two days of culture due to the very low seeding density. Although the cultures seeded at $4x10^2$ cells/cm^2 entered exponential growth phase, by day 9 (the last time point at which cells were harvested) the cells were only at ca. $6x10^3$cells/cm^2. The cells seeded at $5x10^3$cells/cm^2 achieved a final cell density of ca. $2.7x10^4$cells/cm^2 on day 5.

The exponential growth phase of the cells in T25 flasks seeded at $4x10^2$ and $5x10^3$cell/cm^2, days 2-9 and 0-5 respectively, was plotted to determine the growth rate as shown in Figure 12.

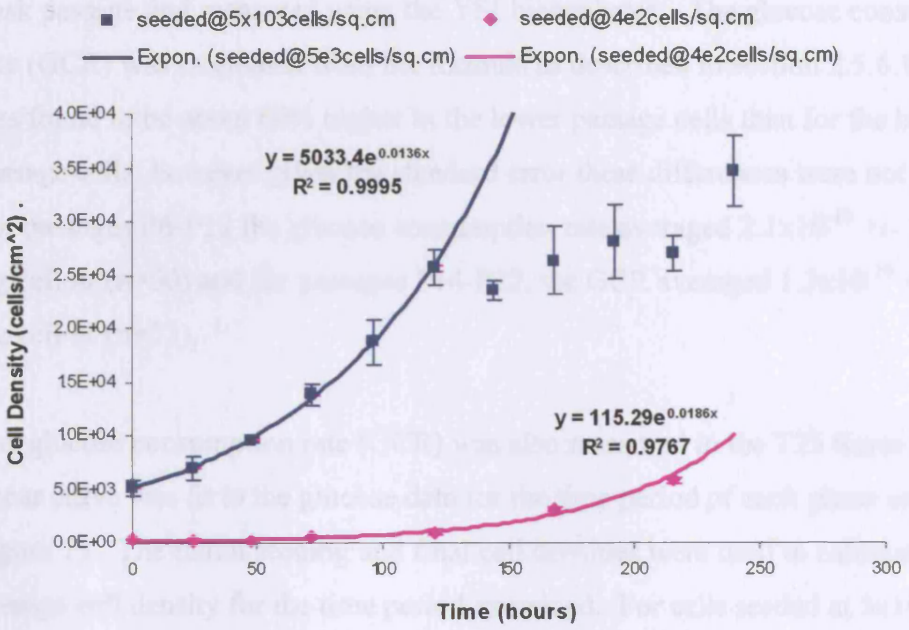

Figure 12. Cell growth curves for rSMCs cultured in T25 flasks at $2x10^4$ and $5x10^3$cells/cm^2. The data points for days 6-10 for cells seeded at $5x10^3$cells/cm^2 and for days 0-1 for cells seeded at $4x10^2$cells/cm^2 were excluded such that only the exponential growth phase of the culture was selected for analysis.

An exponential curve was fit to the cell growth data to determine the growth rate constant. The data points for days 6-10 for cells seeded at $5x10^3$cells/cm^2 and for days 0-1 for cells seeded at $4x10^2$cells/cm^2 were excluded such that only the exponential growth phase of the culture was selected for analysis. The exponential of the cells seeded at $4x10^2$cells/cm^2 was 0.019 hr^{-1} and for cells seeded at $5x10^3$cells/cm^2 was 0.014 hr^{-1}, respectively. Thus the doubling time was 71 hours for the cells seeded at $4x10^2$cells/cm^2 versus 53 hours for the cells seeded at $5x10^3$cells/cm^2. The growth rate, μ, was calculated by dividing the natural log of 2 by the doubling time and multiplying by 24 to convert hours to days. The growth rates were 0.23 day^{-1} and 0.31 day^{-1}, respectively. The viability of the cultures was also determined using trypan blue dye. Cells seeded at $4x10^2$cells/cm^2 maintained a viability $\geq$ 92% for the 9 days observed; and cells seeded at $5x10^3$cells/cm^2 maintained a viability $\geq$ 92% out to day 6 in culture and then gradually decreased to 85% on day 10.

3.3.1.2. Glucose consumption rate of rSMCs

Glucose measurements were taken from the spent medium from each T150 tissue flask passage and measured using the YSI bioanalyzer. The glucose consumption rate (GCR) was calculated from the formula as described in section 2.5.6.1. The GCR was found to be about 60% higher in the lower passage cells than for the higher passage cells; however given the standard error these differences were not significant. For passages P6-P13 the glucose consumption rate averaged $2.1x10^{-10}$ +/- $1.3x10^{-10}$g/cell/hr (n=50) and for passages P14-P22, the GCR averaged $1.3x10^{-10}$ +/- $0.4x10^{-10}$g/cell/hr (n=33).

The glucose consumption rate (GCR) was also measured in the T25 tissue flasks. A linear curve was fit to the glucose data for the time period of each phase as show in Figure 13. The initial seeding and final cell densities were used to calculate an average cell density for the time period examined. For cells seeded at $5x10^{3}$cells/cm^2 during the exponential growth phase between days 0-5, the glucose consumption rate was calculated to be $7.7x10^{-11}$g/cell/hr. For cells in stationary phase at a concentration of ca. $2.7x10^{4}$cell/cm^2 between days 5-10, the GCR was calculated to be $5.3x10^{-11}$g/cell/hr. Similarly for cells seeded at $4x10^{2}$cells/cm^2, the GCR during exponential growth between days 2-9 was calculated to be $6.5x10^{-11}$g/cell/hr.

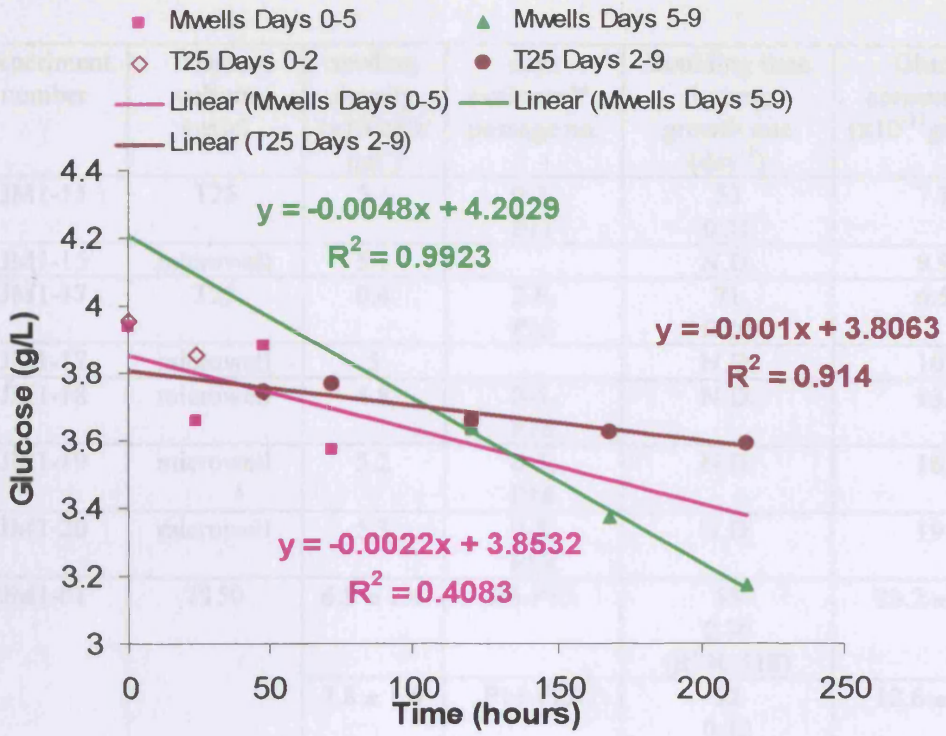

Figure 13. Glucose data for determination of glucose consumption rates in T25 flasks seeded at $4x10^2$cell/cm^2 and microwells seeded at $5x10^3$cells/cm^2.

Glucose consumption rates were also measured for cell growth in microwells. The average of 5 studies, all seeded at ca. $5x10^3$cells/cm^2, produced a glucose consumption rate of $1.4x10^{-10} \pm 4.2x10^{-11}$g/cell/hr. A summary table of the glucose consumption rates for all of these studies is shown in Table 10.

Overall, the glucose consumption rates were similar between flasks and microwells for SMC seeding densities between $4x10^2$ and $1x10^4$cells/cm^2. Therefore, the A7r5 rSMCs can be grown in either microwells or flasks for experimental purposes.

Experiment number	Tissue culture vessel	seeding density ($x10^3$cell/ cm^2)	days evaluated*, passage no.	Doubling time (hours); growth rate (day^{-1})	Glucose consumption ($x10^{-11}$g/cell/hr)
JM1-15	T25	5.1	0-5, P11	53 0.31	7.73
JM1-15	microwell	5.1		N.D.	9.94
JM1-17	T25	0.4	2-9, P15	71 0.23	6.53
JM1-17	microwell	5		N.D.	10.2
JM1-18	microwell	4.8	0-5, P16	N.D.	13.0
JM1-19	microwell	5.2	0-5, P18	N.D.	16.6
JM1-20	microwell	5.3	0-5, P19	N.D.	19.5
JM1-01	T150	6.8 ± 1.4	P6-P13	55 0.30 (R^2=0.518)	23.2 ± 15.4
		7.8 ± 1.6	P14-P22	52 0.32 (R^2=-0.249)	12.6 ± 6.04
JM1-12	T150	6.0 ± 1.7	P6-P13	59 0.28 (R^2=0.838)	19.0 ± 11.1
		8.5 ± 2.0	P14-P21	52 0.32 (R^2=-0.333)	12.6 ± 2.09
JM1-21	T150	7.8 ± 2.1	P6-P13	53 0.31 (R^2=0.576)	20.1 ± 10.8
		8.2 ± 1.2	P14-P20	50 0.33 (R^2=-0.360)	12.4 ± 2.96
* = days evaluated for exponential growth phase, P = passage number of cells , N.D. = not determined					

Table 10. Summary of doubling times, growth rates and glucose consumption rates for rSMCs grown in tissue vessels. The cells were grown in microwells, T25 and T150 flasks. The growth rate and GCR were similar for cells seeded at the same density. T150 flasks were used for cell passaging and T25 flasks were used for some growth curve studies. Microwell comparability to T-flasks was needed as an adequate control condition for the cell densities used with rSMCs immobilized in alginate beads.

3.3.2. RSMCs and non-derivatized alginate matrices

Initially matrix studies were performed using rSMCs with non-derivatized alginate hydrogels formed into sheets, tubes and beads as described in section 2.4. This section describes the results from these early studies and the progression that was made toward alginate-GRGDY hydrogels with an interlude exploring collagen as a matrix.

3.3.2.1. Effect of trisodium citrate on rSMCs viability

Once the rSMCs were incorporated into the alginate matrix, the matrix needed to be evaluated for cell density and viability using hemacytometer and trypan blue. The cells first needed to be released from the alginate hydrogel using 0.1M trisodium citrate as per section 2.5.5. Initial studies were performed to determine the effect of exposing the rSMCs to 0.1M trisodium citrate. Typical viability assessments took an average length of 10 minutes to complete three replicate counts and usually never exceeded 15 minutes. Therefore, a maximum time of 30 minutes was used to evaluate the effect of trisodium citrate.

As can be seen in Figure 14, the average overall viability of cells exposed to 0.1 M trisodium citrate solution was similar to that of the control cells which were resuspended in complete DMEM. In the first experiment, the average viability of cells exposed to trisodium citrate was 73 ± 7 % compared to the viability of control cells, which were not exposed to trisodium citrate, which was 79 ± 6% for the 20 minute evaluation period. In the second experiment, the viability of the cells exposed to trisodium citrate was 88 ± 4% and the viability of the control cells was 91 ± 4% for the 30 minute evaluation period. In addition, the cells exposed to 0.1M trisodium citrate did not appear to gradually decrease in viability during the evaluation periods.

Since the viability of cells exposed to trisodium citrate was similar to the viability of the control cells, 0.1M trisodium citrate solution can be used to release the cells from the alginate hydrogel in order to assess viability.

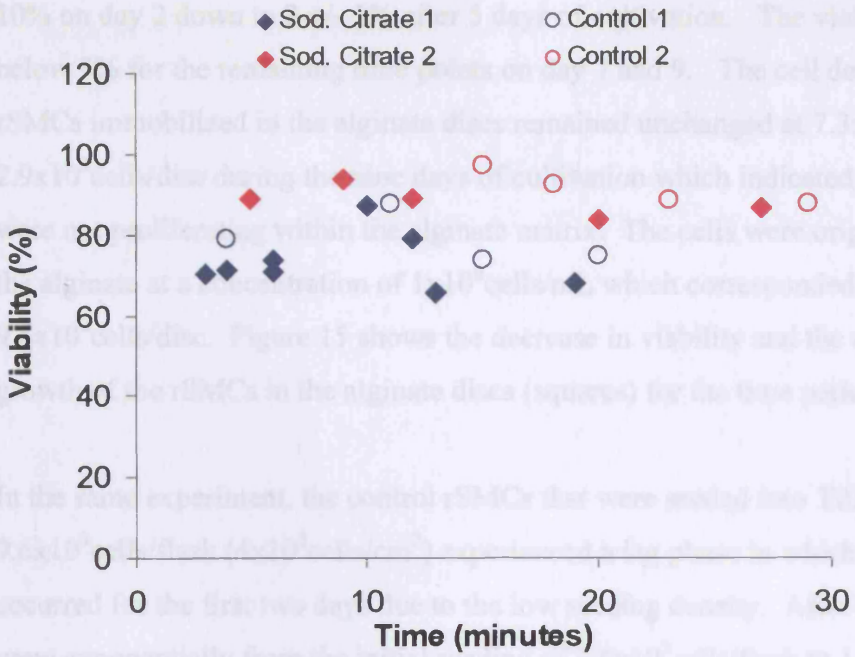

Figure 14. Effect of trisodium citrate on cell viability. RSMCs were exposed to 0.1M trisodium citrate for up to 30 minutes to determine if there was any decrease in viability of the cells during assessment as compared to control cells that were not exposed.

3.3.2.2. RSMCs immobilized in non-derivatized alginate tubes and beads

Initially rSMCs were immobilized in various formulations of sodium alginate and cross linked using $CaCl_2$ as per sections 2.3.1, 2.4.1, 2.4.3 and 2.4.4. In all experiments when n-saline or PBS was used to formulate the alginate, and the cells were centrifuged and resuspended in DPBS or complete DMEM, and the tube or beads were cross linked using 0.5 to 2% $CaCl_2$, the initial cell viability was high. The average cell viability immediately after cross linking for 42 different combinations of alginate, $CaCl_2$, and cell resuspension formulations was 89 +/- 9%. However for all these experiments, cell viability dropped significantly during the first 4 to 5 days in culture and the cells did not proliferate within the alginate matrix.

One experiment conducted in which cells were extruded in alginate tubes and discs were cut and placed into microwell plates as described in section 2.4.3.1, the average cell viability of the rSMCs immobilized in alginate disc was 87+/- 5% on day 0 and 60 +/- 10% on day 1. Thereafter, cell viability decreased significantly from 38 +/-

10% on day 2 down to 3 +/- 1% after 5 days of cultivation. The viability remained below 3% for the remaining time points on day 7 and 9. The cell density of the rSMCs immobilized in the alginate discs remained unchanged at $7.3x10^3$ +/- $2.9x10^3$cells/disc during the nine days of cultivation which indicated that the cells were not proliferating within the alginate matrix. The cells were originally seeded in the alginate at a concentration of $1x10^6$cells/mL which corresponded to ca. $9.6x10^3$cells/disc. Figure 15 shows the decrease in viability and the unchanged cell growth of the rSMCs in the alginate discs (squares) for the time period evaluated.

In the same experiment, the control rSMCs that were seeded into T25 control flasks at $9.6x10^3$cells/flask ($4x10^2$cells/cm^2) experienced a lag phase in which no growth occurred for the first two days due to the low seeding density. After day 2, the cells grew exponentially from the initial seeding of $9.6x10^3$cells/flask to $1.4x10^5$cells/flask on day 9. This growth corresponded to a population doubling level (PDL) increase of 3.9. The average control cell viability for the T25 flasks was ≥ 92% during the nine days of cultivation. The exponential increase in cell growth and high viability for the control cells are shown in Figure 15 (triangles).

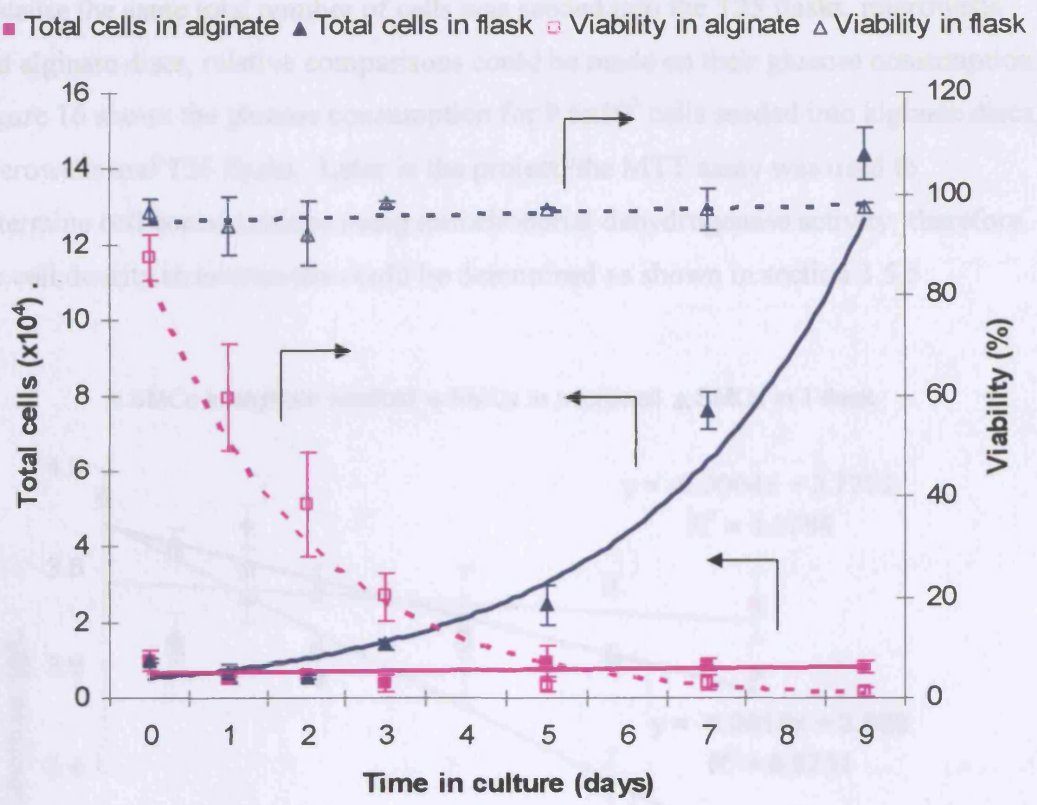

Figure 15. Total cells and viability for rSMCs in alginate discs and tissue flasks. The viability of the rSMCs in the alginate decreased from 87% to 3% over the 9 days; whereas the total cells remained the same at $7.3x10^3$ +/- $2.9x10^3$cells/disc. The control rSMCs in the flasks were >92% viable for the 9 days, and the cells grew exponentially from $9.6x10^3$ to $1.4x10^5$cells/flask.

In addition to cell growth and viability assessment, glucose measurements were taken of the spent medium from the microwells containing the cells in alginate discs seeded at $9.6x10^3$cells/disc/well and T25 flasks containing control cells seeded at $9.6x10^3$cells/flask ($4x10^2$cells/cm^2). Due to the very low seeding density of the control cells in the T25 flasks, control cells were also seeded into microwells at $9.6x10^3$cells/well ($5x10^3$cells/cm^2) which was a more optimal density per square cm. Controls cells were set up in both flasks and microwells because rSMCs seeded into microwells could not be adequately trypsinized and evaluated for density and viability. In order to detach the rSMCs from the growth surface, the culture vessels need to be tapped firmly against the palm of the hand; hence the liquid contents easily spilled out of the shallow, open-topped microwells during this step. Therefore, control rSMCs seeded into microwells were only evaluated for glucose consumption.

Because the same total number of cells was seeded into the T25 flasks, microwells and alginate discs, relative comparisons could be made on their glucose consumption. Figure 16 shows the glucose consumption for $9.6x10^3$ cells seeded into alginate discs, microwells and T25 flasks. Later in the project, the MTT assay was used to determine cell concentrations using mitochondrial dehydrogenase activity; therefore the cell density in microwells could be determined as shown in section 3.5.5.

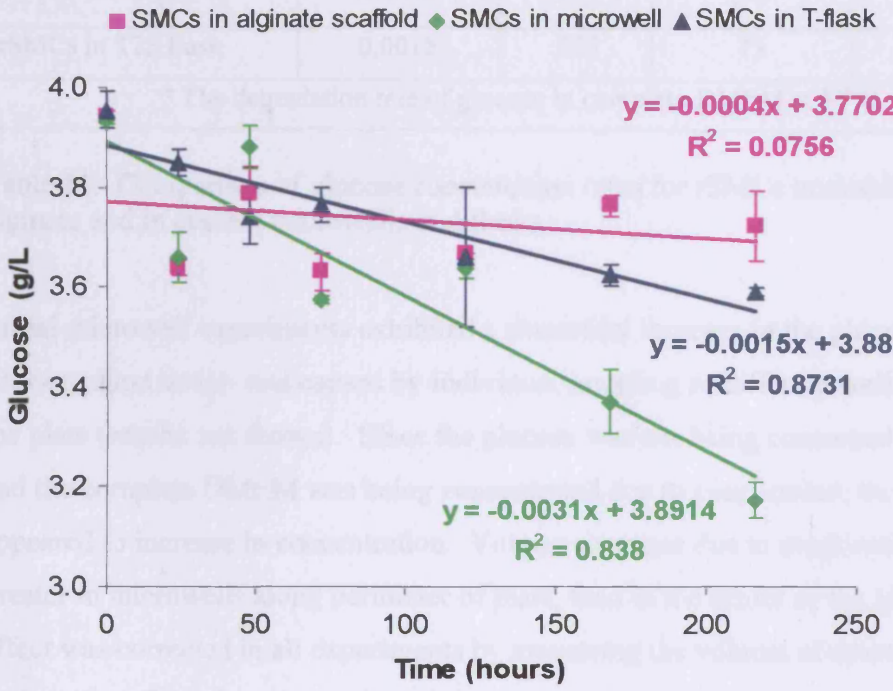

Figure 16. Glucose consumption for rSMCs immobilized in alginate versus control cells in tissue flasks and microwells. The GCR for the rSMCs in the alginate was zero, which indicated the cells were not proliferating compared to rSMCs in the tissue culture plastic.

A linear curve was fit to the glucose data, and then the glucose consumption rate (GCR) was calculated for the different vessel volumes (1mL for microwells and 5mL for T25 flasks). The GCRs are summarized in Table 11. In addition, the degradation rate of glucose in the complete DMEM at 37°C was also measured to be 0.0002g/hr. The GCR for the cells in alginate discs was 0.0004g/hr, only 2 fold higher than glucose degradation rate. This increase was insignificant when compared to the 15.5 fold increase in GCR for the cells in microwells and 37.5 fold increase in flasks. Overall the low GCR indicated that the rSMCs immobilized in alginate were not proliferating as compared to the control cells.

	Glucose consumption or degradation rate (g/L/hr)	Volume per vessel (L)	Glucose consumption or degradation rate ($x10^{-7}$g/hr)	Fold increase over the degradation of glucose at 37°C
complete DMEM*	0.0002	.001	2.0	-
rSMCs in alginate disc	0.0004	.001	4.0	2
rSMCs in microwell	0.0031	.001	31	15.5
rSMCs in T25 flask	0.0015	.005	75	37.5
* The degradation rate of glucose in complete DMEM at 37°C.				

Table 11. Comparison of glucose consumption rates for rSMCs immobilized in alginate and in control microwells and flasks.

Initial microwell experiments exhibited a sinusoidal increase in the glucose concentration which was caused by individual sampling of different well locations in the plate (results not shown). Since the glucose was not being consumed by the cells and the complete DMEM was being concentrated due to evaporation, the glucose appeared to increase in concentration. Volume decrease due to evaporation was greater in microwells along perimeter of plate, than in the center of the plate. This effect was corrected in all experiments by measuring the volume of spent medium in each well or flask that was evaluated. The individual glucose concentrations were then corrected by multiplying the measured glucose concentrations by the ratio of original medium volume to the measured medium volume at each time point.

Another experiment was conducted to determine the effect of the type of complete medium and alginate on cell proliferation and viability. RSMCs were immobilized in 1% Sigma and 1% Fluka alginate beads as per section 2.4.1 and 2.4.4. Two complete medium formulations, DMEM and αMEM, were used to resuspend the rSMCs and as the growth medium for cultivating the beads in microwells. In addition one tube was made with Sigma alginate and αMEM medium and cut into 7mm discs to compare to the same condition made into beads. Another condition included cells in Sigma alginate beads with αMEM which were refed daily with fresh αMEM out to day 7 to compare to static cultures.

During the 16 days of assessment, the cell density for all conditions remained unchanged at ca. $1x10^4$cells/well from two 2 mm beads (data not shown). The cell viability of all alginate and medium conditions immediately after immobilization of the cells was very high at 94 +/- 2%; however, thereafter all viabilities decreased. Both the Fluka and Sigma alginates using complete DMEM had the sharpest decrease in viability down to 3 +/- 1% by day 5 (Figure 17, dashed lines); whereas, all other conditions using αMEM medium had only decreased down to 42 +/- 7% (solid lines). However all of the conditions using αMEM medium decreased down to 7 +/- 3% viable by day 16. It was apparent that the presence of additional nutrients (e.g. nonessential amino acids, antioxidants, deoxy- and ribonucleosides) in the αMEM medium maintained higher cell viability as compared to the complete DMEM.

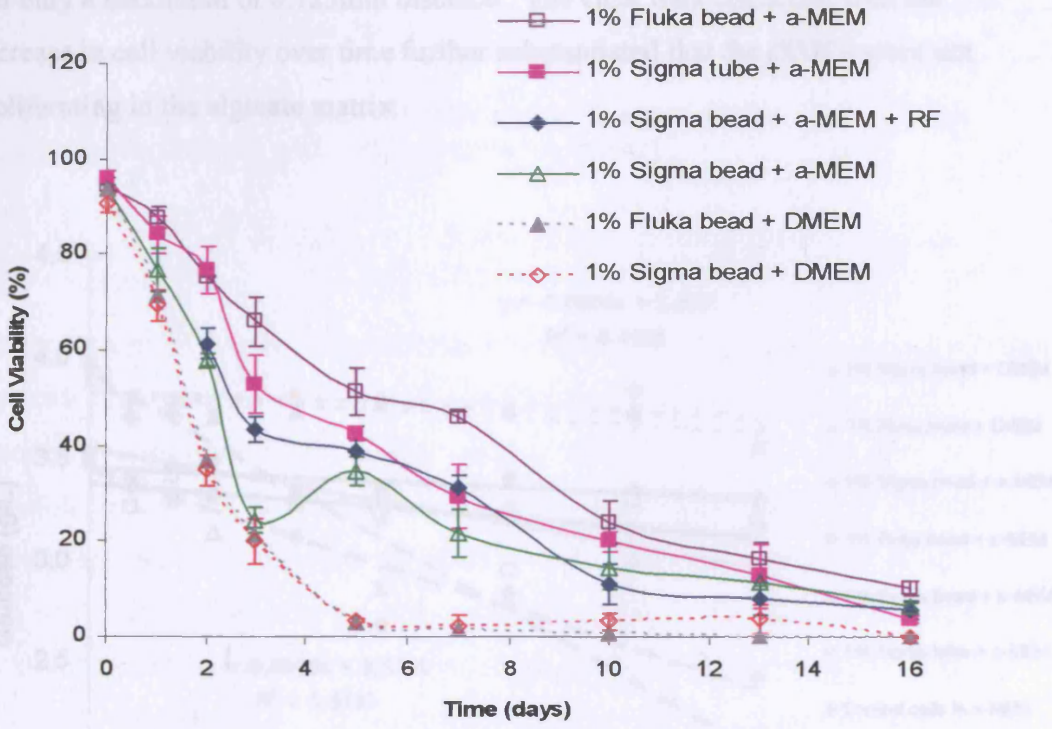

Figure 17. Viability of rSMCs immobilized in different types of alginate and complete media. The viability of the rSMCs cultured in αMEM medium was significantly greater than the viability of the rSMCs in the complete DMEM. The type of alginate (e.g. Fluka or Sigma) appeared to be less significant.

Glucose data were obtained from the spent medium samples collected from each condition. Linear approximations of these data, which are shown in Figure 18, were used to calculate the slope in order to estimate the glucose consumption rate (g/L/hr).

The GCR was multiplied by the microwell volume (0.001L) to achieve a GCR in g/hr. As shown in Table 12, the GCR was greatest in the control cells (not in alginate) seeded at $9.6x10^3$cells/well or $5x10^3$cells/cm^2. The GCR for cells grown in the complete DMEM medium was 24.5 fold higher than the glucose degradation rate at 37°C. Control cells in the αMEM medium were 14 fold higher than the background rate. The highest GCR for the alginate conditions was for the cells immobilized in the Sigma alginate tube and αMEM medium which was 7.5 fold higher than the background rate. All of the other alginate conditions had nominal GCRs only 1.5 to 3.5 fold higher. One possible reason for the higher GCR for the alginate tube condition than for the beads may be due to the wall thickness (mass transfer layer) of the alginate matrix. Cells in the 2mm beads had a maximum diffusion distance of 1mm to the edge of the alginate whereas cells in a 0.25mm thick disc cut from a tube had only a maximum of 0.125mm distance. The GCR data combined with the decrease in cell viability over time further substantiated that the rSMCs were not proliferating in the alginate matrix.

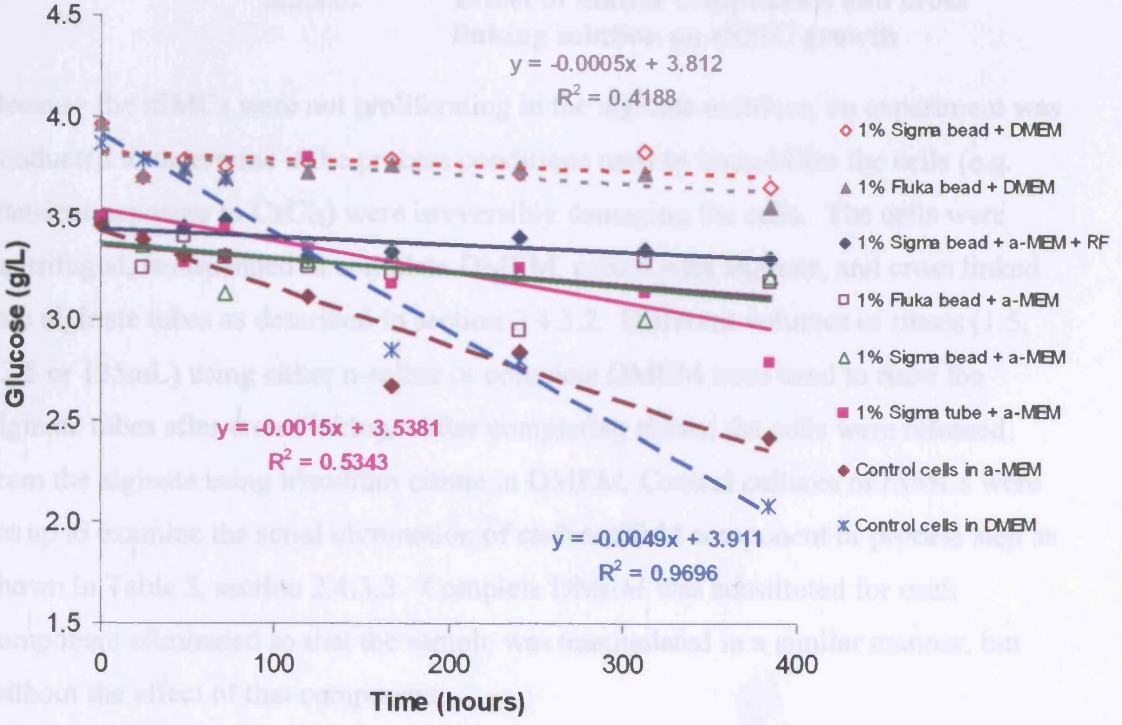

Figure 18. Glucose consumption of rSMCs immobilized in different types of alginate and complete media. The GCR of rSMCs in alginate, regardless of type and media, was significantly lower than the GCR of the control cells (no alginate) in microwells.

	Alginate type	Complete medium type	Glucose consumption or degradation rate ($x10^{-7}$g/hr)	Fold increase over the degradation of glucose at 37°C
Complete medium only *	NA	DMEM	2	-
Control cells	NA	αMEM	28	14
	NA	DMEM	49	24.5
Cells in beads	Sigma	αMEM	7	3.5
	Fluka	αMEM	7	3.5
	Sigma	DMEM	3	1.5
	Fluka	DMEM	5	2.5
Cells in tube	Sigma	αMEM	15	7.5
Cells in beads with refeeds	Sigma	αMEM	4	2
* The degradation rate of glucose in complete DMEM at 37°C.				

Table 12. Comparison of glucose consumption rates for rSMCs immobilized in alginate beads and tube with different complete media.

3.3.2.3. Effect of matrix components and cross linking solution on rSMC growth

Because the rSMCs were not proliferating in the alginate matrices, an experiment was conducted to determine if the process conditions used to immobilize the cells (e.g. transient exposure to $CaCl_2$) were irreversibly damaging the cells. The cells were centrifuged, resuspended in complete DMEM, mixed with alginate, and cross linked into alginate tubes as described in section 2.4.3.2. Different volumes of rinses (1.5, 12.5 or 125mL) using either n-saline or complete DMEM were used to rinse the alginate tubes after cross linking. After completing rinses, the cells were released from the alginate using trisodium citrate in DMEM. Control cultures of rSMCs were set up to examine the serial elimination of each scaffold component or process step as shown in Table 3, section 2.4.3.2. Complete DMEM was substituted for each component eliminated so that the sample was manipulated in a similar manner, but without the effect of that component.

For each alginate tube rinse condition, different initial seeding densities were obtained (see Table 4, section 2.4.3.2) due to the loss of alginate and hence cells during the

washes especially when n-saline was used. The concentration of $CaCl_2$ was expected to be close to 1% (90mM) after completion of the cross linking step. The concentration of $CaCl_2$ was 0.018% (1.6mM) in complete DMEM and 0% in n-saline. Therefore, the diffusion of $CaCl_2$ molecules and exchange of Na^+ ions for Ca^{2+} ions that originally cross linked the alginate molecules occurred more rapidly during the n-saline wash. In fact, the 12.5 and 125mL rinse conditions using n-saline completely dissolved the alginate tube and could not be evaluated in this experiment. Despite these differences in seeded densities, general comparisons could still be made.

Overall, the scaffold components and process steps (1% $CaCl_2$, 0.1M trisodium citrate solution, alginate and centrifugation) did not have a detrimental effect on rSMC growth when rSMCs were released from hydrogel following extrusion and subsequently seeded into microwell plates. Cells from the tube that were rinsed with 1.5mL n-saline exhibited the lowest glucose consumption. This lower glucose consumption is most likely due to the initial lower seeding density than the other conditions. The glucose data are show in Figure 19. The average GCR for all of the alginate tubes and control cells conditions was $3.6x10^{-6} \pm 4.7x10^{-7}$g/hr. These results were comparable to the other microwell studies done with a similar seeding density ($5x10^3$cells/cm^2) for which the average GCR over the culture period was $3.9x10^{-6} \pm 1.3x10^{-7}$g/hr. Therefore the matrix components/process conditions did not significantly effect cell growth as measured by GCR.

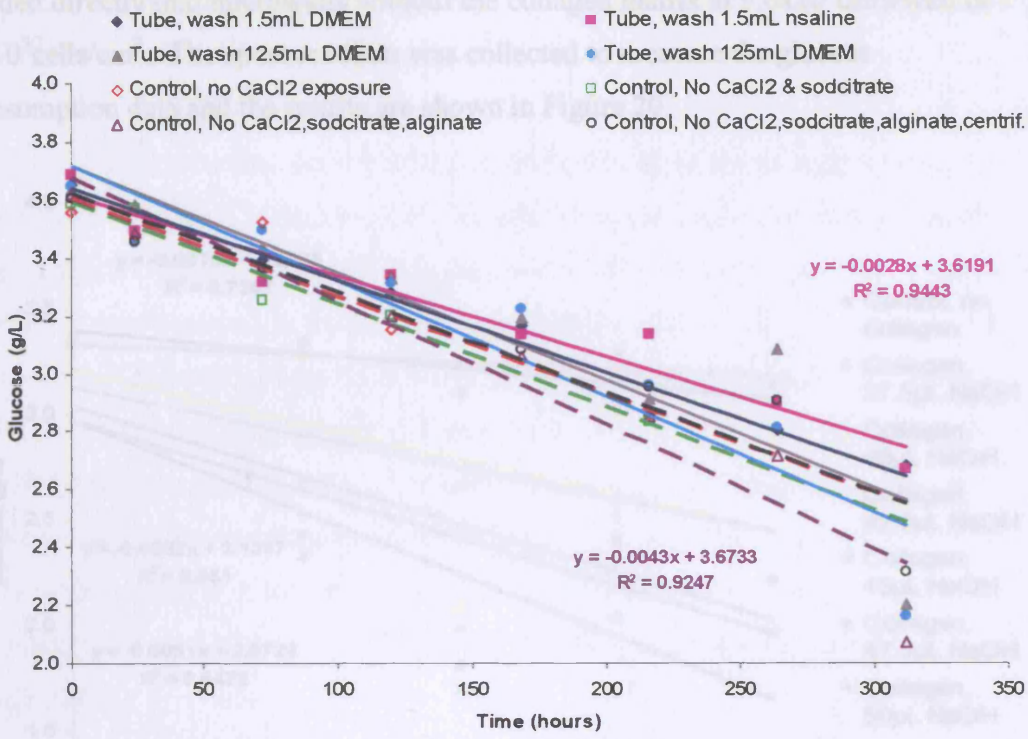

Figure 19. Glucose consumption of cells extruded into alginate tubes, released from the hydrogel using trisodium citrate and then cultured in microwells. The tubes (solid lines) were rinsed with 1.5mL of n-saline or 1.5, 12.5 or 125mL of complete DMEM prior to dissolution with trisodium citrate. The control cells (dashed lines) were processed with the serial elimination of one step of the matrix component or process step (e.g. exposure to $CaCl_2$, dissolution with trisodium citrate, combining with alginate and centrifuging). The GCR was similar for all the conditions.

3.3.3. RSMCs immobilized in collagen

This section describes the interlude during which collagen matrices were explored to provide cell adhesion sites for the rSMCs and to further understand the effects of the matrix components and cross linking solutions on the rSMCs.

Collagen solutions were prepared as described in section 2.3.2 and sheets were prepared as per section 2.4.2.2. Briefly, the rSMCs were trypsinized, centrifuged and resuspended in 50µL of complete αMEM medium and added to 450µL of collagen and 10X EMEM and various concentrations of 1N NaOH ranging from 37.5 to 50µL/well in a 24 well microplate. The NaOH was used to adjust the original acidic pH of the collagen solution to a basic pH to permit the collagen matrix to set. The cells within the collagen matrix were seeded at $5x10^5$cells/well. Control cells were

seeded directly into microwells without the collagen matrix at $9.6x10^3$cells/well or $5x10^3$cells/cm^2. The spent medium was collected to measure the glucose consumption data and the results are shown in Figure 20.

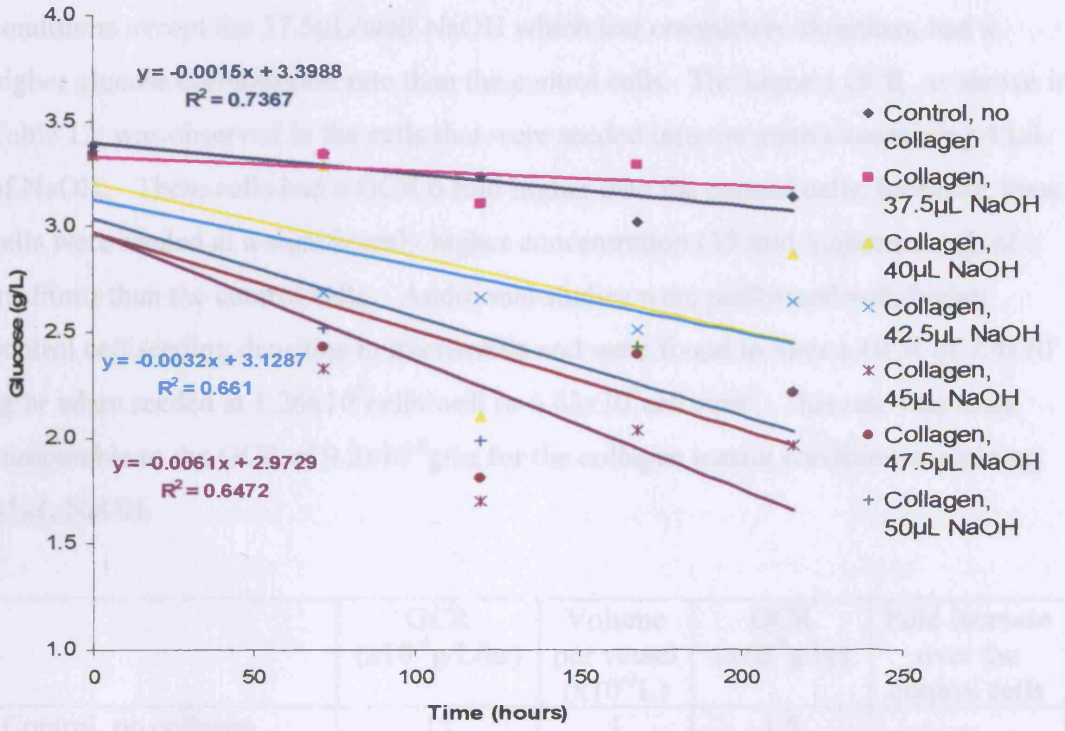

Figure 20. Glucose consumption of cells immobilized in collagen and then cultured in microwells. The collagen matrix was set with 1N NaOH, ranging from 37.5 to 50µL/well.

All of the different volumes of NaOH investigated allowed the collagen matrix to set. However, the integrity and strength of the matrix varied for the different NaOH volumes and hence pH of the final collagen and SMC matrix composition. On day 1 for all of the NaOH concentrations, the rSMCs appeared to be associated with the collagen matrix and exhibited elongation in a 3-D star-burst form. By day 3, the collagen and SMC matrices containing 37.5µL/well NaOH were significantly shrunken to a pellet size clump which primarily contained rounded cells throughout due to the collapse of the matrix. In the matrices containing 42.5 and 45µL/well NaOH, the cells were observed to still have well-formed star-burst shaped clusters throughout the matrix. The 40, 47.5 and 50µL/well NaOH contained primarily rounded cells, and the 40µL/well NaOH condition had slight shrinkage of the matrix

around the perimeter of the well. By day 5, the 40 and 42.5μL/well NaOH exhibited a slight to medium amount of shrinkage.

Due to the lower seeding density of the control cells, all of the collagen matrix conditions except the 37.5μL/well NaOH which had completely shrunken, had a higher glucose consumption rate than the control cells. The highest GCR, as shown in Table 13, was observed in the cells that were seeded into the matrix containing 45μL of NaOH. These cells had a GCR 6 fold higher than the control cells; however, these cells were seeded at a significantly higher concentration (35 fold higher per mL of medium) than the control cells. Additional studies were performed with higher control cell seeding densities in microwells and were found to have a GCR of 7.4×10^{-6} g/hr when seeded at 1.26×10^5 cells/well or 6.63×10^4 cells/cm^2. This rate was more comparable to the GCR of 9.2×10^{-6} g/hr for the collagen matrix condition containing 45μL NaOH.

	GCR ($\times 10^{-4}$ g/L/hr)	Volume per vessel ($\times 10^{-3}$ L)	GCR ($\times 10^{-6}$ g/hr)	Fold increase over the control cells
Control, no collagen	15	1	1.5	--
Collagen, 37.5μL NaOH	7	1.5	1.1	0.7
Collagen, 40μL NaOH	35	1.5	5.3	3.5
Collagen 42.5μL NaOH	32	1.5	4.8	3.2
Collagen, 45μL NaOH	61	1.5	9.2	6.1
Collagen, 47.5μL NaOH	47	1.5	7.1	4.7
Collagen, 50μL NaOH	47	1.5	7.1	4.7

Table 13. Comparison of glucose consumption rates for rSMCs immobilized in collagen matrix.

The pH of the mixture containing collagen, 10X EMEM and NaOH matrix was measured subsequently to the experiment. RSMCs were not added to the matrix for these measurements. The pH of each matrix was 6.8, 6.5, 9.0, 10.5, 11.5 and 12.0 for each of the conditions respectively between 37.5 and 50μL/well NaOH. After measuring the pH, it was difficult to understand why cells immobilized in collagen matrices under very alkaline conditions (the highest amount of NaOH) resulted in cell growth with the highest glucose consumption rate. However, in actuality, the rSMCs were exposed to this alkaline pH for only ca. 15-20 minutes, during the formation and

setting of the collagen matrix (from the time the cells were added to the mixture until the matrix was allowed to set). Thereafter, 1mL of complete αMEM was added to each microwell containing the collagen matrix. The addition of the αMEM complete medium would have buffered any difference in pH in the individual matrix formulations. The growth of the cells in the collagen matrix was most likely affected by the amount that the collagen matrix shrunk/collapsed or was able to support the outgrowth of the rSMCs. As the cells proliferated, the edges of the collagen matrix around the perimeter of the microwell separated slightly and pulled away from the well. The matrices containing 37.5 and 40μL/well NaOH which appeared to have a pH closest to physiological 7.0 were significantly collapsed. These matrices would not have supported cell proliferation and therefore would have had lower GCRs. In fact, cells lying at the bottom of the collagen matrix were observed to have attached to the bottom of the microwell and formed a bridge between the collagen and polystyrene, thus preventing the collapse. Although the matrices containing greater than 42.5μL/well NaOH had initially a very alkaline pH, the matrices maintained their rigidity to support the attachment and proliferation of the rSMCs.

3.3.4. RSMCs immobilized in collagen and alginate

The A7r5 rSMCs were shown to proliferate in collagen and not to be detrimentally affected by the matrix components/process conditions used to immobilize the cells within an alginate matrix. The next experimental goal was to determine if alginate could be combined with the collagen and cell matrix and then cross linked to determine if the cells would proliferate in presence of the alginate and any residuals from the cross linking solutions.

Collagen and alginate matrices were made as per section 2.4.2.3 by adding 4% w/v Fluka alginate in a n-saline solution to the collagen formulation in order to achieve a final 1% alginate concentration that comprised ca. 24% v/v of the matrix composition. Because alginate was added into the matrix formulation the final concentration of the collagen in the scaffold was reduced from 1.6g/mL (ca. 74% v/v) down to 1.25g/mL (ca. 58% v/v). In addition, the amount of complete DMEM that was used to resuspend the cells after centrifugation was also reduced to maintain a high collagen concentration. The addition of alginate and the lower collagen concentration in the

matrix still permitted the collagen to set after formulation, however, the ingredients had to be added in a particular order and mixed homogeneously to prevent premature setting of the collagen or cross linking of the alginate (see section 2.4.2.3). After formulation, the collagen was allowed to set in individual microwells, then the cross linking agent ($CaCl_2$ or $BaCl_2$) was added to cross link the alginate. Three concentrations (1%, 0.5% and 0.1%) of $CaCl_2$ or $BaCl_2$ were examined. These cross linking solutions were all made in n-saline; therefore, one of the control solutions used to compare against the cross linking solutions was just n-saline. The other control solution was complete DMEM.

Approximately 18 hours after the cells were incubated, the microwells were first observed. The rSMCs in the control matrices that were exposed to complete DMEM and n-saline were associated with the scaffold. The cells were spreading out within the scaffold in 3-D star-burst, spindly structures as shown in Figure 21.A. The rSMCs in the matrices treated with 0.5% and 1% $CaCl_2$ or $BaCl_2$ were rounded with no association with the surrounding matrix nor elongation as shown in Figure 21.B. However, a few rSMCs in the 0.1% $CaCl_2$ or $BaCl_2$ treated matrices were slightly elongated within the matrix especially around the perimeter of the microwell where the matrix was thicker due to meniscus effect. Throughout the remaining time points, these condition remained the same: the cells remained rounded and had a grainy appearance in the matrices exposed to 1% and 0.5% $CaCl_2$ or $BaCl_2$ cross linking solutions; the cells exhibited slight elongation, but no proliferation in the 0.1% $CaCl_2$ or $BaCl_2$ cross linking solutions; and continued proliferation in the control matrices which used complete DMEM and n-saline as cross linking solutions.

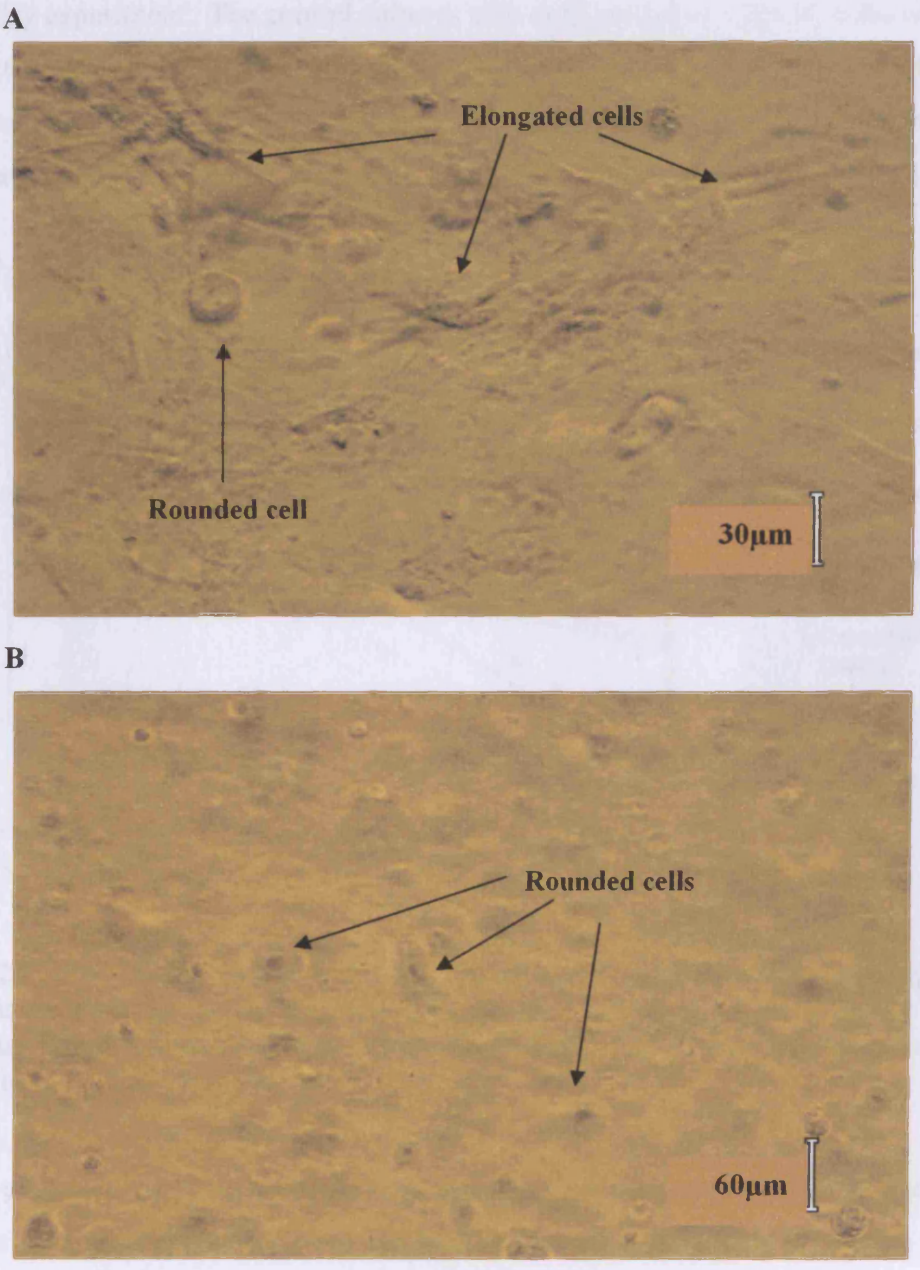

Figure 21. RSMCs immobilized in collagen/alginate matrix on day 1. (A) Control matrix that had complete DMEM as the cross linking solution. Cells were elongated within matrix. (B) Matrix that had 1% $CaCl_2$ used as cross linking solution. Cells remained round within the matrix. Photos 200X and 100X magnification.

The glucose concentration in the spent medium for each cross linking condition was corrected for evaporation. Figure 22 shows the glucose data for each condition over the 13 day experiment. The control cultures with cells seeded at $1.26x10^5$cells/well ($6.63x10^4$cells/cm^2) directly into the microwell with no matrix (pink line). All of the matrix conditions were also seeded at $1.26x10^5$cells/well in order to help compare GCR based upon similar starting conditions. The GCR are summarized in Table 14.

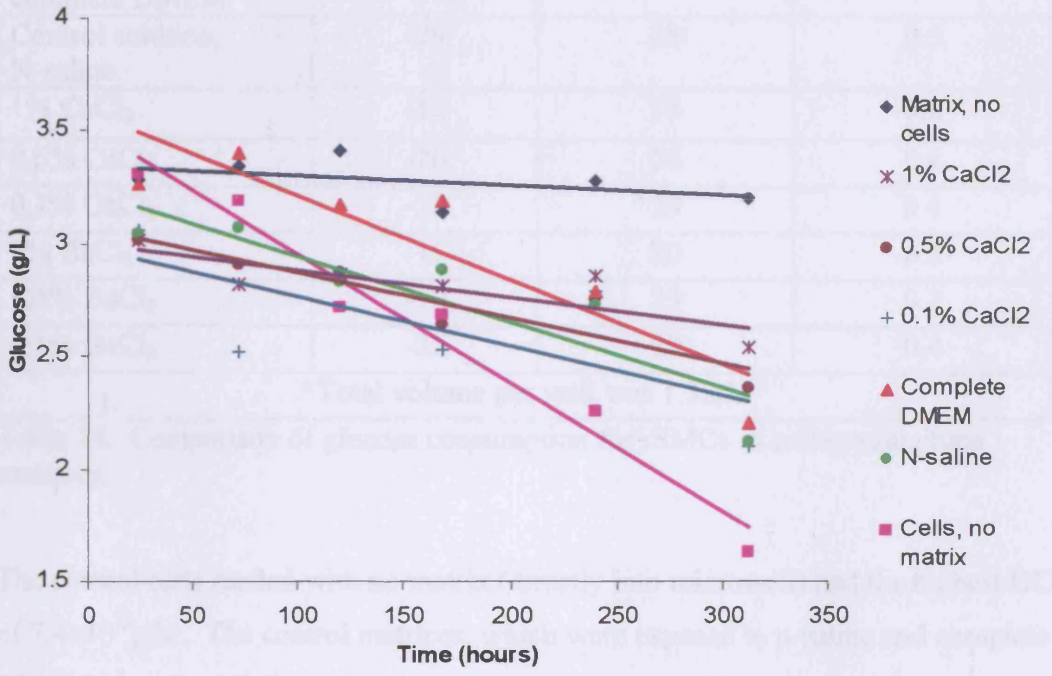

Figure 22. Glucose consumption of rSMCs in collagen/alginate matrices exposed to different crosslinking agents. The cells with no matrix had a significantly higher GCR than the cells within the matrices crosslinked with $CaCl_2$. $BaCl_2$ results were similar to the $CaCl_2$ (data not shown).

During glucose testing, the spent medium samples from the complete DMEM and n-saline cross linking conditions were observed to have become slightly gelatinous after thawing. The samples were dissolved upon addition of collagenase, so it was assumed that the freezing step realigned the residual collagen molecules such that they reset after thawing. This phenomenon was not observed in any of the other conditions using $CaCl_2$ or $BaCl_2$ as the cross linking solution.

Matrix condition with cross linking solution	slope of linear fit ($x10^{-4}$g/L/hr)	Glucose consumption rate (GCR) ($x10^{-7}$g/hr)*	Fraction of GCR compared to control cells with no matrix
Matrix with no cells	-5	6.5	0.09
Cells with no matrix	-57	74	--
Control solution, complete DMEM	-37	48	0.6
Control solution, N-saline	-29	38	0.5
1% $CaCl_2$	-12	16	0.2
0.5% $CaCl_2$	-20	26	0.4
0.1% $CaCl_2$	-22	29	0.4
1% $BaCl_2$	-15	20	0.3
0.5% $BaCl_2$	-19	25	0.3
0.1% $BaCl_2$	-22	29	0.4
*Total volume per well was 1.3mL			

Table 14. Comparison of glucose consumption for rSMCs in collagen/alginate matrices.

The control cells seeded with no matrix (directly into microwell) had the highest GCR of $7.4x10^{-6}$g/hr. The control matrices, which were exposed to n-saline and complete DMEM instead of $CaCl_2$ or $BaCl_2$, had the next highest GCR of $4.8x10^{-6}$g/hr for complete DMEM medium and $3.8x10^{-6}$g/hr for n-saline. The GCR for matrices exposed to 0.1% $CaCl_2$ and $BaCl_2$ cross linking solutions was $2.9x10^{-6}$g/hr. The 1% and 0.5% $CaCl_2$ and $BaCl_2$ solutions were both lower. Thus it appeared that the cross linking solutions had a negative impact on SMC attachment and proliferation, even in the presence of collagen. These GCR can be easily compared in Figure 23.

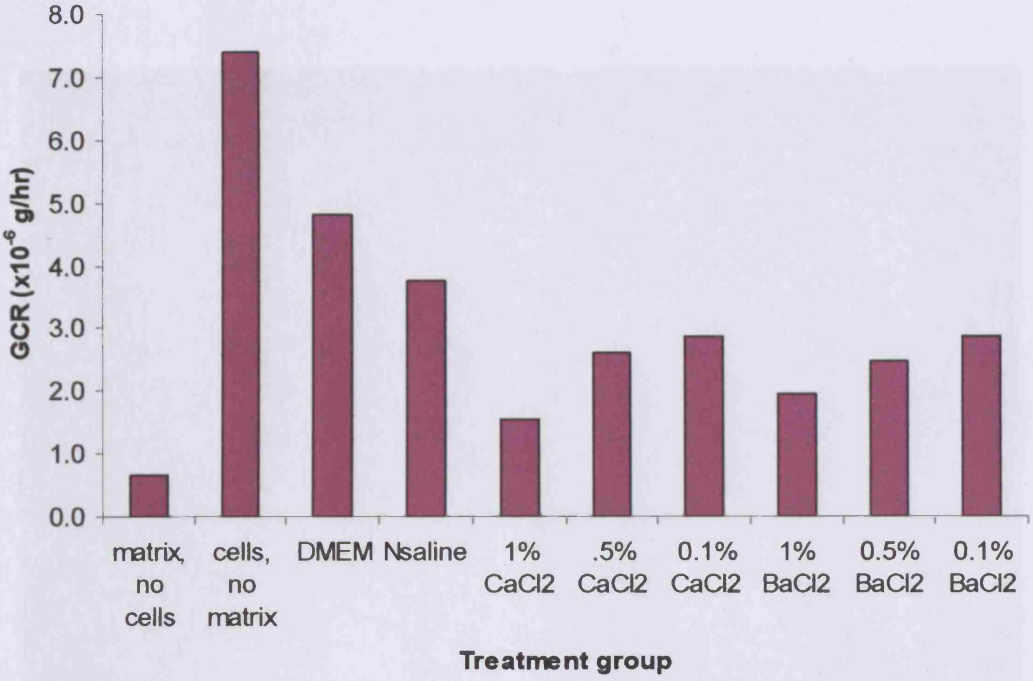

Figure 23. Comparison of rSMC GCR (g/hr) for collagen/alginate matrices with different cross linking solutions.

By day 10 in culture, only the control matrices, which were exposed to n-saline and complete DMEM instead of $CaCl_2$ or $BaCl_2$, had shrunken slightly around the perimeter of the microwell. The amount of shrinkage may have been less in these matrices than the previous collagen matrices due to the presence of alginate, the lower concentration of collagen, or the lower seeding density. All the other matrices that were exposed to cross linking solutions had no shrinkage. Figure 24 shows cell growth in the day 14 culture of the control matrix in which n-saline was used as the substitute for $CaCl_2$ or $BaCl_2$ cross linking solutions. The rSMCs were bridged between the polystyrene of the microwell surface and the collagen/alginate matrix. The cells held the matrix in place to prevent it from shrinking significantly around the perimeter of the microwell.

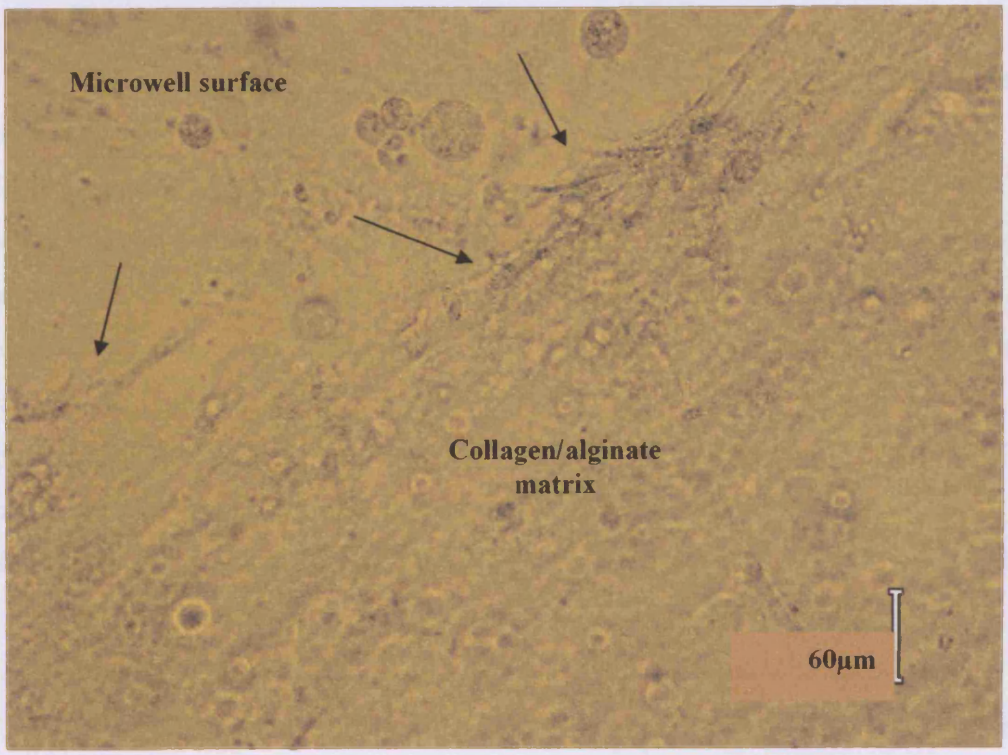

Figure 24. RSMCs immobilized in collagen/alginate matrix on day 14. Control condition which used n-saline as the cross linking solution. The arrows indicate the rSMCs bridging between the collagen/alginate matrix and the polystyrene surface of the microwell. 100X magnification

3.3.5. RSMCs immobilized in alginate-GRGDY

Experimental findings had progressed from observing no growth in alginate matrix to achieving some growth in alginate/collagen matrices in which very low concentrations of $CaCl_2$ or $BaCl_2$ cross linking solution had been used. The ultimate research goal was to incorporate a cell adhesion site onto the alginate molecules so that alginate can be used to encourage cell attachment and proliferation. Research performed in Mooney's lab (Rowley, 1999) had indicated that the pentapeptide glycine-arginine-glycine-aspartic acid-tyrosine (GRGDY) can be incorporated. The results from experiments performed to incorporate this bioactive molecule are

discussed below. References to alginate incorporated with this pentapeptide have been shortened for convenience to alginate-GRGDY.

3.3.5.1. RSMCs seeded onto alginate-GRGDY sheets

Results from cross linking experiments containing alginate/collagen matrices indicated that $CaCl_2$ and $BaCl_2$ cross linking solutions resulted in lower cell attachment and glucose consumption rates. Since the cross linking solutions appeared to be detrimental to rSMCs, initial experiments with alginate-GRGDY were conducted by pre-forming the alginate-GRGDY matrices as sheets in the bottom of a microwell and then seeding the cells separately onto the surface of the alginate. Alginate-GRGDY sheets were constructed as described in section 2.4.2.1. After formation, the alginate sheets were rinsed thoroughly of excess $CaCl_2$ prior to the addition of rSMCs. Initial experiments were performed using 0X, 1X, 10X, and 50X alginate-GRGDY (Fluka), as described in section 2.3.3.2 from Rowley's (1999) reactant concentrations, where 1X was 1mg of alginate containing 38μg of sulfo-NHS, 67μg of EDC and 1μg of peptide; 10X was ten times the reactants and 50X was fifty times the reactants. The 0X alginate was not taken through the peptide incorporation chemistry so it could be was used as the control.

RSMCs were added at a high concentration of $3x10^5$cells/well ($8x10^4$cells/cm^2) in 2mL of complete DMEM to the microwells containing alginate sheets. After incubation of these cultures, no cell attachment was observed in the 0X, 1X, and 10X alginate-GRGDY sheets. However, the rSMCs did attach to the 50X alginate-GRGDY. Figures 25.A and 25.B show images of rSMCs attached to the alginate surface which were slightly elongated and bridged small spaces between adjacent cells between day 2 and 3 in culture. However, on day 5 of the culture no further outgrowth of these cells was observed. These alginates had been lyophilized in order to prepare known concentrations of the alginate after dialysis.

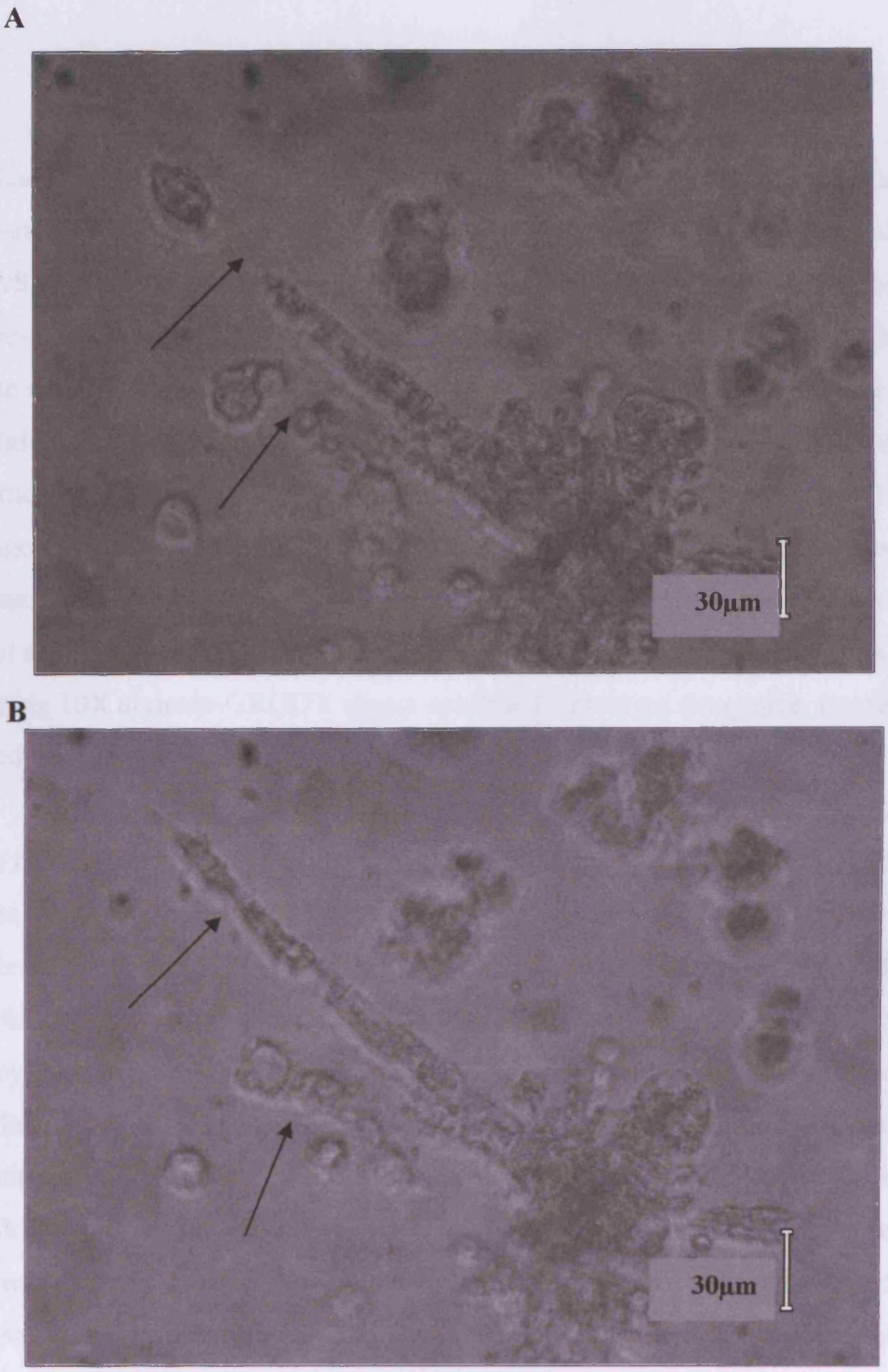

Figure 25. RSMCs seeded onto surface of 50X Fluka alginate-GRGDY sheet. (A) Day 2 of culture. Arrows indicate spaces between adjacent cells. (B) RSMCs bridged the gap between spaces of adjacent cells on the surface of sheet on day 3. 200X magnification.

Significant improvement in cell attachment was observed when the alginate-GRGDY was treated with activated charcoal, filtered through Celite, and not lyophilized. When rSMCs were seeded at $4x10^4$cells/cm^2 into the microwells containing the alginate-GRGDY sheets; the rSMCs attached to both Manugel and Fluka (high G) alginate sheets containing 50X pentapeptide. The rSMCs did not attach to the 1X and 10X alginate-GRGDY sheets. Micrographs were taken over the time course of the experiment and day 2 results are shown in Figure 26.A. The 50X alginate-GRGDY (Manugel) sheets exhibited the best cell attachment and highest percent confluency (cell density) which were similar to the control cells seeded directly into microwells without an alginate matrix (Figure 26.C). RSMCs seeded into the microwells containing 10X alginate-GRGDY sheets exhibited almost no elongation and remained rounded throughout the culture period (Figure 26.B).

Due to the very low concentration of alginate (~0.5%) after the dialysis step, the alginate solutions needed to be lyophilized to prepare higher concentrations of alginate solutions (~1-3%) to permit addition of cells to the solution. During the lyophilization cycle, the bottles were inadvertently removed part-way through the cycle by other users. Although drying was eventually completed at a later time, the 50X Manugel bottle was inadvertently broken. The remaining alginate-GRGDY was reconstituted to ~2% concentration and alginate sheets were made. However, very few rSMCs were associated with the 50X Fluka alginate-GRGDY (data not shown). It was assumed that improper lyophilization or being removed part way through the cycle was detrimental to the cell binding sites on the alginate-GRGDY since the cells had attached prior to lyophilization. However, it was also possible that the biological stability of the alginate-GRGDY also decreased with age of the alginate.

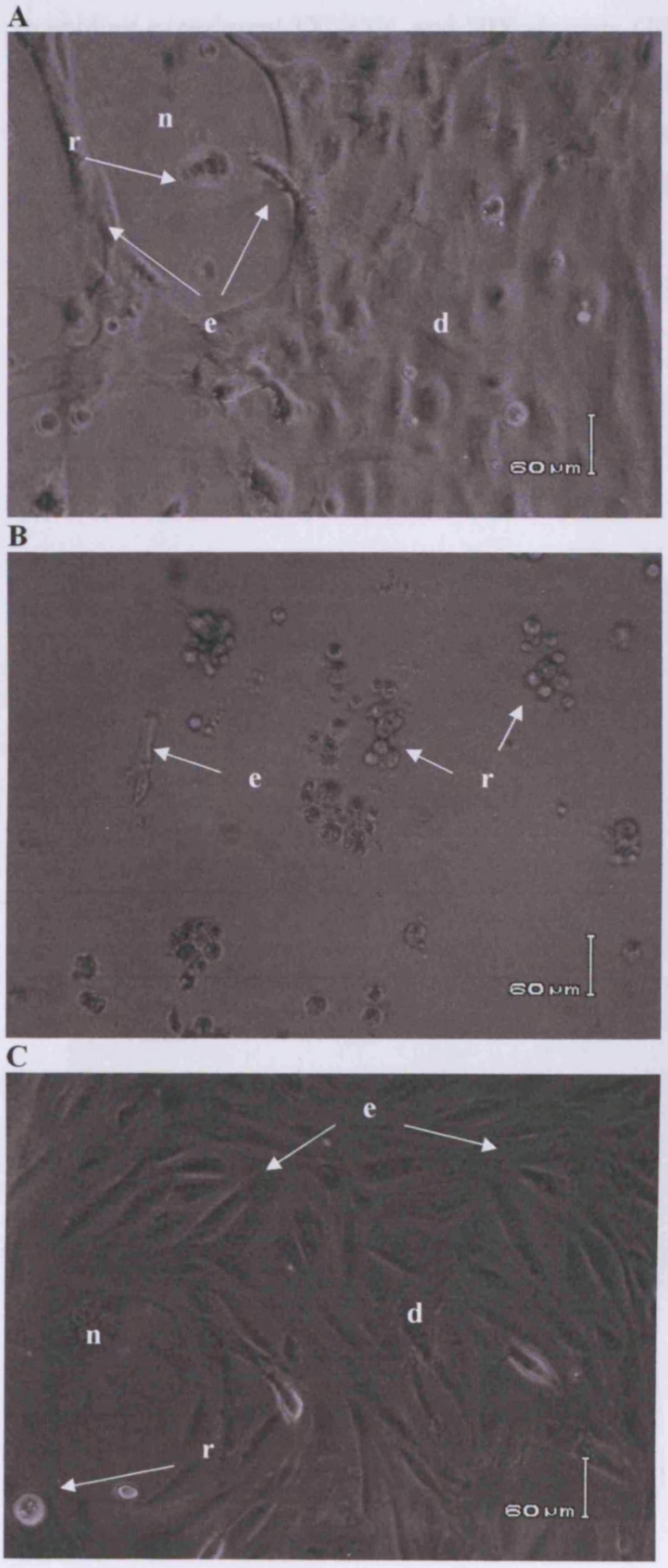

Figure 26. RSMCs seeded on Manugel (High G) alginate-GRGDY sheets on day 2 of culture. (A) Cells on 50X alginate-GRGDY sheet were elongated and networked. (B) Cells on 10X alginate-GRGDY sheet were rounded and were not attached to the surface. (C) Control cells seeded onto microwell surface were attached and nearly 100% confluent.

Cells are designated as: (e) elongated or (r) rounded. Areas are designated as: (d) densely packed cells or (n) no cells.

All photos at 100X magnification.

In another experiment 1X, 10X, and 50X alginate-GRGDY were synthesized using Pronova MVG alginate, a high grade commercial material. Alginate sheets were constructed and seeded with rSMCs as previously described. On day 1 the rSMCs had associated with the 50X alginate-GRGDY, only a few (<1%) associated with the 10X concentration, and none to the 1X. The rSMCs seeded onto the 50X alginate-GRGDY did not grow and expand beyond the point that was observed on day 1 (Figure 27).

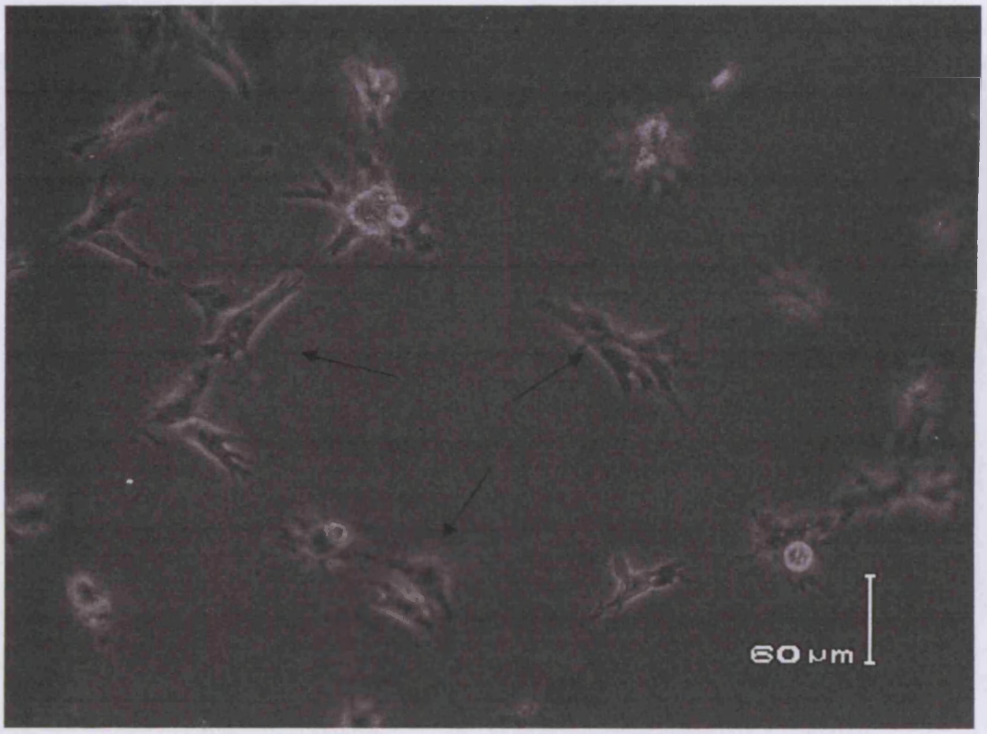

Figure 27. RSMCs seeded on Pronova MVG alginate containing 50X GRGDY on day 1. Cells were attached and just starting to elongate. Arrows indicate cells attached to surface of sheet. 100X magnification.

3.3.5.2. RSMCs immobilized within alginate-GRGDY hydrogels

Although the alginate was very dilute after dialysis, several attempts were made to immobilize rSMCs within the alginate-GRGDY. Cells were added to Fluka alginate-GRGDY as per section 2.4.1 and made into beads using 0.5% and 1% $CaCl_2$ solution for between 5 to 15 minute exposure times as per section 2.4.4. The beads were very fragile (not rigid hydrogel spheres) after rinsing in complete DMEM. The 50X alginate-GRGDY beads completely dissolved by day 2. However, prior to the beads dissolving, on day 1 several cells were observed to have elongated within the bead (Figure 28). The 0X, 1X, 10X beads showed no cell outgrowth and remained intact out to day 10.

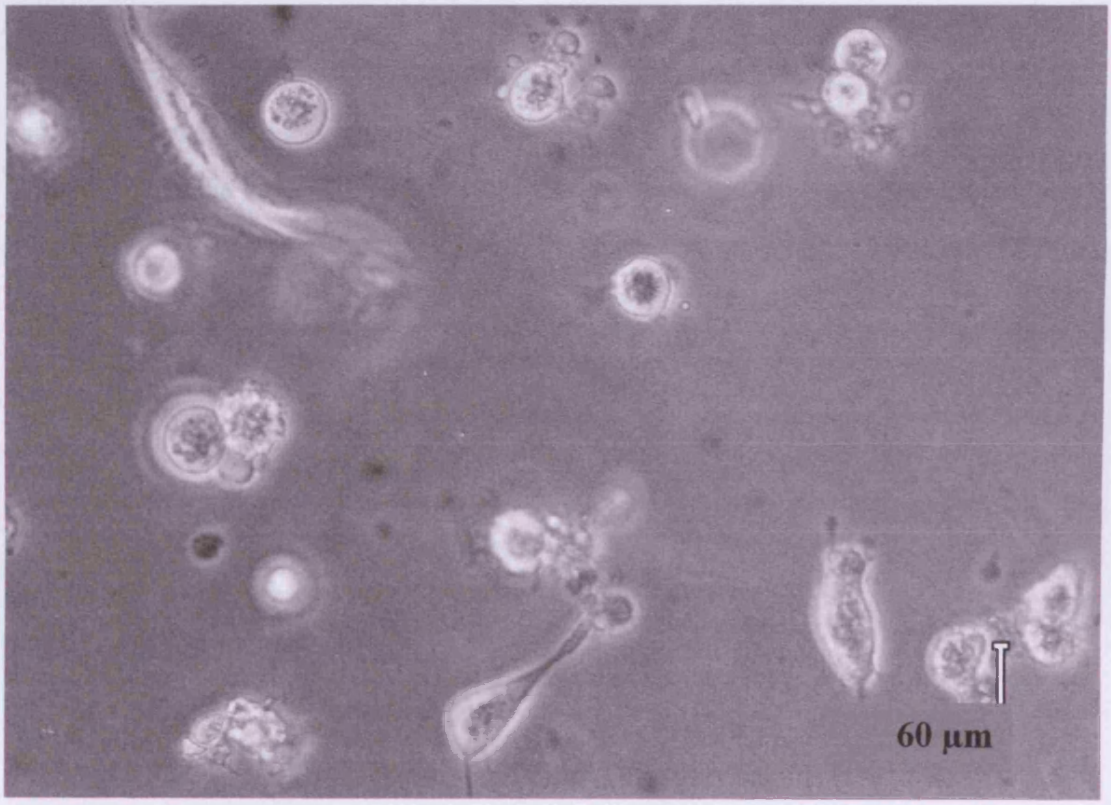

Figure 28. RSMCs elongated within 50X Fluka alginate-GRGDY hydrogel. Day 1 after immobilization in hydrogel, the beads were very fragile (not rigid spheres) and then completely dissolved by day 2 of culture.

In another experiment, rSMCs were resuspended in a very small volume of complete DMEM in order to combine with the 1X, 10X and 50X Pronova MVG alginate-GRGDY solution to make into alginate sheets. Some of these rSMCs elongated within the 50X alginate-GRGDY hydrogel, but not to the same extent as the rSMCs that were seeded onto the surface of pre-formed alginate sheets.

RSMCs were also mixed homogeneously with 50X Pronova MVG alginate-GRGDY and extruded into tubes at $8x10^6$cells/mL using a 3.8mm diameter bullet as the float. These tubes were cross linked using 1% $CaCl_2$ in n-saline. The alginate tubes were incubated *in situ* within the glass tubes in complete DMEM as described in section 2.4.3.3. Fresh medium was added each day from days 0 to 9 and every two days thereafter. Photographs of these constructs were slightly distorted and out of focus due to the reflection of the light and the curvature of the glass tube. Figure 29 shows the growth of the rSMCs over the culture period on day 3, 11, and 17. The cells appeared to attach, elongate and proliferate within the tube. However, it was not known if the cells grew within the alginate or grew along the glass tube surface. As the rSMC culture aged, the cells began to form larger aggregates which could be visualized in the day 11 and 17 photos.

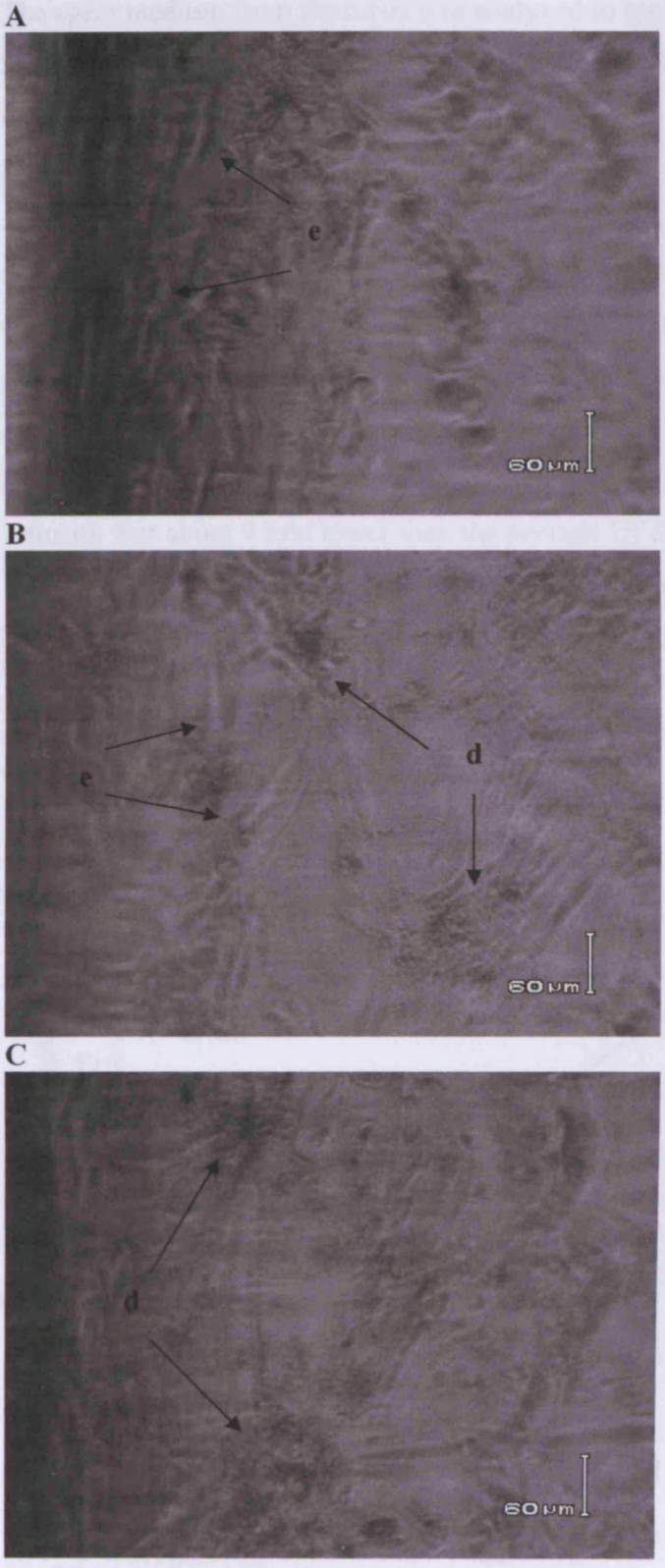

Figure 29. RSMCs immobilized in 50X Pronova MVG alginate-GRGDY tubes at $8x10^6$cell/mL. Micrographs show the growth of cultures on (A) day 3, (B) day 11 and (C) day 17. Due to the curvature of glass tube, the images were slightly distorted.

Cells are designated as (e) elongated within alginate along wall of glass tube. Areas are designated as (d) densely packed cell aggregates.

All photos at 100X magnification.

The spent medium from the tubes was analyzed to see if glucose consumption and lactate production were similar to cells grown in tissue flasks. Figure 30 shows the cumulative glucose consumption of the rSMCs from a representative tube. The glucose consumption rate (GCR) of 0.0187 g/L/hr was determined from the linear approximation for the cumulative amount of glucose consumed. Using the vessel volume of the tube as 1.5mL, the cells consumed $2.8x10^{-5}$g/hr. The final number of cells per tube was not determined, but they were originally seeded with $8x10^6$cells/mL and ca. 147µL was used to make the tube with 100µm wall thickness with outside diameter of 4mm (Volume = Pi * $(r_2^2-r_1^2)$* h = 3.14 * $((4/2)^2 - (3.8/2)^2)mm^2$ * 120mm / $1000mL/mm^3$) which equaled $1.18x10^6$cells, or a GCR of $2.4x10^{-11}$g/cell/hr. This estimate was about 9 fold lower than the average GCR of $2.1x10^{-10}$ +/- $1.3x10^{-10}$g/cell/hr (n=50) which was obtained from tissue flasks for the same cells (P12) from section 3.3.1.2. It was likely that the actual number of cells in the tube was significantly lower than $1.68x10^6$cells due to the daily refeeds with fresh medium. Some fragments of alginate and cells were dissociated from the tube and washed away during the addition of new medium.

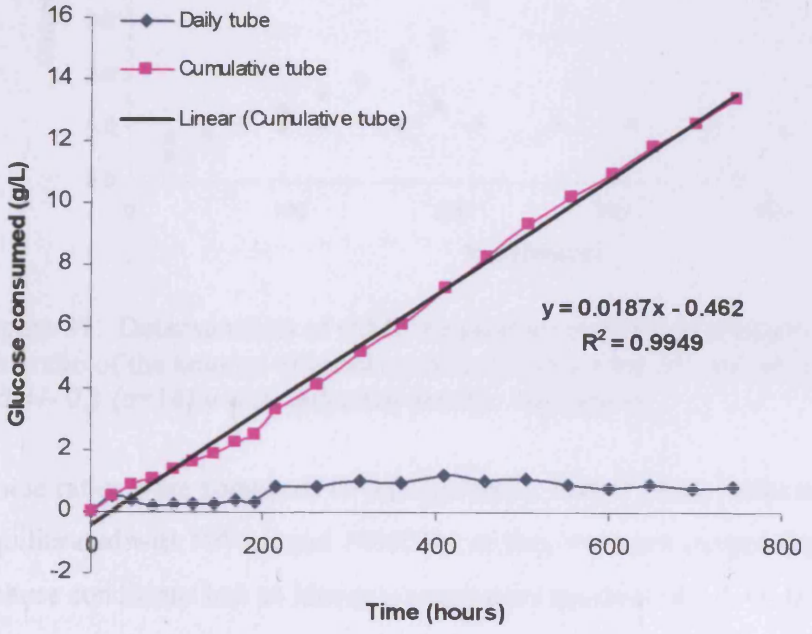

Figure 30. Glucose consumed by rSMCs immobilized in 50X Pronova MVG alginate-GRGDY tube seeded with ca. $1.18x10^6$cells. The tube was refed daily with fresh complete DMEM. The GCR was estimated from the slope of the linear approximation for the cumulative amount of glucose consumed.

Since the tubes were batch fed daily, there was concern about oxygen deprivation between refeeds. The respiratory quotient was calculated to be the ratio of the amount of lactate produced versus the amount of glucose consumed as per section 2.5.6.2. This number was used to determine if the culture's metabolism was anaerobic and aerobic. A respiratory quotient of 1 indicated aerobic metabolism, a ratio of 2 indicated anaerobic metabolism, and a value in between indicated something intermediary (Carrier, 1999). Figure 31 shows that the tube had a respiratory quotient ranging from 0.9 to 1.5, which was maintained even after the daily refeeds were extended to two days.

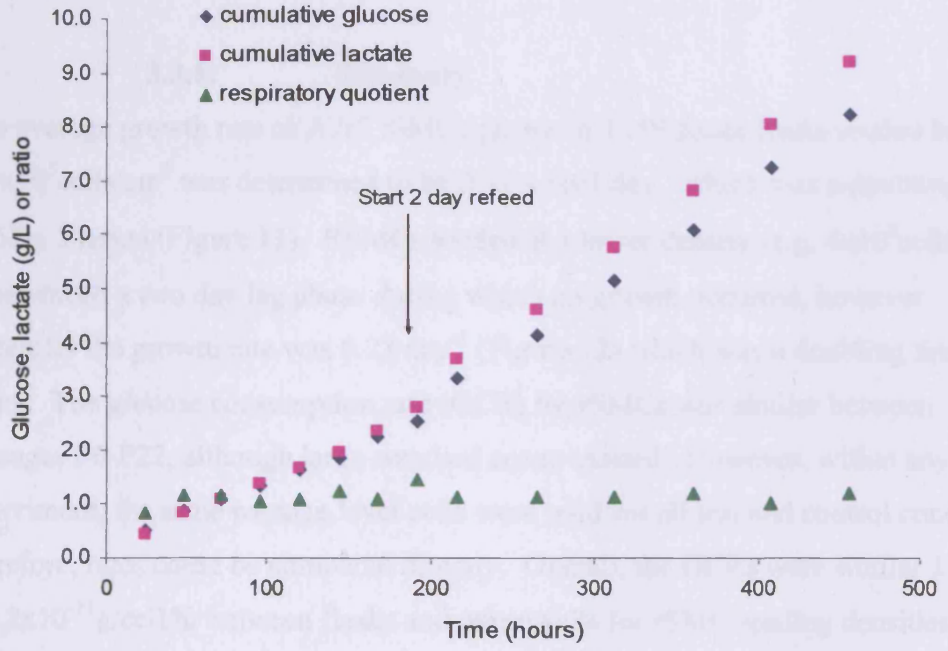

Figure 31. Determination of rSMC respiratory quotient in alginate-GRGDY tubes. The ratio of the amount of lactate produced versus the amount glucose consumed was 1.1 +/- 0.1 (n=14) which indicated aerobic respiration.

These ratios were compared to cells grown in vented tissue flasks which were equilibrated with 90%air and 10%CO_2, so they were not oxygen deprived. These culture conditions had an identical respiratory quotient of 1.1 +/- 0.1 (n=19).

Alternatively to batch feeding, flow circuits were set up using the glass tubes as the bioreactor containing the rSMCs immobilized in the alginate-GRGDY. The bioreactor volume was ca. 1.5mL (4mm diameter tube, 12cm in length). The flow of the complete DMEM through the tube was originally set very low ca. 5mL in 24

hours (0.2mL/hr). Thus the complete DMEM in the reactor volume was replenished ca. three times within the 24 hour period. In the future, the flow of the medium through the tube should be programmed throughout the cultivation period based upon pre-set parameters such as glucose consumption, lactate production or oxygen levels. Initially the flow may need to be low to allow the cells to elongate and network within the hydrogel. Then the flow can be gradually increased since the cell-to-cell binding will make the cell/alginate construct stronger and less susceptible to dissociation of the alginate due to calcium ion exchange into the culture medium. The flow circuit will need to be constructed with tubing that does not contain any leachable toxic substances that will inhibit cell growth.

3.3.6. Summary

The average growth rate of A7r5 rSMCs grown in T150 tissue flasks seeded between 5-9x10^5cells/cm^2 was determined to be 0.31 ± 0.01 day^{-1} which was a doubling time of 53 ± 2 hours (Figure 11). RSMCs seeded at a lower density (e.g. 4x10^2cells/cm^2) experienced a two day lag phase during which no growth occurred; however thereafter the growth rate was 0.23 day^{-1} (Figure 12) which was a doubling time of 71 hours. The glucose consumption rate (GCR) for rSMCs was similar between passages P6-P22, although large standard errors existed. However, within any given experiment, the same passage level cells were used for all test and control conditions; therefore, rates could be compared directly. Overall, the GCRs were similar 1.4x10^{-10} ± 4.2x10^{-11}g/cell/hr between flasks and microwells for rSMC seeding densities between 4x10^2 and 1x10^4cells/cm^2 (Table 10).

High cell viability was achieved following extrusion of rSMCs in alginate and cross linking with $CaCl_2$. The average cell survival measured was 87 ± 7% (n= 42) using trypan blue dye exclusion assay. However, cell viability dropped rapidly from 87% down to 3% in just 9 days; and there was no increase in the number of cells within the alginate hydrogel discs (Figure 15) as compared to the rSMCs in control flasks. An alternative culture medium, αMEM, which was richer in supplements than complete DMEM was tested. The rSMCs' viabilities were higher in the αMEM as compared to complete DMEM, but they still decreased to 20% by day 10 (Figure 17). Glucose measurements were taken from the spent medium from the microwells of the rSMC/alginate beads and discs and confirmed that the cells in the hydrogels were not

surviving (Figures 16 and 18). A separate experiment was conducted to determine the effect of matrix components and cross linking solution on rSMC growth. Alginate tubes of rSMCs were extruded, rinsed with medium and then dissolved using trisodium citrate. Control cells were set up which serially eliminated each step of the process or component. The rSMCs from all of the conditions were plated into microwells and similar GCRs were obtained (Figure 19). Therefore the immobilization process (and dissolution process) was not detrimental to the rSMCs. Therefore, because the rSMCs were strongly anchorage dependent cells and the alginate matrix did not provide cell adhesion sites, the rSMCs could not attach and died.

Collagen matrices were used to confirm that the rSMCs proliferated in matrices in which cell adhesion sites were provided. Glucose consumption was used to measure cell proliferation (Figure 20). In further studies performed with rSMCs in alginate/collagen matrices, rSMCs were sensitive to increased concentrations of divalent cations in the cross linking solution (Figures 21-23). Control conditions in which complete DMEM and n-saline were used as mock cross linking solutions had the highest GCR and the 1% cross linking solutions had the lowest GCR. It was concluded that the higher concentration of cross linking solution caused more alginate hydrogel to be formed, thereby obstructing the rSMCs interaction with the collagen. Studies performed with rSMCs in collagen/alginate matrices also demonstrated the importance of the physical strength of the matrix because cell elongation and proliferation caused the matrix to shrink/collapse. RSMCs were observed bridging the space between the polystyrene microwell surface and the collagen matrix to prevent the matrix from collapsing (Figure 24).

Carbodiimide chemistry was used to incorporate GRGDY peptides onto the alginate polysaccharide chains, thus providing cell adhesion sites. RSMCs attached and elongated on the surface of 50X alginate-GRGDY sheets (Figure 25, 26A, 27). Very few observations were made of rSMCs elongation when immobilized within alginate-GRGDY hydrogel beads (Figure 28) and appeared to occur only when the hydrogel was rapidly dissociating. RSMCs within rigid alginate-GRGDY hydrogel beads never showed elongation. When rSMCs were extruded within 50X alginate-GRGDY tubes, cell elongation was observed (Figure 29); however the cells' association with

the wall of the glass tube cannot be discounted. Alginate preparations containing only 1X and 10X reagent concentrations (as per section 2.3.3.2) did not allow rSMC attachment nor elongation on the surface of sheets (Figure 26B) and within beads and tubes. The GCR was measured for rSMCs cultured in an alginate-GRGDY tube (Figure 30) and found to be $2.4x10^{-11}$g/cell/hr which was 9 fold lower than the GCR of rSMCs in tissue flasks. The respiratory quotient for rSMCs cultured in alginate-GRGDY tubes within the glass tube reactor was measured (Figure 31) and found to be 1.1 indicating aerobic metabolism. RSMCs grown in tissue flasks had the same respiratory quotient as rSMCs in the alginate-GRGDY tube.

The next section describes the work conducted using adult human mesenchymal stem cells (hMSCs). Similar methods and measurements were used to characterize the hMSCs as described in this section for rSMCs cultured in tissue flasks and alginate hydrogel constructs.

3.4. The characterization of hMSCs in tissue flasks and alginate matrices

In order to understand and characterize hMSC growth within alginate hydrogels, the growth characteristics of hMSCs in tissue flasks needed to be established. Each cell source used for this research was assessed according to its percent viability post-thaw (if frozen), percent viability at each passage, the doubling time (hr), the population doubling per day (PD/day), the specific growth rate (cells/cm^2/hr) and the glucose consumption rate (g/cell/hr). The cell concentration was measured using a hemacytometer, viability using trypan blue dye and the glucose and lactate concentrations in the culture medium using the YSI bioanalyzer. Following these measurements, the specific growth rate, glucose consumption rate (GCR) and respiratory quotient were calculated.

HMSCs were immobilized within alginate and alginate-GRGDY matrices, and the interactions of the hMSCs with the matrices were studied. Cell studies were used to concurrently establish the alginate-GRGDY derivatization process. The biological activity of the alginate matrices was assessed by observing the cells' interaction with the matrices, such as the change in morphology. The cells remained rounded (spherical) indicating no interaction, or the cells elongated indicating association with the peptide incorporated onto the alginate. These interactions were observed with the hMSCs either seeded on the surface of hydrogel sheets or within beads or tubes.

During preparation and culturing of 3-dimensional hydrogels, measurements such as viability of the cells post-immobilization into the alginate, cell density and glucose consumption were taken and compared to data for hMSC in 2-dimensional (tissue flasks) environments. In addition the metabolic activity of the cells was measured using the MTT assay. All of the MTT data and results are discussed in section 3.5.

3.4.1. Growth of hMSCs in tissue culture plastic

Due to the limited supply of hMSCs from bone marrow transplant donations, it was necessary to produce frozen stocks of cells for this research. Fresh and frozen sources of hMSCs were obtained from the Wolfson Institute, UCL and were used for these studies. One isolation of hMSCs directly from bone marrow cells (BMCs) was

performed, but cell growth was slow. The reason for poor growth was not known, but the Wolfson Institute had similar experience with a separate sample from the same BMCs. A frozen vial from these cells at P2 was also expanded and growth was lower compared to other banks previously used.

Fresh hMSCs were passaged and used to produce frozen working cell banks of hMSCs. Vials of hMSCs were removed from liquid nitrogen storage and thawed in a 37°C water bath and planted into tissue flasks to expand the number of cells to conduct the experiments described in this section. The cell banking and passaging methods are described in detail in section 2.2.2.

One primary cell bank of hMSCs was produced at passage 4 (P4); however several additional sources were obtained which were frozen at P2, P3 and P4 levels from the Wolfson Institute. In addition a higher passage cell bank was established at P8; however this bank had limited use due to its higher passage level. For the primary P4 cell bank established, the cells maintained a consistent and high viability over the length of storage (ca. 5 months) as determined by trypan blue dye exclusion assay (section 2.5.3). Table 15 shows a summary of each cell source's characteristics in chronological order that the cell sources were used. These data were generated from 5 different hMSC sources (2 fresh and 5 frozen banks) for a total of 24 individual cell expansions.

The first data column 'Fresh hMSC' was derived from freshly isolated cells (never frozen). The remaining data columns represent cell sources that were all derived from frozen hMSCs stocks which were cryopreserved as per section 2.2.2.1. Since the initial cell concentration of hMSCs isolated from BMCs cannot be determined due to the presence of other mononuclear cells, the earliest cell growth data was obtained from passage 2 after the density was determined from the harvest of the P1 cells.

	Fresh hMSC JM2-31, 2-37 Used: 10/02-12/02	P8 JM CB Banked:11/02 Used: 7/03-12/03	P4 JM CB Banked:11/02 Used: 1/03-5/03	P4 SE CB Banked:8/03 Used: 10/03-11/03	P2/P3 MC Banked:12/03 Used: 1/04-3/04
Derived from cell source		JM2-31	JM2-37		
Number of vials		17	16		
% Viability - post thaw		88.4 ± 5.4 (n=6)	87.6 ± 3.9 (n=7)	89.7 ± 0.6 (n=2)	NA
% Viability Passage ≤ 7	98.6 ± 1.3 (n=11)		99.0 ± 0.8 (n=25)	98.0 ± 0.9 (n=8)	97.7 ± 0.8 (n=12)
% Viability Passage ≥ 8	98.7 ± 1.0 (n=13)	98.1 ± 1.6 (n=13)	98.7 ± 0.5 (n=25)	97.9 ± 0.8 (n=2)	94.7 ± 1.6 (n=3)
Doubling time ≤ P7 (hrs.)	64 ± 16 (n=9)		76 ± 18 (n=24)	50 ± 9 (n=8)	72 ± 36 (n=11)
Doubling time ≥ P8 (hrs.)	76 ± 15 (n=12)	146 ± 84 (n=12)	168 ± 108 (n=20)	98 ± 36 (n=2)	102 ± 11 (n=2)
PD/day ≤ P7	0.28 ± 0.07 (n=9)		0.23 ± 0.05 (n=24)	0.34 ± 0.07 (n=8)	0.26 ± 0.07 (n=11)
PD/day ≥ P8	0.23 ± 0.05 (n=12)	0.15 ± 0.09 (n=12)	0.14 ± 0.10 (n=20)	0.18 ± 0.07 (n=2)	0.16 ± 0.02 (n=2)
Growth rate ≤ P7 ($x10^2$ cells/cm^2/hr)	2.30 ± 0.91 (n=6)		1.29 ± 0.56 (n=14)	3.40 ± 0.75 (n=6)	1.31 ± 0.56 (n=5)
Growth rate ≥ P8 ($x10^2$ cells/cm^2/hr)	1.89 ± 1.27 (n=3)	0.90 ± 0.65 (n=9)	0.63 ± 0.20 (n=6)	1.00 (n=1)	0.58 ± 0.57 (n=2)
GCR ≤ P7 ($x10^{-10}$ g/cell/hr)	0.73 ± 0.32 (n=7)		ND	1.72 ± 0.45 (n=8)	1.98 ± 1.33 (n=6)
GCR ≥ P8 ($x10^{-10}$ g/cell/hr)	1.02 ± 0.48 (n=12)	2.13 ± 2.17 (n=11)	ND	4.10 ± 2.16 (n=2)	ND

Table 15. Summary of hMSC growth in tissue flasks including percent viability of cells post-thaw, passaging viability, doubling time, growth rate and glucose consumption rate (GCR). The data were grouped and summarized for cells at passage levels less than or equal to P7 and for cells above P7. (P = passage level; PD = population doubling; GCR = glucose consumption rate; ND = not determined)

The data for Table 15 were grouped and divided into two groups – cells below or at P7 or cells above P7 (at P8 or greater). This distinction was made due to the gradual decrease in growth rate of the hMSCs over increasing passage level. This observation will be discussed further below.

Overall the average viability of the thawed hMSCs was similar for all the cell banks produced averaging 87.6 +/- 4.2% (n=19). The viability of the cells at each passage

after trypsinization was uniformly high >98% at all passage levels, except the cells above P7 from the P2/P3 MC banks (last data column of Table 15). This decreased viability may have been due to a higher bacterial contamination level in those cells (discussed further in section 3.4.3) because penicillin/streptomycin was not utilized in these cultures. The viability of the cells at each passage did not appear to be affected by increasing passage level, at least to passage 12 which was the highest level that these hMSCs were grown for this research.

The doubling time and growth rate of the hMSCs were calculated according to section 2.5.4 and found to be 69 +/- 23 hours (n=52) for hMSCs ≤P7 and 134 hours +/- 88 hours (n=48) for hMSCs ≥P8. The growth rate from these doubling time calculations at every passage was also calculated to be 0.26 +/- 0.07 hr^{-1} for ≤P7 and 0.17 +/- 0.09 hr^{-1} for ≥P8.

3.4.1.1. Specific growth rate of hMSCs

The hMSCs' growth kinetics appeared to be greatly influenced by the passage level with the lowest passage cells having the highest growth rate and the higher passage cells having a significantly lower rate. Due to this observation, cells were not used for experiments above P12. Figure 32 shows the graph of the hMSCs' specific growth rate versus passage number for the cells used from 5 independent BMC sources (n=59). The specific growth rates were determined by the linear approximation of the increase of cell density over the culture length. These rates were generated at each cell passage and contained between 1 to 3 data points from the number of total cells harvested/cm^2. The majority of the specific growth rate data was collected from frozen P4 JM cell bank (n=27) which ranged from 2.2 +/- 0.74x10^2cells/cm^2/hr at P5 down to 0.70 +/- 0.30x10^2cells/cm^2/hr at P10. However data from fresh stocks (n=9) and other frozen cell stocks at P2/P3 MC (n=7), P4 SE (n=7) and P8 JM (n=9) were also used in these analyses.

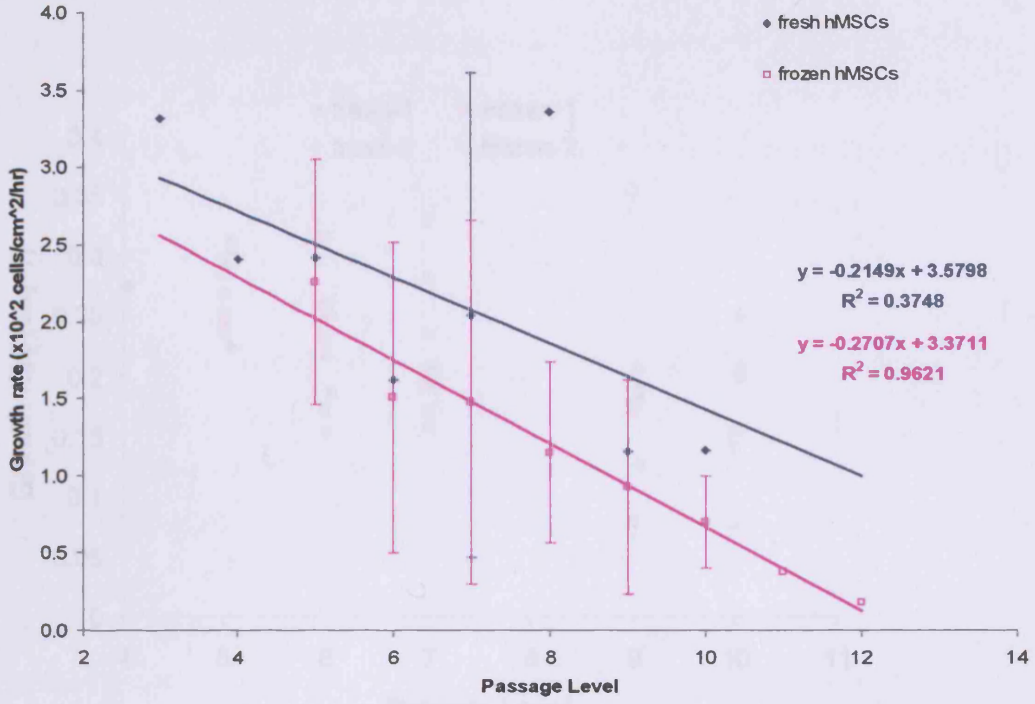

Figure 32. HMSC specific growth rate versus passage level for fresh cells and frozen cells grown in tissue flasks. Frozen cells were derived from frozen cell banks. The fresh hMSCs (not previously frozen) appeared to have a higher growth rate than frozen cells. The growth rate of both fresh and frozen hMSCs significantly decreased between passages 2 and 12. The majority of hMSC growth data was collected from cells expanded from a frozen P4 cell bank. For the frozen cells, the specific growth rate ranged from 2.2 +/- 0.74 $x10^2$cells/cm^2/hr at passage 5 down to 0.70 +/- 0.30$x10^2$cells/cm^2/hr at passage 10. These data were generated from a total of 59 observations (9 for fresh cells, 50 for cells from frozen source).

Although these results suggested that the frozen hMSCs have ca. 50% lower growth rate than fresh cells; these data were from 5 different donor sources, a factor which can contribute to the greatest variability in growth rate (Phinney, 1999). When the growth rates from the same donor(s) were compared directly between freshly passaged hMSCs and the same cells after freezing; a different result was obtained as shown in Figure 33. Growth rates were calculated according to section 2.5.4, and were compared for one donor between P5 and P7, for another donor between P9 and P10.

A

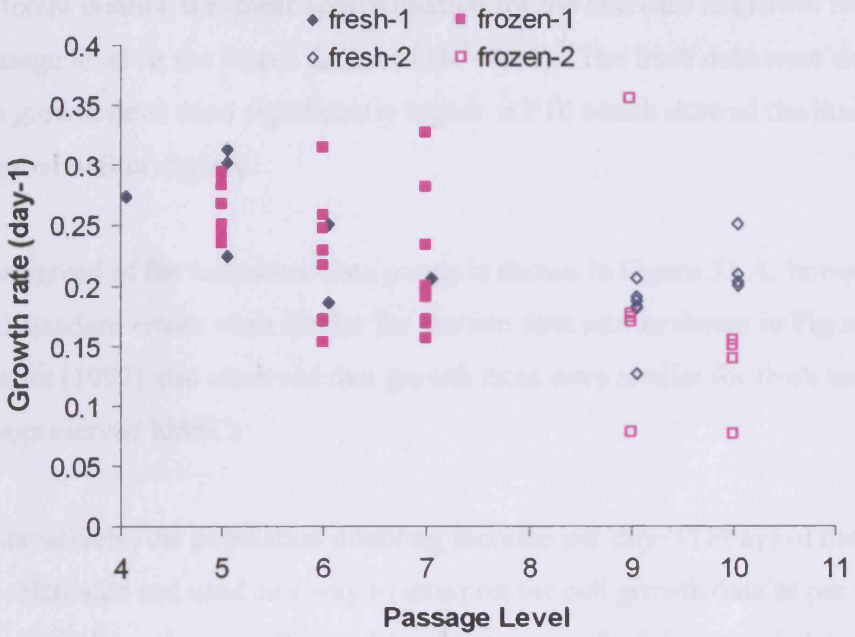

B

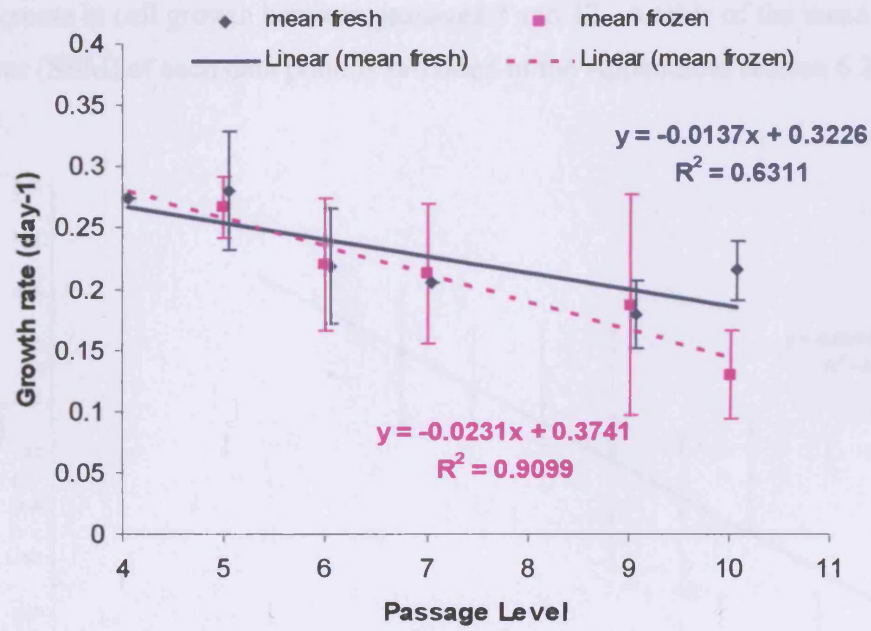

Figure 33. Growth rate comparison between freshly passaged hMSCs and the same cells after cryopreservation. Two donors were compared, one between P5 and P7 and another between P9 and P10. (A) Individual data points obtained from donor 1 designated as '1' and donor 2 as '2'. (B) The mean and standard error of the growth rates determined from each donor for each passage.

The linear approximation was determined from the pooled data from the two donors for the cells passaged fresh and the cells passage after freezing. Despite being two different donors, the linear approximation for the decrease in growth rate versus passage level fit the frozen data well (R^2=0.91). The fresh data were similar; however the growth rates were significantly higher at P10 which skewed the linear approximation slightly.

The spread of the individual data points is shown in Figure 33.A; however the mean and standard errors were similar for the two data sets as shown in Figure 33.B. Bruder (1997) also observed that growth rates were similar for fresh and cryopreserved hMSCs.

Alternatively, the population doubling increase per day (PD/day) of the hMSCs can be calculated and used as a way to interpret the cell growth data as per section 2.5.4. These data are shown in Figure 34 and represent all of the growth data from all hMSCs used in this research. These data also show that there was a substantial decrease in cell growth between passages 2 and 12. A table of the mean and standard error (SEM) of each data point is provided in the Appendices section 6.2.1.1, Table 18.

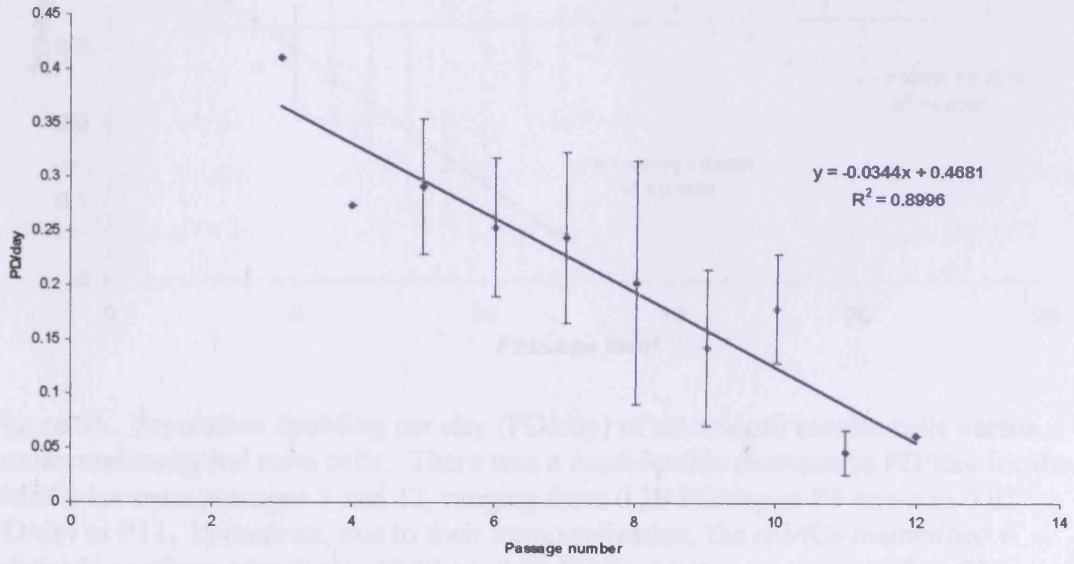

Figure 34. Population doublings per day (PD/day) of hMSCs in tissue flasks from passage 3 to 12. Early passage cells (P3-P5) were 0.3-0.4 PD/day; however, this decreased considerably at later passages (P9-P12) which were 0.05-0.15 PD/day. These growth data were generated from the mean and standard error from all hMSCs used (n=101).

These growth rate data were compared against data published by Kinner (2002) who found that after three passages the hMSCs underwent 9-11 population doublings. The growth kinetics used in their study varied among 10 patients from 0.24 to 0.45 PD/day or an average of 0.4 +/- 0.05doublings/day (Kinner, 2002). After converting their PD/day calculation from ln to log, the rates became 0.1 to 0.2 PD/day or an average of 0.17 +/- 0.02 PD/day and were similar to these results.

The growth data for hMSCs were also compared to the growth data obtained from the rSMCs used initially in this project. As can be seen in Figure 35, the hMSCs have very different growth characteristics as would be expected between primary cells versus immortalized cells. As previously shown, there was a considerable decrease in PD/day for the hMSCs between passages 3 and 12. In contrast, due to their immortalization, the rSMCs maintained a relatively constant growth rate (0.32 +/- 0.06 PD/day) between passages 2 to 22.

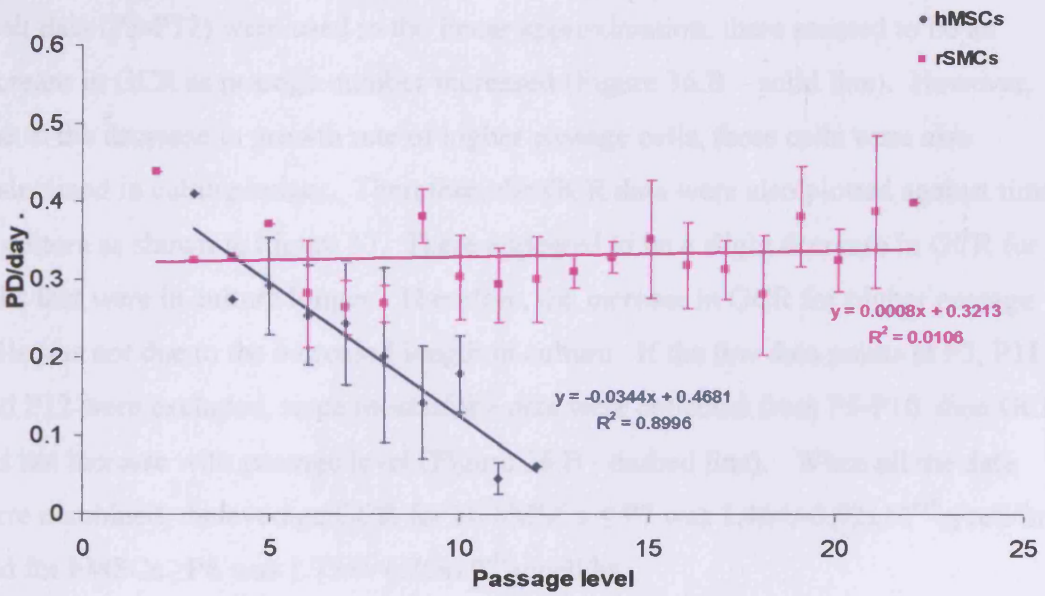

Figure 35. Population doubling per day (PD/day) of rat smooth muscle cells versus human mesenchymal stem cells. There was a considerable decrease in PD/day for the hMSCs between passages 3 and 12, ranging from 0.29 PD/day at P5 down to 0.05 PD/day at P11. In contrast, due to their immortalization, the rSMCs maintained a relatively constant growth rate (0.32 +/- 0.06 PD/day) between passages 2 to 22.

Bruder (1997) and Phinney (1999) have also noted the decreased growth rate of hMSCs cultures *in vitro* as the number of population doublings (e.g. passage level) increased.

3.4.1.2. Glucose consumption rate of hMSCs

At each passage, a sample of the spent medium from the tissue flask cultures was tested for glucose concentrations using the YSI bioanalyzer. In addition, the initial concentration of glucose was measured from the MSCCM. From these data and the average number of cells during the culture period, the GCR was calculated as described in section 2.5.6.1. The average GCR for each cell source was summarized previously in Table 15. The GCR appeared to be slightly higher at passages ≥P8 for several of the cell sources used; although the data were highly variable with large standard errors. These data were plotted against passage level in Figure 36.A to see if this observation was significant.

If all data (P3-P12) were used in the linear approximation, there seemed to be an increase in GCR as passage number increased (Figure 36.B – solid line). However, due to the decrease in growth rate of higher passage cells, these cells were also maintained in culture longer. Therefore, the GCR data were also plotted against time in culture as shown in Figure 37. There appeared to be a slight decrease in GCR for cells that were in culture longer. Therefore, the increase in GCR for higher passage cells was not due to the increased length in culture. If the few data points at P3, P11 and P12 were excluded, since most of the data were collected from P5-P10, then GCR did not increase with passage level (Figure 36.B - dashed line). When all the data were combined, the average GCR for all hMSCs ≤ P7 was $1.46+/-0.92x10^{-10}$g/cell/hr, and for hMSCs ≥P8 was $1.75+/-1.75x10^{-10}$g/cell/hr.

A

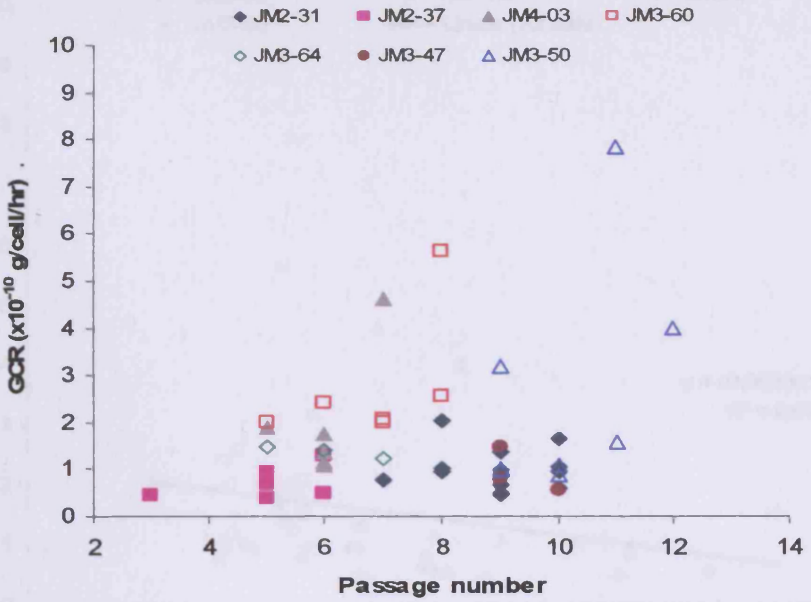

B

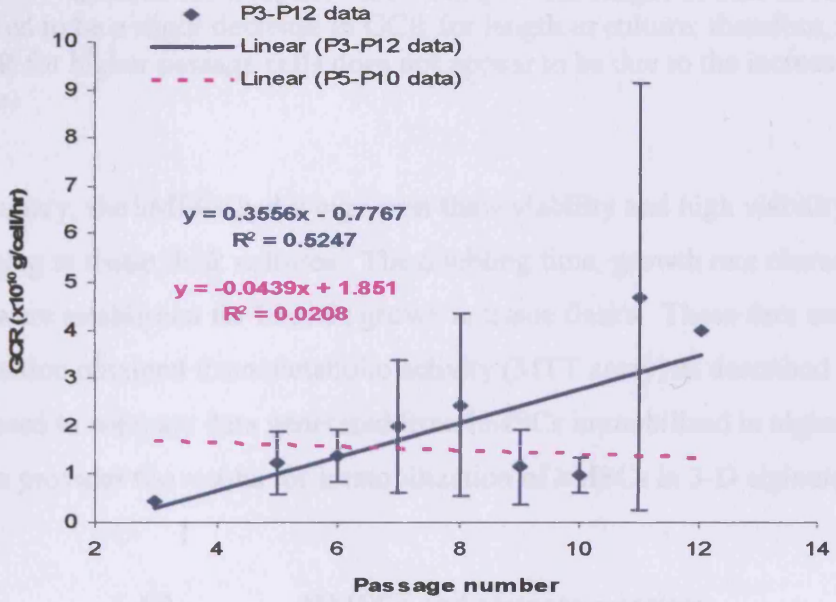

Figure 36. Glucose consumption rate (GCR) verses passage number of hMSCs. The GCR appeared to increase as the passage number of the cells increased, not only for individual cell sources (A), but also as a general trend for all the data collectively (B) when data from P3 to P12 were used (solid line). However, if the few data points at P3, P11 and P12 were excluded, since most of the data was generated for P5-P10, the GCR did not increase with passage level (dashed line).

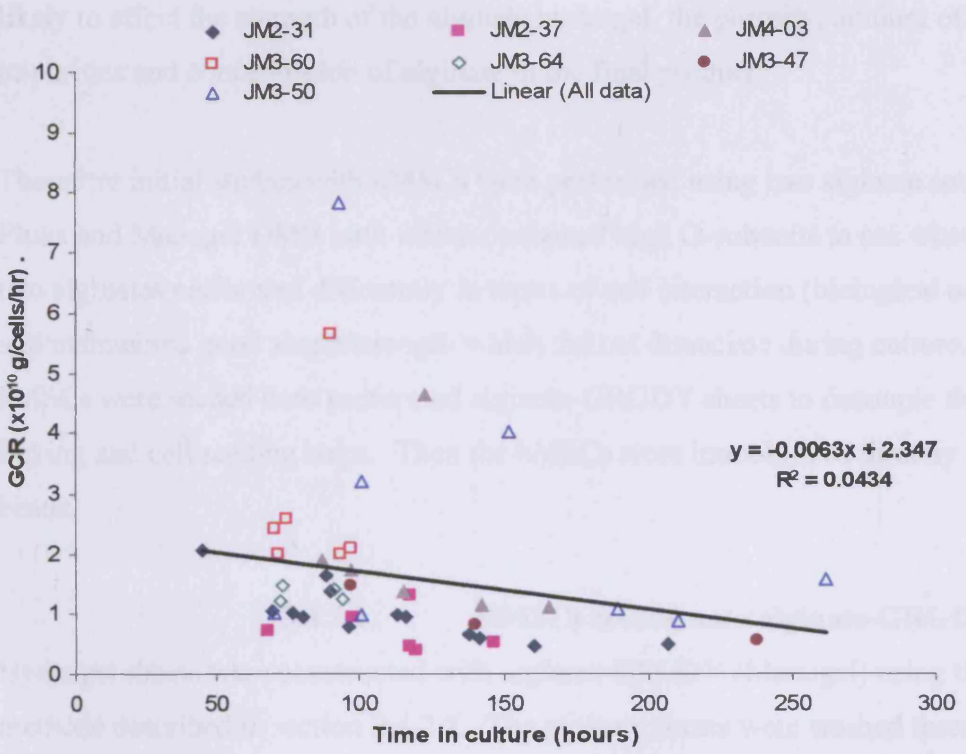

Figure 37. Glucose consumption rate (GCR) versus length of time in culture. There appeared to be a slight decrease in GCR for length in culture; therefore, the increase in GCR for higher passage cells does not appear to be due to the increased length in culture.

In summary, the hMSCs had a high post thaw viability and high viability during passaging in tissue flask cultures. The doubling time, growth rate characteristics and GCR were established for hMSCs grown in tissue flasks. These data and additional information obtained from metabolic activity (MTT assay) as described in section 3.5 were used to compare data generated from hMSCs immobilized in alginate. The next section provides the results for immobilization of hMSCs in 3-D alginate hydrogels.

3.4.2. HMSCs and alginate matrices

Preliminary results using rSMCs showed that alginate-GRGDY had a different degree of biological activity (e.g. cell association) based upon the concentration of the reactants (e.g. 10X versus 50X) that were used to derivatize the Fluka, Manugel or Pronova MVG alginate as described in section 3.3.5. In addition, the reaction parameters (e.g. time and temperature), length of dialysis, treatment with activated charcoal, filtration using Celite and concentration using lyophilization also were very

likely to effect the strength of the alginate hydrogel, the porosity, amount of impurities and concentration of alginate in the final product.

Therefore initial studies with hMSCs were performed using two alginate sources: Fluka and Manugel DMB both which contained high G-subunits to see whether the two alginates performed differently in terms of cell interaction (biological activity), and maintained good shape/strength which did not dissociate during culture. First hMSCs were seeded onto preformed alginate-GRGDY sheets to decouple the cross linking and cell seeding steps. Then the hMSCs were immobilized directly into beads.

3.4.2.1. HMSCs seeded onto alginate-GRGDY sheets

Hydrogel sheets were constructed with alginate-GRGDY (Manugel) using the methods described in section 2.4.2.1. The alginate sheets were washed three times with WFI and then once with MSCCM to remove excess $CaCl_2$ from the sheet fabrication step. HMSCs at P10 were seeded at $6x10^4$cells/mL onto the surface of 10X and 50X alginate-GRGDY sheets with 2mL of MSCCM per well using a 12 well microplate (Corning). At this concentration the cells would have been seeded at $3x10^4$ cells/cm^2, if the 12 well surface area of 3.9cm^2 was used as the estimated surface area of the alginate sheet. After four days of culture at 37°C, the hMSCs seeded onto the surface of 10X alginate-GRGDY sheets remained rounded and did not attach to the surface of the sheet (Figure 38.A). Whereas the hMSCs seeded onto the surface of the 50X alginate-GRGDY sheets elongated and formed a monolayer of cells (Figure 38.B). The hMSCs elongation on the surface of the 50X alginate-GRGDY was comparable to the control hMSCs seeded on the surface of a microwell (Figure 38.C); although the cells on the hydrogel appeared to be at a lower density and more spindle-shaped than in the microwell. This apparent difference in cell density was attributed to the cells sliding or settling off the surface of the alginate hydrogel onto the microwell surface below, as a large number of cells were observed growing under the hydrogel on the surface of the microwell. Due to the thickness of the alginate hydrogel, the microscope field of focus could easily be distinguished from cells positioned on the surface of the hydrogel as opposed to the surface of the microwell.

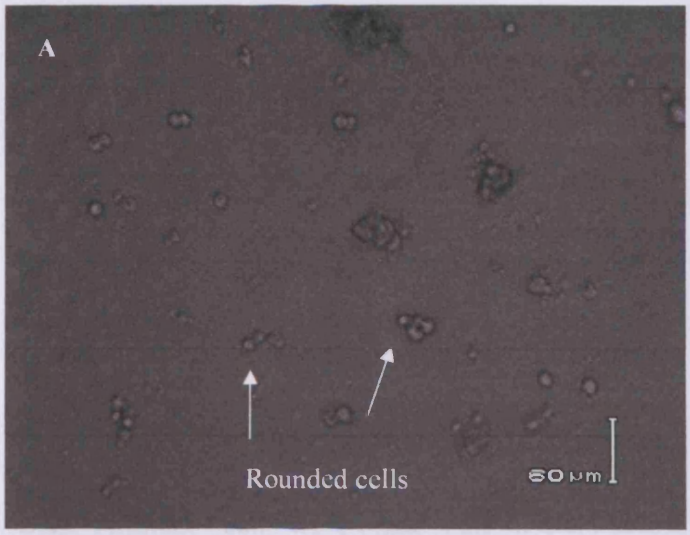

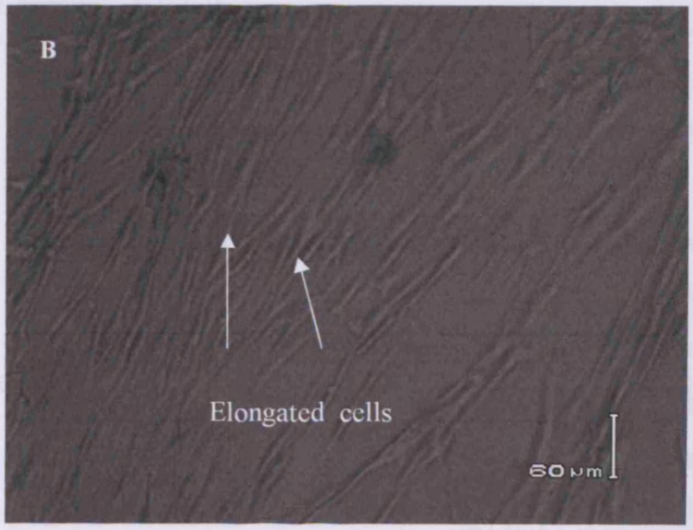

Figure 38. 10X and 50X alginate-GRGDY (Manugel) sheets seeded with hMSCs after 4 days of culture. (A) 10X - All cells remained round and did not attach to surface of alginate. (B) 50X - The cells attached to the surface of the alginate and elongated forming a network of spindle-shaped cells. (C) Control cells seeded onto the microwell surface after 4 days of culture. All cells are attached to surface, elongated and densely packed. All photos 100X magnification.

3.4.2.2. Comparison of hMSCs immobilized in non-derivatized versus derivatized alginate beads

Fluka alginate was derivatized using 50X reactants and GRGDY peptide, dialyzed for 2½ days, treated with activated charcoal and filtered through Celite as described in section 2.3.3. Then it was lyophilized and reconstituted with WFI. Non-derivatized Fluka alginate was prepared using 2% w/v of Fluka alginate in n-saline (0.9% NaCl) solution, pH7.3, and autoclaved for 22min at 121°C. The alginate was mixed with 1g activated charcoal per 15mL of alginate and then filtered through a 1.2μm Supor® membrane filter (Pall, Gelman Laboratory, Acrodisc® syringe filter, Portsmouth, UK). Alginate beads were made with 50% v/v hMSCs at P8 resuspended in MSCCM to a final concentration of $2x10^6$cell/mL in the two alginate solutions using the method described in section 2.4.4. A time course of photos were taken of the hMSCs interaction with the alginate matrices. Immediately after immobilization, the hMSCs were all rounded within both hydrogel matrices. The hMSCs in the non-derivatized alginate matrix remained rounded and did not elongate within the hydrogel during the 7 day study (Figures 39.A-C). In contrast, the hMSCs in the alginate-GRGDY elongated within 24 hours (Figure 39.D) and even more extensively by day 3 and 7 (Figures 39.E-F). Day 1 and 3 photos were taken with a phase contrast microscope. Whereas photos C and F were taken with a fluorescence microscope showing hMSCs that were stained with calcein AM, for cytoplasm of live cells after 7 days in culture.

These results indicated for the first time that hMSCs were able to elongate within a alginate-GRGDY hydrogel. Previous findings using rSMCs demonstrated that these cells were not able to elongate within the alginate-GRGDY hydrogels, but only when seeded freely on the surface of the hydrogel. These results also confirmed that hMSCs do not interact with non-derivatized alginate as was found with rSMCs. Later studies also continued to support this finding; and furthermore, it was found that any amount of non-derivatized alginate (within the range examined) mixed into alginate-GRGDY immediately rendered the hydrogel biologically inactive. These results confirmed earlier collagen and alginate studies with rSMCs which showed that alginate rendered the collagen biologically inactive after cross linking the alginate.

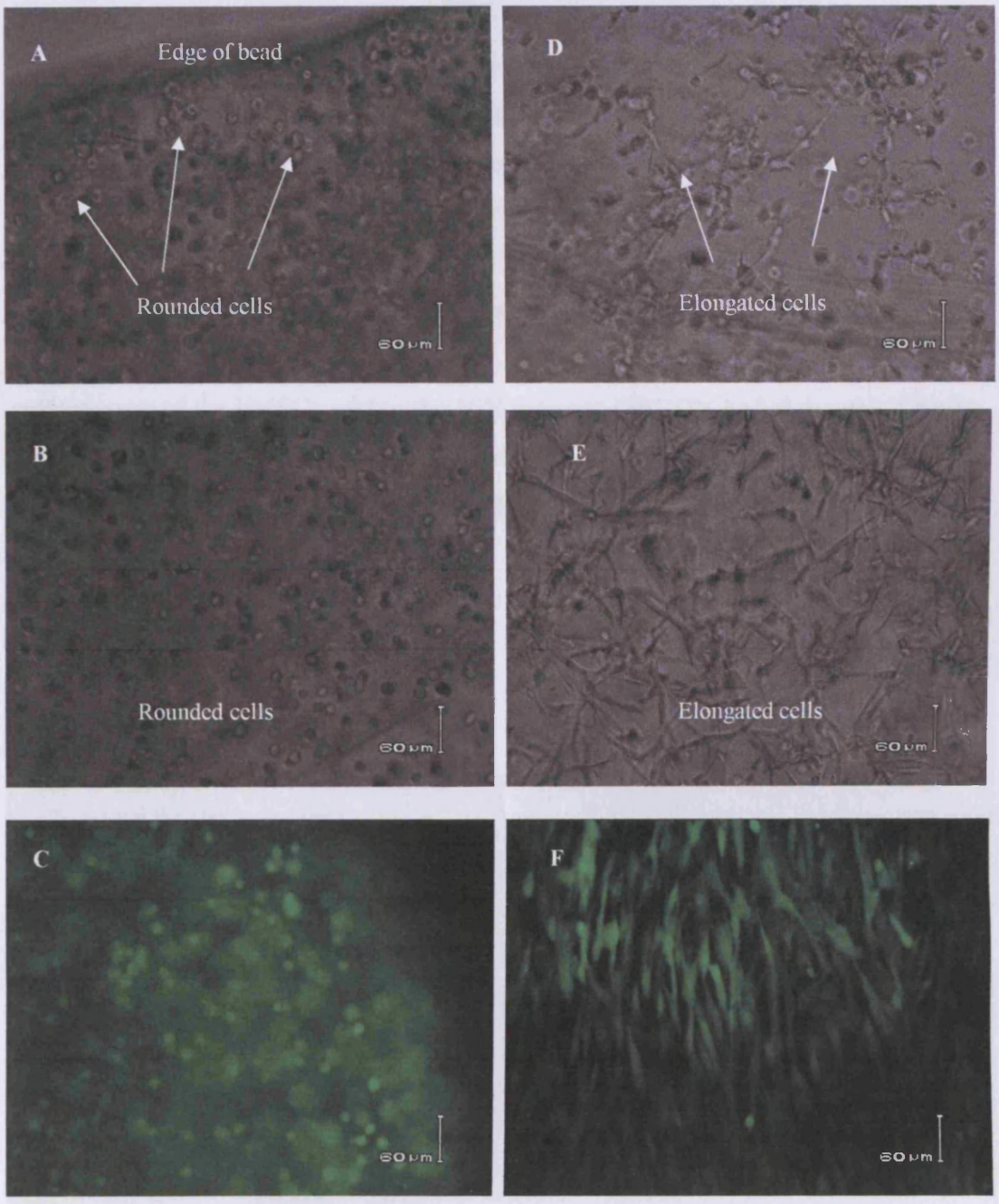

Figure 39. Time course of hMSC seeded at $2x10^6$cells/mL within non-derivatized (0X) alginate beads and 50X alginate-GRGDY beads (Fluka). (A) HMSCs on day 1, (B) day 3 and (C) day 7 in non-derivatized alginate beads. (D) HMSCs on day 1, (E) day 3 and (F) day 7 in 50X alginate-GRGDY beads. Photos A, B, D and E are taken with phase contrast microscope. Photos C and F are taken with fluorescence microscope using calcein AM, which stains the cytoplasm of live cells. All photos 100X magnification.

3.4.2.3. Effect of reactant and cell concentrations on immobilized hMSCs in alginate-GRGDY beads

Additional studies were performed with beads constructed with hMSCs using 10X and 50X alginate-GRGDY (Manugel) as described in section 2.4.4. The cell pellet was resuspended in MSCCM at a concentration $5x10^6$cells/mL and added at 25% v/v to the alginate-GRGDY. Immediately after cross linking with 1% $CaCl_2$ in n-saline, the beads were rinsed twice with MSCCM and transferred into 24 well microplates containing 1mL of MSCCM and incubated at 37°C. Initially the hMSCs are all rounded within the alginate hydrogel after immobilization. However after 4 days of culture some of the hMSCs within the 10X alginate-GRGDY had elongated slightly within the matrix (Figure 40.A). However the hMSCs within the 50X alginate-GRGDY were all elongated and extensively networked within the matrix (Figure 40.B).

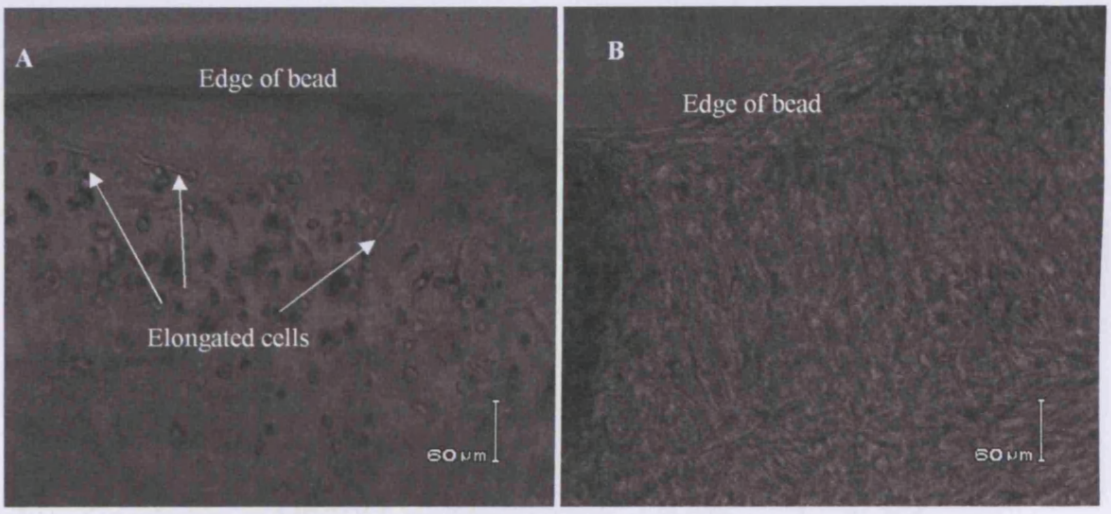

Figure 40. HMSCs seeded at $5x10^6$cells/mL in 10X and 50X alginate-GRGDY beads (Manugel) after 4 days of culture. (A) 10X alginate-GRGDY - A few cells around the perimeter of the bead have elongated. The majority of remaining cells remained rounded and did not elongate. (B) 50X alginate-GRGDY - All of the cells elongated and were extensively networked throughout the entire bead. All photos 100X magnification.

In this study the hydrogels with higher cell density ($5x10^6$cell/mL) had notably better networking of cells than the previous study which had only $2x10^6$cells/mL (Figure 39.E versus Figure 40.B). Throughout the course of research the concentrations of hMSCs varied from $1x10^6$ up to $2x10^7$cells/mL of alginate. It was found that the highest concentration, $2x10^7$cells/mL, produced the best consistency of cell elongation throughout the bead and the most cell-to-cell networking as assessed microscopically. At lower concentrations ($<10^7$cell/mL), the hMSCs were spaced further apart and physically could not bridge the gaps between adjacent cells. In some cases the cells elongated inconsistently throughout the bead, and some cells remained rounded or took longer to eventually elongate. This result could be a growth factor-release event or triggered by a product of metabolism, as it is well documented that cells at low density in tissue culture flasks (such as for cell cloning) have much slower growth rates than cells seeded at high densities (Freshney, 1994). During cell growth the medium is conditioned by release of small molecular metabolites and macromolecules (Takahashi and Okada, 1970). Therefore cells at low density or immobilized in a substrate such as a hydrogel with mass transfer restrictions, may be adversely influenced by these factors.

Because the GRGDY peptide was an expensive reagent, the amount of peptide added to the carbodiimide reaction was examined to see if the concentration required for biological activity (e.g. cell elongation) could be reduced. Alginate was derivatized according the protocol described in section 2.3.3 using 12.5mL of 1% Manugel DMB alginate (125 mg) with three peptide concentrations including 1X (0.125mg) GRGDY, 10X (1.25mg) and 50X (6.25mg). A 50X concentration of reactants (237.5mg of sulfo-NHS and 418.75mg of EDC) was used in each formulation. HMSCs at P6 were combined at 20% v/v to the alginate at $5x10^6$cells/mL. After 1 day of incubation in MSCCM, the hMSC beads were observed and all three conditions had the same high degree of cell elongation and networking throughout the beads. This was a significant finding since previous studies with both Manugel and Fluka alginate showed that 10X reactants produced considerably lower biological activity than the 50X reactants; therefore the amount of reactants, EDC and sulfo-NHS, were limiting the extent of derivatization of peptide onto the alginate and not

the concentration of peptide. Therefore a lower peptide concentration could be used in the derivatization process.

3.4.2.4. Culturing hMSCs in alginate-GRGDY tubes

In addition to the observations made with sheets and beads, hMSCs were combined with alginate-GRGDY and immobilized into tubes as described in section 2.4.3, Figure 7 and 2.4.3.3. The cell-alginate solution was composed of 25% v/v cell suspension and 75% v/v 50X alginate-GRGDY (Manugel DMB). Two tubes with P4 hMSCs at $5x10^6$cells/mL were extruded in glass tubes using a large diameter ball (ca. 3.71mm) as the float. After cross linking was completed using 1%$CaCl_2$ in n-saline, the tubes were rinsed and filled with MSCCM. The tubes were incubated at 37°C as a static culture and refed with ca. 5mL fresh MSCCM every 10-14 hours. The glass tubes held a total volume of 1.5mL MSCCM. Samples of the spent medium were taken and frozen at each time point and analyzed on the YSI bioanalyzer for glucose and lactate. In addition a time course of photos was taken. On day 3, the hMSCs were elongated, but the cell-cell networking was low (Figure 41.A). By 12 days in culture, the cells were densely networked (Figure 41.B).

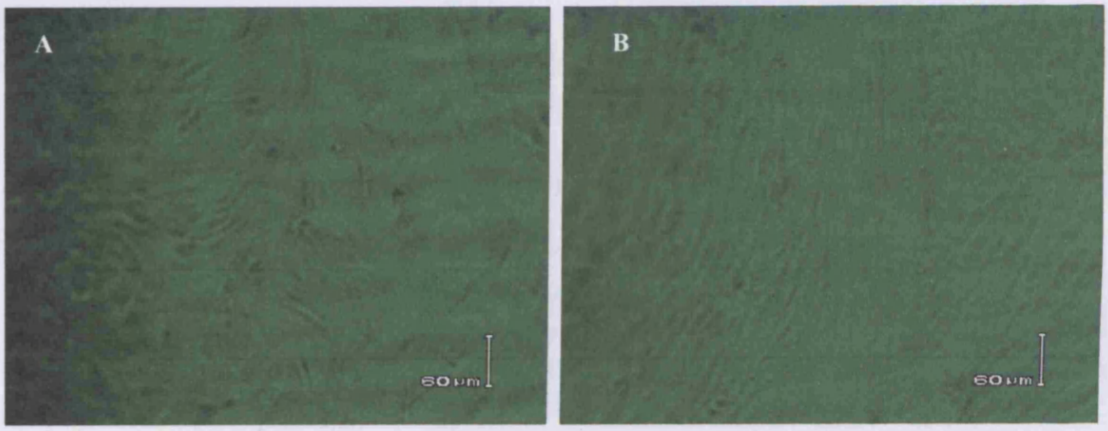

Figure 41. Time course of hMSC growth in 50X alginate-GRGDY (Manugel) extruded into tubes seeded at $5x10^6$cells/mL. (A) HMSCs after 3 days of culture and (B) after 12 days of culture. Due to the curvature of glass rod, the field of view was blurred slightly at edges at 100X magnification.

As shown in Figure 42, analysis of the glucose consumed showed that both tubes had similar rates. The glucose consumption increased slowly between 0-100 hours and then reached a steady-state thereafter. A linear approximation was made for the

cumulative glucose consumed for tube 2 between 100 and 200 hours in culture. The slope of this line was 0.0219 g/L/hr. Therefore using the vessel volume of 1.5mL, the cells consumed $3.3x10^{-5}$g/hr. The final number of cells per tube was not determined, but they were originally seeded with $5x10^{6}$cells/mL and ca. 210µL was used to make the tube 145µm thick with outside diameter of 4mm (Volume = Pi * $(r_2^2-r_1^2)$* h = 3.14 * $((4/2)^2 - (3.71/2)^2)mm^2$ * 120mm / $1000mL/mm^3$) which equaled $1.05x10^{6}$cells, or a glucose consumption rate of $3.1x10^{-11}$g/cell/hr. This estimate was lower than the GCR data obtained from hMSCs grown in tissue flasks for the same cells (JM2-37) below P7 which from Table 15 was $7.3x10^{-11}$ +/- $3.2x10^{-11}$g/cell/hr (n=7).

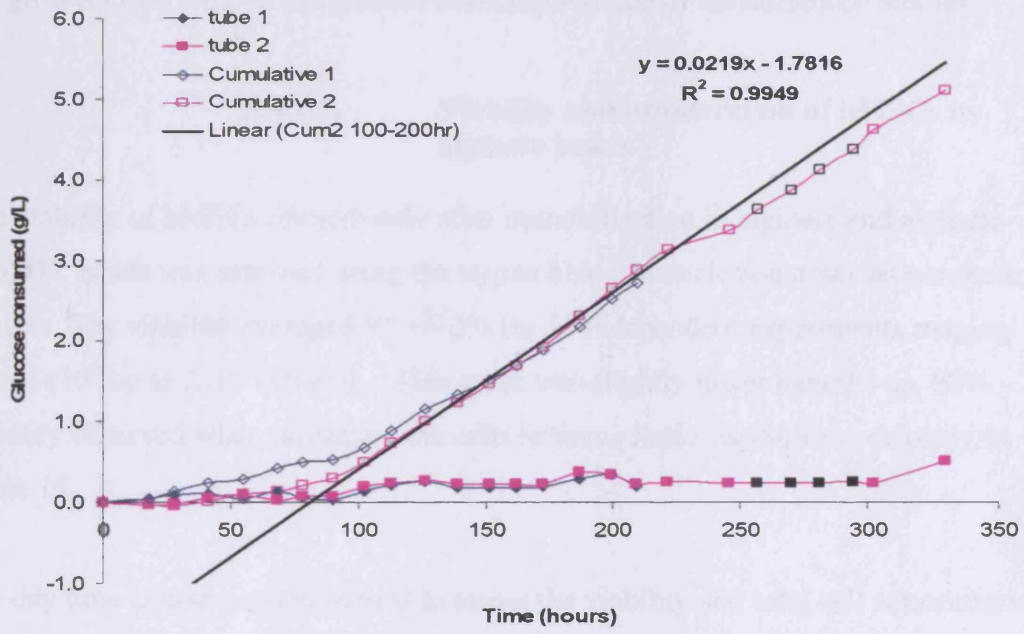

Figure 42. Glucose consumption of hMSCs in 50X alginate-GRGDY (Manugel) tubes seeded with $1.05x10^{6}$cells. The daily measurements of glucose consumed are shown by the closed symbols. The cumulative glucose consumed is shown by the open symbols. Four data points (black) were estimated from actual glucose consumed from four data points surrounding these time points as the tubes were refed but samples were not taken. The linear approximation was estimated from the cumulative glucose consumed in tube 2 between 100-200 hours in culture.

The respiratory quotient (ratio of lactate produced versus glucose consumed) was calculated for this experiment and found to be 2.4+/-1.2 in the first five days of cultures and then decreased to 1.14+/-0.17 for the remaining culture period. This indicated that the cultures were primarily anaerobic during the initial culture and more oxygen was required by the hMSCs. Therefore, in future experiments constant flow

should be supplied to the bioreactor containing hMSCs. The respiratory quotient of representative tissue flask cultures of hMSCs was measured to be 0.90+/-0.18 (n=46) which, as expected, indicated aerobic metabolism.

In addition to providing continuous medium flow through the glass bioreactor, further refinement to the glass bioreactor also requires surface treatment to ensure that the hMSCs do not adhere to the glass tube surface, since it would be undesirable to have the cells attach and grow outside the hydrogel construct. Low binding microwell plates were used for bead studies to ensure cells that dissociated from the alginate did not grow and attribute to the glucose consumption rate in the microwell studies.

3.4.2.5. Viability and proliferation of hMSCs in alginate beads

The viability of hMSCs immediately after immobilization in alginate and alginate-GRGDY beads was assessed using the trypan blue dye exclusion assay as per section 2.3.2.6. The viability averaged 95 +/- 3% for 10 independent experiments ranging from $1x10^6$ up to $2x10^7$cells/mL. This value was slightly lower than the ca. 98% viability observed when passaging the cells in tissue flasks as shown previously in Table 15.

A 5 day time course was performed to assess the viability and total cell concentration of hMSCs immobilized in non-derivatized alginate (Manugel) at 0.5% and 0.75% w/v composition (Figure 43). The viability and total cell concentration were determined by releasing the cells from the alginate using trisodium citrate and counting the cells on a hemacytometer using trypan blue. The 0.5% w/v alginate composition was formulated using 1% Manugel in WFI and combining with 50% v/v of cell suspension in MSCCM, and the 0.75% w/v formulation was made by combining the 1% Manugel in WFI with 25% v/v of cell suspension. The cells were prepared at a concentration of $1x10^6$cell/mL with an average of 2-3 beads counted at each time point. The initial viability was 98% for both conditions. The viability in the 50% v/v alginate beads (final 0.5% w/v alginate) decreased to 70% after 4 days; whereas the viability of the 75% v/v alginate beads (final 0.75% w/v alginate) maintained 85% viability after 5 days in culture. The reason for the decrease in viability was not known, other than the cells were immobilized in non-derivatized alginate without any attachment sites for

the cells. Additional time course experiments that assessed hMSC percent viability and total number of cells per bead were performed during experiments conducted with the MTT assay. These results are discussed in section 3.5.

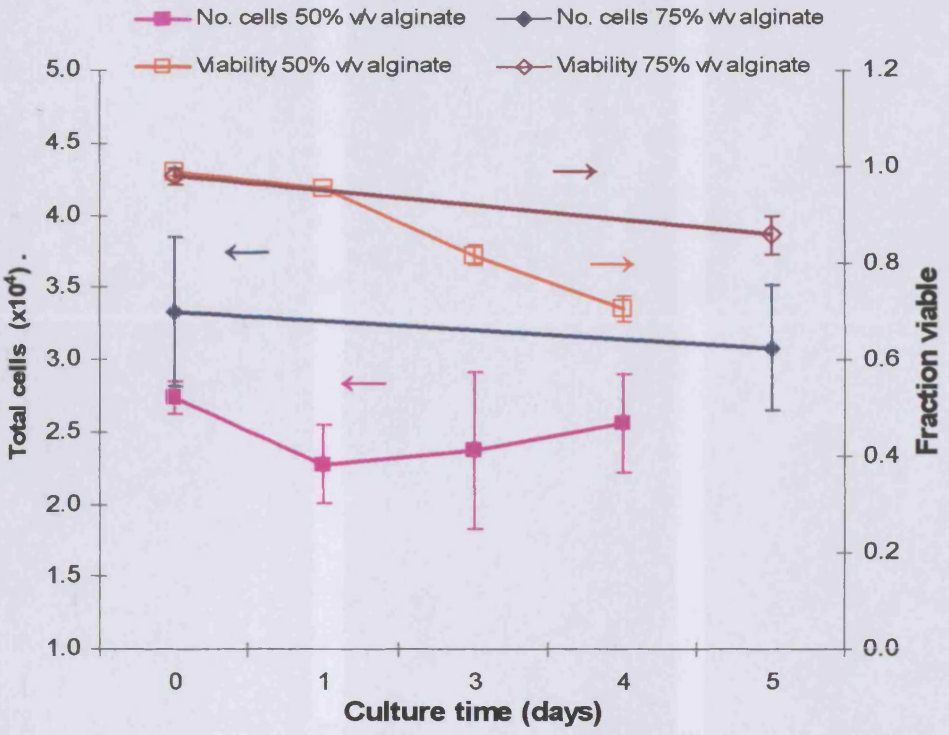

Figure 43. Viability and total number of hMSCs in non-derivatized alginate beads (Manugel) at 50% v/v and 75% v/v composition. The initial viability was 85% for both conditions. The 50% v/v alginate beads decreased to 70% viable after 4 days, whereas the 75% v/v beads maintained 85% viability after 5 days in culture.

An additional time course study was performed using the live/dead fluorescence assay as described in section 2.5.7. The two probes were calcein AM (green) indicating cytoplasm of live cells and ethidium homodimer (red) staining nucleic acids of dead cells. These studies only provided a qualitative as opposed to a quantitative result for cell viability. The study was conducted using hMSCs immobilized in 9X Pronova SLG100 alginate-GRGDY beads at $9x10^6$cells/mL using 1% $CaCl_2$ in n-saline. Immediately after immobilization the beads were rinsed with complete DMEM; then cultured in either complete DMEM or in MSCCM for 17 days. Figure 44 shows the sequence of the three images of hydrogel beads cultured in complete DMEM on day 3 (A-C) and day 17 (G-I); and in MSCCM on day 3 (D-F) and day 17 (J-L). Each sequence was taken without moving the field of view.

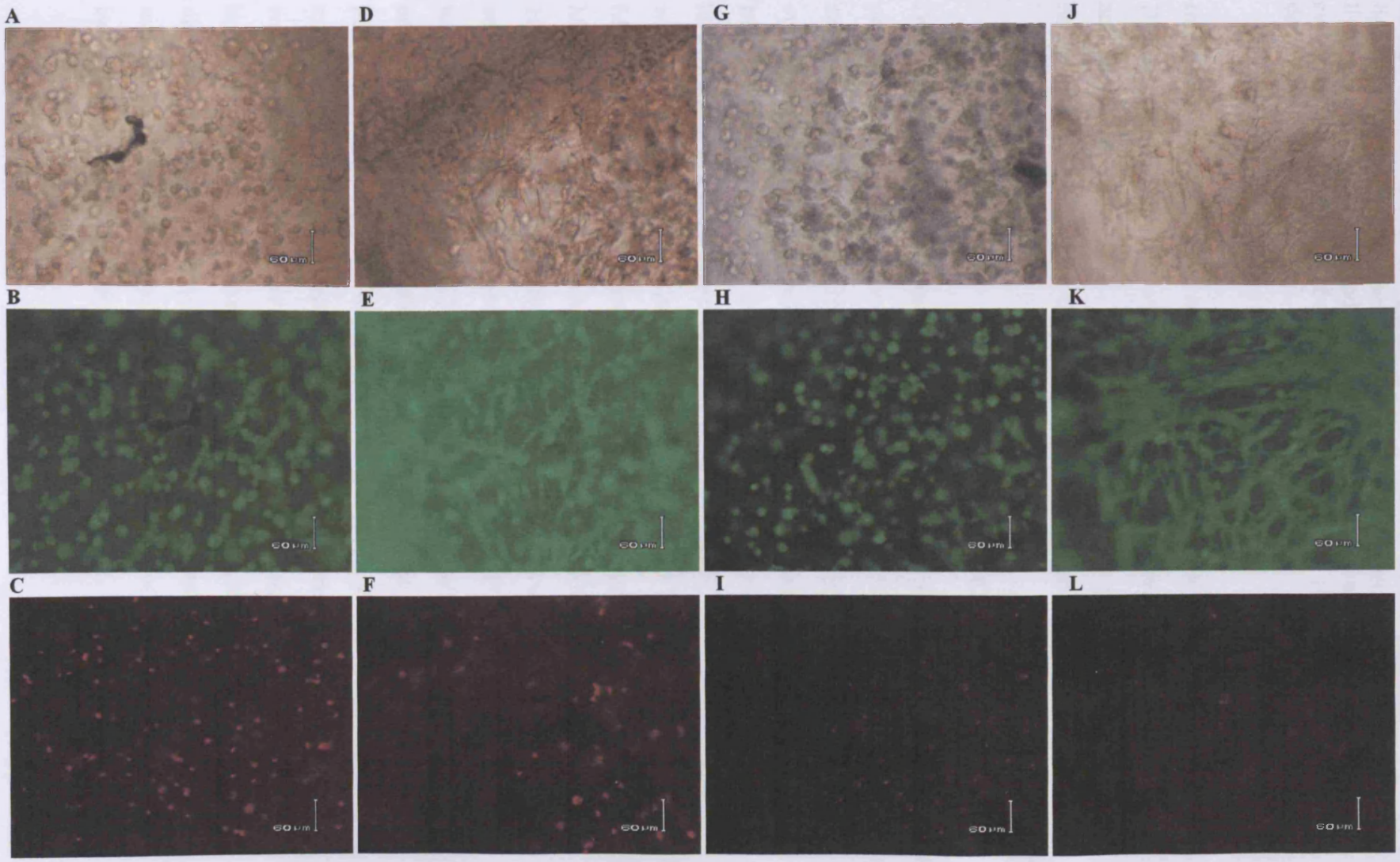
A
D
G
J
B
E
H
K
C
F
I
L
50 µm

Figure 44. (On previous page) Live/dead fluorescence assay for time course of hMSCs immobilized in 9X alginate-GRGDY beads (Pronova SLG100). Sequence of light and fluorescence microscopy with calcein AM (green) indicating cytoplasm of live cells and ethidium homodimer (red) staining nucleic acid of dead cells. Beads cultured in complete DMEM on day 3 (A-C) and day 17 (G-I); and in MSCCM on day 3 (D-F) and day 17 (J-L). 100X magnification.

Interestingly the hMSCs did not elongate within the hydrogels cultured with complete DMEM; whereas the hMSCs within the hydrogels cultured with MSCCM elongated and networked within 1 day. The complete DMEM was most likely deficient in the necessary growth factors for this to occur (e.g. bFGF is added to the MSCCM).

3.4.3. Sterility issues with hMSCs cultures

During the course of this research project the sterility of the alginate derivatization process was continually improved until a sterile process was achieved as described in sections 2.3.3.7 and 3.2.8. However it became apparent that the alginate was not the only possible contributing factor to microbes within the system. So the fresh MSCCM and spent medium from cultures of hMSCs were visually examined in microwells to detect the presence of microbes as per section 2.2.2.3. Terrific broth was not used because precipitates formed when MSCCM was added. The formulated MSCCM was also sterile filtered for added sterility assurance. Once filtered, the MSCCM was rarely contaminated. Despite the presence of 100Upenicillin/mL and 100μL streptomycin/mL (P/S) in the MSCCM, microbes were observed in the cultures of hMSCs that did not appear to be sensitive to P/S nor to other antibiotics tested in MSCCM including 50mg/L gentamycin, 100mg/L kanamycin and 100mg/L erythromycin. The microbes had no adverse macroscopic effect on the culture (e.g. pH or turbidity change) and the cells continued to grow. However after the spent medium in the microwells settled overnight, cellular debris, dead cells and microbes were observed at 400X magnification or greater. The microbes were not homogeneously dispersed throughout the microwell, but outgrowth appeared in discrete foci throughout the well (Figure 45). Samples were provided to the microbiology lab at UCLH to try to identify the organism(s), but they could not isolate any microbes from the spent medium.

The presence of microbes was exacerbated when the hMSCs were immobilized in alginate-GRGDY due to the high cell concentrations used (e.g. $2x10^7$cells/mL) in the beads. The microbes were observed microscopically as tiny dots within the bead, but they also dissociated from the bead and dropped onto the microwell surface below the beads. Occasionally these beads were observed to undergo discoloration as discussed in the next section.

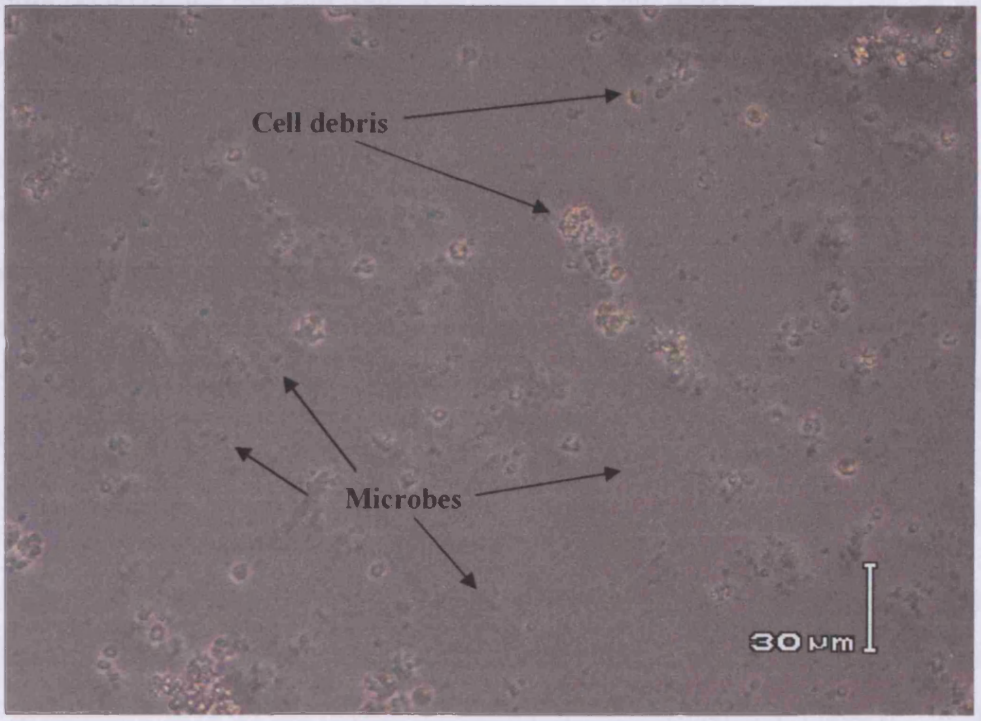

Figure 45. Microscopic image of spent medium from hMSCs cultures which contained small microbes, cell debris and dead cells. The microbes moved slightly and appeared in discrete foci through the microwell. 200X magnification.

3.4.4. Discoloration of alginate beads

A further challenge to the hMSC-alginate system was the discoloration of beads that occasionally occurred during culture. This problem was first experienced when the alginate (Manugel) was autoclaved to sterilize prior to the derivatization process which caused the activation of thermophilic bacillus spores, B.*licheniformis*, as was described in section 3.1.2. The beads appeared to be contaminated when they started turning an opaque whitish-gray color, while appearing black under the microscope. After completing the sterile derivatization process, this problem still persisted so the

culture medium and hMSCs were scrutinized as described in the previous section. Microbes were observed in the spent medium.

Communication with the alginate manufacturers (NovaMatrix) also shed some understanding into the possible cause(s) of the discoloration that may or may not have also been attributed to contaminants present in the hMSCs cultures. The alginate beads actually turned white, but appeared black under the microscope light. This loss of light transmission through bead was caused by calcification within the gel network as a result of the presence of phosphate in the culture medium. Hydrogels made from Pronova SLG100 alginate contained high amounts of calcium due to their high content of guluronic (G) subunits; therefore they were susceptible to calcification. Low G alginates were less susceptible to calcification (Email correspondence with Jan Egil Melvik, NovaMatrix/FMC Biopolymer, March 2004). Also other calcium chelating compounds such as phosphate, lactate and citrate in the medium should be avoided or minimized. Likewise large amounts of sodium will weaken the beads due to the exchange of calcium ions from the hydrogel.

An experiment was conducted using Pronova SLG100 alginate in which beads without cells were made by the standard protocol and then incubated in MSCCM or complete DMEM medium. The beads cultured in the MSCCM where initially clear but gradually turned a yellow/brown tint after about 7-13 days in culture, whereas the beads in complete DMEM medium were not discolored. Based upon this information, it was likely that phosphate present in the MSCCM had caused some calcification within the hydrogel network. Another experiment was conducted in which hMSCs and rSMCs were immobilized at $5x10^6$ and $2x10^7$ cells/mL in the non-derivatized Pronova SLG100 alginate. The beads containing the high cell concentration of hMSCs rapidly turned brown within a few days; and the beads with the low cell concentration gradually turned yellow then brown over a couple weeks. In contrast, the beads containing the rSMCs at both concentrations never discolored during the study. These results showed that increased levels of lactate produced by cells at high concentration within the beads also created a microenvironment which would cause further calcification. Finally the presence of microbes (both in the alginate and in the hMSC cultures) could further exacerbate the system and cause further calcification. Separate studies also showed the derivatization of the alginate and the size of the bead

were not a contributing factor, as small beads (<1mm) were just as likely to calcify as large beads (>2mm). Figure 46 shows micrographs taken of calcified 12X alginate-GRGDY beads (Pronova SLG100) seeded at $1x10^7$cells/mL and cultured in MSCCM for 6 days. The beads were smaller than those typically produced manually due to disruption of the stream (spray) during bead formation which produced smaller beads, but without control of sphere size.

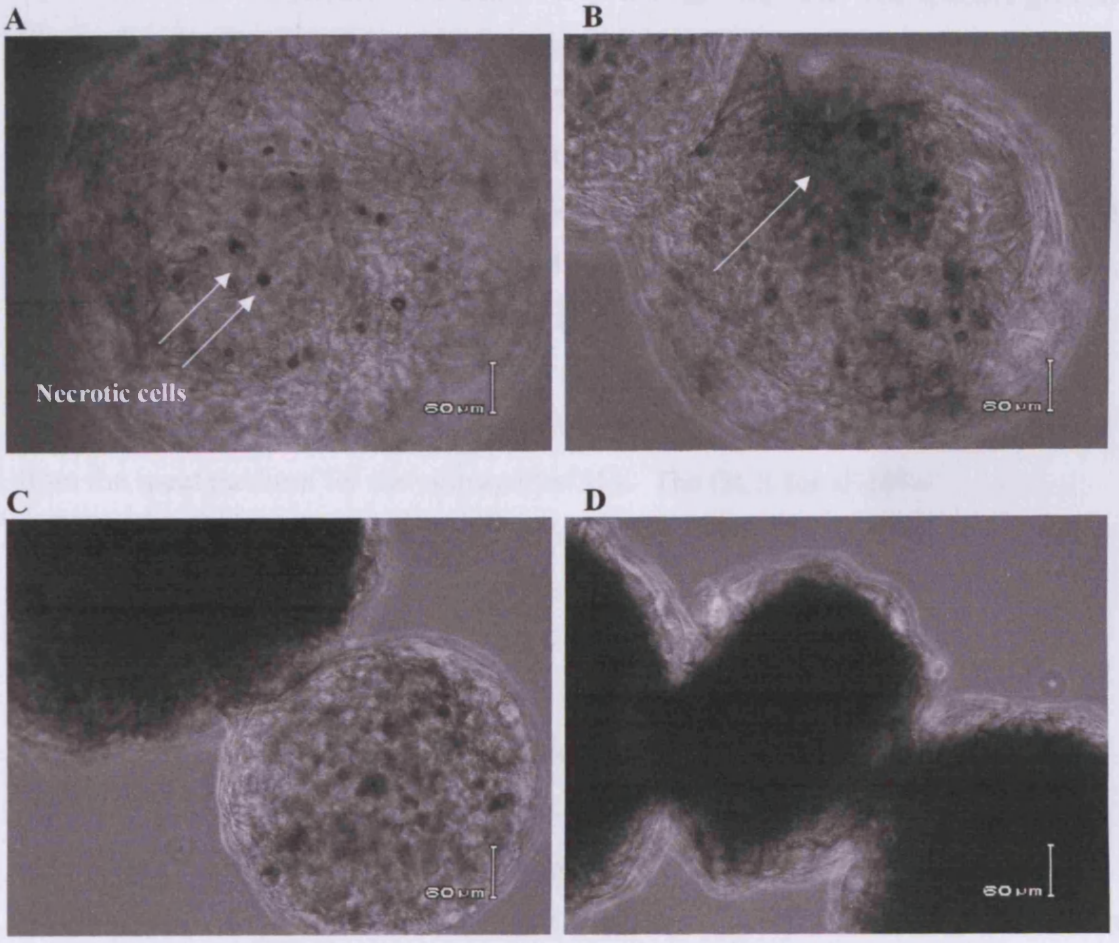

Figure 46. Micrographs of calcified 12X alginate-GRGDY beads (Pronova SLG100) with hMSCs seeded at $1x10^7$cells/mL. All beads were cultured for 6 days in MSCCM. (A) Normal bead with cells completely networked. A few black necrotic cells are present. (B) Bead with small section starting to calcify. (C) Small, iridescent normal bead adjacent to large, black calcified bead. (D) Several linked beads which are completely calcified. All photos 100X magnification.

3.4.5. Summary

Frozen stocks of hMSCs were prepared from isolation of BMCs from a Ficoll gradient and tissue culture plate adherence. The hMSCs had viability post thaw of 88 +/- 4% (n=19), and during passaging a viability of >98% (n=109). The growth kinetics of hMSCs appeared to be greatly influenced by the passage level. The doubling time was 69 +/- 23 hours (n=52) for hMSCs ≤P7 and 134 hours +/- 88 hours (n=48) for hMSCs ≥P8. The growth rate as calculated from the doubling time was 0.26 +/- 0.07 hr^{-1} for hMSCs ≤P7 and 0.17 +/- 0.09 hr^{-1} for ≥P8. The specific growth rate (on a per cell basis) for frozen hMSCs ranged from 2.2 +/- 0.74 $x10^2$cells/cm^2/hr at P5 down to 0.70 +/- 0.30$x10^2$cells/cm^2/hr at P10 (Figure 32). The growth rate of fresh and cryopreserved hMSCs was determined to be similar for the same donor (Figure 33.B). Alternatively population doublings were also used to calculate growth rates. Early passage cells between P3 and P5 had 0.3-0.4 PD/day, which decreased between P9 and P12 to 0.05-0.15 PD/day (Figure 34). In contrast, due to their immortalization, the rSMCs maintained a relatively constant growth rate (0.32 +/- 0.06 PD/day) between P2 to P22 (Figure 35). Glucose measurements were taken from the spent medium for the cultured hMSCs. The GCR for all hMSCs ≤ P7 was 1.46+/-0.92$x10^{-10}$g/cell/hr, and for hMSCs ≥P8 was 1.75+/-1.75$x10^{-10}$g/cell/hr (Figure 36). The GCR was found to be independent of passage level and culture length (Figure 37), given the large standard error associated with the data.

HMSCs were immobilized into alginate and alginate-GRGDY hydrogels and the biological activity (e.g. cell elongation) was studied in sheets, tubes and beads. Following immobilization, viability averaged 95 +/- 3% for 10 independent hMSC experiments ranging from 1$x10^6$ up to 2$x10^7$cells/mL. No elongation was observed in the non-derivatized alginate hydrogels (Figure 39.A). The extent of hMSC elongation within the derivatized alginate-GRGDY was dependent upon the concentration of reagents used during the carbodiimide chemistry (e.g. EDC, sulfo-NHS and peptide). Initially 50X reagents were necessary for Manugel and Fluka alginates (Figures 38, 39.B and 40); then a significant experiment demonstrated that only 1X level of peptide was required for equivalent cell elongation and networking using 50X levels of EDC and sulfo-NHS. The cell concentration required for uniform cell elongation

and complete networking was $2x10^7$cell/mL. In addition, elongation of hMSCs within alginate-GRGDY beads was sensitive to the culture medium. HMSCs within hydrogels incubated with complete DMEM did not elongate during a 17 day time course whereas they did using MSCCM. The live/dead assay was used to qualitatively assess the viability and the extent of elongation of the cells within the hydrogel (Figure 44). Cell elongation and networking was observed in hMSCs immobilized in alginate-GRGDY tubes (Figure 41). The GCR was measured to be $3.1x10^{-11}$g/cell/hr (Figure 42). This estimate was lower than the GCR ($7.3 x10^{-11}$ +/- $3.2x10^{-11}$g/cell/hr) obtained from the same hMSCs grown in tissue flasks. The respiratory quotient of the cells in the tubes was calculated to be 2.4+/-1.2 in the first five days of cultures indicating the cells were under anaerobic metabolism.

Two challenges unfolded for the hMSC-alginate hydrogel system. First, microbes were observed in the spent medium from the hMSCs cultures (Figure 45). The microbes were not sensitive to the antibiotics tested, and could not be isolated and identified when sent to UCLH microbiology testing laboratory. This problem was independent of the B. *licheniformis* contaminants found in the alginate (as described in section 3.1.2). Furthermore during culture some of the alginate-GRGDY beads turned white, but appeared black under the microscope (Figure 46). Hydrogels made from high guluronic (high G) alginate, such as Manugel and Pronova, contained high amounts of calcium within the gel network. Therefore they were susceptible to calcification from the presence of chelating compounds such as phosphate in the MSCCM and increased levels of lactate produced at high cell concentration and in the presence of microbes.

Preliminary data was collected on the viability and cell concentration of hMSCs immobilized in alginate beads during a 5 day time course (Figure 43). These quantitative analyses of the hMSC-alginate hydrogels formed the basis on which cell proliferation (metabolic activity) studies were conducted on hMSCs immobilized in alginate-GRGDY beads using the MTT assay. These studies are described in the next section.

3.5. MTT assay for cell proliferation (metabolic activity)

Every aspect of enhancing the expansion of human cells and of preparing engineered tissue rests upon the ability to measure the number of cells at every stage and their metabolic status. (Later measurement of phenotype status will be important.) As the present research developed it became clear that progress was conditional on advancing this aspect. The previous section (3.4) demonstrated that hMSCs would associate within alginate-GRGDY hydrogels and preliminary results showed viability was high (Figure 43). Due to the potential loss of cells or decrease in viability during release of the cells from the alginate matrix using trisodium citrate and trypsin/ETDA, it was desirable to estimate the cell number in the beads using an alternative method. One common technique that has been used to quantitate cell number includes determination of DNA content (Papadimitriou and Lelkes, 1993; Carrier 1999). Early efforts in this research project developing a DNA fluorescence assay (CyQuant) proved unreliable in the presence of alginate and other residual components (see sections 2.6.1.4 and 6.1.2.1, Figure 71). Instead, the MTT assay was used to monitor cell proliferation and metabolic activity within alginate beads.

The MTT assay was first developed by Mosmann (1983) as a quantitative colorimetric assay for mammalian cell survival and proliferation. It was modified and further developed for uses in quantitation of lymphokines (Green, 1984), drug cytotoxicity (Huveneers-Oorsprong, 1997), cell-mediated cytotoxicity (Ferrari, 1990), cell chemosensitivity to antitumor agents (Heo, 1990), evaluation of cell/biomaterials interactions (Ciapetti, 1993) and assessment of cell viability (Ferrera, 1993; He, 1996). More recently it has been used to assess cell viability and proliferation in tissue engineering scaffolds (Carrier, 1999; Chung, 2002; Dar, 2002; Wang, L., 2003; Wang, D., 2003; Yang, 2003; Zund, 1999).

Heo (1990) found the MTT assay to be more sensitive than the ^{51}Cr-release assay in measuring the antitumor activity of effector cells. As a result it required significantly lower number of cells to perform the assay. Ciapetti (1993) confirmed results obtained from materials' cytotoxic effect by MTT assay correlated to data from ^{3}H-thymidine uptake. Ferrera (1993) found MTT reduction activity correlated to oxygen consumption and adenine nucleotide levels in heart biopsy samples.

The assay involves the mitochondrial dehydrogenase conversion of water soluble yellow MTT salt (3-(4,5-dimethylthiazol-2-yl)-2,5-diphenyltetrazolium bromide) into an insoluble, intracellular purple formazan product which only occurs in metabolically active (live) cells (Mosmann, 1983). After the formazan is dissolved using an organic solvent, the concentration is measured using a spectrophotometer and the result quantitated to the number of cells present in the sample. Mosmann found that isopropanol was the most suitable solvent, since ethanol sometimes precipitated the serum proteins in the mixture. In order to minimize the interference of the phenol red component in the tissue culture medium when read at the wave length used to measure the purple dye of the dissolved formazan, acid was added to the isopropanol. This ensured the cell/culture media mixture was fully acidic so that the phenol red color indication was yellow.

A variety of reagents other than isopropanol have been used to dissolve the formazan crystals. Ferrera (1993) and Ciapetti (1993) found dimethyl sulfoxide (DMSO) worked adequately to dissolve formazan. Dar (2002) used a mixture of 20% aqueous sodium dodecyl (lauryl) sulfate (SDS) and formamide (1:1 volume ratio) to dissolve the formazan crystals off alginate scaffolds. Other researchers using polymer scaffolds for tissue engineering applications have utilized primarily DMSO (Wang, L., 2003; Chung, 2002) or isopropanol combined with HCl or formic acid (Carrier, 1999; Wang, D., 2003; Zund, 1999; Yang, 2003) to dissolve the formazan and to minimize interference with the phenol red component in the tissue culture medium.

Initially, the MTT assay was tested on hMSCs and found not to be adversely affected by alginate or residual components as summarized in section 2.6.2.8. However, the assay needed to be conducted on live cells to metabolize the MTT. Therefore, it was important to incorporate a hold/storage step such that multiple time points could be dissolved and analyzed at the same time to reduce day-to-day variability. In addition, the hold step was convenient to incorporate due to the considerable incubation length required to run through the entire assay protocol. Freeze steps had not been reported in the literature and so the affect of the freeze step needed to be compared to samples that had not been frozen. The MTT assay was found to be especially appropriate for this kind of time course study because the cells were assayed *in situ*, stored frozen,

then dissolved and analyzed on the same day. The assay method described in section 2.6.2 was created from experienced gained from the experiments and results described in this section.

3.5.1. MTT assay parameters

For all MTT assays the culture medium was completely removed or rinsed from the bead/cell constructs to eliminate contributions to the phenol red component in the culture medium. Then the MTT stock solution was added to wells containing DPBSG to ensure the cells were not depleted of glucose during the 2 hours incubation with MTT reagent. He (1996) found that 5mM glucose produced maximal color development of MTT reduction by mitochondria, although incubation lengths were 24 hours for their analyses.

The detergent SDS was originally tested as the formazan dissolution agent as per Dar (2002) who used the MTT assay for cardiomyocytes seeded onto alginate scaffolds. However, under the conditions of this protocol, SDS was deemed unsuitable since the solution solidified into a thick paste after adding the SDS to the trisodium citrate dissolved alginate-cell solution. Most likely this was due to the ionic interaction of alginate with the SDS or divalent cations such as calcium in the dissolved alginate solution. Each SDS molecule has two negative charges. It is possible that Dar (2002) did not experience this problem because they used porous (freeze-dried) alginate scaffolds that were not dissolved during the assay. Subsequent to SDS, isopropanol with 0.1N HCl was determined to be a suitable solvent to dissolve the formazan crystals in the presence of dissolved alginate.

A full wavelength scan was performed on a representative sample of dissolved formazan with alginate/cells (Figure 47) using the Uvikon 922 Spectrophotometer (Kontron Instruments, Milan, Italy). In addition, a scan was performed on a MTT/isopropanol/HCl blank (sample without alginate/cells) and a sample of isopropanol/HCl. The peak of the MTT/isopropanol/HCl blank (unreacted – no conversion of MTT into formazan) was below 450nm. The peak of the dissolved formazan with alginate/cells sample (reacted) was below 600nm. These peaks clearly do not overlap at wavelengths greater than 450nm.

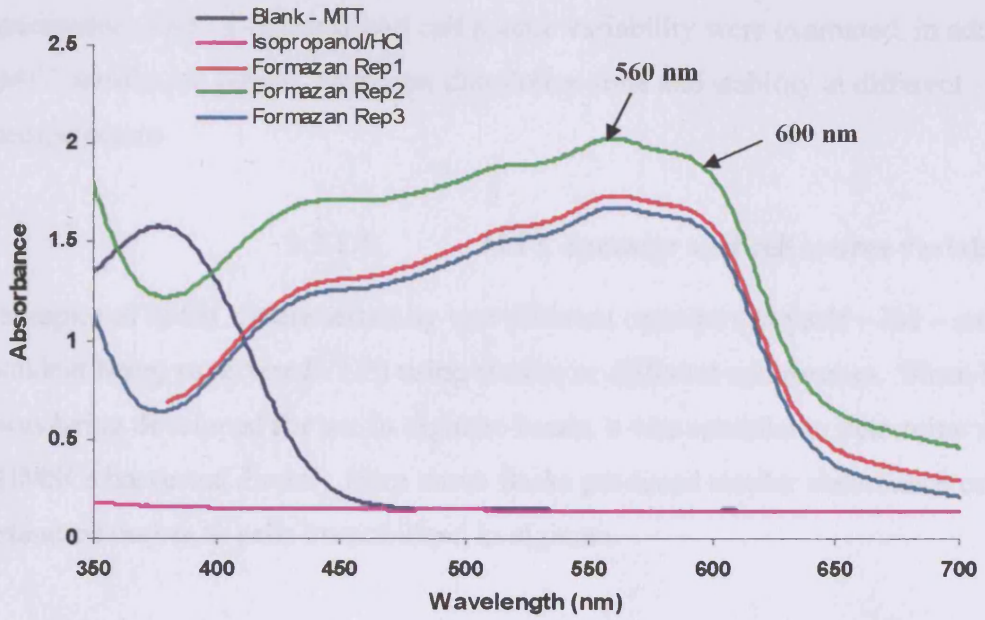

Figure 47. Full wavelength scan of a sample of dissolved formazan with alginate and cells. Arrows indicate the peak wavelength of 560nm and the wavelength of 600nm used to measure the absorbance on the microplate spectrophotometer. The absorbance reading at 600nm was 92% of the reading at 560nm.

The spectrograph also showed that the actual formazan peak occurred at approximately 560nm. However, the absorbance at 600nm was not significantly different from the absorbance at 570nm. For the three replicates performed, the average absorbance at 600nm was 1.65 +/- 0.17 and at 570nm was 1.79 +/- 0.18. Hence, the absorbance readings at 600nm were 92 +/- 0.2% of the readings at 570nm. Because the absorbance readings at 570nm were surrounded by a shallow fall off and the readings at 600nm were on the shoulder of the peak; readings at 600nm be more susceptible to optical error. Future work will be performed with a new spectrometer specified to read at 560-570nm; however since this was the wavelength reading available on the current instrument, the Packard Bioscience Spectracount™ microplate reader was acceptable for reading these samples at 600nm.

The spectrophotometer was also able to perform dual wavelength reading. In the future a reference wavelength set at 670nm could be utilized to also measure each sample so that turbidity of the sample which causes light scatter to improve the data set. The subtracted data would then be a more representative value (Harris, 1996).

Next the MTT assay was tested for reliability and robustness. A number of parameters such as operator and cell source variability were examined, in addition to, MTT incubation length, formazan dissolution time and stability at different temperatures.

3.5.1.1. MTT operator and cell source variability

Samples of hMSCs were tested by two different operators (myself – JM – and a student being supervised - LP) using similar or different cell sources. Since this assay was being developed for use in alginate beads, it was essential to determine whether HMSCs harvested directly from tissue flasks produced similar absorbance cell standard curves to cells immobilized in alginate.

As shown in Figure 48, similar absorbance results for two different operators (JM and LP) were produced for alginate beads after 1 day of incubation (red and black lines). In addition, similar results were obtained using two different cell sources - frozen working hMSC banks at similar passage level (P7 and P8) - when tested simultaneously using two different operators (JM and LP). Figure 48 (green and light blue lines) shows that the two different hMSC banks produced very similar absorbance standard curves, despite the high standard deviations on some of the individual data points. Similar results were also obtained for day 1 cells immobilized in either alginate-GRGDY or alginate beads (Figure 48, pink and dark blue lines), these were tested by same operator (JM). However, overall there seemed to be a large amount of variability among the 3 different assay/cell treatments.

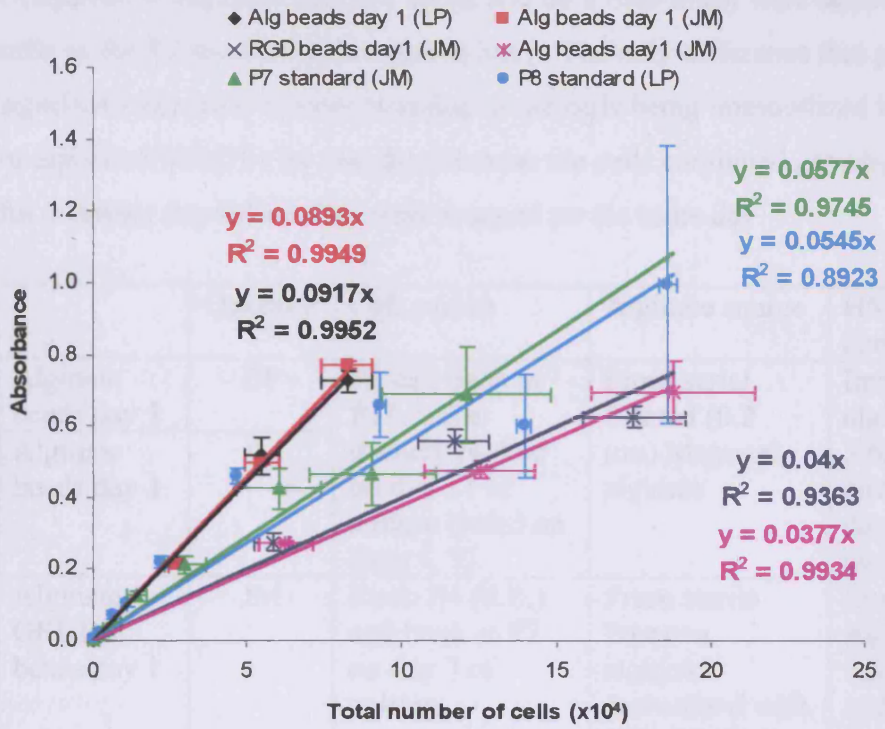

Figure 48. MTT variability using hMSCs from different cell sources and using different operators. HMSCs at P11 in alginate beads after 1 day incubation (red, black lines), hMSCs from P7 or P8 tissue flask cultures (green, light blue lines), hMSCs from P7 cultures in alginate or alginate-GRGDY beads after 1 day incubation (pink, dark blue lines). Absorbance read at 600nm.

The MTT assay has been shown to be sensitive to cell culture methods (Carrier, 1999). The first set of alginate beads (red and black lines) was produced from 0.1% alginate (Manugel DMB) in water (pH 5.6) which was filtered through a series of filters (CUNO) including a carbon zeta plus, a zeta plus and then a 0.2 µm filter as described in section 2.3.1. The filtrate was lyophilized and then reconstituted to $1/10^{th}$ of its original volume to obtain 1% alginate in n-saline. The hMSCs were derived from the P8 cell bank at passage 11 (P11), were densely packed on day 11 of culture (refed on days 4 and 9). The hMSCs were immobilized into the alginate at $5.6x10^6$cells/mL and analyzed on day1. The second set of beads (pink and dark blue lines) was produced using 1% sterile alginate (Pronova SLG100) reconstituted in MES/NaCl buffer and 1% 27X alginate-GRGDY derivatized from Pronova SLG100. The hMSCs were derived from the P4 cell bank from S. Elliman at passage 7 (P7), were 90% confluent on day 3 of culture. The hMSCs were immobilized into the alginate or alginate-GRGDY at $9.6x10^6$cells/mL and analyzed on day 1. These key differences in conditions are summarized in Table 16. Finally, the cells immobilized

in alginate or alginate-GRGDY (pink and dark blue lines) were derived from the same cells as the P7 standard curve (green line). The only difference that produced this significant decrease in slope was due to the cells being immobilized in beads (alginate or alginate-GRGDY) for one day whereas the cells continued growing in tissue flasks for 1 further day before they were assayed on the same day.

	Operator	Cell source	Alginate source	HMSC culture condition
Alginate beads day 1	LP	P8 cell bank at P11, were densely packed on day 11 of culture (refed on days 4, 9).	From serial filtered (0.2 μm) Manugel alginate	Immobilized into alginate at $5.6x10^6$ cells/mL and analyzed on day1 of incubation
Alginate beads day 1	JM			
Alginate-GRGDY beads day 1	JM	From P4 (S.E.) cell bank at P7 on day 3 of culture	From sterile Pronova alginate derivatized with 27X GRGDY	Immobilized into alginate at $9.6x10^6$ cells/mL and analyzed on day1 of incubation
Alginate-GRGDY beads day 1	JM		From sterile Pronova alginate	
P7 standard	JM	From P4 (S.E.) cell bank at P7 on day 4 of culture	No alginate	Cells trypsinized and tested immediately in MTT assay
P8 standard	LP	From P7 cell bank at P8		

Table 16. Key differences among cell sources and culture differences in initial MTT experiments.

The variability from these different culture and alginate immobilization conditions was clearly evident from this early analysis. Several factors still needed to be investigated such as the MTT incubation length and formazan dissolution time. In addition, each set of these assays was conducted and analyzed on different days. This also will contribute to variability. Implementing a frozen storage step may help to improve consistency since time course samples would be analyzed at the same time.

3.5.1.2. Cell passage number

Initial data for different cell banks at similar passage level (P7 & P8) and culture conditions produced similar absorbance curves (Figure 48, green and light blue lines);

however, different passage levels and/or culture conditions seemed to show a difference (Figure 48). It was also shown that hMSCs cultured in tissue flasks at different passage levels have significantly different growth rates (section 3.4.1, Table 15); therefore, cells at different passage levels may have different mitochondrial dehydrogenase activity and produce different MTT results. Experiments performed to date have not been able to directly compared, especially using rigid control of assay parameters which will be discussed in the rest of this section. Therefore, the cell passage level should be studied as future work.

3.5.1.3. Length of incubation for MTT conversion

Ferrera (1993) found that tetrazolium reductase (TR) activity plateaued after 90 minutes of incubation with MTT solution. However, Huveneers-Oorsprong (1997) found that TR activity did not have a maximum after 3 hours incubation in rat and pig hepatocytes. As part of assay development, it was necessary to determine whether a difference in MTT incubation length effected absorbance results for hMSCs. For this study, three plates were loaded with duplicate samples of a hMSC cell standard that was prepared as described in sections 2.6.2.1 and 2.6.2.4 and Table 5. The initial incubation time at 37°C with MTT solution was varied between 1, 2 and 3 hours in length. The final hour of incubation after addition of trisodium citrate was performed for each plate such that the total incubation length at 37°C was 2, 3 and 4 hours. The remaining steps including centrifugation, removal of supernatant, freezing of plates, and dissolution of formazan was performed according to sections 2.6.2.4 and 2.6.2.5 without the addition of 10X trypsin/EDTA. In studies without alginate-GRGDY beads, addition of trypsin/EDTA tended to make the cells more aggregated and sticky due to the trypsin; therefore it was excluded from this study. Each plate was read on the spectrophotometer within 1 hour from isopropanol/HCl addition and again after ca. 20-25 minutes. The absorbance results for the subtracted data (read at 600nm and reference at 670nm) are shown in Figure 49. The assay appeared to be linear for cell densities per well less than $10x10^4$cells/well.

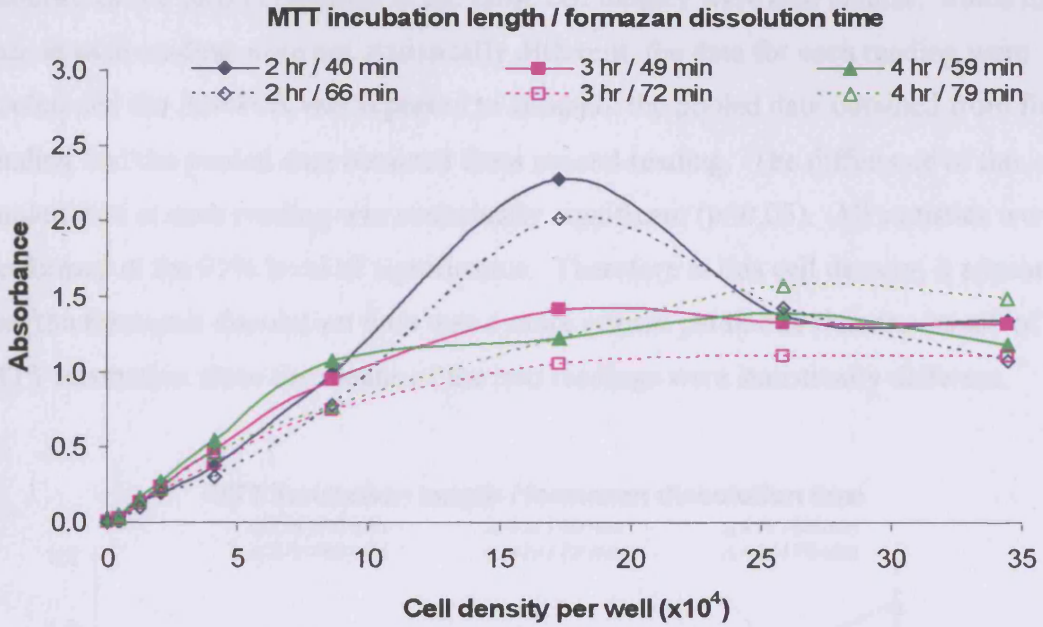

Figure 49. Effect of MTT incubation length (2, 3, 4 hours) and formazan dissolution time (minutes at 37°C) on absorbance readings for cell standard curves. The first reading was performed for formazan dissolution time <1 hour (closed symbols). The second reading was performed for formazan dissolution times >1 hour (open symbols). Incubation and dissolution occurred at 37°C. Absorbance readings appeared to become non-linear for cell densities greater than $10x10^4$cells/well. Absorbances read at 600nm and subtracted against reference at 670nm.

In order to determine whether the incubation length or formazan dissolution time produced different results, linear approximations were performed on the cell standard curves produced below $10x10^4$cells/well. The linear approximations for each data set are shown in Figure 50. The 4 hour MTT incubation length produced greater absorbance readings than both the 2 and 3 hour incubation lengths at the first formazan dissolution times (<1 hour). However, the second readings obtained at the second formazan dissolution time (>1 hour) were all significantly lower than the initial readings at all three incubation lengths (e.g. 2, 3, 4 hours). During this study, formazan dissolution occurred at room temperature (ca. 24°C).

A single factor ANOVA (analysis of variance) was used to determine whether the differences in absorbances for the first reading were statistically different from the second reading. First of all, the mean and variance of the 2, 3 and 4 hour results for the first reading were analyzed (for absorbances at $8.6x10^4$cells/well) and found to be statistically similar ($p>0.05$), see Appendices section 6.2.2.1, Table 20. The mean and

variance of the second readings at the same cell density were also similar. Since the data at each reading were not statistically different, the data for each reading were pooled and the ANOVA was repeated to compare the pooled data obtained from first reading and the pooled data obtained from second reading. The difference of the pooled data at each reading was statistically significant ($p<0.05$). All statistics were performed at the 95% level of significance. Therefore at this cell density, it appeared that the formazan dissolution time was a more critical parameter than the length of MTT incubation since the means of the two readings were statistically different.

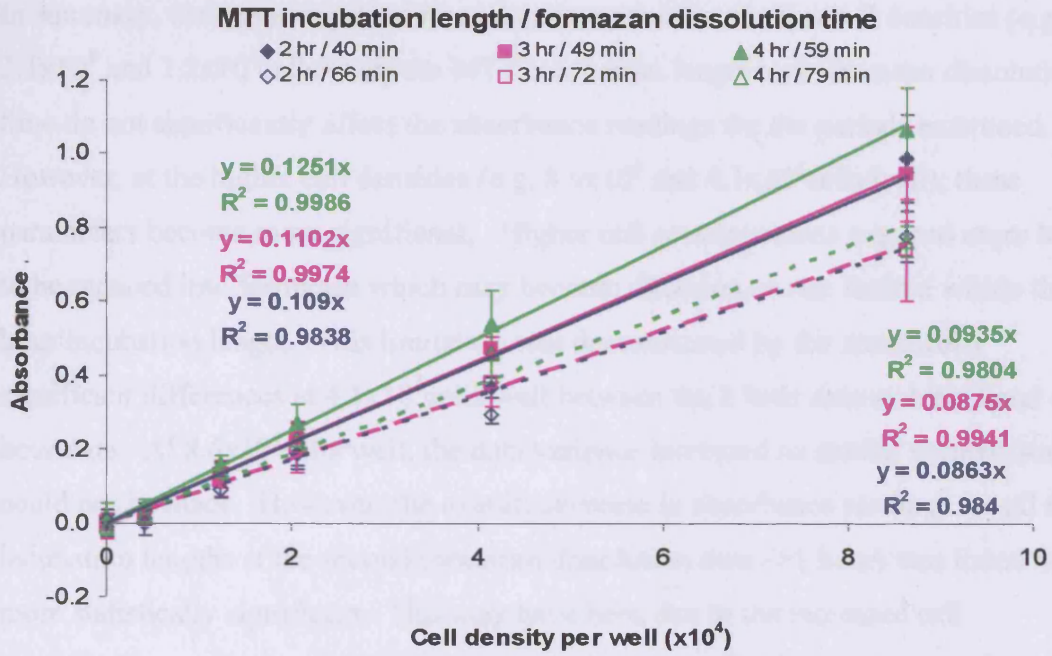

Figure 50. Linear approximations of the cell standard curves for different MTT incubation times (2, 3, 4 hours) and for different formazan dissolution lengths (minutes). Absorbances obtained from the first readings after 2, 3 and 4 hour incubation lengths (solid lines) were overall greater than second readings after 2, 3 and 4 hour incubation lengths (dashed lines). Analysis of the data at 8.6×10^4cells/well demonstrated that the mean of the pooled first readings were statistically different from the pooled second readings ($p<0.05$). Absorbances read at 600nm and subtracted against reference at 670nm.

The single factor ANOVA was repeated for the data set at 4.1×10^4cells/well. At this cell density, there was a statistical difference ($p<0.05$) between the mean and variance of individual time points at both the first and second reading, so the data for each time point could not be pooled. This result meant that MTT incubation length did have an affect on the absorbance, with 2 hour incubation length showing significant

differences between both the 3 and 4 hour incubation lengths for both the first or second dissolution reading. At this cell density only the 2 hour sample showed a difference between the first and second dissolution reading; the 3 and 4 hour samples did not have a statistical difference. The mean, variance and summary of p-values for these analyses are summarized in the Appendices section 6.2.2.1, Table 19 and 20. Further analyses for data at $2.1x10^4$ and $1.2x10^4$ cells/well showed no statistical difference ($p>0.05$) among MTT incubation lengths and between pooled data between first and second dissolution times.

In summary, these statistical analyses demonstrated that for low cell densities (e.g. $2.1x10^4$ and $1.2x10^4$cells/well) the MTT incubation length and formazan dissolution time do not significantly affect the absorbance readings for the periods examined. However, at the higher cell densities (e.g. $8.6x10^4$ and $4.1x10^4$cells/well); these parameters become more significant. Higher cell concentrations required more MTT to be reduced into formazan which may become diffusion or rate limited within the 2 hour incubation length. This limitation was demonstrated by the statistically significant differences at $4.1x10^4$cells/well between the 2 hour data and the 3 and 4 hour data. At $8.6x10^4$cells/well, the data variance increased so similar comparison could not be made. However, the overall decrease in absorbance readings for all three incubation lengths at the second formazan dissolution time (>1 hour) was found to be more statistically significant. This may have been due to the increased cell concentration or the increased formazan concentration. Further analysis on the stability of dissolved formazan needed to be performed.

3.5.1.4. The effect of temperature on stability of formazan absorbance

Previous work indicated that absorbance readings decreased significantly between first readings (taken after <1 hour after addition of the isopropanol/HCl solution) and second readings (taken after >1 hour). A temperature controlled study was performed at three dissolution temperatures (6, 19 and 37°C). HMSCs at P9 were trypsinized, centrifuged and resuspended at $7.8x10^5$cells/mL in DPBSG. Six wells in each of three 96-well microplates were loaded with 100µL of cell suspension. MTT solution was added and incubated at 37°C according to section 2.6.2.4. Following

centrifugation and removal of supernatant, the three plates were frozen at -70°C. Upon thaw and addition of DPBSG and isopropanol/HCl to each well according to section 2.6.2.5, one plate was incubated at each temperature (6, 19 and 37°C). The DPBSG and isopropanol/HCl added to the microplate incubated at 6°C were also chilled before addition to that plate. After 15-20 minutes, the wells were mixed with a micropipet to aid in the formazan dissolution and read on the spectrophotometer. After reading each plate was returned to its designated incubation temperature. After 30 minutes, the wells were mixed again by micropipet, read and incubated. Additional readings (with no mixing) were taken at 30 minute intervals out to ca. 2½ hours. The plates were wrapped in film during incubation to reduce evaporation effects. The results are shown in Figure 51.

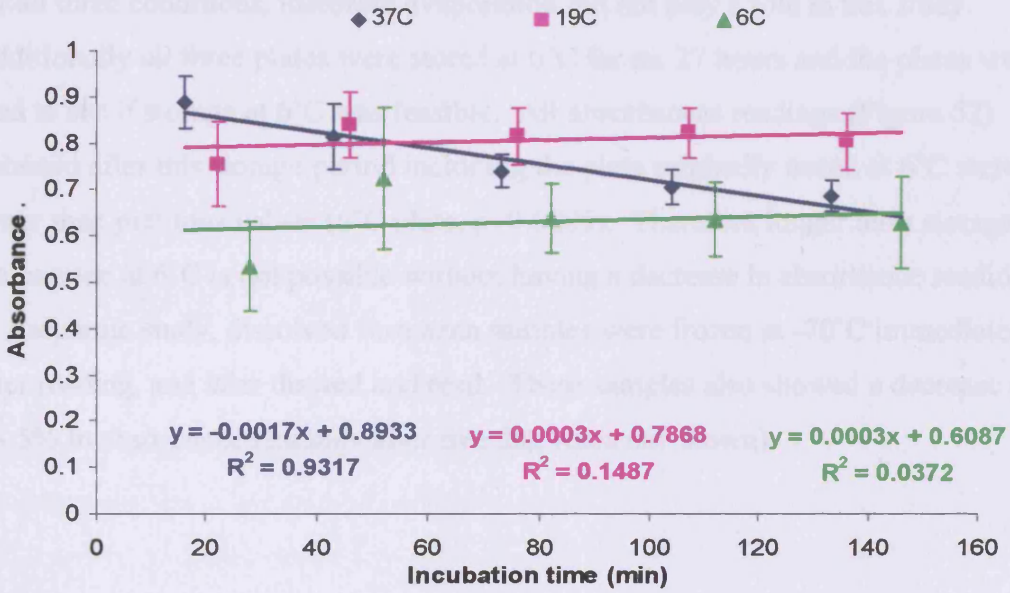

Figure 51. Stability of formazan absorbance at 6, 19 and 37°C. Each data point represents the mean and standard error of 6 wells for each temperature. The cell concentration was 7.8×10^4cells/well. Absorbance read at 600nm.

The formazan product did not appear to be dissolved completely at the initial reading (ca. 20 min.) at 6 and 19°C, hence a second mixing step was performed as indicated, and both absorbance levels increased at the second reading. Thereafter the absorbance readings at 6°C and 19°C appeared to be stable during the 2½ hours of incubation. A single factor ANOVA comparison of the readings at 6°C showed there was a statistical difference in the absorbance readings out to 2 ½ hours when the first reading was excluded from the analysis ($p=0.0263$). In contrast, there was not a

statistical difference in the 19°C absorbance readings, excluding the first reading since dissolution was not complete (p=0.4262). Overall there was a 23% decrease in absorbance reading after 2½ hours at 37°C. ANOVA comparison confirmed a statistically significant difference among those absorbance readings at 37°C (p=0.0000). Overall the absorbances at 6°C were ca. 22% lower than both 19 and 37°C. This difference in absorbance may be due to a difference in formazan dissolution at the lower temperature or may be attributed to the temperature dependance on absorbance (Adams and Berman, 1981).

At the conclusion of the study, the final volume remaining in each well of the three treatment groups was measured. The average volume remaining per well was similar for all three conditions, therefore evaporation did not play a role in this study. Additionally all three plates were stored at 6°C for ca. 27 hours and the plates were read to see if storage at 6°C was feasible. All absorbances readings (Figure 52) obtained after this storage period including the plate originally tested at 6°C were lower than previous values (6°C plate, p=0.0005). Therefore longer term storage of plates even at 6°C is not possible without having a decrease in absorbance readings. In a separate study, dissolved formazan samples were frozen at -70°C immediately after reading, and later thawed and read. These samples also showed a decrease of 31 +/- 5% in absorbance readings after freezing (data not shown).

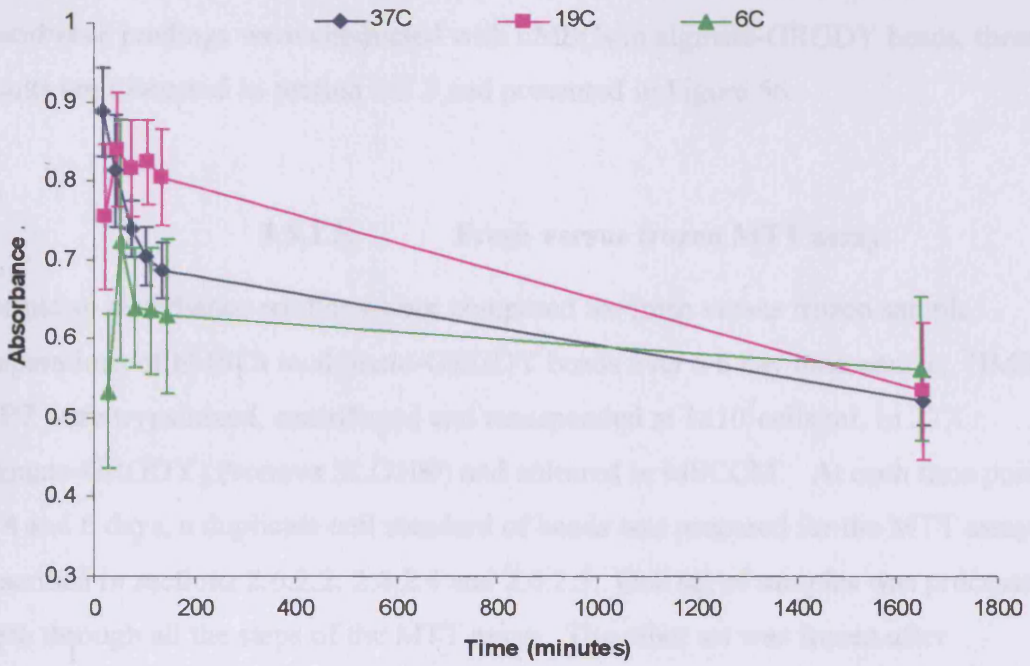

Figure 52. Temperature stability of formazan absorbance after temperature study at 6, 19 and 37°C. All plates held for 27 hours at 6°C then read. ANOVA comparison showed that all samples had a statistically significant decrease in absorbance levels during this storage. Therefore long term storage at 6°C was associated with decreased absorbance readings. Absorbance read at 600nm.

Wan (1994) reported on the stability of dissolved formazan solution in isopropanol at room temperature (temperature not specified) and at 4°C. They found the absorbance decreased by approximately 10% of the original reading during the one hour time period that the samples were held at room temperature. Whereas the samples held at 4°C did not vary significantly during the one hour period. Their results also showed the initial absorbance reading at 4°C was 21% lower than the absorbance reading at room temperature. Previous findings during this research project did show that formazan absorbance levels decreased at 24°C between the first and second reading (section 3.5.1.3, Figure 50). However, the results of this temperature controlled study, showed the absorbance readings at 19°C and 37°C at the second time point (ca. 45 minutes) and the 19°C at the third time point (ca. 70 minutes) were very comparable ($p=0.4492$). Therefore the recommended protocol (as outlined in section 2.6.2.5) was to perform the isopropanol/HCl dissolution at room temperature, mix the samples after 20 and 40 minutes, and then read the plate immediately after the second

mixing (within 1 hour of start of dissolution). Additional stability studies of absorbance readings were conducted with hMSCs in alginate-GRGDY beads, these results are discussed in section 3.5.3 and presented in Figure 56.

3.5.1.5. Fresh versus frozen MTT assay

Formazan absorbance readings were compared for fresh versus frozen sample preparations of hMSCs in alginate-GRGDY beads over a 6 day time course. HMSCs at P7 were trypsinized, centrifuged and resuspended at $1x10^7$cells/mL in 27X alginate-GRGDY (Pronova SLG100) and cultured in MSCCM. At each time point, 2, 4 and 6 days, a duplicate cell standard of beads was prepared for the MTT assay as described in sections 2.6.2.2, 2.6.2.4 and 2.6.2.5. One set of samples was processed fresh through all the steps of the MTT assay. The other set was frozen after centrifugation and removal of supernatant, and then thawed on a subsequent day for dissolution using isopropanol/HCl. Due to these conditions, the fresh samples were processed and read on three separate days and the frozen samples were started (MTT conversion to formazan) on the same days as the fresh, but completed and read on a separate day as a group.

Absorbance values were very similar between the fresh and frozen samples for 1 bead/well for all three time points (Figure 53). A single factor ANOVA comparison indicated that only the day 6 fresh sample was statistically different from the other five samples for 1 bead/well (*, $p<0.05$). The variability of the absorbance readings was much greater for 2 beads/well; however no general trend was noted. The data for 3 beads/well corresponded to a cell density greater than $10x10^4$cells/well and was disregarded as it was outside the linear range of the assay. A summary of the mean, standard error (SEM), variance and statistical comparison (p-value) for the study is provided in the Appendices, section 6.2.2.2, Table 21.

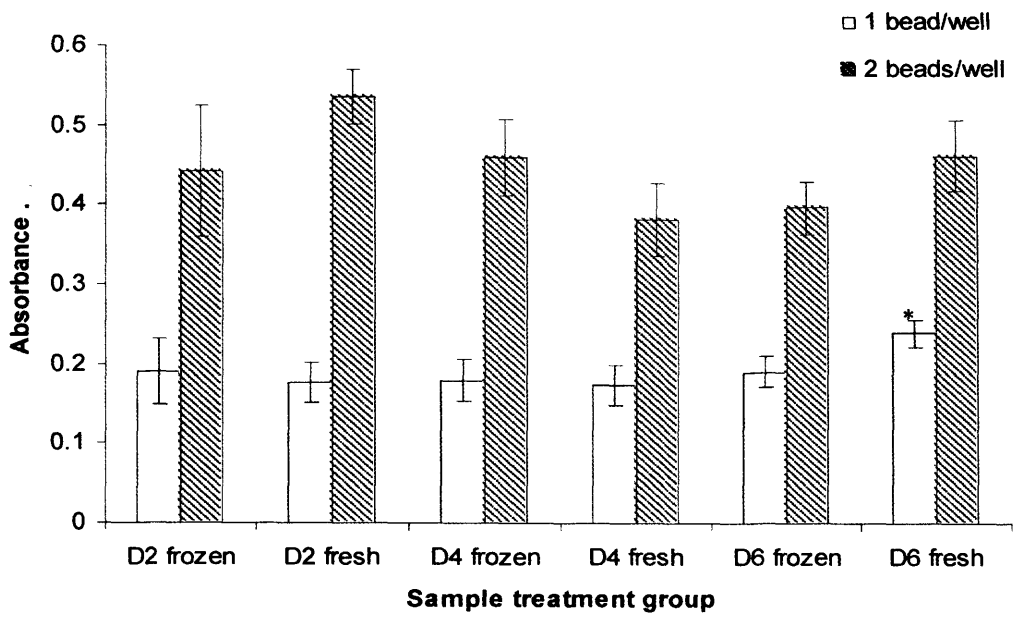

Figure 53. Comparison of MTT assay results using fresh versus frozen samples containing hMSCs in 27X alginate-GRGDY beads (Pronova SLG100) at $1x10^7$cells/mL. The bar graph shows the variability of absorbance corresponding to the number of beads per well for the fresh versus frozen protocol performed on day 2, 4 and 6. The data from 1 bead/well showed no differences in absorbance, except for the day 6 fresh sample (*, $p<0.05$). The data for 2 beads/well was significantly more variable; however no trend could be observed. The data for 3 beads (>$10x10^4$ cells/well) was discounted because it was above the linear range for the assay. Absorbance read at 600nm.

These preliminary data also showed that the absorbance readings did not increase during the six day study, thus this would suggest that the cell number per bead remained constant over the 6 days. This conclusion was substantiated by concurrent analysis performed by dissolving a representative bead at each time point and performing a cell count using a hemacytometer. Using this method, the cell density was found to remain constant (5.05 +/- 0.11 $x10^4$cells/bead) during the 6 days. The cell viability was 85% and 86% on day 2 and day 4, respectively; but dropped to 73% on day 6 (data not shown).

3.5.2. Using MTT assay to monitor hMSC proliferation in alginate and alginate-GRGDY beads

For this experiment, the MTT assay was used to determine whether there was cell growth in alginate-GRGDY beads over a time course. In addition, simultaneous measurements were made for glucose consumption and cell number and viability using hemacytometer and trypan blue dye exclusion assay.

Two sets of hMSC/alginate beads were made using the methods described in section 2.4.4 from hMSCs at P7 which were resuspended at $1x10^7$cells/mL in MSCCM. Alginate beads were made with 40% v/v cells in MSCCM and 60% v/v sterile alginate (Pronova SLG100) reconstituted in 0.1M MES, 0.3M NaCl buffer pH 6.5. Alginate-GRGDY was made using derivatized 27X Pronova SLG100 alginate according to the 'sterile process' method outlined in section 2.3.3, but prior to implementation of every sterilization step. Three beads were placed into each well of a low-binding 24 well microplate (Corning) containing 1mL of MSCCM. These plates were used so that any cells detached from the alginate beads would not attach and grow on the bottom of the microplate; thereby increasing the glucose consumption or lactate production. Time points were performed on day 1, 3, 5, 7. The spent medium volume was measured from each well to measure any loss due to evaporation. An aliquot was frozen for subsequent metabolite analysis using the YSI 2700 Select Biochemistry Analyser as described in section 2.5.6. Beads were removed for the MTT assay and assayed as fresh samples as described in section 2.6.2.2, 2.6.2.4 and 2.6.2.5, except trypsin/EDTA was not yet being utilized to dissociate the beads during the MTT assay. The cell concentration and viability of the beads were determined using a hemacytometer and trypan blue dye as described in section 2.6.2.3. Figure 54 shows the MTT absorbances for the time course performed on the alginate and alginate-GRGDY beads as measured for 1 bead/well and 2 beads/well. Data for 3 beads/well was discounted because the results were highly variable and above the linear range of the assay.

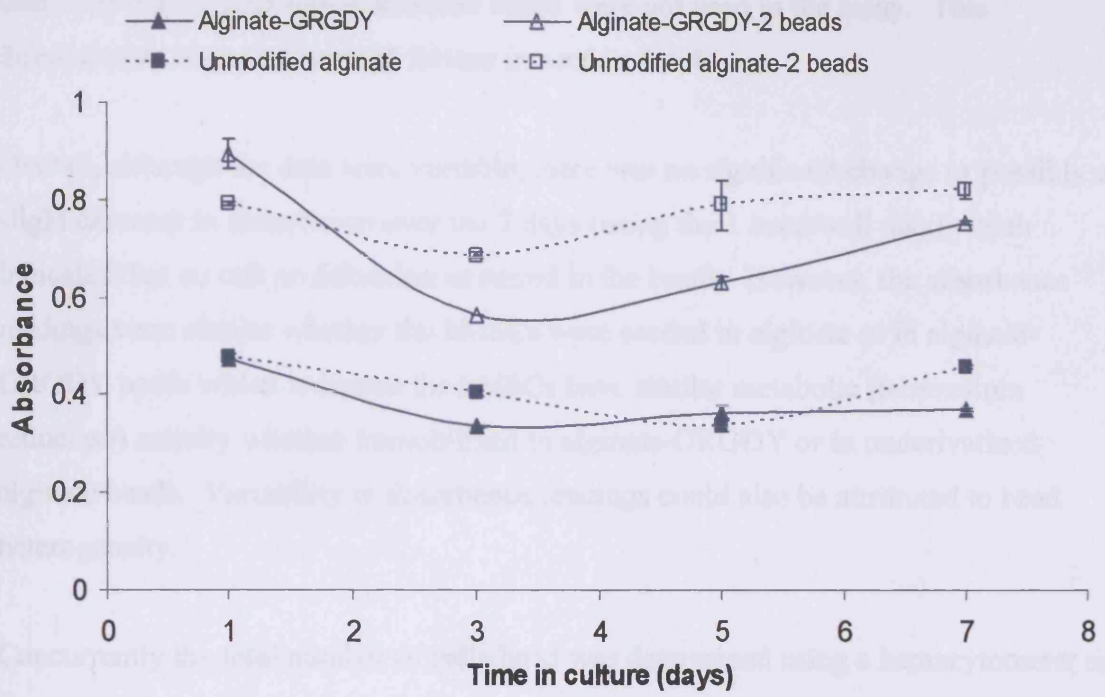

Figure 54. MTT absorbance readings of hMSCs seeded at $1x10^7$ cells/mL in alginate and 27X alginate-GRGDY beads (Pronova SLG) over 7 day time course. Data shown for 1 bead/well and 2 beads/well. The cells were not homogeneously resuspended in the alginate-GRGDY condition on day 3, 5 and 7. Although the data were variable, no significant change in absorbance was noted over the 7 days using the 1 bead/well data. In addition the absorbance results were similar for hMSCs seeded in alginate and in alginate-GRGDY beads. Absorbance read at 600nm.

Because replicate wells were not prepared for each condition (due to restriction in bead numbers), the data were not statistically analyzed. For the alginate bead condition, the cells dissociated homogeneously from the alginate because there was no interaction between the cells and alginate matrix. However, the cells did not dissociate homogeneously from the alginate-GRGDY matrix particularly for the 2 and 3 beads/well on days 3, 5 and 7. Because the cells did not resuspend into a homogeneous suspension; the formazan was not dissolved completely and the absorbance readings were lower. The cell aggregation was caused by the cells' interaction (elongation and networking) within the alginate-GRGDY bead. On day 7 the alginate-GRGDY beads dissolved more consistently than day 3 and 5. This change may have been the result of an increase in contamination level during the course of incubation. Some of the alginate-GRGDY beads were discolored at the

later time points; although discolored beads were not used in the assay. This discoloration issue is discussed further in section 3.4.4.

Overall, although the data were variable, there was no significant change or possibly a slight decrease in absorbance over the 7 days (using the 1 bead/well data) which indicated that no cell proliferation occurred in the beads. However, the absorbance readings were similar whether the hMSCs were seeded in alginate or in alginate-GRGDY beads which indicates the hMSCs have similar metabolic (tetrazolium reductase) activity whether immobilized in alginate-GRGDY or in underivatized alginate beads. Variability in absorbance readings could also be attributed to bead heterogeneity.

Concurrently the total number of cells/bead was determined using a hemacytometer as per section 2.6.2.3. The total number of cells/bead decreased by ca. 25% over the 7 day period in both bead conditions (Figure 55.a), this may have been due to cell lysis and the loss of cells during the dissolution of the beads with trisodium citrate and trypsin/EDTA using a micropipet. Disrupting the beads into a single cell suspension subjected the cells to high shear stresses during multiple, vigorous pipetting. Additionally the contamination causing discoloration of the beads may have also contributed to cell death. The fraction of cells viable was similar in both conditions and was ca. 85-90% on day 1 and ca. 79-85% on day 7.

The glucose consumption was plotted (Figure 55.b) and determined to be the similar in both the alginate and alginate-GRGDY beads. The slope of the lines used for the linear approximation of the glucose consumption was used along with the number of cells obtained from hemacytometer counts and the culture volume to obtain the specific GCR on a per cell basis. If a constant cell concentration was assumed ($6.2x10^4$cells/bead) over the culture period and each well contained three beads and 2mL of MSCCM, the GCR was calculated to be $4.33x10^{-11}$g/cell/hr. The volume of each well was measured during the 7 days to adjust losses due to evaporation.

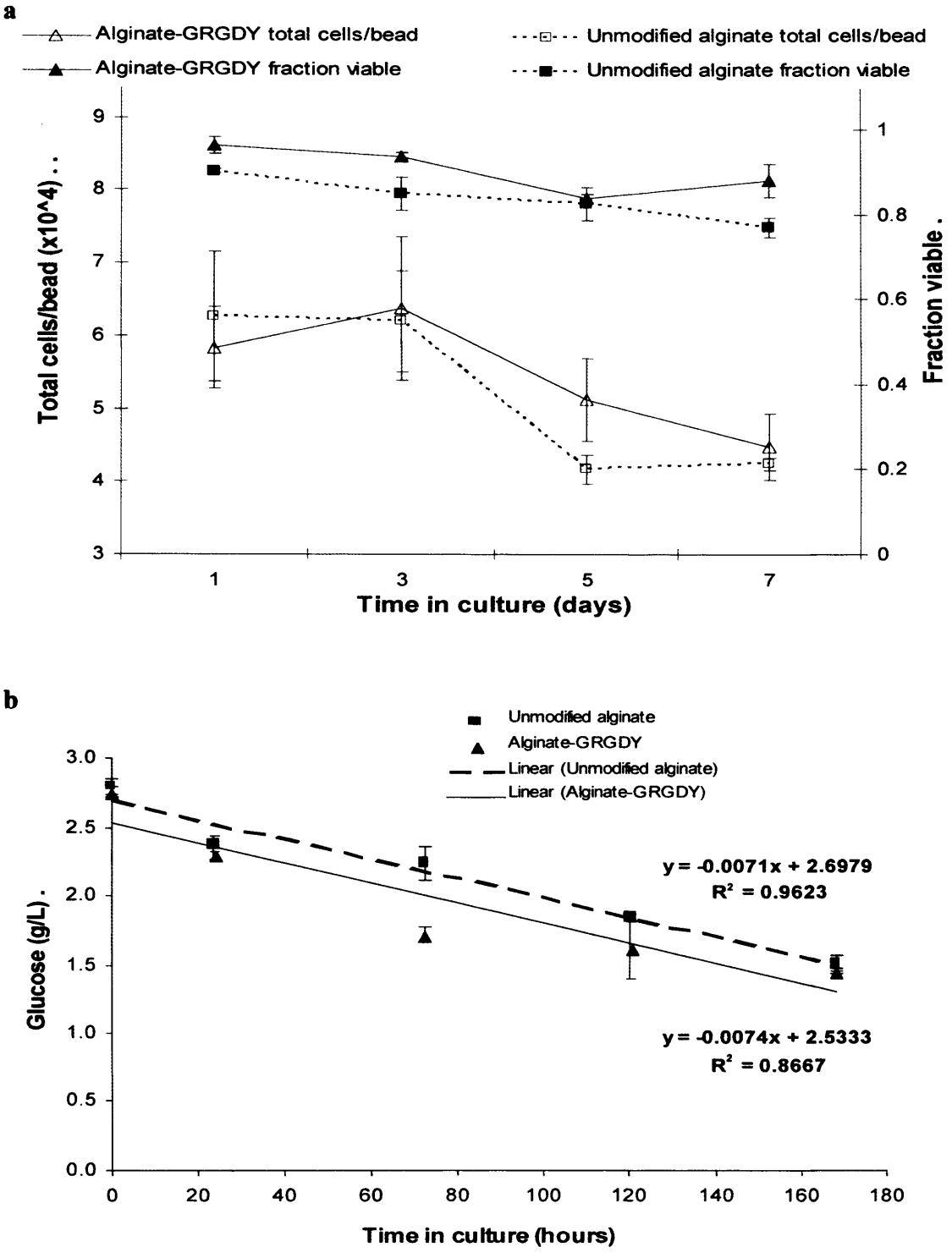

Figure 55. HMSCs in alginate or 27X alginate-GRGDY beads (Pronova SLG100), corresponding results for (a) total number of cells and fraction viable, and (b) glucose consumption. The cell number and viability decreased during the experiment, possibly due to cell lysis during evaluation. The GCR was similar for both conditions.

The main conclusion from this experiment was that a step for dissolution of the alginate-GRGDY beads using trypsin/EDTA needed to be introduced to improve resuspension of the cells into a homogeneous suspension. A concentrated trypsin solution was needed due to the micro-scale volumes needed for a 96 well microplate assay. In addition, the buffer solution could not contain phenol red due to interference with absorption values. This eliminated the 0.25% trypsin/0.2% EDTA that was already being used for cell trypsinization and counting of cells in beads. Therefore, 10X trypsin/EDTA in saline solution (5g trypsin, 2g EDTA 4Na/L in 0.9% NaCl, Sigma T4174) was selected and tested for these reasons.

3.5.3. Addition of 10X trypsin/EDTA in saline to improve bead dissolution

This section describes the experiments implementing the use of 10X trypsin/EDTA in saline to aid in complete resuspension of the cells from alginate-GRGDY beads. For further clarification, the MTT assay steps referenced in this section are those listed in the Appendices, section 6.1.1.2.

In the first set of experiments, 20μL of 10X trypsin/EDTA in saline was added to each microwell at the same time (e.g. step 5) as the trisodium citrate after 1 hour incubation with MTT solution. Then after a total of 2 hours of MTT incubation, the beads were resuspended with a micropipet to break up the cell aggregates. However, the cells were very sticky after addition of 10X trypsin/EDTA in saline and many adhered to the inside of the pipet tip. In addition, the cells would not pellet after centrifugation at 100g, nor at a higher force (160g). As a result it was concluded that trypsin/EDTA did not help resuspend the cells into a single cell suspension when introduced at this step in the MTT assay protocol. The results of this experiment are discussed further in section 3.5.4.

In the next experiment, 0-20μL of 10X trypsin/EDTA in saline was added to the 12X alginate-GRGDY (Pronova SLG100) beads after the beads had been frozen, thawed and DPBSG had been added (e.g. step 10). The absorbance results are presented in Figure 56. The dashed line represents the control condition in which no 10X trypsin/EDTA in saline was added. As observed during the dissolution of these beads

and as shown by the lower overall absorbance readings, this condition was not adequate to homogenize the cell suspension. The remaining solid lines represent the conditions containing 10-20µL of 10X trypsin/EDTA in saline. All of these conditions greatly improved the homogeneity of the suspension such that the formazan crystals were completely dissolved. This study also incorporated additional absorbance readings to confirm previous results on the stability of the formazan absorbance. This study confirmed that the addition of 10X trypsin/EDTA in saline did not adversely affect the stability of the absorbance readings over a 2 hour time course with the plates stored at 19°C. A single factor ANOVA comparison indicated that there was no statistical change in each individual sample over the 2 hour dissolution time. There was a statistically significant difference between the absorbance readings for the sample with no trypsin/EDTA treatment and the samples containing trypsin/EDTA for each time point. A summary of the comparison is provided in the Appendices, section 6.2.2.3. In addition this plate was held at 6°C for 27 hours after the study and then read on the spectrophotometer. All absorbance readings dropped significantly during the storage at 6°C (data not shown). Storage of the dissolved formazan samples for greater than 2 hours is not recommended.

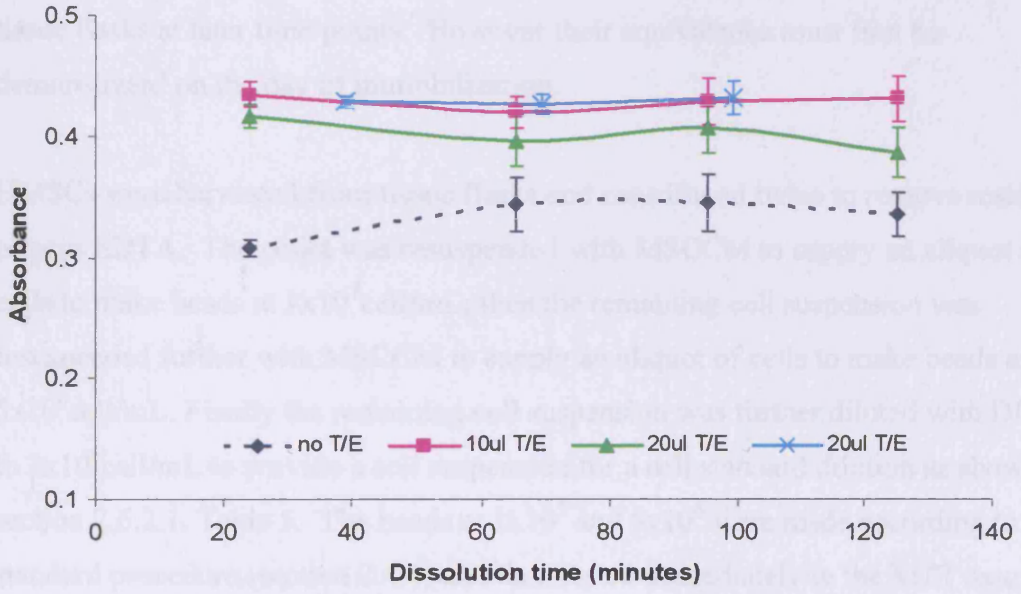

Figure 56. Addition of 10X trypsin/EDTA in saline to 12X alginate-GRGDY (Pronova SLG100) beads to aid in dissolution of beads during MTT assay. The blue line was the control condition in which no trypsin/EDTA was added. These absorbances were overall lower than the conditions using trypsin/EDTA. Additional readings were taken during the dissolution to examine the stability of the absorbance readings at 19°C. All samples were found to be stable during the 2 hours. Absorbance read at 600nm.

In summary, a reliable dissolution step for alginate-GRGDY beads was incorporated into the MTT assay using 10X trypsin/EDTA in saline. These cells had been in culture in the alginate-GRGDY beads for 17 days prior to the experiment. In addition, the trypsin/EDTA was determined to have no affect on the stability of the formazan absorbance readings during a 2 hour dissolution study at 19°C.

3.5.4. Comparison of MTT absorbances for cell standards produced from tissue flasks and alginate beads

This experiment was conducted to determine whether cells immobilized in alginate-GRGDY beads (on day 0) at two different concentrations produced the same absorbance readings as a cell standard dilution performed from the same cells harvested from tissue flasks but never immobilized in alginate. It had already been seen that beads from a time course can produce different cell standard curves (section 3.5.1.1). Due to the differences in metabolic activity between cells in tissue flasks and cells immobilized in alginate beads, it may be more suitable to determine a cell standard from cells immobilized in alginate beads rather than trypsinized cells from tissue flasks at later time points. However their equivalence must first be demonstrated on the day of immobilization.

HMSCs were harvested from tissue flasks and centrifuged twice to remove residual trypsin/EDTA. The pellet was resuspended with MSCCM to supply an aliquot of cells to make beads at $1x10^7$cell/mL; then the remaining cell suspension was resuspended further with MSCCM to supply an aliquot of cells to make beads at $5x10^6$cell/mL. Finally the remaining cell suspension was further diluted with DPBSG to $2x10^6$cell/mL to provide a cell suspension for a cell standard dilution as shown in section 2.6.2.1, Table 5. The beads at $1x10^7$ and $5x10^6$ were made according to the standard procedure (section 2.4.4) and then tested immediately in the MTT assay (section 2.6.2.2 and 2.6.2.4) alongside the cell standard dilutions made from the cell suspension at $2x10^6$cells/mL. After MTT incubation, 20µL of 10X trypsin/EDTA in saline was added to each microwell at the same time (at step 5, Appendices, section 6.1.1.1 and section 6.1.1.2) as the trisodium citrate after 1 hour incubation with MTT solution to aid in homogenating the cells. Then after a total of 2 hours of MTT

incubation, the beads were resuspended with a micropipet to break up the cell aggregates. However, the cells were very sticky after addition of 10X trypsin/EDTA in saline and many adhered to the inside of the pipet tip. In addition, the cells would not pellet after centrifugation at 100g, nor at a higher force (160g). Therefore the addition of trypsin/EDTA did not aid in resuspension of the cells when introduced at this step.

Despite these difficulties, the assay was continued and the plates were frozen. Thereafter the plates were thawed, the formazan was dissolved and then the plates were read (section 2.6.2.5). Again these data were highly variable at cell densities greater than $7.5x10^4$cells/well, probably due to the stickiness of the cells. If data above this concentration were eliminated from analyses, then the linear approximations produced very similar results. As can be seen in Figure 57, cells immobilized into 9X alginate-GRGDY (Pronova SLG100) beads at two densities, $1x10^7$ and $5x10^6$cells/mL, produced the same standard curve when plotted against the number of cells/well; however these data were only generated from 1 data point and 2 data points respectfully. The cell standard curve was generated from 4 data points.

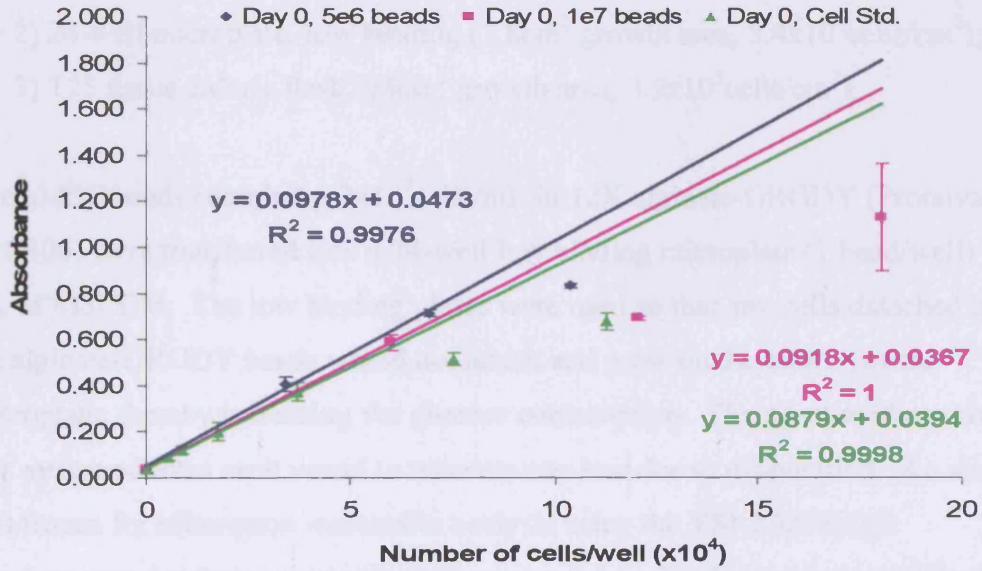

Figure 57. MTT absorbance for freshly harvested cells compared to same cells immediately after immobilization into 9X alginate-GRGDY (Pronova SLG100) beads. Linear curves were estimated from absorbance data below $7.5x10^4$cells/well, since the data above these points were non-linear. The cells immobilized at $5x10^6$cells/mL (blue line) and $1x10^7$cells/mL (pink line) in alginate-GRGDY produced the same cell standard curve as the original cells (green line). Absorbance read at 600nm.

These results confirmed that similar MTT absorbance standard curves are produced using a dilution series of hMSCs immediately after immobilization into alginate-GRGDY beads at two different concentrations and a standard curve produced from a cell dilution series from the original cell suspension.

3.5.5. Use of the MTT assay to monitor proliferation of hMSCs in alginate-GRGDY beads, microwells and tissue flasks

A final experiment was performed to evaluate cell proliferation in various tissue culture plastic (TCP) as compared to alginate-GRGDY beads. HMSCs at P7 were trypsinized, centrifuged and immobilized into alginate-GRGDY beads at $2x10^7$cells/mL according to the standard manual protocol. The exact number of cells per bead and viability was determined after dissolution of the bead with trisodium citrate and trypsin/EDTA using a hemacytometer and trypan blue dye as described in section 2.6.2.3. This same number of cells ($9.8x10^4$) was also seeded into the following TCP (all from Corning), each with 2mL of MSCCM:

1) 24-well microplate, cell culture-treated ($1.8cm^2$ growth area, $5.4x10^4$cells/cm^2);
2) 24-well microplate, low binding ($1.8cm^2$ growth area, $5.4x10^4$cells/cm^2);
3) T25 tissue culture flask ($25cm^2$ growth area, $3.9x10^3$cells/cm^2).

The hMSC beads containing $2x10^7$cells/mL in 12X alginate-GRGDY (Pronova SLG100) were transferred into a 24-well low binding microplate (1 bead/well) with 2 mL of MSCCM. The low binding plates were used so that any cells detached from the alginate-GRGDY beads would not attach and grow on the bottom of the microplate; thereby increasing the glucose consumption. The spent medium volume was measured from each vessel to measure any loss due to evaporation. An aliquot was frozen for subsequent metabolite analysis using the YSI 2700 Select Biochemistry Analyser as described in section 2.5.6. Beads were removed for the MTT assay as described in section 2.6.2.2, 2.6.2.4 and 2.6.2.5; 10X trypsin/EDTA in saline was utilized to help dissolve the beads after the plates were thawed at step 10, Appendices, section 6.1.1.2. HMSCs from one T25 flask were trypsinized, centrifuged and resuspended in ca. 325µL DPBSG. HMSCs from the low binding plates were removed with the spent medium, centrifuged and resuspended in ca.

325μL DPBSG. Then 100μL of each cell suspension was added to a 96 well plate then 10μL of MTT solution was added and the normal protocol was performed. These results were multiplied by a factor of 3.25 (100μL of 325μL cells used in MTT assay) and compared to the absorbance results obtained from one alginate-GRGDY bead. The hMSCs from the cell culture treated microwell plates were tested by the cell adherent MTT assay method outlined in section 2.6.2.7. These results were multiplied by a factor of 3.0 (3 times volume of DPBSG and isopropanol/HCl are added to a 24 well microplate compared to the 96 well microplate) to compare to the absorbance results obtained from one alginate-GRGDY bead.

Figure 58 shows the MTT absorbances for the 10 day time course performed on hMSCs under the 4 conditions (T25 flask, alginate-GRGDY bead, microwell-low binding plate and microwell-cell culture treated) which all were seeded on day 0 at $9.8x10^4$cells/vessel. Only the hMSCs cultured in the T25 flask exhibited cell growth as indicated by the 230% increase in absorbance readings. The other culture conditions resulted in either no significant change in absorbance readings (microwell-treated) or a decrease in absorbance (microwell-low and alginate-GRGDY beads) over the 10 day period. The absorbance reading of the hMSCs in the alginate-GRGDY beads decreased by ca. 33% over the 10 days. An additional absorbance data point was collected at day 15 for the alginate-GRGDY beads which continued this downward trend (Abs_{600nm} = 0.47±0.01).

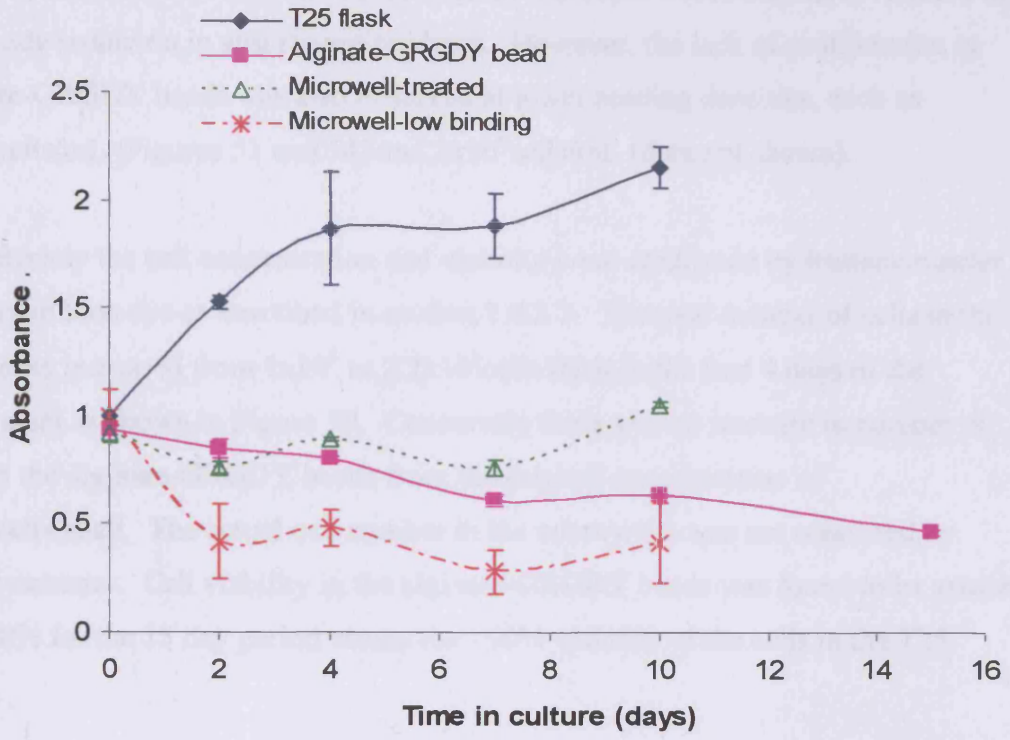

Figure 58. Use of MTT assay to monitor cell proliferation in T25 tissue flasks, 12X alginate-GRGDY (Pronova SLG100) beads, low binding microwells and cell culture treated microwells. All four conditions were seeded at $9.8x10^4$ cells/vessel. Only the cells in the T25 flasks exhibited an increase in absorbance readings over the 10 days. The cells in the alginate-GRGDY beads showed a 33% decrease in absorbance. Absorbance read at 600nm.

These results can be explained by the characteristics of the four different culture vessels/types. The T25 flasks were the only condition in which the cells were not space-constrained when seeded at $3.9x10^3$cells/cm^2. Therefore the cells were able to grow during the 10 day incubation. In contrast, the cells in the 24-well cell culture treated microplate were seeded at $5.4x10^4$cells/cm^2, which resulted in densely packed conditions after the cells attached to the growth surface. Thus, the hMSCs would have minimal space for growth, would become contact-inhibited and growth arrested (Batt and Roberts, 1998). The cells in the 24-well low binding microplate were seeded at a high density of $5.4x10^4$cells/cm^2, but the plate treatment inhibited the attachment of the cells to the surface. Therefore, most of the cells aggregated into large clusters. These conclusions were all confirmed by phase contrast microscopy. Finally the cells seeded in the alginate-GRGDY beads at $2x10^7$cells/mL were also very tightly packed. After the cells elongated within the alginate forming a dense

network, nutrient mass transfer would become restricted which may have resulted in the steady reduction in absorbance readings. However, the lack of proliferation in alginate-GRGDY beads was also observed at lower seeding densities, such as $1x10^7$cells/mL (Figures 53 and 54) and $2x10^6$cells/mL (data not shown).

Concurrently the cell concentration and viability were confirmed by hemacytometer and trypan blue dye as described in section 2.6.2.3. The total number of cells in the T25 flasks increased from $1x10^5$ to $2.7x10^5$cells/flask in the first 4 days of the experiment as shown in Figure 59. Conversely there was no increase in number of cells in the alginate-GRGDY beads from the original concentration of $1x10^5$cells/bead. The actual cell number in the microwells was not measured by hemacytometer. Cell viability in the alginate-GRGDY beads was found to be greater than 80% for the 15 day period versus the >90% viability of the cells in the T25 flasks.

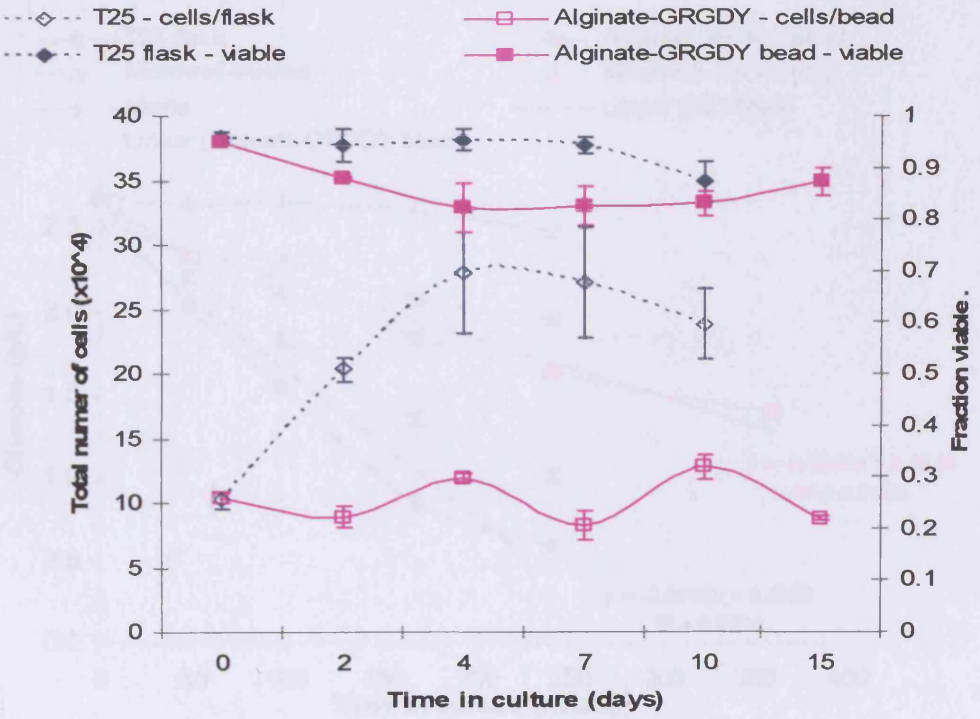

Figure 59. Total number of cells and fraction viable in T25 flask and 12X alginate-GRGDY (Pronova SLG100) beads over a 15 day time course. Cultures were seeded at ca. $9.8x10^4$ cells per flask and per bead which is equivalent to seeding density achieved for $2x10^7$cell/mL in the beads. The total number of hMSCs in the T25 flasks increased, whereas the total number in the alginate-GRGDY beads remained relatively constant during the experiment.

The GCR was highest for the hMSCs in the T25 flasks due to the increase in cell number per flask (Figure 60). The GCR for hMSCs in alginate-GRGDY beads was lower than both the cells grown in T25 flasks and microwell cultures. The cells in the microwells with no adhesion surface had the lowest rate. The baseline degradation rate of glucose in the culture medium with no cells was also measured.

The slope of the linear approximations of the glucose consumption, the hemacytometer count and the culture volume were used to obtain the specific GCR on a per cell basis. The GCR of hMSCs seeded at $2x10^7$cells/mL in the alginate-GRGDY beads with 1 bead/well was $7.1x10^{-11}$g/cell/hr as compared to $9.5x10^{-11}$g/cell/hr in the T25 flasks during exponential growth (first four days) and $6.5x10^{-11}$g/cell/hr in the T25 flasks during stationary growth (days 4-10). These rates were also comparable to the GCR of $4.3x10^{-11}$g/cell/hr from hMSCs seeded at $1x10^7$cells/mL in the alginate and alginate-GRGDY beads (section 3.5.2).

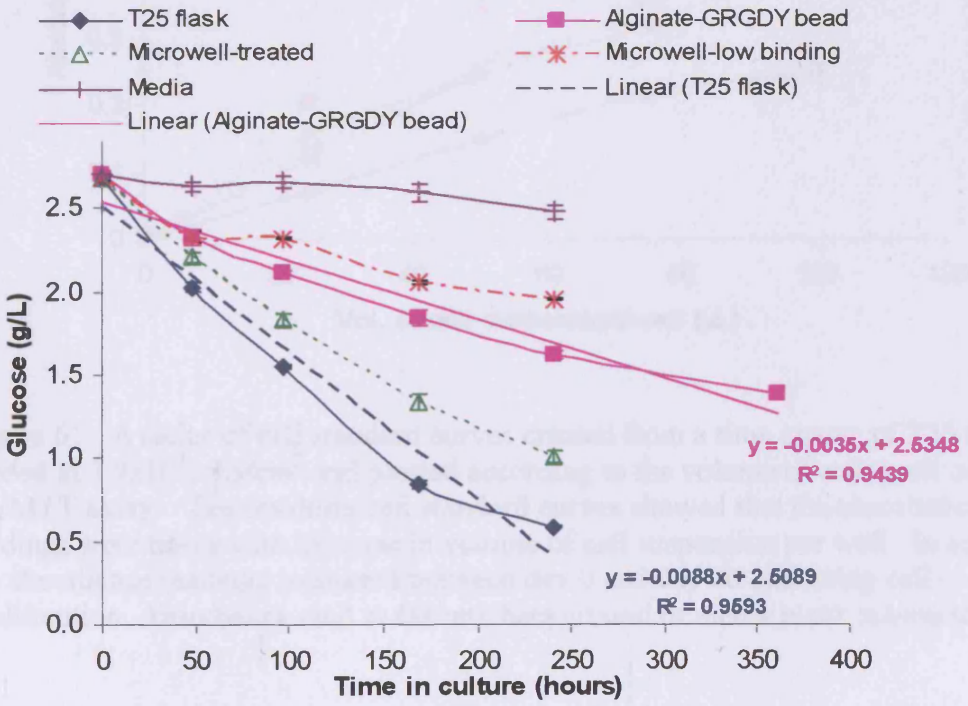

Figure 60. GCR of hMSCs seeded at $9.8x10^4$cells in TCP (T25 flasks, microwells treated for cell culture and microwells with low binding surface) and 12X alginate-GRGDY (Pronova SLG100) beads over a 15 day time course. The T25 flasks had the highest GCR due to the increase in number of cells/flask. The hMSCs in alginate-GRGDY appeared to have a lower GCR; however, when calculated on a per cell basis the GCR of $7.1x10^{-11}$g/cell/hr was similar to $6.5x10^{-11}$g/cell/hr for stationary growth in T25 flasks.

3.5.6. Comparison of cell number derived from MTT absorbance readings and from hemacytometer

In addition to the results previously described in section 3.5.5, the linearity of the MTT assay was confirmed by using a series of cell standard curves created from the individual cell suspensions from the 10 day time course experiment using T25 flasks. The absorbance readings were plotted according to the volume of cells/well used for the MTT assay (e.g. 0, 25, 50, 75 and 100µL). Figure 61 shows the data for the 10 day time course that the cells were trypsinized and assayed.

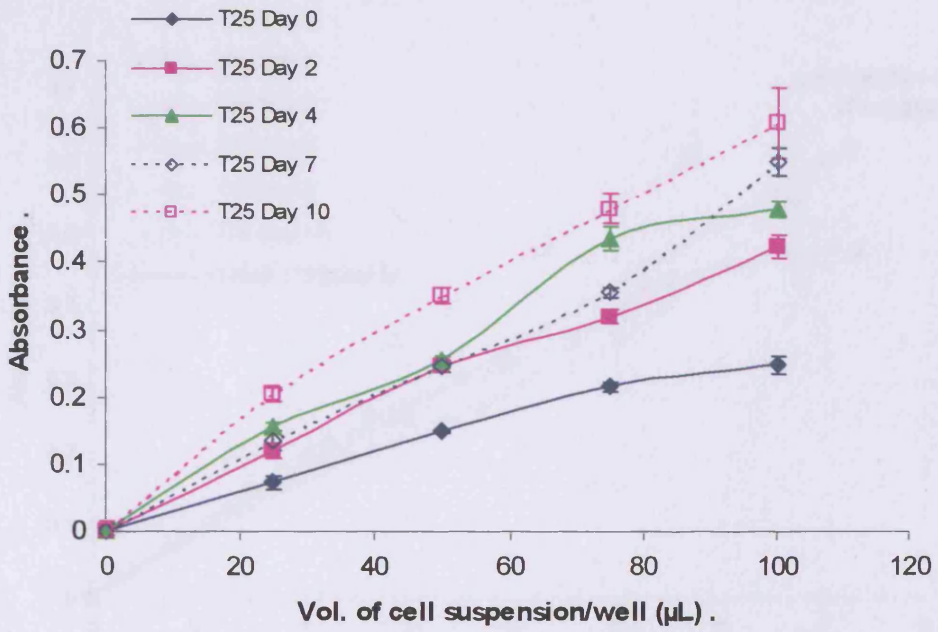

Figure 61. A series of cell standard curves created from a time course of T25 flasks seeded at $3.9x10^3$cells/cm^2 and plotted according to the volume of cells/well used in the MTT assay. The resulting cell standard curves showed that the absorbance readings were linear with increase in volume of cell suspension per well. In addition, the absorbance readings increased between day 0 and day 10 indicating cell proliferation. Absorbance read at 600nm, background of media blank subtracted.

The same cell standard curves for the T25 flasks were plotted by their corresponding cell number/well as was measured simultaneously by hemacytometer count (Figure 62). All of the cell standard curves, except from day 10, align very closely to the day 0 standard curve and each other, indicating that the absorbance readings correlated very closely to cell number. The day 10 cell count obtained by hemacytometer was

lower than expected (see Figure 59). This was due to cell aggregation which commonly occurs when flasks are trypsinized after a long time in culture or after the cells reach a high density (Lombarts, 1992). Aggregation would have most likely caused the actual cell density to be underestimated. This would result in a cell standard curve with a greater slope (higher corresponding absorbance readings). If a higher cell density was substituted for the day 10 absorbance readings (e.g. those obtained for day 4 or day 7), the data line would shift closer to the other standard curves. This decrease in hemacytometer count was also observed for long term cultures with rat smooth muscle cells when comparing the CyQuant fluorescence results to the actual hemacytometer counts (see section 2.6, data not shown).

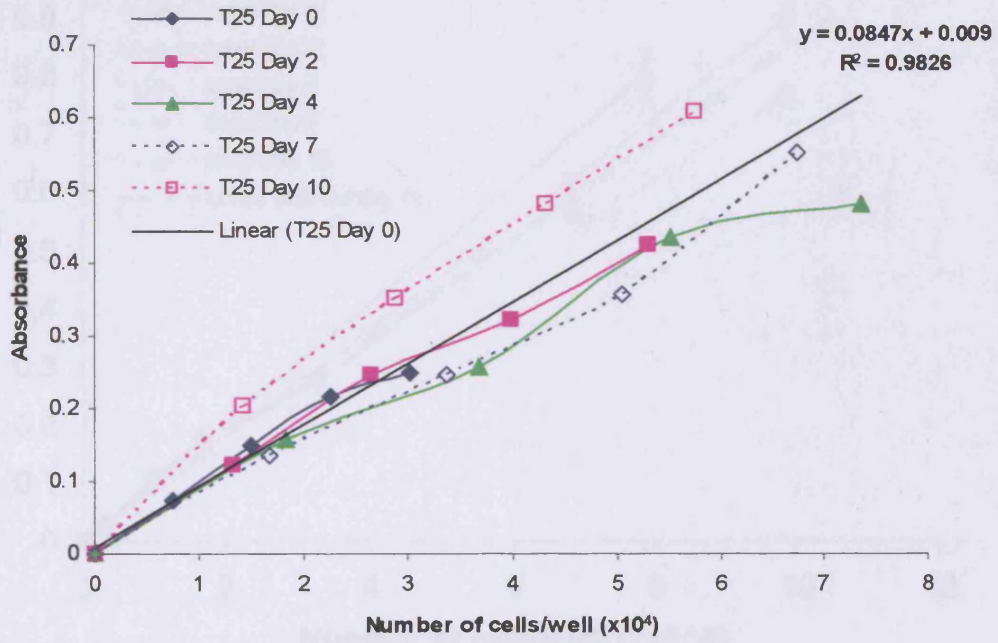

Figure 62. T25 flask absorbance readings corrected for actual cell count obtained by hemacytometer. The actual cell density obtained by hemacytometer on day 10 was much lower than expected due to cell aggregation (see Figure 59). Therefore, higher corresponding absorbance readings were produced (T25 Day 10). The remaining cell standard curves from days 2, 4 and 7 all closely align to the day 0 data. Absorbance read at 600nm, background of media blank subtracted.

The MTT absorbance readings obtained for hMSCs immobilized in 12X alginate-GRGDY (Pronova SLG100) beads were also plotted against the actual cell number obtained by hemacytometer (Figure 63). The cell standard curves generated from day

0, 2, 4 and 7 bead samples conformed well to the initial (day 0) cell standard curve which did not contain alginate. The actual cell concentration of the day 10 bead was slightly higher than expected (Figure 59); therefore the corresponding absorbances caused the standard curve from day 10 to shift considerably below the other standard curves. Due to the large size of the beads made by the manual method (ca. 2mm diameter) and the high cell concentration used ($2x10^7$cells/mL), all of the bead standard curves (day 0, 2, 4, 6, and 10) were based upon absorbance readings from only 1 bead. Data above $10x10^4$cells/well was excluded from analysis because these data were above the linear range of the assay.

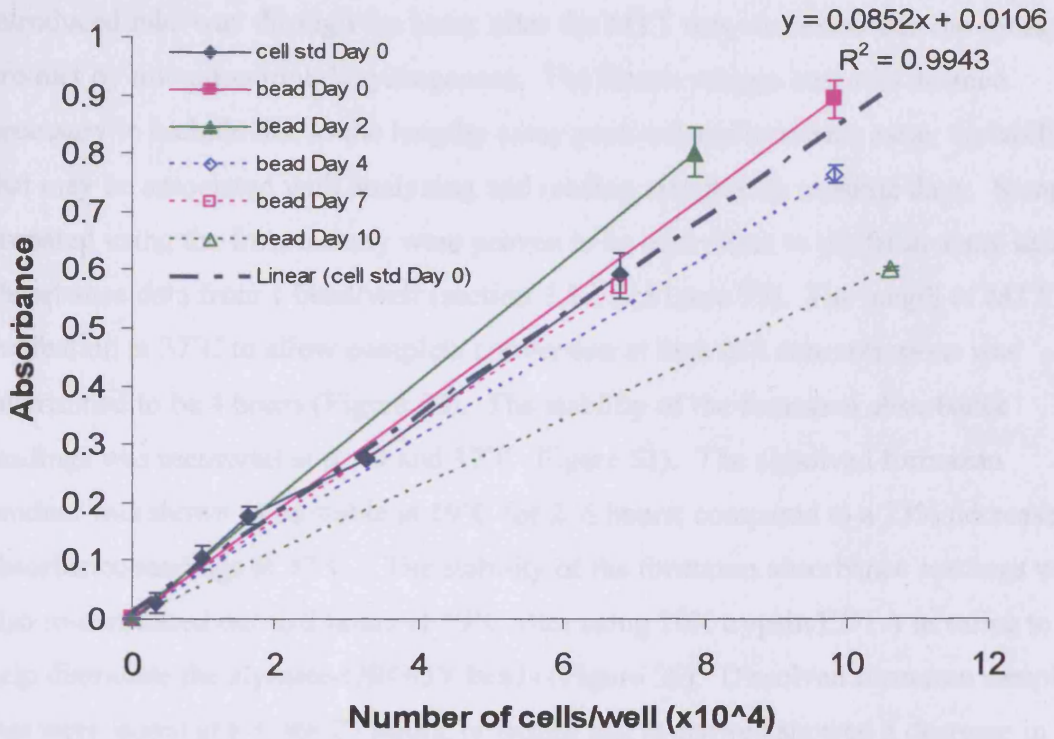

Figure 63. MTT absorbance for 12X alginate-GRGDY (Pronova SLG100) beads plotted versus actual number of cells/well. All data above $10x10^4$cells/well were excluded from analysis due to the non-linearity of the assay above this concentration. Most of the data, except the day 10 sample, conformed well to the day 0 cell standard curve which did not contain alginate. Absorbance read at 600nm, background of media blank subtracted.

Overall, the consistency of the results would be improved if more data points could be generated. This would be possible using smaller diameter beads or a lower cell concentration per bead to obtain more data points within the linear range of the assay. Previous cell standard data obtained from alginate-GRGDY beads made at

$5x10^6$cells/mL and $1x10^7$cells/mL showed good conformity to the cell standard curve on day 0 (Figure 57). However this previous experiment used 10X trypsin/EDTA in saline to improve the dissolution of the beads at the trisodium citrate addition step, so good linearity could not be achieved above $7.5x10^4$cells/well.

3.5.7. Summary

A modified MTT assay was produced to analyze a time course of hMSCs immobilized in alginate and alginate-GRGDY beads. A frozen storage step was introduced mid-way through the assay after the MTT was converted into the formazan product by mitochondrial dehydrogenase. The frozen storage step was deemed necessary to include due to the lengthy assay protocol and to reduce assay variability that may be associated with analyzing and reading samples on separate days. Samples prepared using the frozen assay were proven to be equivalent to the fresh assay using absorbance data from 1 bead/well (section 3.5.1.5, Figure 53). The length of MTT incubation at 37°C to allow complete conversion at high cell concentrations was determined to be 4 hours (Figure 50). The stability of the formazan absorbance readings was measured at 6, 19 and 37°C (Figure 51). The dissolved formazan product was shown to be stable at 19°C for 2 ½ hours; compared to a 23% decrease in absorbance readings at 37°C. The stability of the formazan absorbance readings were also re-confirmed out to 2 hours at 19°C after using 10X trypsin/EDTA in saline to help dissociate the alginate-GRGDY beads (Figure 56). Dissolved formazan samples that were stored at 6°C for 27 hours, or frozen and re-thawed showed a decrease in absorbance readings. All of the absorbance data were read at 600nm on a microwell plate spectrophotometer. A full wavelength spectrograph was found to produce similar readings at 600nm as compared to the peak absorbance at 560nm (Figure 47). Additional improvement in the data may be possible using the dual wavelength measurements by subtracting the absorbance at the reference wavelength of 670nm. Dual readings account for increased light scattering cause by turbidity in the sample which may slightly skew absorbance readings obtained from just the single wavelength (e.g. 600nm) (Harris, 1996).

A number of factors were determined to potentially affect the results of the MTT assay. These factors are listed below with the method or condition used to minimize the variability:

1. Length of incubation to permit MTT conversion to formazan – optimized to 4 hours for high cell concentrations.
2. Dissolution of the formazan product, including release from cells – used a freeze step to lyse cell membrane, and isopropyl alcohol was added to dissolve the formazan product for ca. 40 minutes - 1 hour
3. Dissolution of alginate – trisodium citrate was added to reverse cross linking of the alginate hydrogel
4. Dispersion of formazan/hMSCs in alginate-GRGDY beads – 10X trypsin/EDTA in saline was added and multiple pipetting steps were used to disperse the cells
5. Stability of the formazan absorbance readings – performed dissolution at room temperature and read plate within 1 hour after isopropanol/HCl added.
6. Residual excipients (e.g. alginate) – the supernatant was removed prior to freezing
7. Volume variability per well – the supernatant was removed until an 'o ring' appeared on bottom of well.
8. Loss of material in pipet tips clinging to inside wall – no pipetting was performed prior to freezing, mixing was performed after isopropanol addition.
9. Phenol red (pH indicator) contained in the culture medium – samples were dissolved with isopropanol containing 0.1N HCl, the HCl ensured an acidic pH causing the phenol red indicator to be yellow versus orange/red in neutral or basic pH which would interfere with absorbance readings.

Wan (1994) investigated the reproducibility of the MTT assay within the same plate, between plates and between different culture vessels. They found that the reproducibility of the assay was not satisfactory for any of these conditions. That is, the data obtained for these conditions were statistically different, when the results were expected to be the same. They determined that the cell number variability was the most significant factor influencing the reproducibility of the MTT assay. So it was essential that the cell suspension was homogeneously mixed before seeding the microplate to minimize the variation in cell number. In addition they also looked at

non-random and random sampling across the microplate. Statistically significant differences were measured when a sample was measured by order, left to right across the plate. However, random sampling eliminated this difference. For the purpose of this MTT assay application (e.g. use as a cell number titration which requires using a serial dilution scheme) random sampling was not possible. However if the assay was used as a screening or toxicity test; random sampling could be utilized for evaluation of a biomaterial or the effect of a drug.

Randomized sampling was used to improve the reliability of these MTT results by randomizing the bead selection for analysis. In addition more replicates could be performed at each time point, depending upon availability of material. However the most important factor for generating reproducible results was the complete dissolution of formazan product which required 30 minutes of exposure to 10X trypsin/EDTA addition for cells in alginate-GRGDY beads and multiple pipetting during the isopropanol/HCl dissolution. Ferrara (1993) also found that one hour was sufficient to dissolve the formazan using DMSO; however some formazan was trapped in the compact tissue section that did not dissolve properly unless the sample was shaken vigorously to release the formazan during dissolution. If complete, homogeneous release of formazan was not achieved a linear relationship between tetrazolium reductase (TR) activity and cell viability could not be ascertained. Huveners-Oorspong (1997) found that the formazan crystals dissolved completely using both DMSO and isopropanol. DMSO gave higher absorbance readings; however, the coefficient of variation (CV) was higher using DMSO than isopropanol, and sometimes there was a color shift in some of the wells. In addition, the evaporation rate of isopropanol was overcome by chilling the plates to 4°C after removal of medium and adding ice-cold isopropanol to the wells. In these studies plastic film was used to reduce evaporation, however when the plates were dissolved at room temperature and read immediately (within 1 hour), minimal evaporation was noted. When the formazan was dissolved at 6°C, the absorbance readings were lower than expected, most likely due to incomplete dissolution; therefore 19°C (room temperature) was the chosen temperature. Finally, an alternative tetrazolium salt that produces a more water-soluble formazan could be utilized to improve dissolution (Ishiyama, 1997).

In addition to the factors described above, a number of experimental conditions also affected the reproducibility of the results. These factors would not affect the performance of the assay; however, they would affect the reliability of the data.

1. Homogeneity of cells mixed within alginate prior to bead formation
2. Homogeneity of bead size/shape
3. Sterility of alginate/cells/medium
4. Purity of alginate (toxins causing cell death or decreased metabolism)

After tight assay parameters were established (e.g. for MTT incubation length, formazan dissolution time and temperature control) and a homogeneous cell suspension was achieved (i.e. by addition of 10X trypsin/EDTA at the appropriate step to dissociate the cells within the alginate-GRGDY matrix), a linear relationship was established between formazan absorbance readings and concentration of hMSCs. This relationship was established for a cell suspension of hMSCs from tissue flask cultures over a series of 7 days (Figure 62) and from a dilution series of cells immobilized in GRGDY-alginate beads over a 7 day time course (Figure 63). However, the day 10 data for both cell standard preparations were outliers in the study (refer to section 3.5.6). Combining these data with some additional studies generated using tight assay controls (Table 17), there appeared to be close agreement to a linear relationship between absorbance and cell concentration that was estimated to be $y = 0.085x$; where y was the absorbance measured at 600nm and x was the cell density per well ($x10^4$).

Since it has been shown that the growth rate of hMSCs varies with passage level and with donor source (section 3.4.1, Table 15; Bruder, 1997; Phinney, 1999); it is also likely that these parameters will also affect the linear relationship of the formazan absorbance readings and cell concentration. These two parameters were not investigated during this research.

Study	Corresponding figure number	Range of slope estimates	Level of assay control
Initial – Alginate beads	48	0.89 to 0.92	Parameters not established
Initial – cell standards	48	0.055 to 0.058	Parameters not established
Initial – Alg. vs. alg.-GRGDY beads	48	0.038 to 0.040	Parameters not established
MTT incubation length and formazan dissolution time	50	0.086 (2hr MTT inc.)* 0.125 (4hr MTT inc.)	Tight control
Fresh vs. frozen samples	53 (all data not shown)	0.037 to 0.047	Trypsin/EDTA not used
Alg. vs. alg.-GRGDY beads	54 (all data not shown)	0.059 to 0.157 0.043 to 0.092	Trypsin/EDTA not used
Equivalence of beads and flasks on day 0	57	0.088 to 0.98 *	Tight control
T25 cell standard	62	0.085 * day 10 – 0.104	Tight control – Day 10 outlier
Bead cell standard	63	0.085 * day 10 – 0.057	Tight control – Day 10 outlier

Table 17. Linear relationship between formazan absorbance readings and cell concentration established for MTT experiments with tight assay parameters. The slope of the standard curves were highly variable in initial experiments in which parameters had not been established or when 10X trypsin/EDTA was not used to dissociate the alginate-GRGDY beads. The remaining data (*) produced similar slopes (using 2 hour MTT incubation length) which were estimated to be $y = 0.085x$; where y was the absorbance measured at 600nm and x was the cell density per cell ($x10^4$).

Under these conditions, the MTT was linear up to $1x10^5$cells/well and sensitive down to $3x10^3$cells/well. Heo (1990) also showed that the MTT assay started becoming non-linear at cell densities above $1x10^5$cells/well. Alginate beads made by the manual method were ca. 2-2.5mm in diameter, which was too large for the study, especially when cell densities needed to approach $2x10^7$cells/mL for the complete networking of cells within the alginate-GRGDY bead. For most assays, only 1 bead/well could be used to estimate the slope of the linear approximations because the number of cells/well exceeded $1x10^5$cells/well when 2 or 3 beads/well were tested. A new bead fabrication device is under development that will produce small diameter beads (<1mm) which will therefore have a lower number of cells/bead. This will

allow the MTT assay to be run using multiple beads, without exceeding the non-linear range of the assay.

The MTT assay's absorbance results showed that hMSCs do not proliferate within the alginate-GRGDY or unmodified alginate matrix (Figure 54) cultured for 7 days. In fact, there was a gradual decrease in absorbance readings (ca. 33%) within the alginate-GRGDY beads cultured for 15 days (Figure 58). This decrease may be due to diffusion limitations in these large diameter (2mm) beads. Similarly, there was no increase in absorbance levels for hMSCs that were seeded at a high density ($5.4x10^4$cells/cm^2) in microwell plates. Only the cells seeded at a low density ($3.9x10^3$cells/cm^2) in T25 flasks showed an increase in MTT absorbance over the 15 day study (Figure 58). These results were due to availability of space in the T25 flasks since primary cells become contact-inhibited at high density as shown in the microwell plates. Concurrently the cell numbers and viabilities of the beads were confirmed by hemacytometer and trypan blue dye. The viability of the hMSCs seeded at $2x10^7$cells/mL in alginate-GRGDY beads was greater than 80% for the 15 days evaluated in culture (Figure 59). Comparable results were also found in the 7 day studies with hMSCs seeded at $1x10^7$cells/mL in alginate and alginate-GRGDY beads (Figure 55.a).

The experiments conducted in this research project showed no proliferation of rSMCs or hMSCs in alginate or in alginate-GRGDY matrices out to 2 weeks in culture. Similarly, Dar (2002) reported no proliferation of rat neonatal cardiac cells in alginate scaffolds despite retaining some spontaneous contraction for 2 weeks. More recently, Ma (2003) showed that alginate encapsulated MSCs become growth arrested. In addition, this research showed that the presence of cell-adhesion sites in the alginate-GRGDY does not encourage proliferation. Bone marrow cells have only been reported to proliferate on the surface of unmodified alginate as well as express osteoblast associated markers when exposed to differentiation medium (Wang, L., 2003).

If the hMSCs do not proliferate within this system, it may not be a concern provided the cells are healthy and can be seeded at a high enough density to form an integral network throughout the alginate-GRGDY construct. In fact, these studies showed

hMSCs had similar GCRs whether grown on 2-D TCP or immobilized 3-D alginate and alginate-GRGDY matrices. The GCR of hMSCs seeded at $2x10^7$cells/mL in the alginate-GRGDY beads with 1 bead/well was $7.1x10^{-11}$g/cell/hr as compared to $9.5x10^{-11}$g/cell/hr in the T25 flasks during exponential growth (first four days) and $6.5x10^{-11}$g/cell/hr in the T25 flasks during stationary growth (days 4-10) (section 3.5.5, Figure 60). These rates were also comparable to the GCR of $4.3x10^{-11}$g/cell/hr from hMSCs seeded at $1x10^7$cells/mL in the alginate and alginate-GRGDY beads (section 3.5.2, Figure 55).

3.6. Differentiation studies using hMSCs

HMSCs derived from bone marrow cells (BMCs) have been shown to differentiate *in vitro* into adipocytes, chondrocytes and osteoblasts (Bruder 1997; Phinney, 1999; Pittenger, 1999; Kinner, 2002), as well as myoblasts and myotubes (Wakitani, 1995). At the time of this research, the exact components of a specialized differentiation medium for smooth muscle cells had not been published; therefore, the idea of using conditioned medium from rSMC co-cultures (CDMEM) was tested. The preparation of rSMCs co-cultures for differentiation studies of hMSCs immobilized in alginate-GRGDY beads is described in sections 2.7.2 and 2.7.3.

Charbord (2000) proposed a sequential model of differentiation from hMSCs to vascular-smooth muscle-like stromal cells from cytoskeletal and extracellular matrix protein expression analyses in both humans and murine using principal component analysis. The human protein markers are summarized in section 1.7.3, Table 1, and include fibronectin and α-smooth muscle actin (ASMA) as early indicators of differentiation along the smooth muscle cell (SMC) pathway (Charbord, 2000). They determined that the default differentiation pathway for hMSCs was toward vascular SMCs if they received no other definitive biological factors or cues to an alternative differentiation pathway (Galmiche, 1993).

The presence of undefined biochemical components including proteins, growth factors and/or hormones in the fetal bovine serum (FBS) in the culture medium imparted further ambiguities that may have influenced the differentiation pathway of

these hMSCs. For these reasons, a media differentiation study was conducted with hMSCs grown long term in MSCCM (control), complete DMEM, and in conditioned DMEM from rSMC cultures (CDMEM) in microwell plates as described in section 2.7.4 to establish a base-line of ASMA expression for cultured hMSCs. The results from these 2-D media differentiation studies conducted with hMSCs in long term culture in microwells are discussed in section 3.6.1.

The results from the 3-D differentiation studies carried out using hMSCs immobilized in alginate-GRGDY beads and cultured in CDMEM with rSMC co-cultures are described in section 3.6.2. Samples were taken over a time course; and histology preparations were made from the cross sections of the hMSC/alginate beads and immunostained for ASMA as described in 2.5.8. Some of these studies were compared directly to cultures of hMSCs/alginate beads in control medium (DMEM). The extent of differentiation of the hMSCs was also monitored using fluorescence activated cell sorting (FACS) to observe the change in cell surface markers as described in section 2.5.9.

3.6.1. Media differentiation studies in microwells (2-D)

Because hMSCs have been shown to express ASMA in culture (Charbord, 2000), it was important to determine the baseline expression of ASMA in long term hMSC cultures that were not associated with alginate-GRGDY hydrogel matrix and not exposed to the growth factors and intermediate biochemical products of metabolism produced by the rSMC co-cultures. HMSCs were seeded into microwells at $5x10^3$cells/cm^2 as described in section 2.7.4. The cultures were confluent after 5 days, when the spent MSCCM was removed and the wells were refed with MSCCM (control medium), complete DMEM (control medium) or CDMEM. Over a 9 day time course, the hMSCs were scrapped from the microwell surface, smeared onto a microscope slide, fixed with acetone and exposed to hematoxylin which stains the cells' nuclei blue and to cell-specific antibodies against ASMA which stain the cells' cytoplasm brown. Figure 64 shows the time course results. The cytology smears of the hMSCs showed distinct blue nuclei and some non-specific ASMA staining, as indicated by the brown fiber-like strands (photos A-C), on the initial time point on day 3 of the study which was post-seeding day 8. The staining was non-specific

because it was not confined to the cytoplasm of the cell which would be the expected location of these cell-specific proteins. The cytology smears of the hMSCs cultured in MSCCM continued to show a small level of non-specific ASMA staining, whereas the cells cultured in DMEM and CDMEM had an increased level of non-specific ASMA staining after day 6 in culture (photos D-F). By day 9, both DMEM and CDMEM cultures had a high degree of non-specific ASMA staining; however the staining was still not confined to the cytoplasm of the cell (photos G-I). Higher magnification (400X) micrographs are shown in the Appendices, section 6.2.3, for these same preparations for day 6 (Figure 73) and for day 9 (Figure 74). These photos further help show the individual cell structure.

In conclusion the brown non-specific staining from the 2-D hMSC cultures grown in MSCCM, DMEM and CDMEM was determined to be an artifact of the method of preparation and not an indication that the cells were expressing ASMA. Due to this result, a biotin blocker (Dako) was used in future preparations to minimize the non-specific binding of endogenous biotin in the samples.

Figure 64. (On next page) Time course of hMSCs in confluent microplate cultures grown in MSCCM, DMEM and CDMEM. All preparations were fixed with acetone and exposed to hematoxylin (blue nuclear stain) and ASMA (brown cytoplasmic stain). Small amounts of non-specific ASMA staining were observed in day 3 preparations as indicated by brown fiber-like strands (A-C). No cytoplasm-specific staining was observed in the MSCCM cultures (A,D,G). However an increased level of non-specific ASMA staining was evident on day 6 and day 9 in the DMEM (E,H) and CDMEM (F,I) cultures; however, it was not confined to the cytoplasm of the cells.

Day 3
Day 6
Day 9
A
MSCCM
B
DMEM
C
CDMEM
Non-specific
ASMA staining
Non-specific
ASMA staining
D
E
F
G
H
I
30 μm
30 μm
30 μm
30 μm
30 μm
30 μm
30 μm
30 μm
30 μm

3.6.2. Differentiation studies in alginate-GRGDY beads

In previous bead studies described in section 3.4.2.2, it was shown that hMSCs readily attached and elongated within alginate-GRGDY hydrogel beads within 1 day of immobilization. And when seeded at high densities (e.g. 10^7cells/mL), hMSCs formed dense networks within the bead (section 3.4.2.3). In these differentiation studies, hMSC/alginate-GRGDY beads were removed from co-cultures of rSMCs and conditioned DMEM (CDMEM) over a time course and placed into formal saline (10% formaldehyde in buffered saline) for characterization using immunohistology. In addition, fluorescence activated cell sorting (FACS) was used to analyze the hMSCs immobilized within the alginate-GRGDY beads to monitor the change in hMSC surface markers during co-culture with rSMCs. For these studies the hMSC/alginate-GRGDY beads were physically separated from the rSMC co-cultures by using cell culture inserts.

3.6.2.1. Immunohistological analysis of beads

During initial histology preparations, it was nearly impossible to locate the clear alginate beads within the paraffin block. Therefore preparations were made by smearing the 10% formaldehyde-fixed bead across a glass slide and then staining with hematoxylin and eosin (H&E) for overall morphology as described in section 2.5.8. Hematoxylin stains the cell nucleus blue, and eosin stains the cell cytoplasm pink. Figure 65 shows the results from a differentiation study.

The hMSCs were immobilized in 50X alginate-GRGDY (Manugel DMB) beads at $5x10^6$cells/mL and placed into cell culture inserts as described in section 2.7.1 and 2.7.3. On day 1 the inserts were transferred into microwells containing rSMC co-cultures and CDMEM. Phase contrast micrographs showed the hMSCs were elongated within the bead on day 1 (photo A) and on day 7 (photo C) of the time course study. The beads were noted to be more compact on day 7 of the study. The corresponding H&E preparations of the hMSCs are shown from day 1 (photo B) of culture which was day 0 of the differentiation study, and from day 7 (photo D) of culture which was day 6 of the differentiation study. The pink/purple color in the micrographs was due to background staining of the alginate from the eosin. The

grainy, brown sections were caused by formalin pigmentation due to the smear preparation of the samples. Upon examination under higher magnification (400X), these H&E preparations showed a distinct difference in morphology of the hMSCs between day 1 and day 7. The day 1 beads contained a majority of hMSCs with narrow, pointy nuclei (photo E) which were indicative of primitive stem cells. Whereas the day 7 beads contained a greater number of hMSCs with larger, oval-shaped nuclei (photo F) which were indicative of terminally differentiated cells (Bruder, 1997; Phinney, 1999).

Figure 65. (On next page) Differentiation studies of hMSCs at $5x10^6$cells/mL in 50X alginate-GRGDY (Manugel) beads cultured in CDMEM with rSMC co-cultures. Phase contrast micrographs of the hMSCs elongated within the bead are shown from day 1 (photo A) and day 7 (C). Initial histology preparations were performed by smearing the hMSCs/alginate bead across glass slide. The corresponding H&E staining is shown on day 1 (B) and day 7 (D). The majority of hMSCs within the bead on day 1 contained narrow, pointy nuclei (E); whereas the day 7 beads contained a greater number of hMSCs with larger, oval-shaped nuclei (F), also circled in (D). The pink/purple background in photos B, D and E was due to eosin staining of the alginate. Some brown formalin pigmentation was present (arrows) due to the smear preparation. (A-D: 100X magnification, E-F: 400X magnification)

A Phase contrast - Day 1

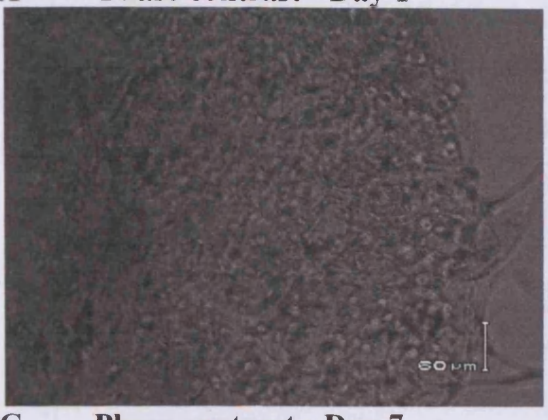

B H&E - Day 1

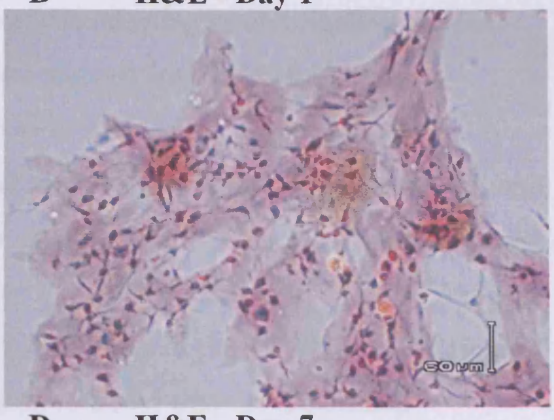

C Phase contrast - Day 7

D H&E - Day 7

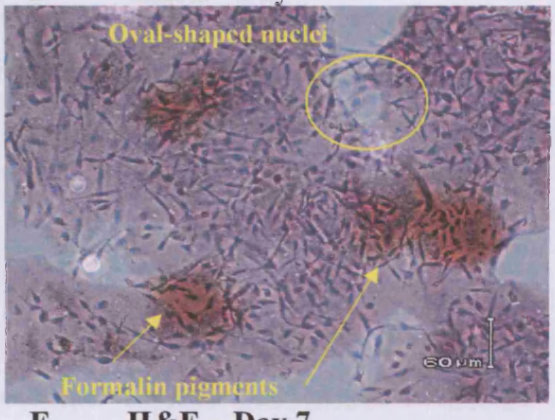

E H&E – Day 1

F H&E – Day 7

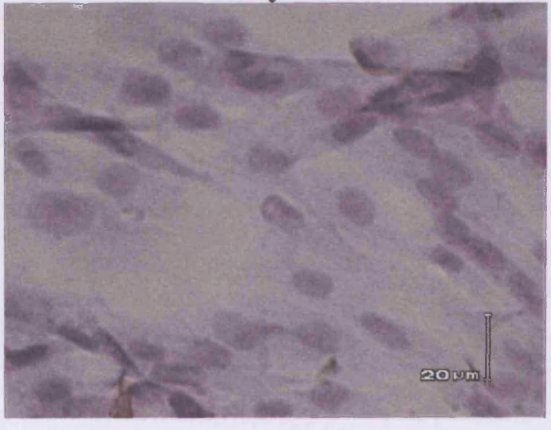

In later differentiation studies, microsectioning of the hMSC/alginate bead was possible after the edge of the formaldehyde-fixed bead was marked with histological marking ink. Then the beads were placed in biopsy capsules and cassettes and underwent standard overnight histopathologic processing as described in section 2.5.8. The microsections were dewaxed and stained with H&E for overall morphology. The results from a differentiation study in which hMSCs were immobilized in 50X alginate-GRGDY (Manugel DMB) beads at $5x10^6$cells/mL and cultured in CDMEM with rSMC co-cultures are shown in Figure 66. Control hMSCs in 50X alginate-GRGDY beads were cultured in DMEM medium. Figure 66 shows H&E preparations of the hMSCs after immobilization on day 0 within the alginate-GRGDY bead (photos A&B). The cells were rounded after cross linking. Immunohistological preparations using a specific antibody stain for ASMA were used to assess the presence of ASMA, one of the specific cell proteins for SMCs. The day 0 beads showed that some of the hMSCs initially stained positively for ASMA as was evident by the brown cytoplasmic staining of the cells in the sectioned bead (photo C). However, under higher magnification (400X) many of the cells also had a dark membrane (photo D) with no cytoplasmic staining which indicated the hMSCs may have taken up the stain due to the delicate condition of the cells immediately after immobilization in the alginate-GRGDY bead and exposure to the 'harsh' conditions (e.g. pressure cooking for 4 hours) of antigen recovery during histological preparation. This observation was further supported by the micrographs from day 3 & 4, which showed that the cells had elongated within the alginate (H&E – photo E); but the level of ASMA staining was very low (photos F&G) with only a couple positive cells, if any. It was also observed that the surface of the bead was uneven in appearance due to contraction of the cells/alginate (photo G). By day 11 of culture in the CDMEM with rSMC co-cultures there was a 40μm layer of positive ASMA cells around the rim of the bead (photo H).

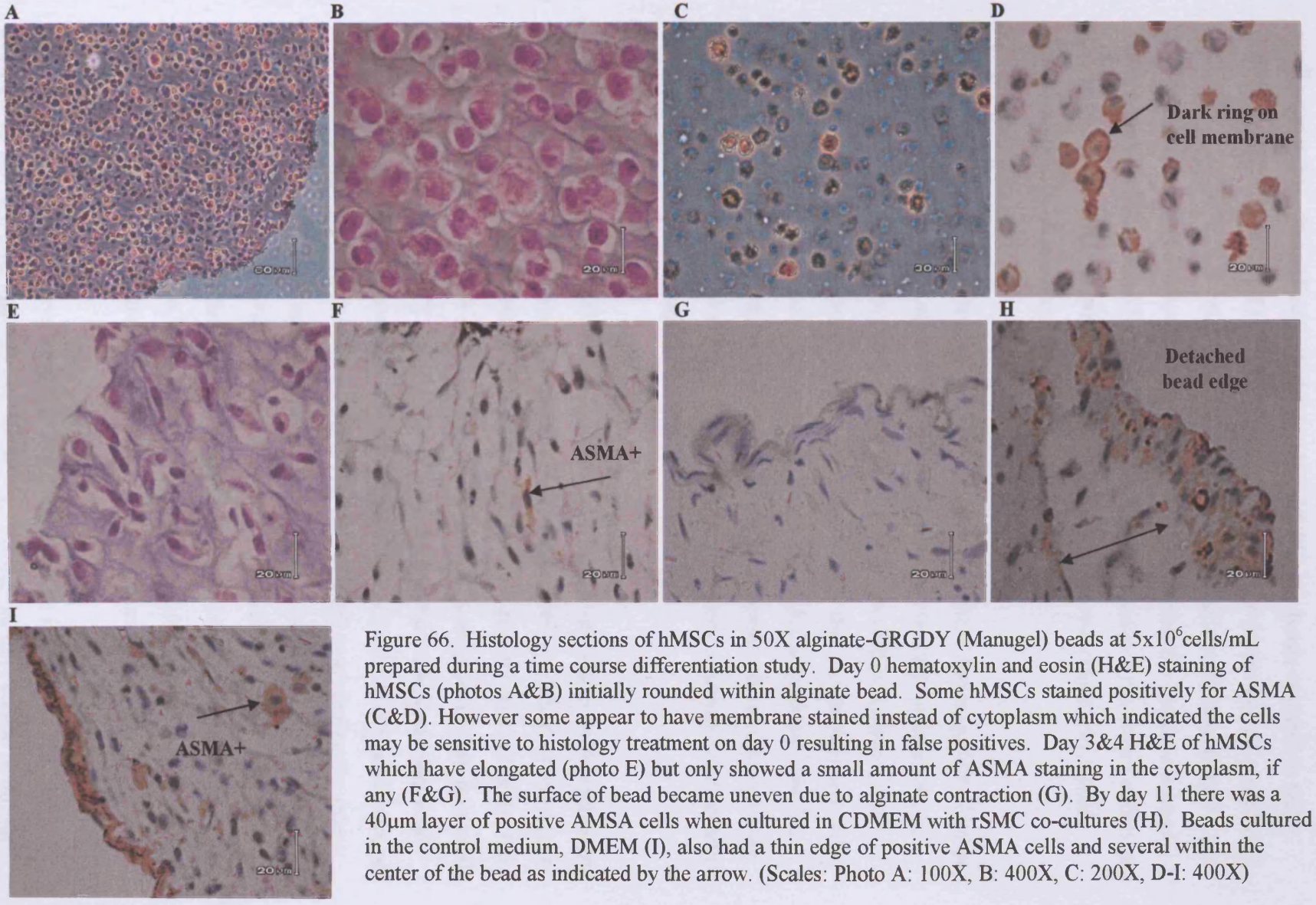

Figure 66. Histology sections of hMSCs in 50X alginate-GRGDY (Manugel) beads at $5x10^6$cells/mL prepared during a time course differentiation study. Day 0 hematoxylin and eosin (H&E) staining of hMSCs (photos A&B) initially rounded within alginate bead. Some hMSCs stained positively for ASMA (C&D). However some appear to have membrane stained instead of cytoplasm which indicated the cells may be sensitive to histology treatment on day 0 resulting in false positives. Day 3&4 H&E of hMSCs which have elongated (photo E) but only showed a small amount of ASMA staining in the cytoplasm, if any (F&G). The surface of bead became uneven due to alginate contraction (G). By day 11 there was a 40μm layer of positive AMSA cells when cultured in CDMEM with rSMC co-cultures (H). Beads cultured in the control medium, DMEM (I), also had a thin edge of positive ASMA cells and several within the center of the bead as indicated by the arrow. (Scales: Photo A: 100X, B: 400X, C: 200X, D-I: 400X)

Part of the bead edge was detached during microsectioning which indicated the sections may have been sliced too thinly. In addition, the beads cultured in the control medium, complete DMEM, also had some hMSCs which stained positively within the bead as well as on the edge (photo I). A comparison of these samples is provided in the Appendices, section 6.2.3, Figure 75 between the negative control slides (unstained) and the ASMA-stained slides. When possible the same bead cross section was compared directly to show the difference between these two media conditions on day 4 versus day 11.

These early differentiation studies used 50X alginate-GRGDY (Manugel DMB) that was filtered through Celite after treatment with activated charcoal as described in section 2.3.3, Figure 4 by the 'initial process'. Additional differentiation studies were conducted using alginate-GRGDY (Manugel DMB) that was autoclaved and was not treated with activated charcoal and filtered through Celite as described in section 2.3.3 by the 'intermediate process'. In order to increase the cell networking within the alginate bead, these studies used a higher cell concentration $2x10^7$cells/mL in 9X alginate-GRGDY beads.

Immunohistological preparations showed the cell density was higher at the edge (rim) of the beads. After 9 days in culture in CDMEM with rSMC co-cultures there was a 40-60μm rim of positive ASMA cells around the bead (Figure 67, photo A&B). On day 16, the extent of ASMA staining seemed to be significantly lower than previously observed on day 9 (photo C). On day 23 of culture, positive ASMA staining was again apparent (photo D); however, the hMSCs within the center of the bead were not networked completely (photo E), and gradually the bead fell apart during the micro sectioning by day 37 when only the rim of the bead survived histological preparation (photo F). A comparison of some of these slides is also provided in the Appendices, section 6.2.3, Figure 76. The negative control slides (unstained) and the ASMA-stained slides from the same bead cross section were compared directly to demonstrate the difference between time points on day 9 versus day 23.

The bead instability may have been due to decreased cross linking of the alginate hydrogel as calcium ions diffused out of the bead during the time course or during

storage in the formal saline. Therefore in future studies 10mM $CaCl_2$ should be added to the formal saline to help maintain bead integrity during storage. These beads were ca. 2-2.5mm in diameter since they were made manually. This bead size was much greater than desired; therefore a bead device that will produce beads of smaller diameter (400-600μm) is being fabricated for future work. The large bead diameter was likely to have caused diffusion limitations of nutrients and oxygen into the center of the bead. In addition, during cross linking it was also possible that the outer shell of the alginate bead was well formed and very tightly cross-linked; whereas the center of the bead was less strongly cross-linked due to a diffusion limitation or gradient during exposure to the $CaCl_2$ solution. Other researchers have observed a nonuniform distribution of biomass with a tendency toward growth at the surface (Leo, 1990; Constantinidis, 1999; Goosen, 1999).

The most likely cause for the bead instability would have been due to use of the autoclaved Manugel alginate during the 'intermediate process' (see Figure 4, section2.3.3). Autoclaving lowered the alginate viscosity to 5mPa·s, and thus the molecular weight and gel strength. In addition it was discovered that the autoclaved alginate contained activated thermophilic bacillus spores that may have contributed to the degeneration of the alginate within the center of the beads. The earlier differentiation studies by the 'initial process' used Manugel alginate that was not autoclaved, which was treated with activated charcoal and filtered through Celite. These steps, although not sterile processes, would have reduced the amount of bacillus spores and alginate impurities that may otherwise have resulted in degradation of the alginate or cell death during incubation. Further instability of the bead may have been caused by microbial contamination from the hMSC cultures. These contamination issues were discussed in detail in sections 3.1.2 and 3.4.3.

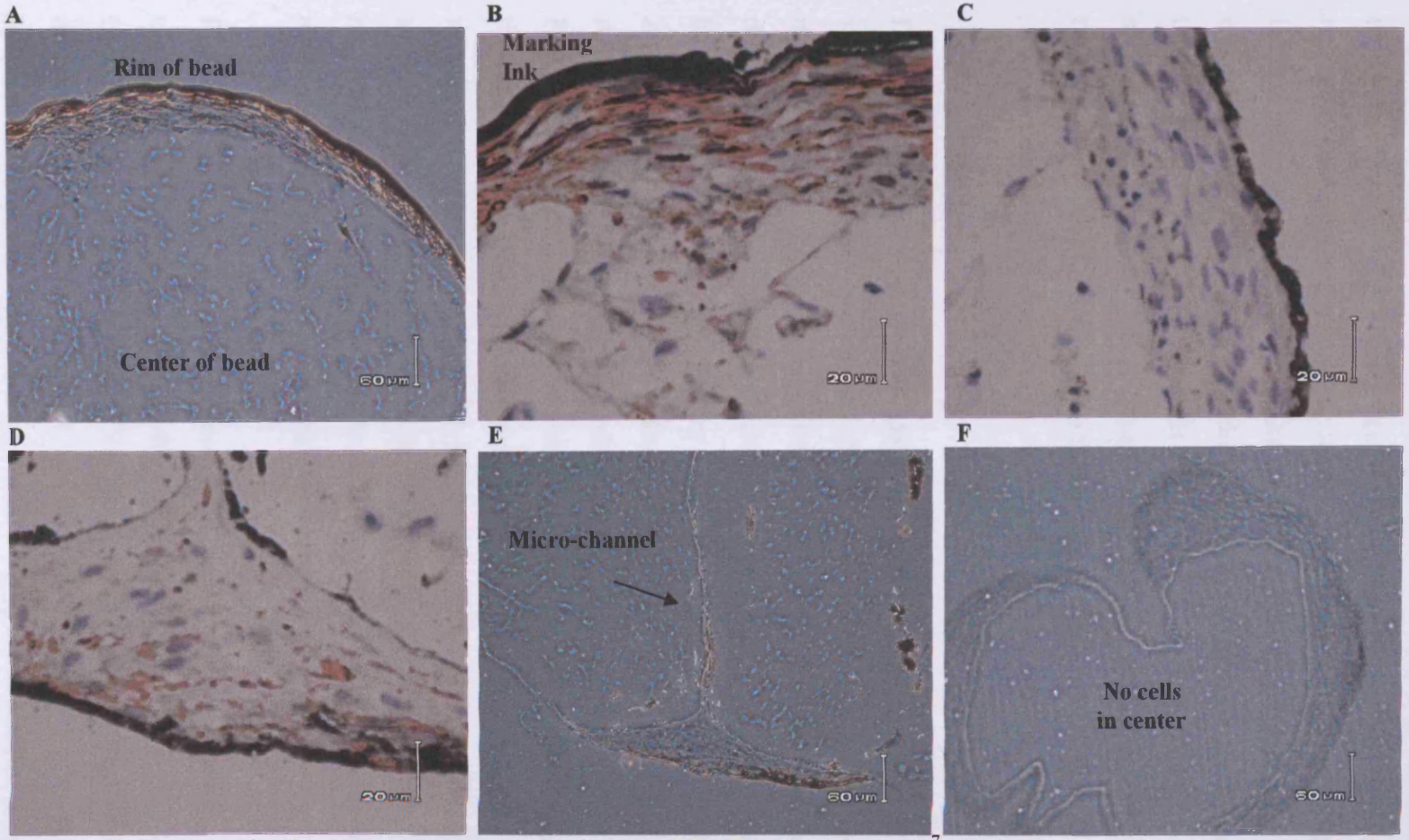

Figure 67. Immunohistology preparations of 9X alginate-GRGDY beads at $2x10^7$ cells/mL prepared using autoclaved Manugel DMB prepared by the 'intermediate process'. All beads were cultured in CDMEM with rSMC co-cultures. On day 9 there was a 40-60 µm rim of hMSCs that stained positively for ASMA (Photo A: 100X, B: 400X). On day 16 the rim of the bead seemed to have no positive ASMA staining (Photo C: 400X). On day 23 some positive ASMA staining (Photo D: 400X, E: 100X) was evident along rim of bead and through a center channel through the bead. However, the center of the bead was more detached from the rim and by day 37 microsections revealed just the rim of the bead and no cells in the center section (F: 100X).

As previously observed, the hMSC/alginate-GRGDY beads seemed to become more compact with increased length in culture. This was most likely due to the contraction of the cells/alginate within the rim of the bead. However, future work will need to be performed using smaller sized beads to determine whether 1) the rim of these tightly networked cells formed initially due to better cross linking/hydrogel formation at the rim rather than in the center of the bead, 2) the rim of cells caused diffusion limitations of oxygen and/or nutrients to the bead center, 3) the presence of microbes caused instability in the center of the bead, or 4) the alginate slowly diffused out of the rim of the bead leaving the cells tightly networked within the rim. Reagents specific for staining polysaccharides such as alginate include periodic acid-Schiff reagent, Toluidine blue and Alcian blue (Lee, 1997).

3.6.2.2. FACS analysis of beads

During differentiation studies, hMSC/alginate-GRGDY beads were dissociated into a single cell suspension by exposing the beads to 0.1M trisodium citrate and 0.25% trypsin/0.02% EDTA and gently micropipetting until the bead was completely dispersed. After the cells were centrifuged and washed with DPBS, the hMSCs were labeled with monoclonal antibodies with a fluorescent tag as described in section 2.5.9. Briefly the primary monoclonal antibodies used were against CD34 and ASMA which were conjugated to secondary mouse immunoglobulins/RPE Goat F(ab), as well as, SH2 and SH4 monoclonals which were conjugated to FITC. After the cells were exposed to the monoclonal antibodies labeled with the fluorescent marker, the cells were washed with DPBS to remove unbound antibodies. Then the samples were run through a FACS machine which produced graphical outputs showing the distribution of the cells and those labeled with the fluorescent tag. The actual outputs are provided in the Appendices, section 6.2.4.

Figure 68 shows the summary of the FACS results which were used to monitor the change in hMSC surface markers after being immobilized within the 50X alginate-GRGDY (Manugel) beads at $5x10^6$cells/mL and cultured in either DMEM (control medium) or in CDMEM with rSMC co-cultures for 6 days. Each cell was designated by a dot on the graph. The gated region of the graph was selected using an 'empty' sample (one prepared without any antibodies) from the distribution of the cells on the

graph of side scatter (SSC-H) vs. forward scatter (FSC-H) as described in methods in section 2.5.9. Cells within the gated region on the graph of RPE tag (FL2-H) versus FITC tag (FL1-H) were negative for the surface marker. Cells that expressed the surface marker, and hence were positive for the antibody with fluorescent tag, fell outside the gated region (in R2). Both bead culture conditions were negative for CD34 surface marker as shown by the cell distribution falling within the gated region (Figure 65, graph A&B). This result was expected since *ex vivo* cultures of hMSCs are typically CD34-; although some groups have identified precursors as CD34+ (Deans and Moseley, 2000). HMSCs are positive for SH2 and SH4 surface markers; whereas marrow-derived hemopoietic cells are negative for SH2 and SH4 surface markers (Haynesworth, 1992). In this differentiation study, the control bead cultures of hMSCs in DMEM retained their expression of SH2 and SH4, as indicated by the dots lying outside of the gated region (Figure 65, graph C&E). In sharp contrast, the bead cultures in CDMEM with rSMC co-cultures lost most of their expression for SH2 (Figure 65, graph D) and all of their expression for SH4 (Figure 65, graph F). Although ASMA is a cytoplasmic protein rather than a surface marker, this monoclonal antibody was also tested and the hMSC beads cultured in CDMEM with rSMC co-cultures had a slightly higher level of positive ASMA expression (Figure 65, graph H) than the cells culture in the DMEM (Figure 65, graph G).

The complete FACS reports are provided in the Appendices, section 6.2.4. They show the histograms of the cell distribution and the percentage of cells within and outside the gated regions. The loss of expression of SH2 and SH4 surface markers in the hMSC/alginate beads cultured in CDMEM with rSMC co-cultures demonstrated that these hMSCs were differentiating by day 6 in culture.

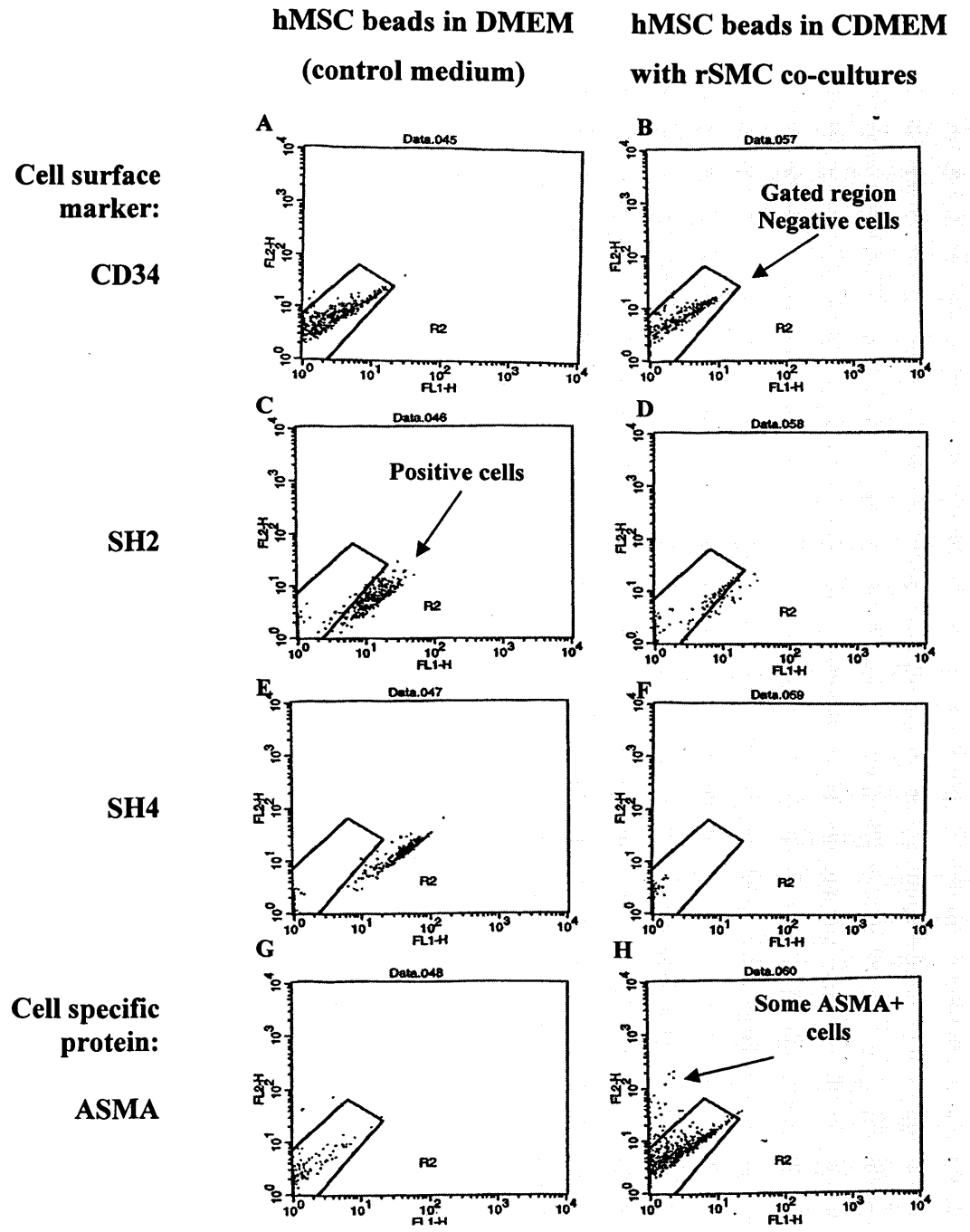

Figure 68. FACS results for cell surface markers CD34, SH2 and SH4 and for cytoplasmic protein ASMA on day 6 of culture. Cells that were negative (non-fluorescent) for the surface marker were contained within the gated region. First column: Control hMSC/50X alginate-GRGDY (Manugel) beads cultured for 6 days in DMEM medium remained CD34- (A), SH2+ (C), SH4+ (E), and ASMA- (G). Second column: hMSC/50X alginate-GRGDY (Manugel) beads cultured for 6 days in CDMEM with rSMC co-cultures were CD34- (B), SH2- (D), SH4- (F) and slightly more ASMA+ (H). Axes represent RPE tag (FL2-H) versus FITC tag (FL1-H).

The FACS results coupled with the changes observed in cell morphology by day 7 of culture and the immunohistology data that showed positive ASMA staining by day 9-11 in culture provided preliminary evidence that the hMSC differentiation may be along the SMC pathway. In addition these results show, the biochemical components and/or intermediate products within the CDMEM/rSMC co-cultures provided at least some of the factors necessary to differentiate the hMSCs as compared to the control DMEM medium.

3.6.3. Summary

Differentiation studies were conducted on the hMSC/alginate-GRGDY beads using conditioned medium with rSMC co-cultures. Since long term cultures of hMSCs have been shown to differentiate along the vascular SMC pathway (Charbord, 2000), a time course media study was first conducted growing hMSCs in microwell (2-D) plates using three media conditions - MSCCM, DMEM and CDMEM - to determine the level of ASMA in hMSCs grown to confluency (high density) with these media. Cytology preparations were made; hematoxylin and ASMA were used to stain the cells. The hMSCs cultured in MSCCM showed no specific ASMA staining. The samples prepared from hMSCs cultured in DMEM and CDMEM exhibited a higher level of non-specific staining after 6 days in culture, and especially after 9 days (Figure 64). The staining was not defined to the cytoplasm of the cells; therefore, the staining was determined to be an artefact of the sample preparation.

When hMSCs were immobilized into 50X alginate-GRGDY beads and cultured in CDMEM with rSMC co-cultures, there appeared to be a change in the cell morphology within the beads. Initial H&E smears of the alginate beads, showed that the hMSCs within the bead on day 1 contained cells with narrow, pointy nuclei (Figure 65.E); whereas the day 7 beads contained a greater number of hMSCs with larger, oval-shaped nuclei (Figure 65.F) which was indicative of terminally differentiated cells. After satisfactory sample preparation for immunohistology was achieved on the hMSC/50X alginate-GRGDY beads, cross sections were prepared and stained with hematoxylin and the cell-specific protein, ASMA. Day 0 results of hMSCs immobilized in the beads showed that initially some cells were positive for ASMA (Figure 66.D); however, these results may have been false positives due to the 'harsh' conditions used to reverse cross linking of the cell antigens in the sample

during histological preparation. Day 3-4 samples expressed little, if any, ASMA (Figure 66.F). As the culture time increased the perimeter of the beads was found to have nicely networked cell layers (ca. 20-60 μm thick) that were positive for ASMA by ca. day 9-11 in culture (Figures 66.H and 67.B). The center of the beads seemed to have significantly lower cell densities and lower levels of staining or no staining. 9X alginate-GRGDY beads prepared from autoclaved Manugel by the 'intermediate process' appeared to fall apart at later time points in culture (e.g. day 23-37 in Figure 67.F). This may have been due to decreased stability of the alginate in the large diameter beads during culture due to the lower alginate molecular weight, diffusion of calcium ions out of the hydrogel, the presence of microbes, or poor hydrogel formation in the center of the bead at the cross linking step.

Differentiation studies combined with FACS analysis were performed and showed that within 6 days of culture hMSCs/50X alginate-GRGDY beads cultured in CDMEM with rSMC co-cultures lost expression of the hMSC surface markers SH2 and SH4; whereas hMSCs cultured in DMEM remained positive for SH2 and SH4 (Figure 68). Concurrent immunohistological preparations of these cells showed low levels of ASMA staining on day 4 and significantly increased levels of ASMA for both cultures grown in both DMEM and CDMEM with rSMC co-cultures on day 11 (Figure 66, photos F-I). Other cell-specific proteins for SMCs such as calponin, heavy chain myosin and h-caldesmon were not tested in these early studies, but will be incorporated in future studies.

Finally cell culture inserts with a 0.4μm membrane were used to physically separate the beads from the rSMCs co-cultures. In addition the supernatant collected from the CDMEM was centrifuged at 200g to ensure rSMCs and cell debris were not introduced into the hMSC cultures. Therefore differentiation of the hMSCs into SMCs by cell fusion would not have been possible. Although this possibility was not proven by analytical techniques such as PCR of known rSMC DNA sequences (not found in hMSCs); these analyses can be performed in future studies.

4. Discussion and conclusions

4.1. Alginate as a tissue engineering matrix

Alginate is a natural, biodegradable polymer that sets rapidly within a solution of divalent ions. Alginate hydrogels have been used successfully to entrap secretory (e.g. pancreatic islet) cells (Mullen, 2000) and transformed producer-cell lines (Constantinidis, 1999; Joki, 2001; Tobias, 2001; Zheng, 2003) and have been used in some tissue engineering applications for soft tissue (Halberstadt, 2002), myocardium (Leor, 2000; Zimmerman, 2003), cartilage (Atala, 1994; Hauselmann, 1994; Wong, M., 2001; Lee, 2003; Kamil, 2004) and bone (Alsberg, 2001; Simmons, 2004). Human clinical studies have shown alginate to be well-tolerated (Hasse, 1997; Laham, 1999; Caldamone and Diamond, 2001) and it has been used extensively in bandage dressings in surgery and wound management (Thomas, 2000). The 3-D configuration of a hydrogel provides structural support, preserves phenotypic expression and function of the cells that may not be achieved in 2-D cultures (Jen, 1996). For these aforementioned reasons, sodium alginate was utilized as the matrix for conducting cell studies toward investigation of a tissue engineered blood vessel (TEBV). University College London has developed and patented a novel method of extruding alginate into a hydrogel tube using an automated device (Mason and Town, 2002).

In this research immortalized rat smooth muscle cells (rSMCs) were initially used to study cell-alginate interactions. Immortalized rSMC were used due to the limited proliferation of adult SMCs *in vitro* (McKee, 2003). For all studies conducted, despite high initial cell viability, the rSMCs rapidly died after immobilization within the alginate hydrogels. In contrast, rSMCs proliferated within collagen matrices and within collagen/alginate matrices in which cross linking solutions were not used. The rSMCs' remained spherical within the alginate (since no adhesion sites were present); whereas the rSMCs elongated within the collagen. In collagen/alginate matrices in which cross linking solutions were used, the rSMCs remained spherical. This change in morphology was thought to be one of the key indications of viability and proliferation, and demonstrated the need to incorporate cell adhesion sites, such as RGD, onto the alginate using carbodiimide chemistry.

The pentapeptide GRGDY (Gly-Arg-Gly-Asp-Tyr) was chosen to incorporate onto the alginate polymer matrix based upon success reported by Rowley using myocytes (Rowley, 1999). This research found that the concentrations of reagents (i.e. EDC, sulfo-NHS and peptide) used in the carbodiimide chemistry were critical in order to obtain sufficient cell association while simultaneously maintaining the hydrogel strength because the peptide was incorporated into the same moiety as the calcium binding site during cross linking. Too much peptide incorporated onto the alginate polymer resulted in rapid dissociation of the hydrogel. The alginate source and preparation, including method of sterilization, were also critical to the peptide derivatization process as summarized in section 3.2.9. Using cultured rSMCs and the 'initial process' of alginate-GRGDY derivatization which included 2 days of dialysis followed by adsorption with activated charcoal and filtration through Celite, it was found that all alginates (e.g. Fluka, Manugel, and Pronova MVG) worked best with 50X reactants. RSMCs were shown to attach and elongate on the surface of 50X alginate-GRGDY sheets (Figure 26A and 27); whereas no association occurred for the lower concentrations tested (Figure 26B). These results confirmed the results originally reported by Rowley (1999, 2002) using myocytes.

When entrapped within 50X alginate-GRGDY hydrogels, the rSMCs were observed, for the most-part, to remain spherical in morphology. Only in a few instances the rSMCs elongated within the 50X alginate-GRGDY hydrogel (Figure 28) and this appeared to occur only when the hydrogel was rapidly dissociating (due to too many peptides incorporated into the polymer) as summarized in section 3.3.6. RSMCs were shown to attach and elongate within tubes (Figure 29). However, the possibility that the rSMCs associated with the glass tube surface cannot be discounted. This conclusion was reached because elongation was observed only a few times for rSMCs immobilized within alginate-GRGDY beads, and even when repeated at later stages of the project when rSMCs were immobilized in 27X alginate-GRGDY beads using the final 'sterile process'.

The expectation would have been that the rSMCs would have elongated along the pores of the alginate hydrogel containing the GRGDY peptides. It is possible that the pore size of the alginate-GRGDY matrix may have been too small or restrictive. Eiselt (2000) suggests that alginate used in the physical form of a hydrogel contains

small pore size (nm size scale) that does not allow cell movement. Zmora (2002) created macroporous scaffolds from 1% (high G) alginate scaffolds by freeze-drying methods and found both interconnecting round pores 110+/-30μm in diameter and non-connecting elongated pores 210+/-80μm depending upon the freezing regime. They also found that the seeded rat hepatocytes' morphology was either elongated or spherical based upon the two pore microstructures (Zmora, 2002). Chandy (2003) also measured the pore size of an alginate/elastin/PEG matrix and found them to be 35-75μm. These different pore microstructures were created by freezing the alginate matrix and examining the structure using a scanning electron microscope (SEM). Freezing is likely to alter the pore size; however this issue warrants future work to evaluate the pore size and microstructure.

The stiffness of the alginate hydrogel may have been another factor. Recently Genes (2004) found that chondrocytes would adhere at a level 10-20 times higher on alginate-G_4RGDY than on unmodified alginate. The alginate stiffness regulated the morphology of the chondrocytes – rounded on weak surfaces with little actin expression and flattened on stiff surfaces with actin stress fibers (Genes, 2004). Therefore it was possible that these alginate-GRGDY hydrogels were not stiff enough to support the rSMCs' cytoskeleton because they are composed largely of actin stress fibers. Activation of the cell cytoskeleton via cell adhesion is essential for maintaining proper cell function, proliferation, and differentiation (Saltzman, 2000). The cells would die without activation of the SMCs' cytoskeleton as was observed in these studies. This hypothesis is in agreement with other reports for chondrocyte culture systems which showed cells maintained in a rounded morphology prevented the formation of stress fibers that were believed to mediate dedifferentiation when chondrocytes were grown on adherent surfaces (Takigawa, 1984). In contrast, primary rSMCs have been shown to proliferate within photopolymerized acryloyl-PEG-KQAGDV (Lys, Gln, Ala, Gly, Asp, Val) hydrogels (Mann, 2001). The KQAGDV peptide was identified as the most adhesive peptide for vascular smooth muscle cells (Mann and West, 2001). However, the differences between results with this peptide/polymer system and the current GRGDY/alginate system could not be addressed within the context of this research.

4.2. Adult hMSCs for tissue engineering

A collaboration to investigate cell-alginate interactions using adult human mesenchymal stem cells (hMSCs) was established with the UCL Wolfson Institute of Biomedical Research which permitted more relevant studies using material (i.e. bone marrow cells or whole blood) that was more appropriate for adult autologous cell therapy. Not unexpectedly, the hMSCs showed significantly different growth kinetics compared to the immortalized rSMCs in tissue flask cultures. The growth rate of the hMSCs slowed considerably by passage 12; therefore all experimentation needed to be conducted prior to that level.

In contrast to the rSMCs, the entrapped hMSCs within 50X alginate-GRGDY hydrogels showed a dramatic change in morphology from spherical immediately after immobilization to more elongated within 1 day. These bead constructs were assessed using phase contrast microscopy and standard histological preparations. During this hMSC work the 'initial process' of alginate-GRGDY derivatization (Figure 4) required the highest concentration of reactants (e.g. 50X); whereas if the alginate was autoclaved which reduced its viscosity in the 'intermediate method', 27-35X reactants were sufficient. After changing to a new lot of EDC, 9X was the best concentration. Finally for the purest alginate (Pronova SLG100) used in the 'sterile process', 9X-12X reactants were sufficient for biological activity and maintenance of hydrogel integrity. An initial seeding density of $2x10^7$cells/mL showed that the hMSCs formed dense network of cells within the hydrogel. All of these results are summarized in section 3.4.5. The hMSCs may have been more amenable to elongation within the alginate-GRGDY hydrogel due to their more primitive state (i.e. adult stem cell) or differences in cytoskeleton (i.e. less actin is expressed in undifferentiated stem cells) (Wang, D., 2004).

A modified MTT (3-(4,5-dimethylthiazol-2-yl)-2,5-diphenyltetrazolium bromide) assay was used to examine cell metabolism and proliferation by first exposing the hMSC/alginate beads to MTT and then dissociating the cell/alginate constructs using trisodium citrate and trypsin/EDTA. In addition a frozen storage step was incorporated into the assay so that a time course study could be meaningfully evaluated. Using the MTT assay it was found that hMSCs did not proliferate within

either the unmodified alginate or alginate-GRGDY matrix within the 2 weeks examined. These results were further substantiated by concurrent cell density measurements using a hemacytometer. Cell viability >80% was maintained in the beads during the study. In addition, the glucose consumption rate (GCR) was measured and found to be comparable to hMSCs grown in two-dimensional culture vessels. The MTT assay was found to be a sensitive means for a time course evaluation of the metabolic activity of hMSCs entrapped in the alginate hydrogels. Overall there was ca. 33% decrease in metabolism during the 2 weeks examined as summarized in section 3.5.7.

It was anticipated that conversion of hMSCs to smooth muscle cells could be enhanced in a three-dimensional gel as was found with differentiation of MSCs to chondrocytes (Ma, 2003; Steinert, 2003). Chondrocytes have been shown to proliferate and maintain a stable differentiated phenotype when cultured in alginate as compared to 2-D cultures (Hauselmann, 1994; Lee, 2003). In the studies reported here, alginate-GRGDY hydrogel beads were examined as a surrogate for tubes of the same material which were placed into conditioned medium from rSMC co-cultures (CDMEM). The cultures were physically segregated using a plastic insert with a 0.4μm membrane. Three different analytical techniques were used to determine if the hMSCs were differentiating as was summarized in section 3.6.3. First, cytology slides were prepared from the hMSCs within the alginate-GRGDY beads in CDMEM with rSMC co-cultures and were identified as initially having cells exhibiting a primitive morphology with narrow, pointy nuclei. After further incubation of the hMSCs within the alginate-GRGDY beads in CDMEM with rSMC co-cultures a number of cells contained larger, oval-shaped nuclei. This morphology change was an indication of terminal differentiation (Bruder, 1997; Phinney, 1999).

Next, fluorescence activated cell sorting (FACS) was used to monitor the cell surface markers. In these studies, the hMSCs were initially confirmed to be CD34-, SH2+ and SH4+. The SH2 and SH4 antibodies recognize epitopes present on the surface of hMSCs and not on hematopoietic cells, and the surface antigens disappeared upon differentiation (Haynesworth, 1992). Furthermore, the SH2 antigen was identified to be endoglin, the transforming growth factor-β receptor III, which mediates TGF-β

signaling during differentiation of MSCs into chondrocytes (Barry, 1999; Pittenger, 1999). In the studies performed here, hMSCs/alginate-GRGDY beads cultured in CDMEM with rSMC co-cultures lost expression of the hMSC surface markers SH2 and SH4; whereas control cultures of hMSCs/alginate-GRGDY beads cultured in DMEM retained expression. Therefore the loss of the SH2 and SH4 surface markers was an indication that the hMSCs exposed to CDMEM with rSMC co-cultures had differentiated.

Finally, immunohistochemistry was used to stain the hMSCs/alginate-GRGDY beads for presence of the smooth muscle cell-specific cytoplasmic protein, ASMA, using avidin-biotin complexed to a monoclonal antibody specific for ASMA. Microsections of the beads showed a dense cell layer was formed around the perimeter of the alginate-GRGDY beads. These cells stained positively for ASMA after the beads had been cultured in CDMEM with rSMC co-cultures. Although these three results do not unequivocaly demonstrate differentiation of the hMSCs into smooth muscle cells; they do show the potential for differentiation studies to be pursued using this cell/polymer system. Others have shown the potential for MSCs to differentiate into chondrocytes (Ma, 2003; Steinert, 2003) osteoblasts (Wang, L., 2003) and cardiomyocytes (Xu, 2004) using unmodified alginate. Additional analyses would need to be performed to determine if the hMSCs examined in this study differentiated into functional smooth muscle cells. These would include determining if the cells were sensitive to calcium channel antagonists and positive for additional cell-specific proteins such as caldesmon, calponin and heavy chain myosin during immunohistological preparations.

Three factors may have caused differentiation of the hMSCs within the alginate-GRGDY beads cultured in CDMEM with rSMC co-cultures.

1. The presence of intermediate products of cell metabolism or growth factors from conditioned medium and/or microfiltrate from rSMC cultures (those molecules that diffused through the 0.4μm membrane) triggered differentiation.

Some growth factors have been identified, but the results have been conflicting until recently. For example, Simper demonstrated adult stem cells derived from human whole blood differentiated into SMCs and endothelial cells (ECs) using specific

growth factors. Endothelial outgrowth cells were selected by growing human mononuclear cells (MNCs) in endothelial growth medium (EGM-2). Smooth muscle outgrowth cells were selected by growing the MNCs in EGM-2 with 50ng/mL platelet-derived growth factor-BB (PDGF-BB) (Simper, 2002). On the other hand, Kinner reported that 1ng/mL of transforming growth factor-β1 (TGF-β1) significantly increased ASMA expression and the contractility of MSCs; whereas, 10ng/mL of PDGF-BB decreased expression and contraction (Kinner, 2002). More recently, Seruya (2004) and Wang, D. (2004) have successfully demonstrated MSC differentiation into SMC using TGF-β1.

2. The second factor potentially causing differentiation relates to the density of hMSCs seeded within the 3-D alginate-GRGDY hydrogel bead.

Pittenger showed a high cell density (i.e. pelleted micromass) was necessary for chondrogenic differentiation (Pittenger, 1999). Reyes reported that differentiation of MSCs to all mesodermal lineages required that cells be seeded at high density (greater than $2x10^4 cell/cm^2$). Whether the high cell density caused the cells to exit from cell cycle or whether cell-cell contact itself or factors secreted following cell-cell contact were required was not known (Reyes, 2001).

3. The third factor may have been the presence of GRGDY peptide in the alginate hydrogel.

Cultured SMCs produce ECM components including collagen, elastin, laminin, fibronectin, and glycosaminoglycans (Owens, 1995). RGD is the cell adhesion peptide for fibronectin. Attachment of MSCs to this peptide may signal the cells to differentiate. Several researchers have determined that the default differentiation pathway for hMSCs grown *in vitro* was toward vascular SMCs if they received no other definitive biological factors or cues to an alternative differentiation pathway – e.g. to adipocytes, chondrocytes or osteoblasts (Galmiche, 1993; Remy-Martin, 1999; Charbord, 2000). There have been several recent reports of in-vitro differentiation of MSCs on 3-D matrices as becoming "smooth muscle cell-like" through analyses of the proteins expressed during culture on 3-D matrices. MSCs grown on polyglycolic-acid (PGA) mesh coated with poly-4-hydroxybutyrate (P4HB) using non-specialized growth medium demonstrated myofibroblast-like characteristics by positive staining

for ASMA and vimentin. Protein analysis showed production of collagen type I and III. No staining was noted for desmin (muscle cell marker), collagen II (osteoblast marker), collagen IV, and elastin (Kadner, 2002). In another study, early passage ovine MSCs grown in non-specialized growth medium stained positively for SH2, ASMA, and desmin, and a subset for calponin. These cells were also grown on a PGA-P4HB matrix and were shown to have biomechanical properties similar to native heart valve leaflets (Perry, 2003). The specific markers of differentiated smooth muscle cells include ASMA, smooth muscle myosin heavy chain, myosin light chains, calponin, SM-22a, h-caldesmon, vinculin, metavinculin, tropomyosin and intermediate filament proteins (desmin and vimentin) which are specific for vascular smooth muscle (Owens, 1995).

4.3. HMSCs/alginate-GRGDY hydrogel as a TEBV

In order to grow *ex vivo* a sufficient number of hMSCs to seed autologous tissue engineered blood vessels (TEBV) with $2x10^7$cells/mL, 10.6mL of cell/alginate solution would be required to fabricate 5 tubes (4mm inner diameter x 20cm length x 0.4mm wall thickness). This would require over $2x10^8$ cells, not including cells required for release testing. Growth rate data were collected from fresh and frozen cell bank stocks derived from 5 different donors as measured by the population doubling time (PD/day). A minimum of 5 passages must be performed to achieve these numbers. However, it was noted that there was a substantial decrease in cell growth rate between passages 2 and 12 (section 6, Table 18). This decrease was also reported by Bruder and Phinney; however, in their case the decrease in MSC growth rate was not associated with a loss in differentiation potential when extended subcultivation was used to differentiate cells through an osteogenic lineage (Bruder, 1997; Phinney, 1999). Similar MSC growth rates have also been reported by Kinner (Kinner, 2002).

There is growing *in vivo* evidence that bone marrow cells (BMCs) will differentiate down the SMC pathway and can be used successfully as a cell source for a TEBV. *In vivo* canine studies have shown that bone marrow cells contributed to the construction of tissue engineered vascular autographs (Matsumura, 2003a); and there is now

successful human clinical experience with these grafts in over 22 patients has been reported (Matsumura, 2003b).

Although alginate has not been reported as a potential matrix for TEBV; it has been used successfully for other structural tissues and has been found to be safe in humans. Part of this research focused on the formation of tubular constructs. Both rSMCs and hMSCs were shown to elongate inside alginate-GRGDY hydrogel tubes (Figures 29 and 41). Interactions of the cells with the glass wall could not be discounted; although tubes made of cells with unmodified alginate did not produce any cell elongation. This interaction should be examined and discounted in future studies. All evidence from this research indicated no proliferation of the hMSCs within the unmodified alginate and alginate-GRGDY hydrogels. These results are further substantiated by results from Ma (2003) and Dar (2002). If no cell proliferation occurs in the matrix, then the constructs need to be initially seeded with the final number of cells to achieve 100% confluency. In fact, proliferation may be undesirable in a TEBV because proliferation of SMCs is associated with the pathology of cardiovascular disease (Ross, 1986; Schwartz, 1986).

The strength of the cell/alginate constructs was not addressed in this research. The evaluation of the strength of a TEBV derived from hMSCs/alginate-GRGDY constructs will be critical to determine if this approach is feasible. L'Heureux (1998) showed that fully confluent, overgrown sheets of cells when rolled together and further matured were strong enough (e.g. had burst strength over 2000mmHg) provided that the cells were producing extracellular matrix (ECM). If the alginate-GRGDY hydrogel tubes are seeded at very high density $>2x10^7$cells/mL, then the construct would become densely networked within one day as was observed in beads. The strength of the MSCs can be increased by adding ascorbate to increase ECM (e.g. collagen) deposition or by using mechanical stimulation or pulsatile flow (L'Heureux, 1998; Niklason, 1999; L'Heureux 2001; Thompson, 2002; Solan, 2003). Histological preparations of the large diameter (>2mm) hydrogel beads showed more cells located on or near the outer surface of the alginate construct which has been reported by others using alginate beads (Leo, 1990; Constantinidis, 1999; Goosen, 1999; Stabler, 2002) and in media equivalents for skin (Girton, 2000; Michel, 1993) possibly due to air/liquid interface. This inhomogeneity in the large diameter beads may have been

due to an oxygen or nutrient gradient; and therefore, avoidable using smaller diameter beads and thin walled tubes. Cell to cell contact must be achieved in these constructs in order to obtain the strength needed for a TEBV.

Growth factors could be incorporated into the cell/alginate hydrogel to stimulate growth or differentiation. Others have shown success releasing growth hormones (such as bFGF, VEGF, PDGF, hGH) from PLGA microspheres within alginate scaffolds (Perets, 2003), without alginate (Johnson, 1996) or a combination (Richardson, 2001). The alginate polysaccharide backbone is extremely versatile. Different peptides can be used to study attachment, proliferation and/or differentiation. Degradable peptide sequences could be incorporated onto the alginate backbone such as GGLGPAGGK (collagenase-sensitive) or AAAAAAAAAK (elastase-sensitive) as was shown by Mann using photopolymerized PEG hydrogels (Mann, 2001). It is possible that the lack of cell proliferation in the alginate and alginate-GRGDY beads in this research was due to lack of degradation of the alginate polymer. Degradation of the alginate polymer can be manipulated by altering the molecular weight by gamma irradiation (Alsberg, 2003; Kong, 2003). A lower molecular weight (<48kDa) is also desirable to clear the kidneys (Al-Shamkhani and Duncan, 1995).

Finally several challenges were overcome using this hMSC/alginate system as a tissue engineered construct during this research. Thermophilic bacillus spores were identified in the commercial alginate suppliers which became activated during autoclaving. Reliable and consistent preparation of sterile alginate was not a trivial issue; therefore a sterile supplier (NovaMatrix) was obtained to maintain the progress of this research. As a result, derivatized alginate-GRGDY material was produced by consistent and sterile methods. The purification of alginate remains a topic of much investigation (Klock, 1994; Zimmermann, 2000 and 2001; Orive, 2002).

In addition, a dramatic discoloration of the hMSC/alginate-GRGDY beads was observed and determined to be caused by calcification within the hydrogel network. The calcification was due to the high concentration of calcium ions within the cross linked alginate due to its high guluronic content and the presence of divalent ion chelators. The possible sources of these chelators were identified as high

concentration of phosphate in the MSCCM growth medium, elevated levels of lactate produced locally by the high seeding density of the hMSCs within the alginate, and the presence of microbial contaminants within the system. Differentiation studies were usually not affected by calcification due to the switch to conditioned DMEM during these studies.

4.4. Conclusions

This research indicated that adult hMSCs can be encapsulated in alginate beads with retained viability and that the GRGDY peptide derivative encouraged attachment and elongation to form a dense network of cells which is required for a tissue substitute. Because the availability of autologous human cells is severely limited, beads were examined as a proxy for tubular constructs. Despite providing cell adhesion sites using a GRGDY peptide motif, the hMSCs did not proliferate within the alginate hydrogel. The MTT assay can be used to evaluate the metabolic activity of the cells; and the results using the MTT assay were consistent with measurements by hemacytometer and GCR. A frozen storage stage was incorporated to allow consistent examination of a time course. The lack of cell proliferation in the alginate beads may have been associated with the small pore size, degree of stiffness or lack of degradation after cell elongation and networking; however similar reports of no cell proliferation in unmodified alginate have been made by Dar (2002) using entrapped neonatal cardiac cells. In addition Ma (2003) showed MSC growth cycle arrest within 1 day of encapsulation of MSCs in alginate.

The research described has identified a number of critical issues in the expansion of adult stem cells and their association with alginate scaffold for tissue engineering. The issue of sterility with alginate emphasized the challenge this presents with natural polymers. However, the success in obtaining encapsulated cells which developed and associated once an RGD peptide was incorporated into the polymer indicates that the alginate scaffold has real potential. The action of the microfiltrate from the conditioned rSMC co-cultures probably has not caused more than partial differentiation of the hMSCs but indicates the potential of an equivalent human smooth muscle immortalized line and therefore necessitates further characterization of the active agents. Further progress rests on being able to measure the degree of cell proliferation and metabolism over extended times so that the ability to use the MTT

assay with frozen material, which was established, is valuable. The issue of whether sufficient cell doublings during *in vitro* expansion of the adult hMSCs can be achieved remains as do many others but some of the key issues that will underpin future studies at UCL and elsewhere have been defined.

4.5. Recommendations for future work

4.5.1. Cell-alginate hydrogel construction

Cell/alginate beads of 2-2.5mm diameter were produced manually as described in section 2.4.3. This size was well above the 80-100μm limit of oxygen diffusion in human tissue (Schumacker and Samsel, 1989; Carmeliet and Jain, 2000). The maximum cell density used in these studies was ca. $2x10^7$cells/mL alginate. This density was limited by the minimum volume required for homogeneous resuspension of the pelleted cells and the concentration of the reconstituted alginate-GRGDY (see sections 2.4.1 and 2.4.4). Other reports have indicated that $5x10^7$cells/mL matrix was required to produce homogeneous cartilage (Xia, 2001). Therefore it would be desirable to make beads of higher cell concentration with smaller diameter size (ca. 400-600μm). Producing a smaller diameter bead would also be essential in order to achieve an effective comparison of similar dimensions of tube wall thickness. Alginate bead devices were commercially available (Innotec AG, Dottikon, Switzerland); however they operated at very large input volumes (ca. 100–1000mL). For this project, microliter to milliliter volumes of cells/alginate (ca. 100-1000μL) needed to be processed due to the limited supplies and expense of mammalian stem cell culture and reagents used to produce derivatized alginate. Therefore an in-house fabricated bead device capable of operating with microliter quantities for producing smaller diameter beads would be important.

Future studies should be performed to verify and adjust the pH and osmolality of the reconstituted alginate-GRGDY so that it is physiological to the cells. Initial pH measurements were inconclusive due to the large volume of alginate-GRGDY material needed to test with the current electrode system. A sterilizable, micron-sized pH probe would be ideal. Alternatively, a buffer exchange step could be incorporated during the last stage of dialysis with water that contained enough NaOH for reconstitution after lyophilization. However, this base addition during the dialysis

step would still need to compensate for the final concentration of the alginate-GRGDY product after lyophilization and reconstitution due to the influx of water into the cassette during dialysis. The dependence of the carbodiimide reaction upon temperature and mixing conditions should also be further examined. The temperature used in this research was not well controlled and ranged between 20-26°C for the reaction chemistry. In addition, the dialysis temperature varied from cold (6-10°C) during the 'initial process' to very warm (26-31°C) in the laminar flow hood during the 'sterile process'.

Several items were not well understood regarding the derivatization of alginate-GRGDY. The amount of uronic acid units in the alginate was estimated since this information was not provided by the manufacturers. Therefore the amount of reactants (eg. sulfo-NHS, EDC and peptide) added to the alginate was varied between 1X and 50X, where 1X was 1mg of alginate containing 38μg of sulfo-NHS, 67μg of EDC and 1μg of peptide; and 50X was fifty times the reactants per 1mg of alginate. More analytical chemistry needs to be completed such as determining the amount (number) of uronic acid units in the alginate and determining the amount of pentapeptide incorporated into the alginate. Then the efficiency or possibly rate at which the peptide is incorporated into the alginate can be determined from the concentration of reactants used. Mooney's lab used a radioactive label to measure the amount of peptide incorporated into the alginate (Rowley, 1999), which was not feasible for this research. Levels of peptide incorporated into the alginate may be able to be determined from the tyrosine residue (due to its aromatic ring) which may be measurable using nuclear magnetic resonance (NMR).

Primarily high guluronic-containing alginates, such as Manugel DMB and Pronova SLG100, were used for this research. High guluronic-containing alginates produced strong hydrogels because they were highly cross linked. Because they contained high levels of calcium; they were susceptible to calcification. Low guluronic-containing alginates, such as Pronova SLM and Sigma alginates, are less likely to experience calcification and should be investigated further. The GRGDY-derivatization process of low guluronic-containing alginates will also need to be investigated because the mannuronic subunits may be less susceptible to reaction using carbodiiamide chemistry due to its different moiety. The use of barium chloride as a cross linking

solution should be explored to see if this eliminates calcification. However the rSMCs seemed to be more sensitive to barium when studied initially in collagen/alginate matrices.

Finally the pore size and microstructure of the alginate-GRGDY hydrogels should be examined. The hydrogel pore size may be increased by adding surfactants such as BSA or Pluronic (F68 or F108) to increase pore size (Eiselt, 2000).

4.5.2. MSCs as the cell substrate

It would be advantageous to create a hMSC cell bank that had a longer life-span *in vitro* on which to conduct studies since the cells used in these studies could only be grown to passage 12. This could be accomplished by two methods: isolating and generating a multipotent adult progenitor cell (MAPC) bank which would have unlimited passaging potential without obvious senescence or loss of differentiation potential (Reyes, 2001; Jiang, 2002); or incorporating human telomerase reverse transcriptase (hTERT) gene into a population of isolated hMSCs. HTERT has been successfully incorporated into human SMCs and resulted in cells that proliferated far beyond their normal lifespan but retained characteristics of normal control SMCs (McKee, 2003).

Due to the hMSC/alginate-GRGDY beads dissociating at later time points and to improve the stability of the alginate beads during storage prior to immunohistochemistry preparation, 10mM $CaCl_2$ should be added to the formaldehyde solution. The presence of calcium ions will help maintain the hydrogel structure during storage of the beads until histological preparations are made. Additional antibodies for identification of smooth muscle cell-specific proteins, such as h-caldesmon (now commercially available), desmin, calponin and heavy chain myosin, should be used in immunohistological preparations for verification of smooth muscle cell phenotype. H-caldesmon staining has been reported as being able to differentiate between smooth muscle cells and other cell varieties such as fibroblasts and myofibroblasts that sometimes express ASMA and desmin (D'Addario, 2002). In addition, a protein assay should be used to quantitate the amount of these proteins expressed by the hMSCs in the differentiation studies. A detailed protein analysis

would also confirm whether hMSCs expressed ASMA at the beginning of a differentiation study or after long term culture in growth medium since immunohistology results showed non-specific binding of the biotin in the day 0 hMSCs immobilized in alginate-GRGDY beads, as well as in long term cultures of hMSCs grown in DMEM and CDMEM. Finally, alginate degradation during culturing should be monitored using staining reagents specific for polysaccharides such as alginate including periodic acid-Schiff reagent, Toluidine blue and Alcian blue (Lee, 1997). Alginate may be lost during standard histological preparation (e.g. dewaxing step) so the hydrogels may need to be stained for presence of alginate prior to processing.

Differentiation studies were conducted with conditioned medium containing fetal bovine serum which could have affected growth and differentiation due to presence of undefined components. In the future, studies should be performed in defined medium. Gronthos and Simmons have shown the conditions and factors required for growth of stromal cells under serum deprived conditions *in vitro*. The exogenous factors determined to be essential included their SDM (serum-deprived medium, defined in glossary) containing L-ascorbate, glucocorticoid dexamethasone, PDGF-BB and EGF on fibronectin coated plates (Gronthos and Simmons, 1995). In addition, Seruya (2004) reported serum-free conditions that led to high-efficiency smooth muscle differentiation using rat MSCs isolated from muscle tissue plated on collagen IV-coated surfaces and exposed to transforming growth factor-β1 (TGF-β1). These rat MSCs differentiated into a homogeneous population expressing ASMA and calponin (Seruya, 2004). Wang, D. (2004) also reported that TGF-β1 affected the differentiation of rMSCs into SMCs. Initial research has also indicated that some minimal culture time is needed in MSCCM before transfer of the beads into CDMEM with rSMC cultures due to one study in which no elongation was observed in hMSCs grown in complete DMEM only (Figure 44). Finally further differentiation studies could be conducted to determine if hMSCs immobilized in unmodified alginate (no GRGDY peptide) differentiate when cultured in CDMEM with rSMC co-cultures. Alternatively differentiation studies could be performed using human SMC conditioned medium and co-cultures instead of rat SMC. A female source of hMSCs should be used with a male source of hSMCs such that DNA analysis using fluorescence in situ hybridization (FISH) testing could be performed after the study to

determine if cross contamination of cells occurred. The presence of a Y chromosome in the female hMSCs would indicate contamination from the male hSMC co-cultures; and therefore, indicate differentiation potentially caused by cell fusion instead of by directed differentiation. It has been reported that BMCs can adopt the phenotype of the recipient cells *in vivo* by cell fusion rather than by directed differentiation (Terada, 2002).

The issue of cell/alginate matrix contraction as observed in section 3.6.2.1 (Figure 66.G) will have to be studied further since it would be undesirable to have an uneven surface in the lumen of a mature blood vessel. An uneven surface could result in turbulent flow and thrombosis. Finally the possibility that the hMSCs are associating with the glass wall of the bioreactor needs to be examined and discounted by applying a non-binding surface onto the glass bioreactor.

5. Glossary

Allogeneic - being genetically different although belonging to or obtained from the same species

Amino acid abbreviations – A – alanine (Ala); C – cysteine (Cys); D – aspartic acid (Asp); E – glutamic acid (Glu); F – phenylalanine (Phe); G – glycine (Gly); H- histidine (His); I – isoleucine (Ile); K – lysine (Lys); L – leucine (Leu); M – Methionine (Met); N- asparagine – (Asn); P – proline (Pro); Q – glutamine (Gln); R - arginine (Arg); S – Serine (Ser); T – threonine (Thr); W – tryptophan (Trp); V-valine (Val); Y – tyrosine (Tyr)

Aneurysm - a localized, pathological, blood-filled sac-like dilatation (widening) of a blood vessel caused by a disease or weakening of the vessel's wall

Arteriovenous fistula - abnormal channel between an artery and a vein, bypassing the capillaries, which may be congenital, in which smaller vessels are involved, or acquired due to acute local trauma or to erosion of an arterial aneurysm into an accompanying vein (from The Merck Manual – web version)

Autologous - Derived or transferred from the same individual's body (i.e. patient's own)

CDMEM – conditioned DMEM - the supernatant collected from centrifuged conditioned medium from rSMC cell cultures used for hMSC differentiation studies.

Complete DMEM – culture medium consisting of the formulation of Dulbecco's Modified Eagles Medium (DMEM) completed with 10% FBS, 2 mM l-glutamine, 100 U penicillin/ml and 100 µl streptomycin/ml.

EDTA – Ethylenediaminetetraacetic acid – a divalent cation chelator used in combination with trypsin (porcine-derived proteolytic enzyme) to detach cells from the surface of polystyrene tissue flasks. It also sequesters calcium ions in an alginate hydrogel and causes the gel to dissolve.

FACS – Fluorescence activated cell sorting.

Femoropopliteal bypass - a diseased (blocked) blood vessel located above or below the knee is bypassed by using either a transplanted healthy blood vessel or an artificial graft material (from my.webmd.com).

FITC - fluorescein isothiocyanate is the reactive form of fluorescein, a fluorescent dye for FACS analysis. FITC is a small organic molecule, and is typically conjugated to proteins via primary amines (i.e., lysines). Usually, 3-6 FITC molecules are conjugated to each antibody. Fluorescein is typically excited at 488nm using an argon laser, and emission is collected at 530nm.

Formal saline - 10% formaldehyde in buffered saline used to prepare histology samples

Glucose consumption rate (GCR) – the amount of glucose consumed in the compete medium per hour in culture.

HLA – Human leukocyte antigens are proteins on the surface of the body's cells which identify an individual's tissue type. The immune system uses HLA to recognize self vs. foreign. These proteins are encoded by genes comprising of the major histocompatibility complex (MHC) which in concert with T-cell receptors make possible the immune recognition of foreign antigens.

Homophilically – refers to the type of cell adhesion where the cell surface adhesion proteins in the two cells are the same

Hypertonic – having the higher osmotic pressure of two solutions

Integrins - family of cell surface proteins that are involved in binding to extracellular matrix components in some cases. The first examples described were fibronectin and vitronectin receptors of fibroblasts, which bind to an RGD (Arg Gly Asp) sequence in the ligand protein

Intima - The innermost membrane of an organ or part, especially the inner lining of a lymphatic vessel, an artery, or a vein.

Luminal - The inner open space or cavity of a tubular organ, as of a blood vessel or an intestine

Mitogen - agent that induces mitosis (cell division)

MSC, hMSC – human mesenchymal stem cells derived from bone marrow

MSCCM – mesenchymal stem cell culture medium consisting of the formulation of Mesencult basal medium, MSC growth stimulatory supplements (Stem Cell Technologies), rFGF, penicillin and streptomycin

MTT (3-(4,5-dimethylthiazol-2-yl)-2,5-diphenyltetrazolium bromide) assay

Normal saline (n-saline) – 0.9% w/v NaCl in distilled water, pH adjusted using 1N NaOH to ca. 7-8.

Patency, Patent – the state of being open, expanded or unblocked

RGD-modified alginate – abbreviated term for alginate which has been modified by the addition of a poly-peptide containing arginine, glycine, and aspartic acid (RGD) onto the carboxylic acid moiety of the alginate polysaccharide chain.

RPE - Rhodophyta-phycoerythrin was originally isolated from red algae and is used as a fluorescent probe. Its primary absorbance peak occurs at 566nm with secondary peaks at 496 and 545nm; the relative prominence of the secondary peaks varies significantly among RPEs from different species. Usually one RPE molecule is

conjugated to each antibody for identification of cell-specific surface markers using FACS analysis. It emits at about 575nm.

rSMC – rat smooth muscle cells derived from immortalized cell line ATCC A7r5

SDM – serum-deprived medium as described by Gronthos and Simmons (1995) for hBMCs – αMEM supplemented with 10μg/mL bovine pancreas-derived insulin, 2% BSA, 4μg/mL human low-density lipoprotein, 200μg/mL iron-saturated human transferrin, 2mmol/L L-glutamine, 10nmol/L dexamethasone sodium phosphate, 100μmol/L L-ascorbic acid 2-phosphate, and 50μmol/L β-mercaptoethanol.

SMC – smooth muscle cells

Spent medium – conditioned medium from confluent cultures of SMCs would contain complete medium, trypsin, EDTA, and by-products of cellular metabolism (eg. lactate, ammonia, LDH)

Systolic thickening - increase in apparent tracer activity during systolic contraction

WFI - Water for injection used for cell culture applications prepared by ultrafiltration, reverse osmosis, deionization, distillations and sterile filtration. Obtained from Biowhittaker, catalog 17-724G.

Xenogeneic - derived from a different animal species

6. Appendices

6.1. Materials and methods appendices

6.1.1. Assay protocols

6.1.1.1. MTT assay for MSC cell number standard

Step 1: Trypsinize MSCs from tissue culture flask(s) using procedure in section 2.2.2.2 and determine the cell concentration as per section 2.5.2.

Step 2: Centrifuge the cells, remove the supernatant and resuspend the pellet to $2x10^6$cell/mL in DPBSG. Repeat the cell count using 20μL of cell suspension and add to 80μL of DPBSG to confirm the actual cell concentration in the resuspended pellet.

Step 3: Transfer aliquots of cell suspension into a 96 well microplate as indicated in Table 5 (section 2.6.2.1). Equalize the volume per well by added the volume of DPBSG indicated in Table 5.

Step 4: Add 10μL of 5mg/mL MTT solution to each well. Incubate at 37°C, covered with film.

Step 5: After 3 hours, add 40μL 0.3M trisodium citrate to each well. Incubate at 37°C, covered with film for 1 additional hour. (Trisodium citrate added here to mimic protocol to dissolve alginate beads.)

Step 6: Centrifuge plate at 100g for 5 minutes

Step 7: Remove supernatant without disturbing pellet/bead, until ring appears on bottom of well.

Optional Step 8: Freeze/store plate at -70°C, covered with foil. (Freezing recommended for time course experiment.)

Optional Step 8a: Thaw plate.

Step 9: Add 70μL of DPBSG to each well (Note add 50μL if performing step10). Gently tap plate to loosen cell pellet. (Note optional step 10 and 10a can be performed, but the trypsin/EDTA tends to make the cells sticky).

Optional Step 10: Add 20μL 10X trypsin/EDTA in saline to each well. Incubate at RT for 30 minutes covered with film. (Note this step is only required for alginate-GRGDY beads.)

Optional Step 10a: Using separate micropipets, thoroughly resuspend cells until completely homogeneous within solution.

Step 11: Add 100μL of isopropanol/0.1N HCl solution to each well. Incubate at RT, covered with film for 20 minutes.

Step 12: Using separate micropipets, mix each well thoroughly (formazan crystals may not yet be completely dissolved). Incubate at RT, covered with film for 20 additional minutes.

Step 13: Using separate micropipets, mix each well thoroughly (solution should be completely dissolved).

Step 14: Immediately read plate on spectrophotometer (read setting 600nm, reference setting 670nm) within 1 hour from time of isopropanol/HCl addition.

Note: RT = room temperature (19°C ideal, absorbance readings and stability of dissolved formazan were effected by temperature.)

6.1.1.2. MTT assay for MSCs in alginate beads

Step 1: Transfer beads from microwell culture into petri-dish containing DPBSG. Let bead rinse for ca. 15 minutes.

Step 2: Transfer beads into 96 well microplate; add 0, 1, 2, 3 beads/well for cell standard.

Step 3: Equalize DPBSG volume per well to 100μL/well.

Step 4: Add 10μL of 5mg/mL MTT solution to each well. Incubate at 37°C, covered with film.

Step 5: After 3 hours, add 40μL 0.3M trisodium citrate to each well. Incubate at 37°C, covered with film for 1 additional hour.

Step 6: Centrifuge plate at 100g for 5 minutes

Step 7: Remove supernatant without disturbing pellet/bead, until ring appears on bottom of well.

Optional Step 8: Freeze/store plate at -70°C, covered with foil. (Freezing recommended for time course experiment.)

Optional Step 8a: Thaw plate.

Step 9: Add 70μL of DPBSG to each well (Note add 50μL if performing step10). Gently tap plate to loosen cell pellet.

Optional Step 10: Add 20μL 10X trypsin/EDTA in saline to each well. Incubate at RT for 30 minutes covered with film. (Note this step is required for alginate-GRGDY beads.)

Optional Step 10a: Using separate micropipets, thoroughly resuspend bead(s) until cells completely homogeneous within solution.

Step 11: Add 100μL of isopropanol/0.1N HCl solution to each well. Incubate at RT, covered with film for 20 minutes.

Step 12: Using separate micropipets, mix each well thoroughly (formazan crystals may not yet be completely dissolved). Incubate at RT, covered with film for 20 additional minutes.

Step 13: Using separate micropipets, mix each well thoroughly (solution should be completely dissolved).

Step 14: Immediately read plate on spectrophotometer (read setting 600nm, reference setting 670nm) within 1 hour from time of isopropanol/HCl addition.

Note: RT = room temperature (19°C ideal, absorbance readings and stability of dissolved formazan were effected by temperature.)

6.1.1.3. MTT assay for adherent cells

Step 1: Remove spent medium from (24 well) microwell cultures and add 300µL/well DPBSG.

Step 2: Add 30µL of 5mg/mL MTT solution to each well. Incubate at 37°C, covered with film.

Step 3: After 3 hours, add 120µL 0.3M trisodium citrate to each well. Incubate at 37°C, covered with film for 1 additional hour. (This step mimicked additions performed to dissolve alginate beads but is not required if alginate not used in study.)

Step 4: Remove MTT solution from wells (Note: formazan precipitates trapped when cells attached to plate surface).

Optional Step 5: Freeze/store plate at -70°C, covered with foil. (Freezing recommended for time course experiment.)

Optional Step 5a: Thaw plate.

Step 6: Add 210µL of DPBSG to each well.

Step 7: Add 300µL of isopropanol/0.1N HCl solution to each well. Incubate at RT, covered with film for 20 minutes.

Step 8: Using separate micropipets, mix each well thoroughly (formazan crystals may not yet be completely dissolved). Incubate at RT, covered with film for 20 additional minutes.

Step 9: Using separate micropipets, mix each well thoroughly (solution should be completely dissolved).

Step 10: Immediately remove 100µL from each well, transfer into 96 well plate and read plate on spectrophotometer (read setting 600nm, reference setting 670nm) within 1 hour from time of isopropanol/HCl addition.

Step 11: Actual absorbance should be multiplied by a dilution factor of 3 (3 fold volume of DPBSG/isopropanol used compared to normal cell standard prepared in 96 well) to obtain actual cell concentration compared to the standard.

Note: RT = room temperature (19°C ideal, absorbance readings and stability of dissolved formazan were effected by temperature.)

6.1.2. Assay errors and standard curves

6.1.2.1. CyQuant assay

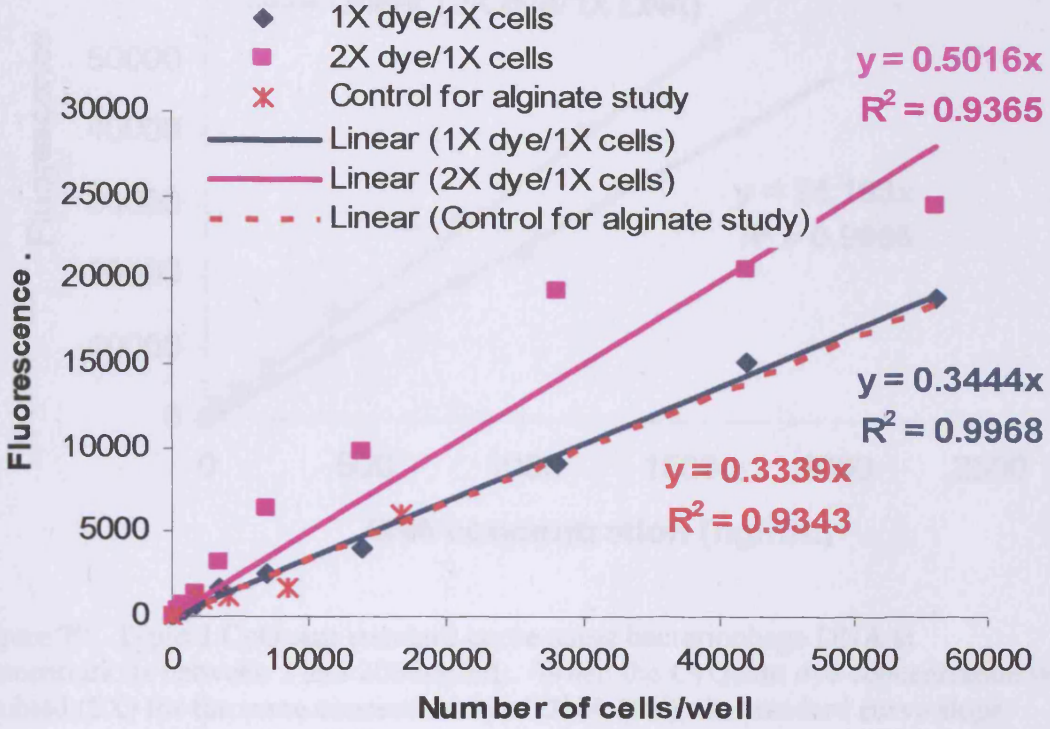

Figure 69. Typical CyQuant standard curve using rSMCs at concentrations between 50 and 56,000cells/well. When the CyQuant dye concentration was doubled (2X) for the same concentration of cells (1X), the standard curve slope increased from 0.34x to 0.50x. The 'control for alginate' sample is the cell standard curve generated for the data shown in Figure 71. The assay was fairly linear between this range when the cell suspension was treated with RNAse as described in section 2.6.1.1. Readings were taken at 900 PMT.

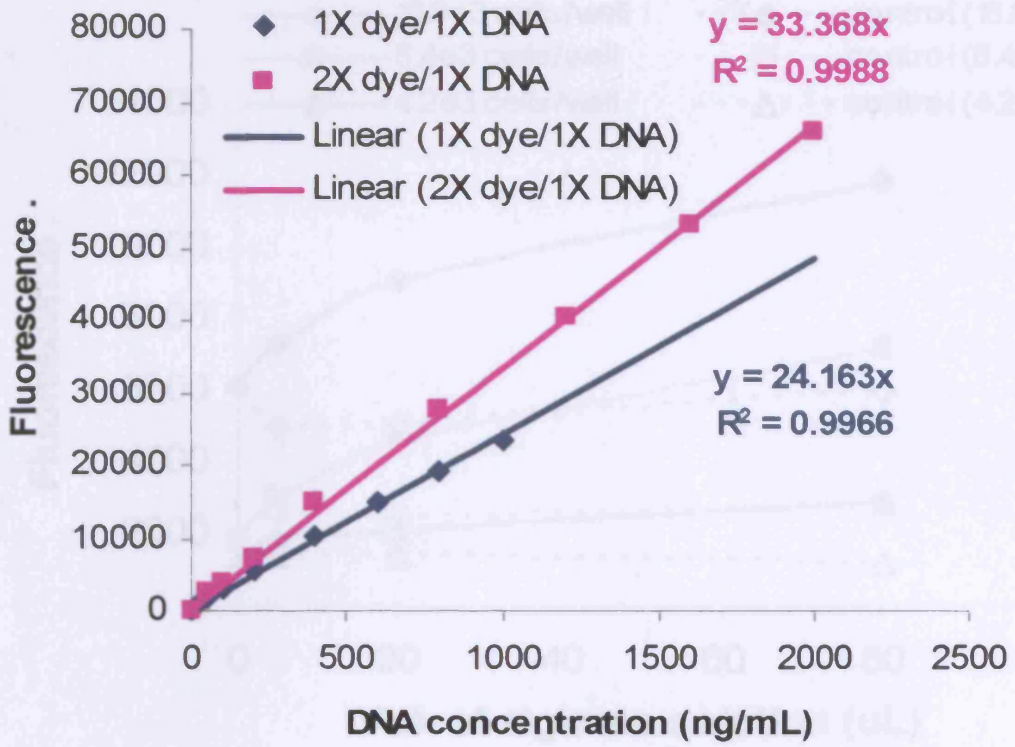

Figure 70. Typical CyQuant standard curve using bacteriophage DNA at concentrations between 5 and 2000ng/mL. When the CyQuant dye concentration was doubled (2X) for the same concentration of DNA (1X), the standard curve slope increased from 24x to 33x. This corresponds to a similar increase observed when the CyQuant dye concentration was doubled in the cell standard curve shown in Figure 69. Readings were taken at 900 PMT.

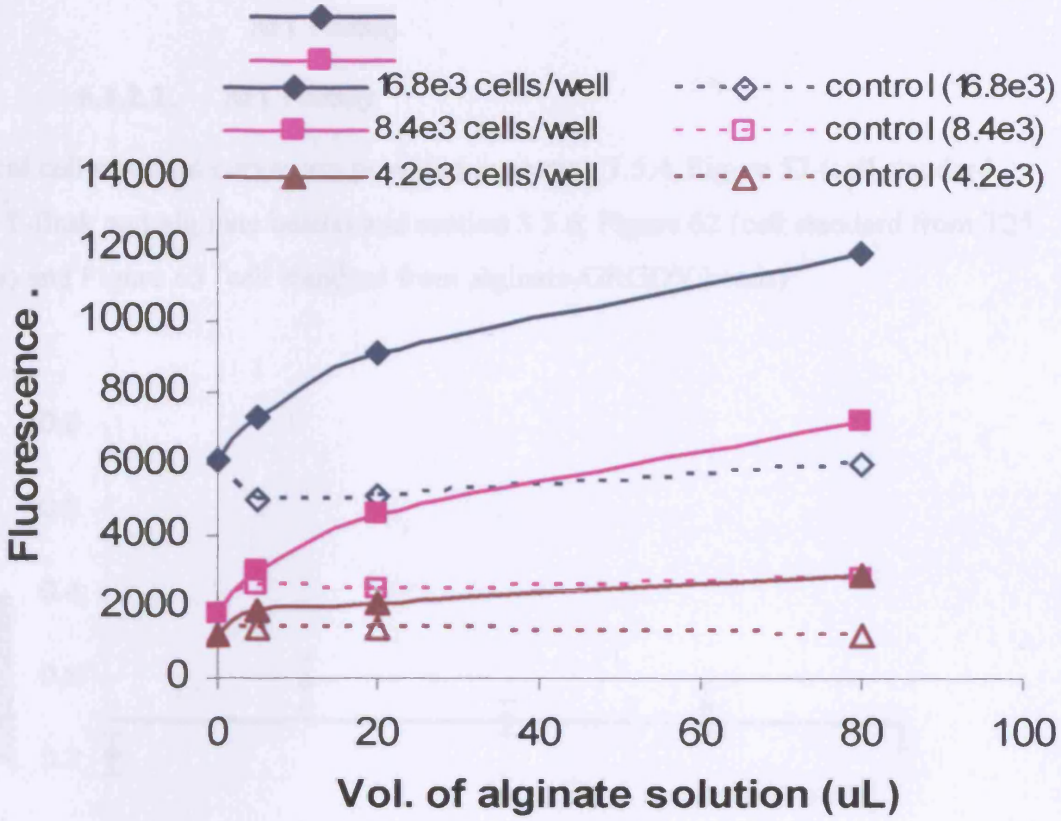

Figure 71. Effect of alginate solution on fluorescence signal of three cell concentrations using CyQuant assay. Three cell concentrations were tested with 0, 5, 20 and 80μL of dissolved alginate solution. As the volume of solution increased the fluorescence signal increased indicating the alginate or other components of the solution adversely affected binding of fluorescence dye to the cellular DNA as compared to the control solution at the same cell concentrations. The cells were RNAse treated prior to addition of solutions and measured at a PMT setting of 900. The cell standard curve is shown in Figure 69 for this experiment. From these data, an alternative proliferation assay was deemed necessary.

6.1.2.2. MTT assay

Typical cell standard curves are provided in section 3.5.4, Figure 57 (cell standard from T-flask and alginate beads) and section 3.5.6, Figure 62 (cell standard from T25 flasks) and Figure 63 (cell standard from alginate-GRGDY beads).

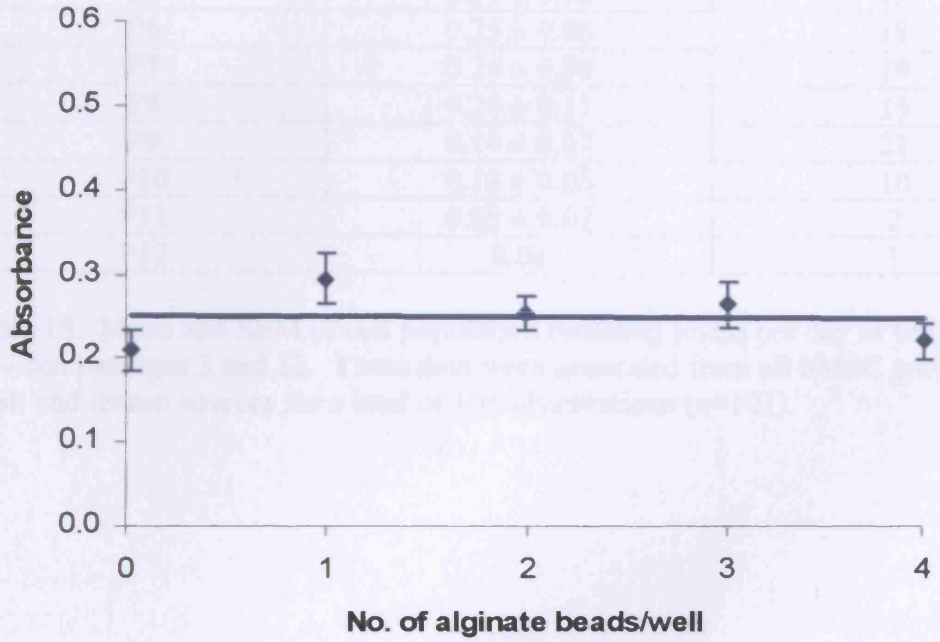

Figure 72. Determination of alginate interference with the absorbance of formazan. The same concentration ($2.05x10^4$cells/well) was tested with an increasing number of alginate beads/well. Absorbance readings were not affected by the increased level of alginate per well. Single factor ANOVA statistical comparison indicated that the results were statistically different ($p=0.0000$) among the 5 samples; however, the statistical difference between absorbance readings for 0 and 4 beads was not significant ($p=0.4023$) and between the absorbance readings for 2 and 3 beads ($p=0.5021$). The statistical difference was significant among the absorbance readings for 1, 2 and 3 beads ($p=0.0405$). The variability of these results was likely due to well-to-well variability, and not due to alginate effect.

6.2. Results appendices

6.2.1. Cell growth data

6.2.1.1. Cell population doubling levels per day for hMSCs

Passage number	Population Doubling/day mean ± SEM	Number of observations (n)
P3	0.41	1
P4	0.27	1
P5	0.29 ± 0.06	13
P6	0.25 ± 0.06	18
P7	0.24 ± 0.08	19
P8	0.20 ± 0.11	15
P9	0.14 ± 0.07	21
P10	0.18 ± 0.05	10
P11	0.05 ± 0.02	2
P12	0.06	1

Table 18. Mean and SEM of cell population doubling levels per day of hMSCs between passages 3 and 12. These data were generated from all hMSC growth from fresh and frozen sources for a total of 101 observations (n=101).

6.2.2. Single factor ANOVA (analysis of variance) of MTT data

6.2.2.1. Length of incubation for MTT conversion and formazan dissolution time

	2 hr mean ± SEM (variance)	3 hr mean ± SEM (variance)	4 hr mean ± SEM (variance)
		$8.6x10^4$ cells/well	
First reading (<1hr dissolution time)	0.989 ± 0.119 (0.014)	0.947 ± 0.130 (0.017)	1.066 ± 0.117 (0.014)
Second reading (>1hr dissolution time)	0.777 ± 0.068 (0.005)	0.738 ± 0.138 (0.019)	0.763 ± 0.041 (0.002)
		$4.1x10^4$ cells/well	
First reading (<1hr dissolution time)	0.367 ± 0.027 (.001)	0.472 ± 0.031 (0.001)	0.539 ± 0.088 (0.008)
Second reading (>1hr dissolution time)	0.293 ± 0.024 (0.001)	0.381 ± 0.063 (0.004)	0.457 ± 0.075 (0.006)
		$2.1x10^4$ cells/well	
First reading (<1hr dissolution time)	0.189 ± 0.046 (0.002)	0.229 ± 0.039 (0.001)	0.269 ± 0.051 (0.003)
Second reading (>1hr dissolution time)	0.186 ± 0.029 (0.001)	0.205 ± 0.068 (0.005)	0.223 ± 0.018 (0.000)
		$1.2x10^4$ cells/well	
First reading (<1hr dissolution time)	0.137 ± 0.028 (0.001)	0.112 ± 0.039 (0.002)	0.158 ± 0.023 (0.001)
Second reading (>1hr dissolution time)	0.091 ± 0.024 (0.001)	0.131 ± 0.035 (0.001)	0.139 ± 0.019 (0.000)

Table 19. The mean, standard error (SEM) and variances of absorbance readings for MTT incubation length and formazan dissolution time (from section 3.5.1.3, shown in Figure 50).

Length of incubation for MTT conversion and formazan dissolution time (continued)

Comparison of p-values among designated time points (2, 3 or 4 hr) (for absorbances at $8.6x10^4$ cells/well)		
	p value (2 / 3 / 4 hr time points)	
First reading (<1hr dissolution time)	p=0.2613	1st readings have same mean
Second reading (>1hr dissolution time)	p=0.7571	2nd readings have same mean

Comparison of p-values between pooled (2, 3 and 4 hr) time points at first and second reading (for absorbances at $8.6x10^4$ cells/well)		
	p value of pooled 1st reading / pooled 2nd second	
Pooled readings	p=0.0000	Therefore, 1st and 2nd readings have different means

Comparison of p-values between designated time points (2, 3 or 4 hr) (for absorbances at $4.1x10^4$ cells/well)				
	p value (2 / 3 / 4)	p value (2 / 3)	p value (3 / 4)	p value (2 / 4)
First reading (<1hr dissolution time)	0.0003	0.0001	0.1090	0.0010
Second reading (>1hr dissolution time)	0.0008 different means	0.0097 different means	0.0848 same mean	0.0004 different means

Comparison of p-values between each time point (2, 3 or 4 hr) at first and second reading (for absorbances at $4.1x10^4$ cells/well)			
	p value (2 first / 2 second)	p value (3 first / 3 second)	p value (4 first / 4 second)
Both readings	0.0005 different means	0.0095 different means	0.1125 same mean

Table 20. Single factor ANOVA statistical comparison of individual time points at first and second absorbance readings at $6.8x10^4$ and $4.1x10^4$ cells/well for MTT incubation length and formazan dissolution time (from section 3.5.1.3, shown in Figure 50). Analyses at $2.1x10^4$ and $1.2x10^4$ cells/well were not statistically different ($p>0.05$) for any comparison.

6.2.2.2. Fresh versus frozen MTT assay

	Mean ± SEM (variance) for 1 bead	Comparison of p-value for 1 bead	Comparison of p-value for 1 bead	Mean ± SEM (variance) for 2 beads	Comparison of p-value for 2 beads	Comparison of p-value for 2 beads
Day 2 - fresh	0.189 ± 0.026 (0.0007)	0.6743	All 6 samples (p=0.0005)	0.549 ± 0.034 (0.0012)	0.0209	All 6 samples (p=0.0000)
Day 2 - frozen	0.198 ± 0.042 (0.0017)		5 samples (excluding D6 fresh) (p=0.3804) *	0.449 ± 0.083 (0.0068)		5 samples (excluding D2 fresh) (p=0.0051)
Day 4 - fresh	0.174 ± 0.025 (0.0006)	0.0579		0.383 ± 0.046 (0.0021)	0.0030	
Day 4 - frozen	0.206 ± 0.026 (0.0007)			0.487 ± 0.047 (0.0022)		4 samples (excl. D2 & D4 fresh) (p=0.0316)
Day 6 - fresh	0.251 ± 0.017 (0.0003)	0.0000		0.475 ± 0.045 (0.0020)	0.0042	
Day 6 - frozen	0.184 ± 0.019 (0.0004)			0.391 ± 0.033 (0.0011)		

Table 21. Summary of the mean, standard error (SEM), variance and statistical comparison for fresh verses frozen MTT samples during 6 day time course. Only the day 6 fresh sample for 1 bead/well was statistically different from all the remaining samples (*, $p>0.05$). The frozen and fresh absorbance results were equally variable for 2 beads/well. Data from the 3 beads was discounted because the cell number was outside the MTT assay linear range. Therefore, the frozen storage step does not appear to adversely affect the MTT assay. Trypsin/EDTA was not used in this study.

6.2.2.3. Addition of 10X trypsin/EDTA in saline to alginate-GRGDY beads

Mean ± SEM (variance)				
	No T/E	10μL T/E	20μL T/E	20μL T/E (replicate)
First reading	0.307 ± 0.007 (0.0000)	0.434 ± 0.010 (0.0001)	0.416 ± 0.010 (0.0000)	ND
Second reading	0.343 ± 0.022 (.0005)	0.420 ± 0.013 (0.0002)	0.396 ± 0.022 (0.0005)	0.428 ± 0.005 (0.0000)
Third reading	0.344 ± 0.023 (0.0005)	0.429 ± 0.020 (0.0004)	0.406 ± 0.019 (0.0004)	0.425 ± 0.008 (0.0000)
Fourth reading	0.335 ± 0.018 (0.0003)	0.431 ± 0.019 (0.0004)	0.386 ± 0.021 (0.0004)	0.431 ± 0.014 (0.0002)
p-value among four readings	0.1249 *	0.7181 *	0.2937 *	0.7884 *

	Comparison of p-values among designated samples	
	All samples	T/E containing samples
First reading	0.0000 #	0.0855 +
Second reading	0.0013 #	0.0900 +
Third reading	0.0017 #	0.2726 +
Fourth reading	0.0005	0.0346
Pooled readings	0.0000	0.0002

Table 22. Summary of the mean, standard error (SEM), variance, and statistical comparison for hMSCs in alginate-GRGDY beads dissolved using 10X trypsin/EDTA (denoted as T/E). Each individual sample was not statistically different (*, $p>0.05$) for all four readings (out to 2 hour dissolution time). There was no statistical difference (+, $p>0.05$) between the samples containing trypsin/EDTA (T/E) for the 1st, 2nd and 3rd readings. There was a significant difference between all the samples and the samples just containing trypsin/EDTA (#, $p<0.05$) for the 1st, 2nd and 3rd readings.

6.2.3. Comparison of negative controls versus ASMA stained immunohistological preparations

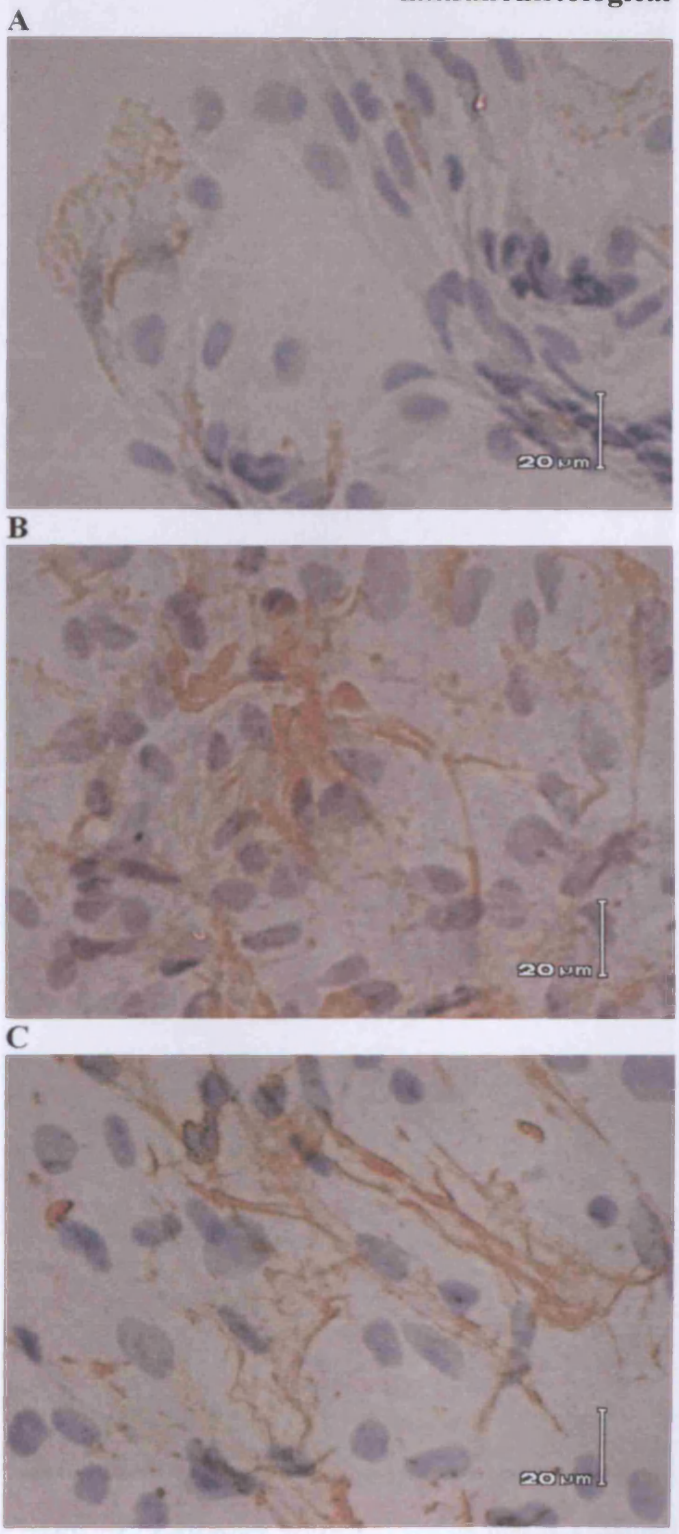

Figure 73. Cytology preparations of hMSCs stained with hematoxylin and ASMA on day 6 of media differentiation study. High magnification (400X) of cells grown with (A) MSCCM, (B) DMEM and (C) CDMEM.

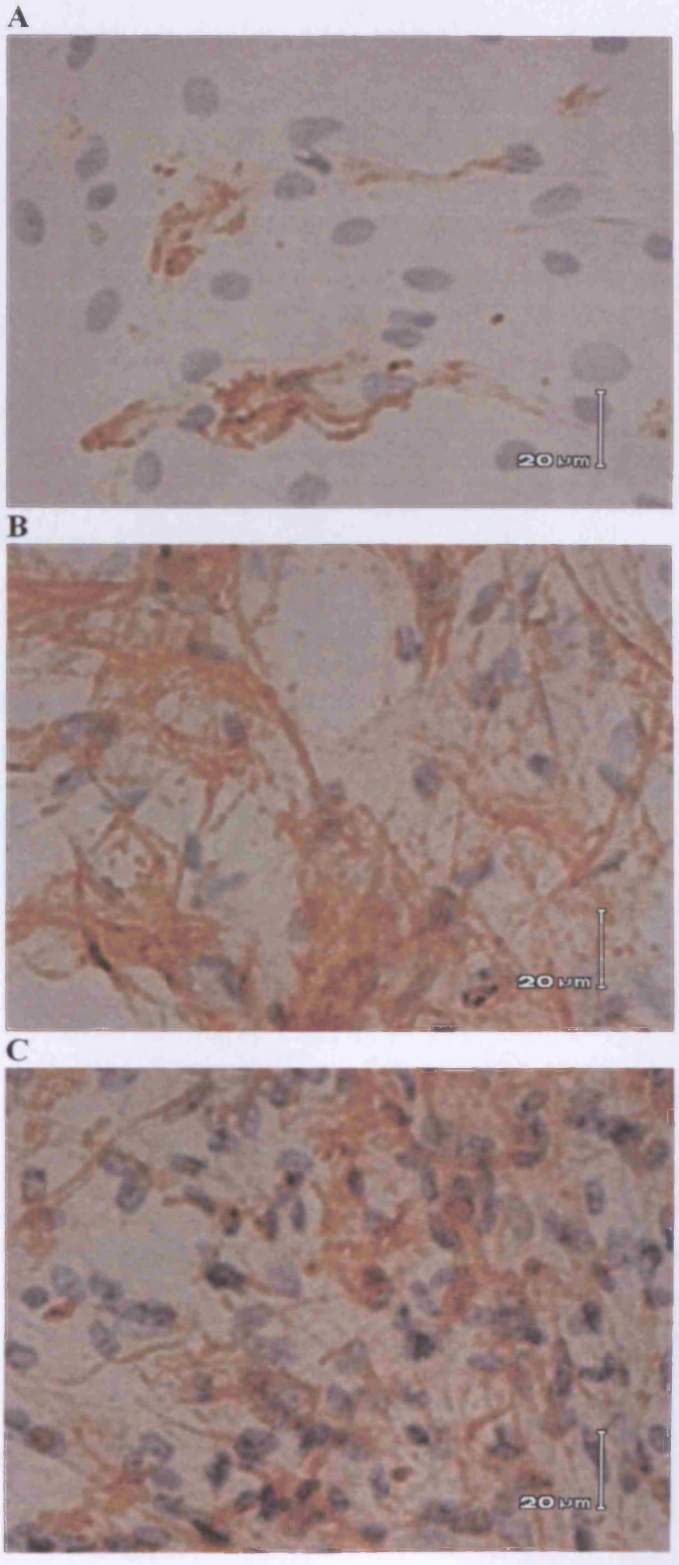

Figure 74. Cytology preparations of hMSCs stained with hematoxylin and ASMA on day 9 of media differentiation study. High magnification (400X) of cells grown with (A) MSCCM, (B) DMEM and (C) CDMEM.

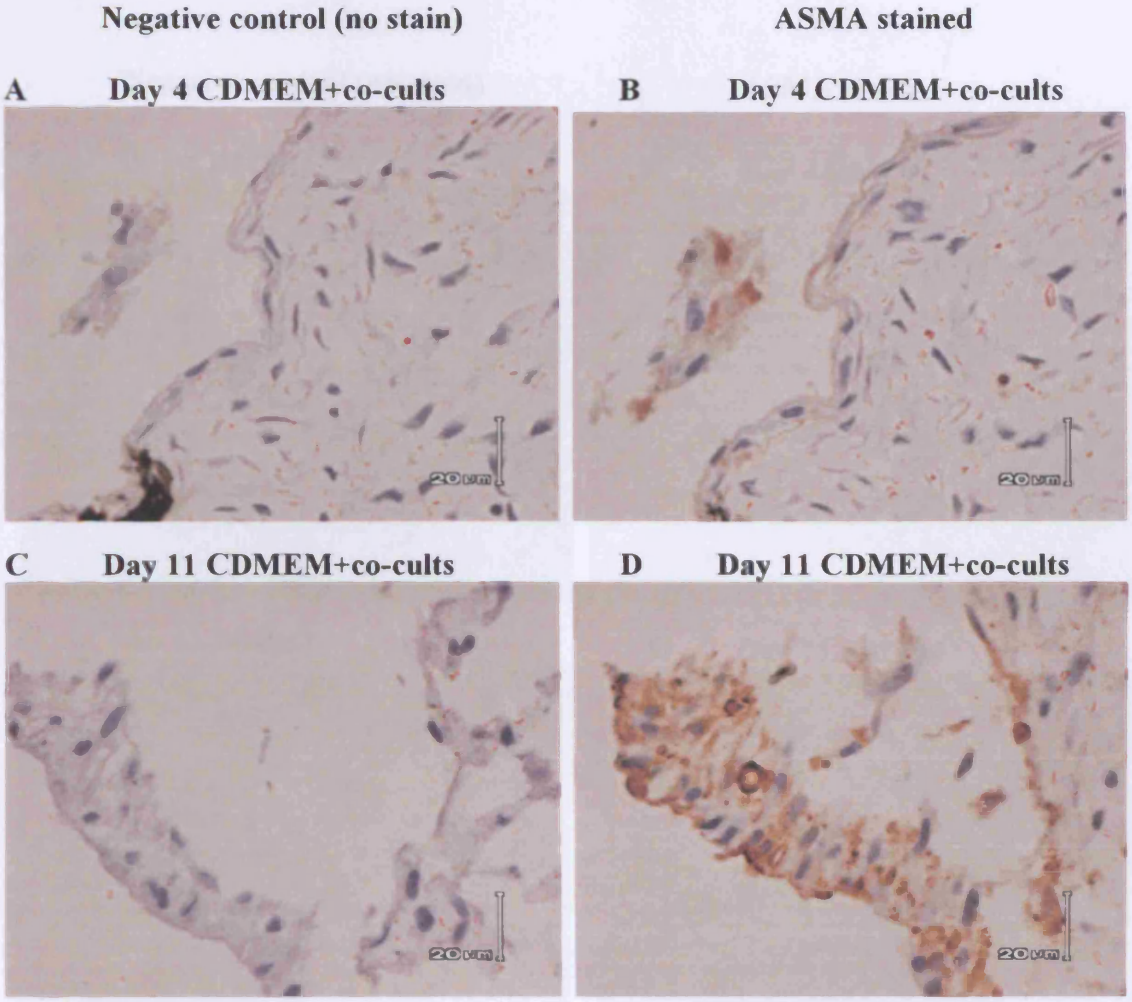

Figure 75. Groupings of immunohistology slides of hMSC/alginate beads to compare ASMA staining to negative controls. When possible the photos were from the same position in the bead cross section. Beads were cultured in CDMEM and rSMC co-cultures for 4 days (Photos A&B) and for 11 days (C&D). Beads were also cultured in DMEM (control medium) for 4 days (E&F) and for 11 days (G&H). (All 400X magnification.)

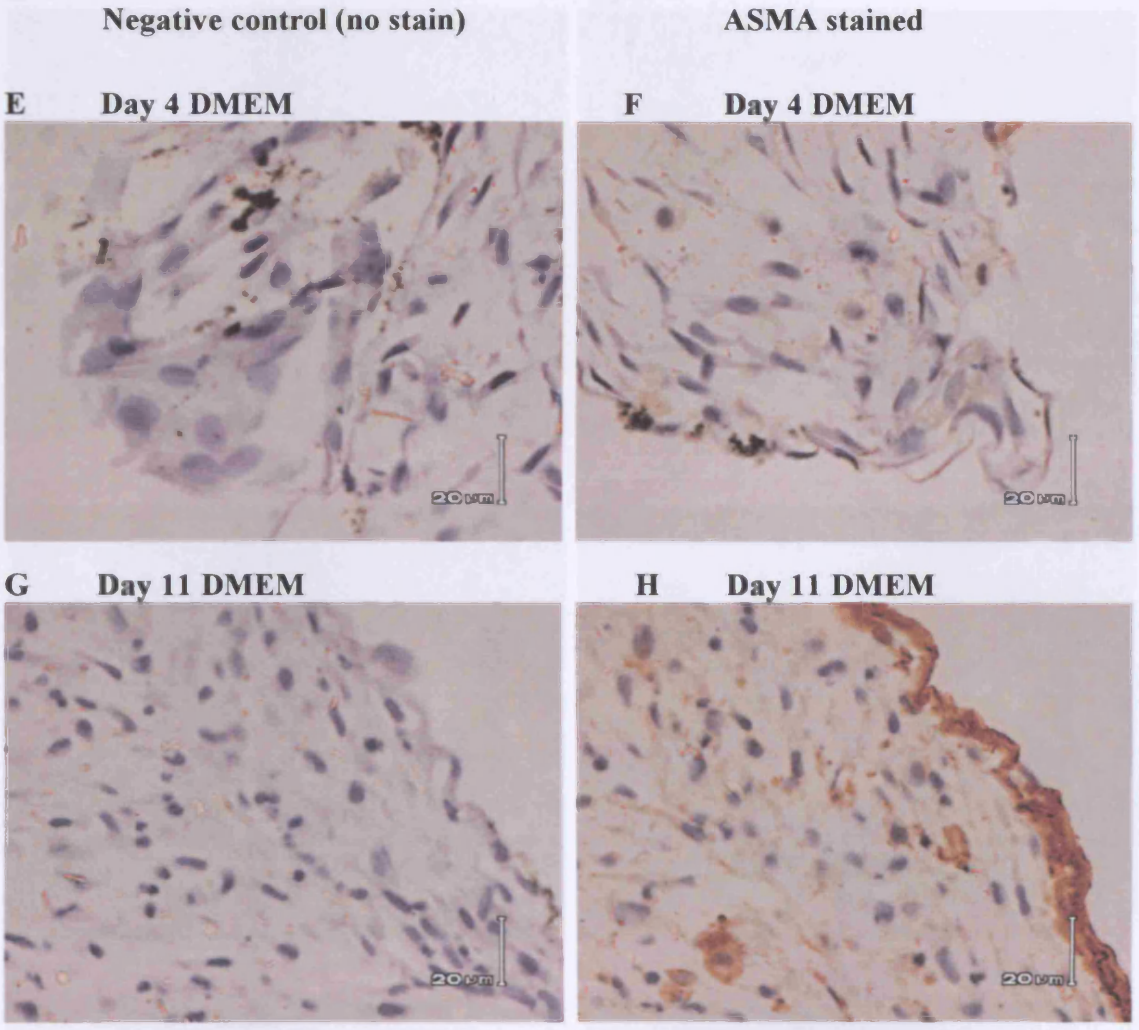

Figure 75. (Continued from previous page) Groupings of immunohistology slides of hMSC/alginate beads to compare ASMA staining to negative controls. When possible the photos were from the same position in the bead cross section. Beads were cultured in CDMEM and rSMC co-cultures for 4 days (Photos A&B) and for 11 days (C&D). Beads were also cultured in DMEM (control medium) for 4 days (E&F) and for 11 days (G&H). (All 400X magnification.)

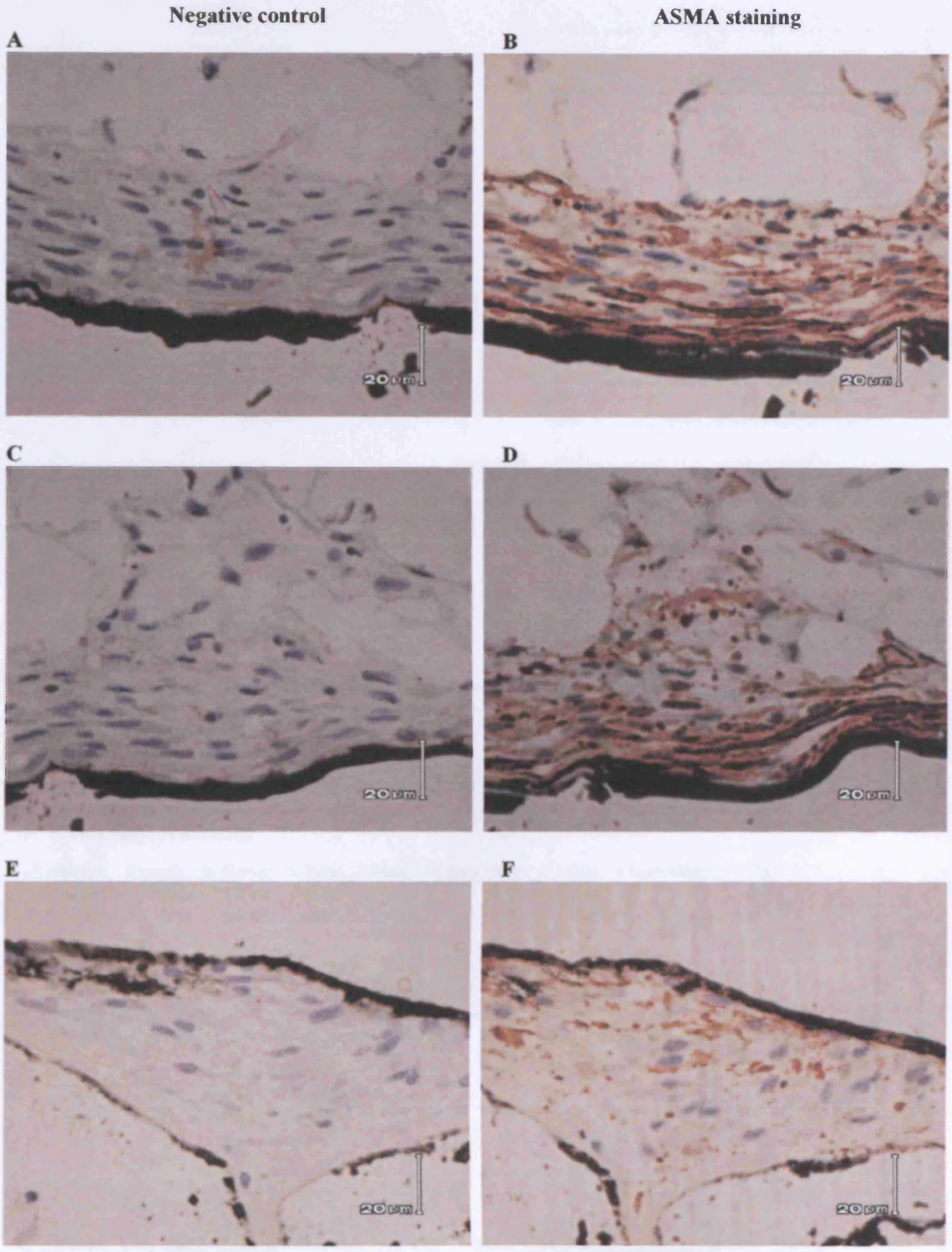

Figure 76. Groupings of immunohistology slides to compare ASMA staining to negative controls in differentiation study using the 'intermediate process'. The photos were obtained from the same position in the bead cross section. Photos A-D: day 9 of culture; and photos E-F: day 23. (All 400X magnification)

6.2.4. FACS reports for hMSC differentiation studies

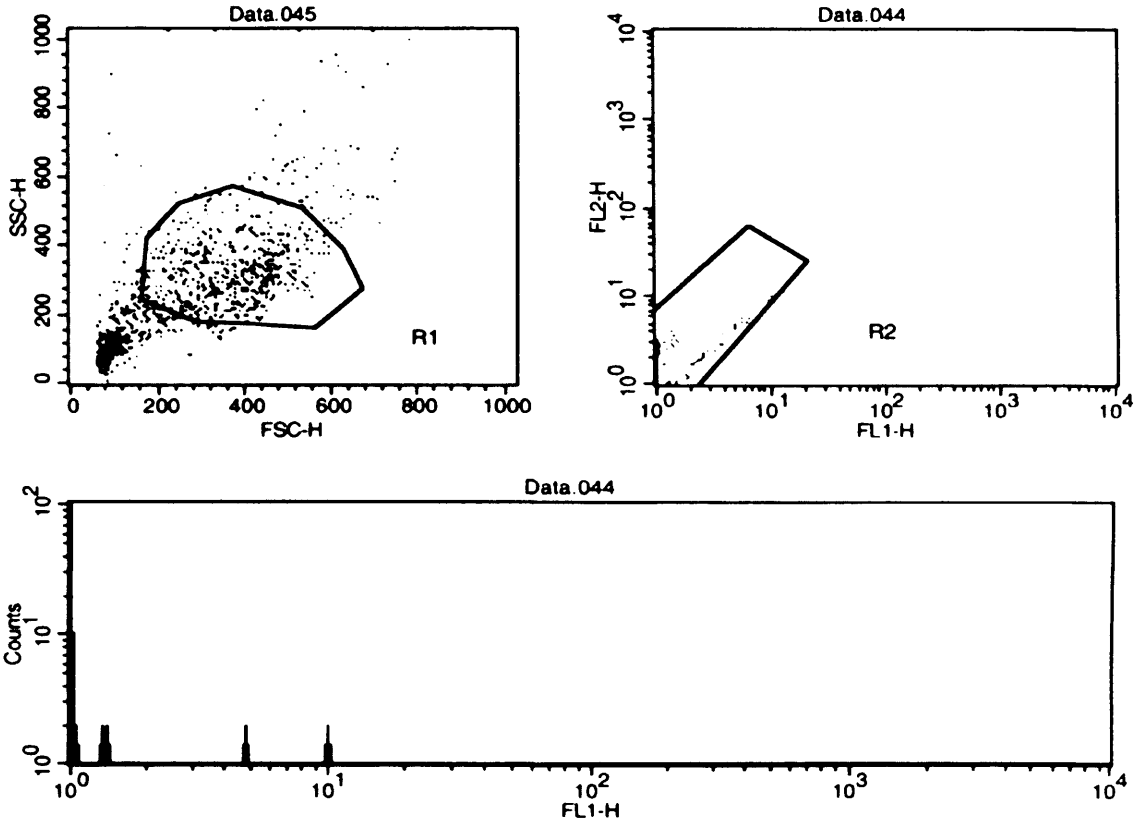

Gate: G1
Total Events: 1000
Y Parameter: FL2-H (Log)
Gated Events: 422
X Parameter: FL1-H (Log)

Region	Events	% Gated	% Total	X Mean	X Geo Mean	Y Mean	Y Geo Mean	Px,Py
R1	422	100.00	42.20	1.29	1.12	1.41	1.22	1, 2
R2	420	99.53	42.00	1.22	1.10	1.35	1.20	3, 4

Gate: G1
Total Events: 1000
Y Parameter: FL2-H (Log)
Gated Events: 422
X Parameter: FL1-H (Log)

Gate	Events	% Gated	% Total
G1	422	100.00	42.20
G2	420	99.53	42.00
G3	2	0.47	0.20

X Parameter: FL1-H (Log)

Marker	Left, Right	Events	% Gated	% Total	Mean	Geo Mean	CV	Median	Peak Ch
All	1, 9910	422	100.00	42.20	1.29	1.12	107.64	1.00	1

Figure 77. FACS results from hMSCs/alginate beads cultured in DMEM (control) and not labeled (empty).

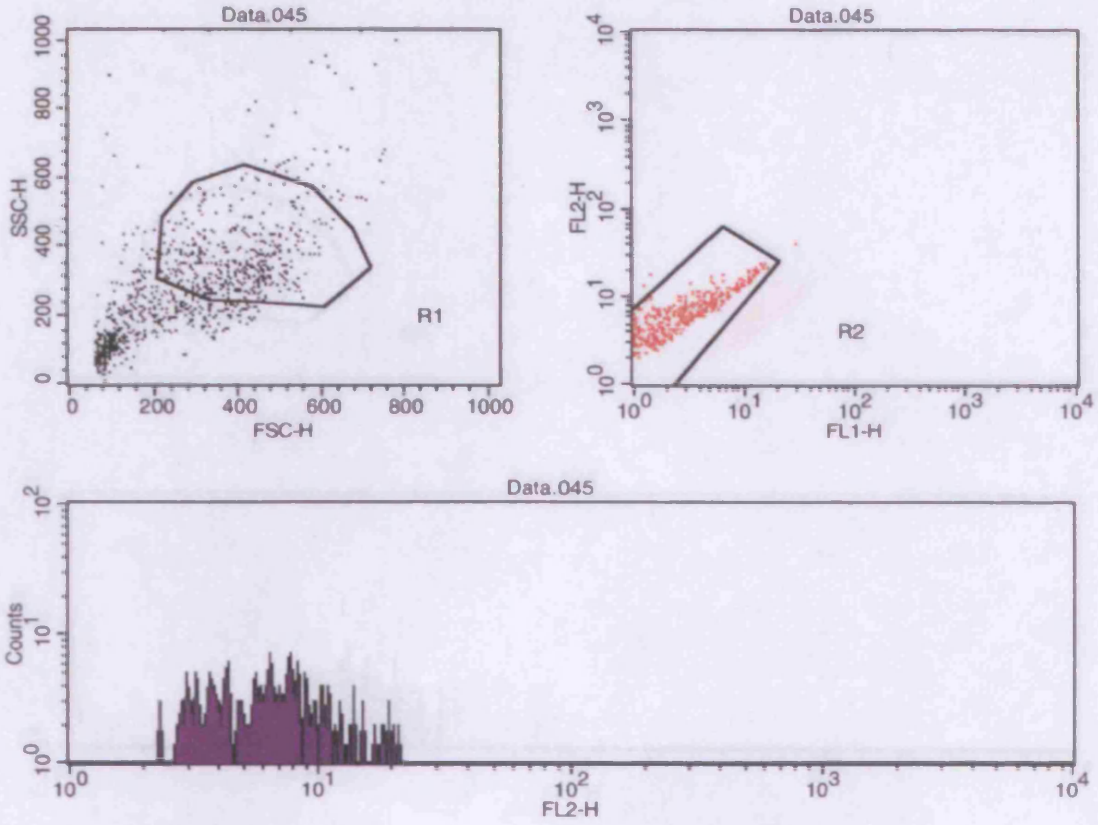

Gate: G1 Gated Events: 427
Total Events: 1000 X Parameter: FL1-H (Log)
Y Parameter: FL2-H (Log)

Region	Events	% Gated	% Total	X Mean	X Geo Mean	Y Mean	Y Geo Mean	Px,Py
R1	427	100.00	42.70	3.80	2.86	7.28	6.25	1, 2
R2	424	99.30	42.40	3.75	2.86	7.17	6.19	3, 4

Gate: G1 Gated Events: 427
Total Events: 1000 X Parameter: FL1-H (Log)
Y Parameter: FL2-H (Log)

Gate	Events	% Gated	% Total
G1	427	100.00	42.70
G2	424	99.30	42.40
G3	3	0.70	0.30

X Parameter: FL2-H (Log)

Marker	Left, Right	Events	% Gated	% Total	Mean	Geo Mean	CV	Median	Peak Ch
All	1, 9910	427	100.00	42.70	7.28	6.25	61.50	6.26	6

Figure 78. FACS results from hMSCs/alginate beads cultured in DMEM (control) and labeled with CD34.

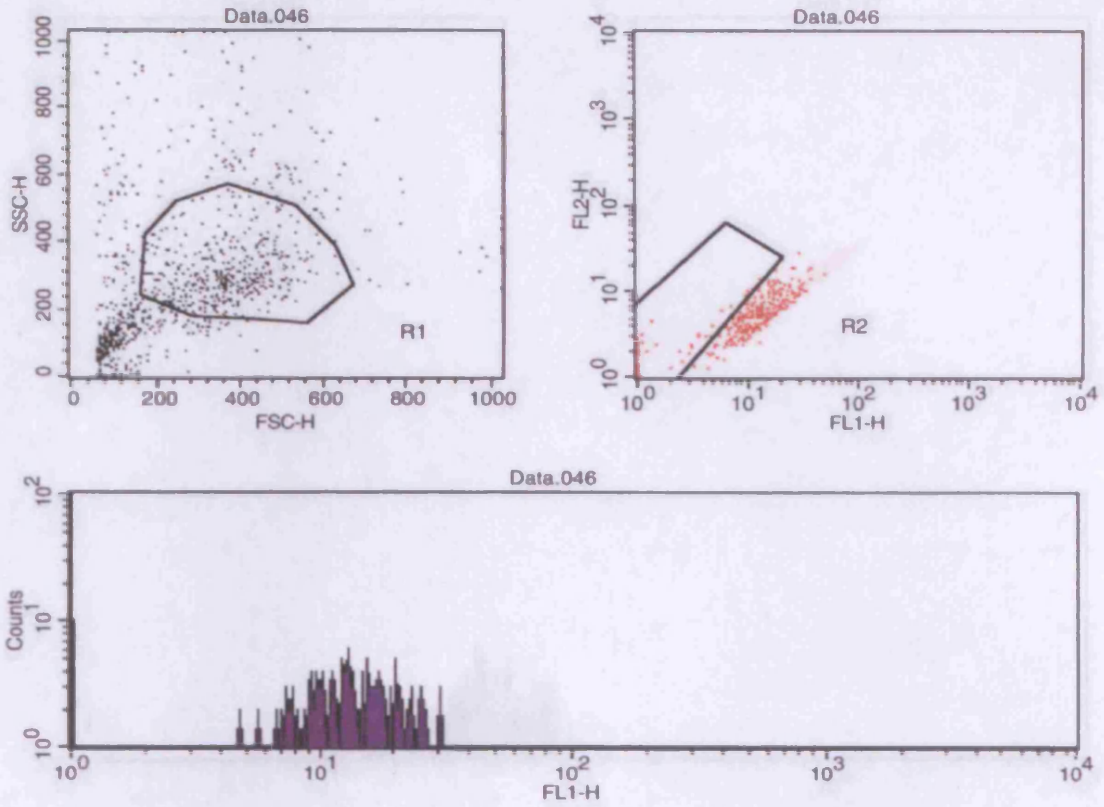

Gate: G1
Total Events: 1000
Y Parameter: FL2-H (Log)

Gated Events: 416
X Parameter: FL1-H (Log)

Region	Events	% Gated	% Total	X Mean	X Geo Mean	Y Mean	Y Geo Mean	Px,Py
R1	416	100.00	41.60	10.53	6.09	4.93	3.52	1, 2
R2	139	33.41	13.90	1.73	1.28	1.80	1.38	3, 4

Gate: G1
Total Events: 1000
Y Parameter: FL2-H (Log)

Gated Events: 416
X Parameter: FL1-H (Log)

Gate	Events	% Gated	% Total
G1	416	100.00	41.60
G2	139	33.41	13.90
G3	277	66.59	27.70

X Parameter: FL1-H (Log)

Marker	Left, Right	Events	% Gated	% Total	Mean	Geo Mean	CV	Median	Peak Ch
All	1, 9910	416	100.00	41.60	10.53	6.09	82.56	9.82	1

Figure 79. FACS results from hMSCs/alginate beads cultured in DMEM (control) and labeled with SH2.

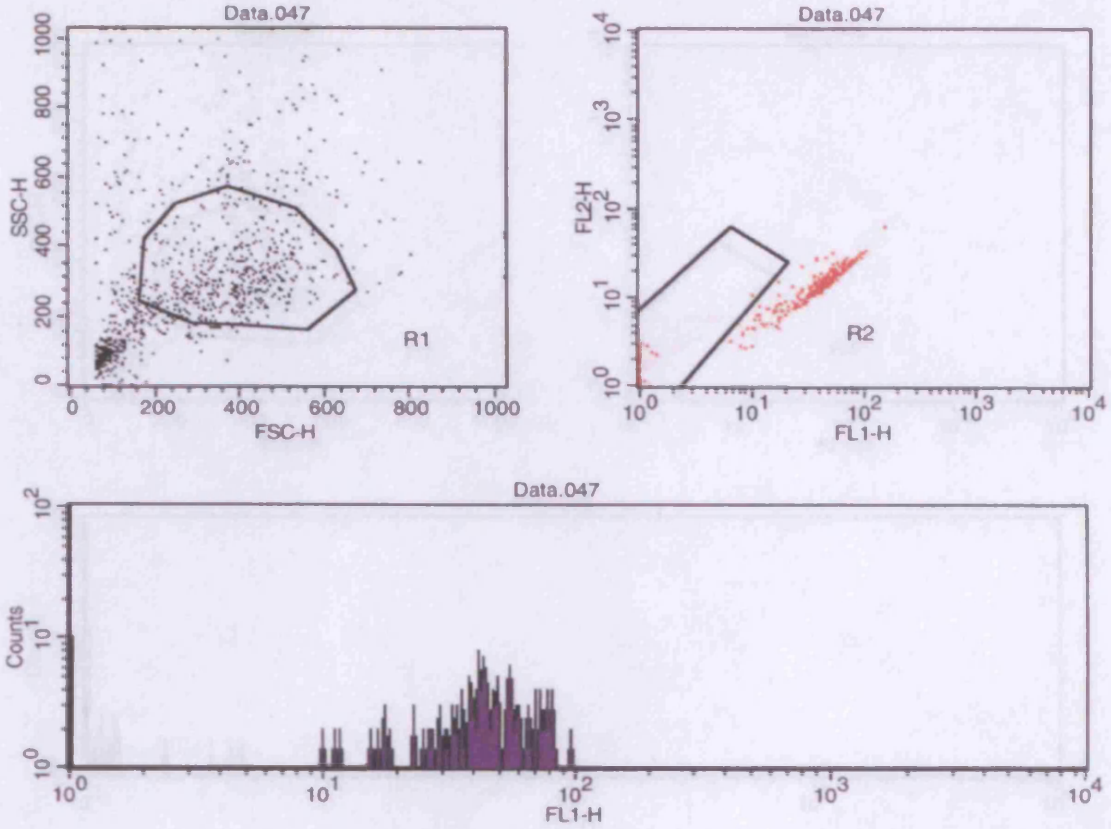

Gate: G1
Total Events: 1000
Y Parameter: FL2-H (Log)

Gated Events: 452
X Parameter: FL1-H (Log)

Region	Events	% Gated	% Total	X Mean	X Geo Mean	Y Mean	Y Geo Mean	Px,Py
R1	452	100.00	45.20	30.33	12.34	10.47	6.13	1, 2
R2	142	31.42	14.20	1.11	1.04	1.25	1.15	3, 4

Gate: G1
Total Events: 1000
Y Parameter: FL2-H (Log)

Gated Events: 452
X Parameter: FL1-H (Log)

Gate	Events	% Gated	% Total
G1	452	100.00	45.20
G2	142	31.42	14.20
G3	310	68.58	31.00

X Parameter: FL1-H (Log)

Marker	Left, Right	Events	% Gated	% Total	Mean	Geo Mean	CV	Median	Peak Ch
All	1, 9910	452	100.00	45.20	30.33	12.34	86.08	32.34	1

Figure 80. FACS results from hMSCs/alginate beads cultured in DMEM (control) and labeled with SH4.

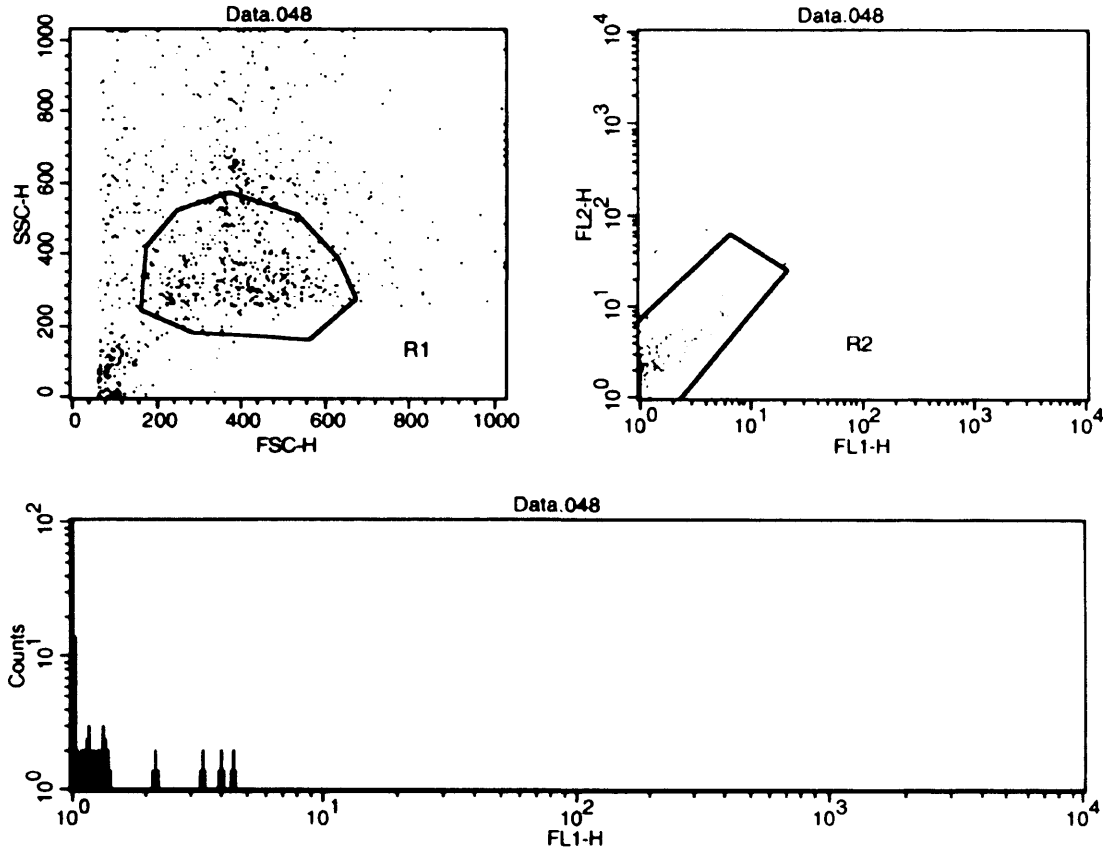

Gate: G1 Gated Events: 441
Total Events: 1000 X Parameter: FL1-H (Log)
Y Parameter: FL2-H (Log)

Region	Events	% Gated	% Total	X Mean	X Geo Mean	Y Mean	Y Geo Mean	Px,Py
R1	441	100.00	44.10	1.31	1.14	2.14	1.43	1, 2
R2	437	99.09	43.70	1.26	1.13	1.75	1.39	3, 4

Gate: G1 Gated Events: 441
Total Events: 1000 X Parameter: FL1-H (Log)
Y Parameter: FL2-H (Log)

Gate	Events	% Gated	% Total
G1	441	100.00	44.10
G2	437	99.09	43.70
G3	4	0.91	0.40

X Parameter: FL1-H (Log)

Marker	Left, Right	Events	% Gated	% Total	Mean	Geo Mean	CV	Median	Peak Ch
All	1, 9910	441	100.00	44.10	1.31	1.14	105.42	1.00	1

Figure 81. FACS results from hMSCs/alginate beads cultured in DMEM (control) and labeled with ASMA.

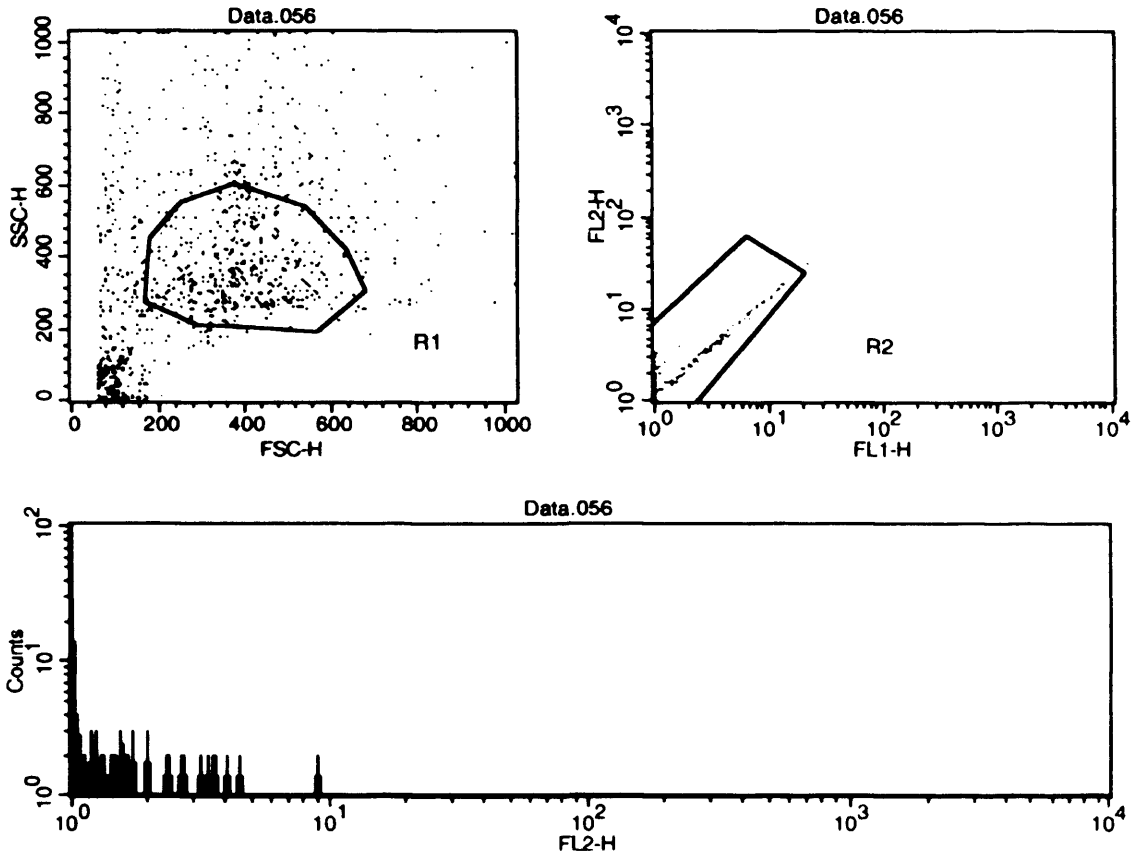

Gate: G1 Gated Events: 424
Total Events: 1000 X Parameter: FL1-H (Log)
Y Parameter: FL2-H (Log)

Region	Events	% Gated	% Total	X Mean	X Geo Mean	Y Mean	Y Geo Mean	Px,Py
R1	424	100.00	42.40	1.68	1.27	2.05	1.43	1, 2
R2	423	99.76	42.30	1.63	1.26	1.98	1.41	3, 4

Gate: G1 Gated Events: 424
Total Events: 1000 X Parameter: FL1-H (Log)
Y Parameter: FL2-H (Log)

Gate	Events	% Gated	% Total
G1	424	100.00	42.40
G2	423	99.76	42.30
G3	1	0.24	0.10

X Parameter: FL2-H (Log)

Marker	Left, Right	Events	% Gated	% Total	Mean	Geo Mean	CV	Median	Peak Ch
All	1, 9910	424	100.00	42.40	2.05	1.43	147.17	1.00	1

Figure 82. FACS results from hMSCs/alginate beads cultured in CDMEM with rSMC co-cultures not labeled (empty).

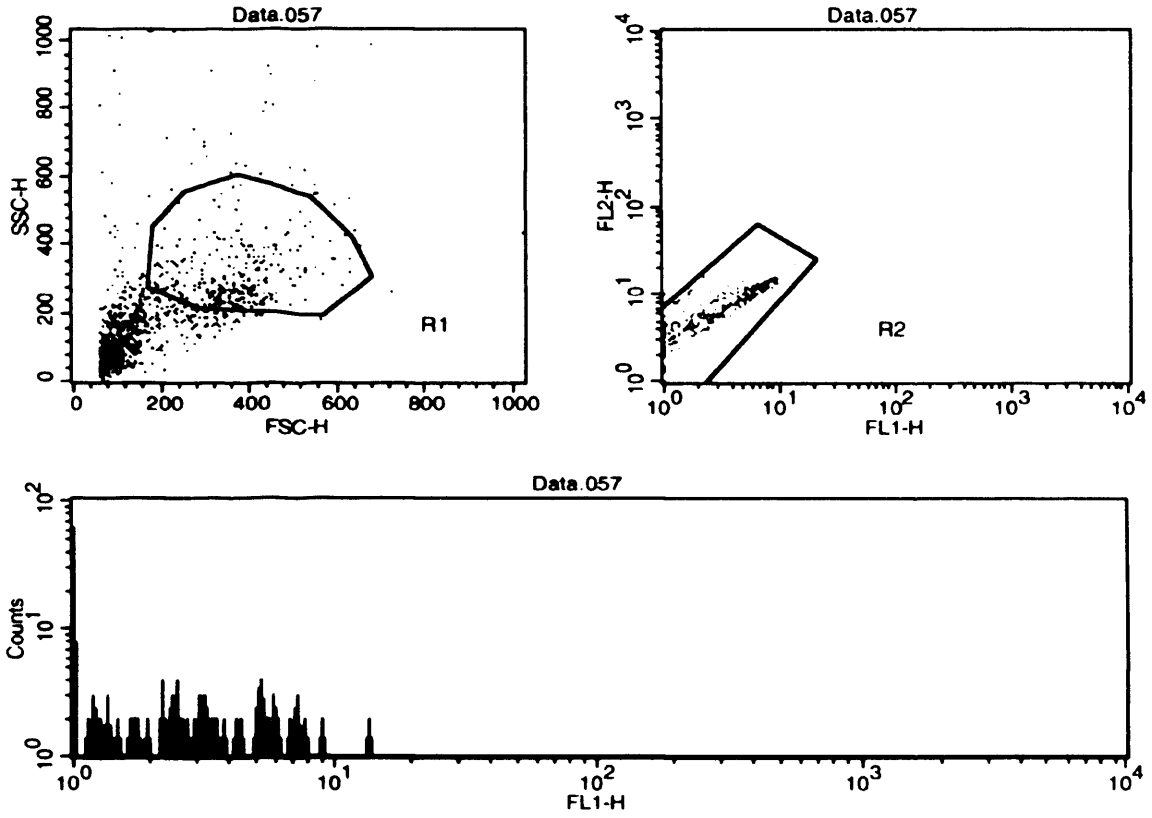

Gate: G1 Gated Events: 278
Total Events: 1000 X Parameter: FL1-H (Log)
Y Parameter: FL2-H (Log)

Region	Events	% Gated	% Total	X Mean	X Geo Mean	Y Mean	Y Geo Mean	Px,Py
R1	278	100.00	27.80	3.35	2.53	6.77	5.34	1, 2
R2	276	99.28	27.60	3.37	2.55	6.76	5.32	3, 4

Gate: G1 Gated Events: 278
Total Events: 1000 X Parameter: FL1-H (Log)
Y Parameter: FL2-H (Log)

Gate	Events	% Gated	% Total
G1	278	100.00	27.80
G2	276	99.28	27.60
G3	2	0.72	0.20

X Parameter: FL1-H (Log)

Marker	Left, Right	Events	% Gated	% Total	Mean	Geo Mean	CV	Median	Peak Ch
All	1, 9910	278	100.00	27.80	3.35	2.53	77.21	2.46	1

Figure 83. FACS results from hMSCs/alginate beads cultured in CDMEM with rSMC co-cultures and labeled with CD34.

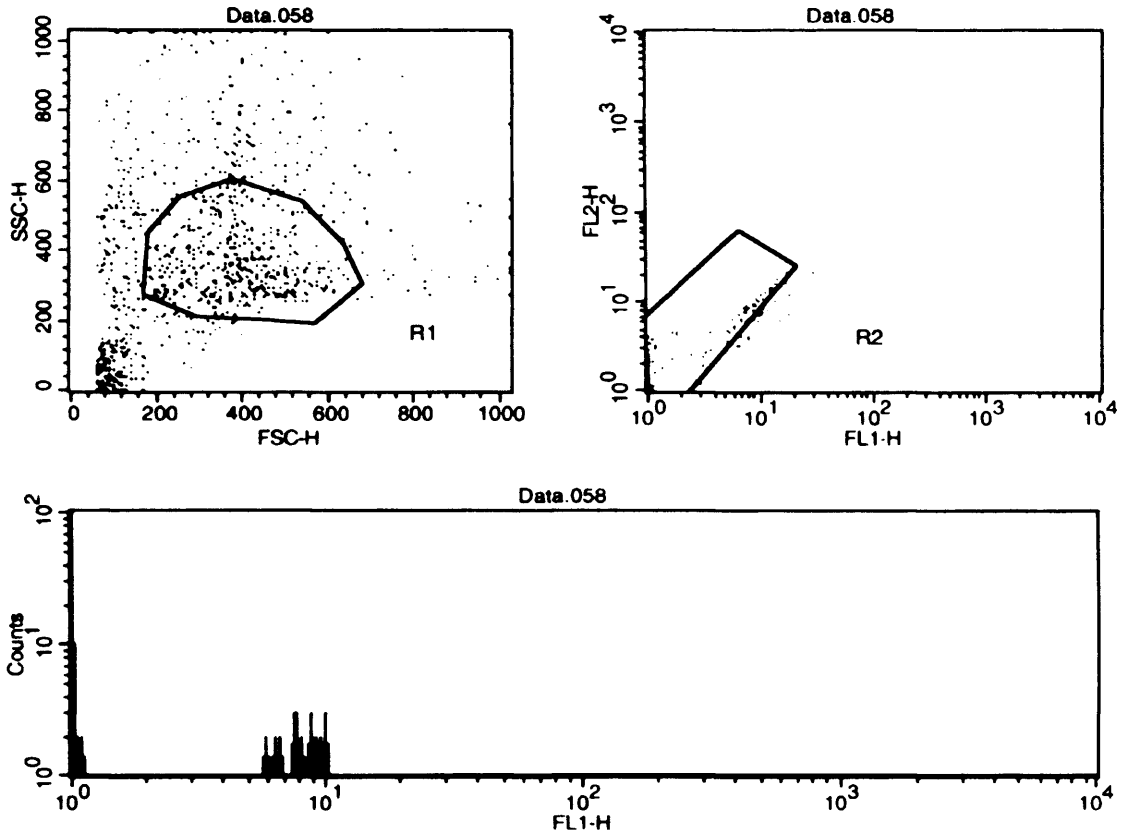

Gate: G1 Gated Events: 454
Total Events: 1000 X Parameter: FL1-H (Log)
Y Parameter: FL2-H (Log)

Region	Events	% Gated	% Total	X Mean	X Geo Mean	Y Mean	Y Geo Mean	Px,Py
R1	454	100.00	45.40	2.50	1.47	2.35	1.56	1, 2
R2	422	92.95	42.20	1.80	1.27	1.99	1.41	3, 4

Gate: G1 Gated Events: 454
Total Events: 1000 X Parameter: FL1-H (Log)
Y Parameter: FL2-H (Log)

Gate	Events	% Gated	% Total
G1	454	100.00	45.40
G2	422	92.95	42.20
G3	32	7.05	3.20

X Parameter: FL1-H (Log)

Marker	Left, Right	Events	% Gated	% Total	Mean	Geo Mean	CV	Median	Peak Ch
All	1, 9910	454	100.00	45.40	2.50	1.47	154.78	1.00	1

Figure 84. FACS results from hMSCs/alginate beads cultured in CDMEM with rSMC co-cultures and labeled with SH2.

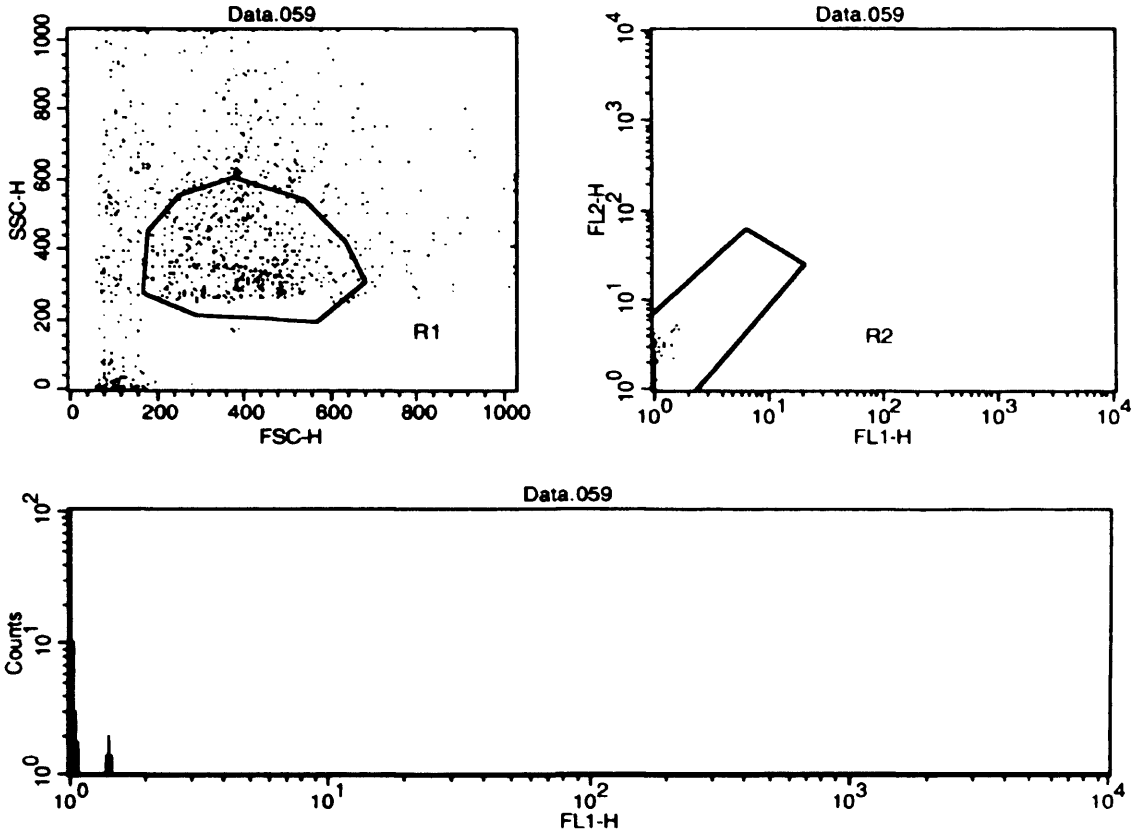

Gate: G1 Gated Events: 485
Total Events: 1000 X Parameter: FL1-H (Log)
Y Parameter: FL2-H (Log)

Region	Events	% Gated	% Total	X Mean	X Geo Mean	Y Mean	Y Geo Mean	Px,Py
R1	485	100.00	48.50	1.01	1.01	1.24	1.16	1, 2
R2	485	100.00	48.50	1.01	1.01	1.24	1.16	3, 4

Gate: G1 Gated Events: 485
Total Events: 1000 X Parameter: FL1-H (Log)
Y Parameter: FL2-H (Log)

Gate	Events	% Gated	% Total
G1	485	100.00	48.50
G2	485	100.00	48.50
G3	0	0.00	0.00

X Parameter: FL1-H (Log)

Marker	Left, Right	Events	% Gated	% Total	Mean	Geo Mean	CV	Median	Peak Ch
All	1, 9910	485	100.00	48.50	1.01	1.01	6.19	1.00	1

Figure 85. FACS results from hMSCs/alginate beads cultured in CDMEM with rSMC co-cultures and labeled with SH4.

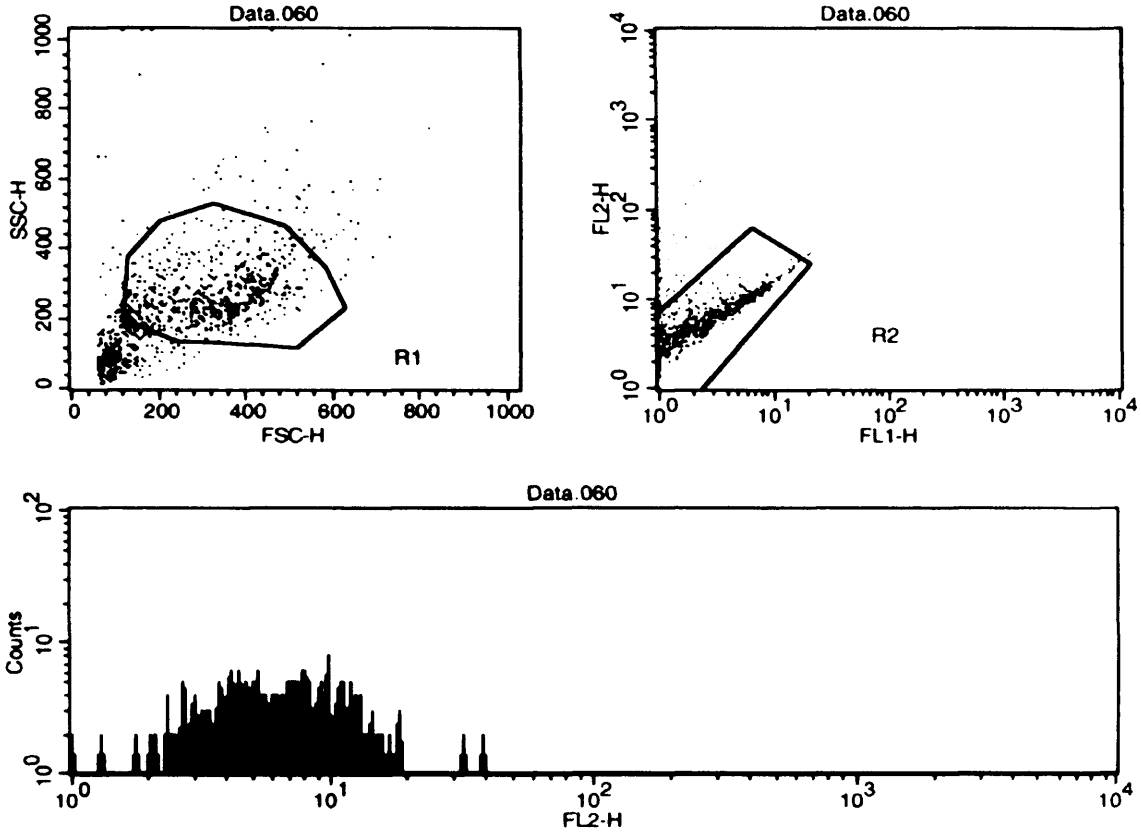

Gate: G1 Gated Events: 584
Total Events: 1000 X Parameter: FL1-H (Log)
Y Parameter: FL2-H (Log)

Region	Events	% Gated	% Total	X Mean	X Geo Mean	Y Mean	Y Geo Mean	Px,Py
R1	584	100.00	58.40	3.47	2.62	9.48	6.76	1, 2
R2	542	92.81	54.20	3.52	2.73	7.24	6.10	3, 4

Gate: G1 Gated Events: 584
Total Events: 1000 X Parameter: FL1-H (Log)
Y Parameter: FL2-H (Log)

Gate	Events	% Gated	% Total
G1	584	100.00	58.40
G2	542	92.81	54.20
G3	42	7.19	4.20

X Parameter: FL2-H (Log)

Marker	Left, Right	Events	% Gated	% Total	Mean	Geo Mean	CV	Median	Peak Ch
All	1, 9910	584	100.00	58.40	9.48	6.76	157.21	6.67	9

Figure 86. FACS results from hMSCs/alginate beads cultured in CDMEM with rSMC co-cultures and labeled with ASMA.

7. References

Adams, P.A. and Berman, M.C. A Kinetic Standard for Precise Calibration of Spectrophotometer Cell Temperature. *Clinical Chemistry* 27:5 (1981) 753-755

Agerholm, J.S., Jensen, N.E., Dantzer, V., Jensen, H.E, Aarestrup, F.M. Experimental Infection of Pregnant Cows with Bacillus Licheniformis Bacteria. *Veterinary Pathology* 36:3 (1999) 191-201

Agerholm, J.S., Jensen, N.E., Giese, S.B., Jensen, H.E. A Preliminary Study on the Pathogenicity of Bacillus Licheniformis Bacteria in Immunodepressed Mice. *Acta Pathologica, Microbiologica, et Immunologica Scandinavica* 105:1 (1997) 48-54

Alsberg, E., Anderson, K.W., Albeiruti, A., Franceschi, R.T., Mooney, D.J. Cell-Interactive Alginate Hydrogels for Bone Tissue Engineering. *Journal of Dental Research* 80: 11 (2001) 2025-2029

Alsberg, E., Kong, H.J., Hirano, Y., Smith, M.K., Albeiruti, A., Mooney, D.J. Regulating Bone Formation via Controlled Scaffold Degradation. *Journal of Dental Research* 82:11 (2003) 903-908

Al-Shamkhani, A. and Duncan R. Radioiodination of Alginate Via Covalently-Bound Tyrosinamide Allows Monitoring of Its Fate In Vivo. *Journal of Bioactive and Compatible Polymers* 10 (1995) 4-13

Atala, A., Kim, W., Paige, K.T., Vancanti, C.A., Retik, A.B. Endoscopic Treatment of Vescoureteral Reflux with a Chondrocyte-Alginate Suspension. *Journal of Urology* 152 (1994) 641-643

Baffi, R.A. and Garnick, R.L. Quality Control Issues in the Analysis of Lyophilized Proteins. *Developments in Biological Standardization* 74 (1992) 181-184

Bak, H., Afoke, A., McLeod, A.J., Brown, R., Ayazi-Shamlou, P., Dunnill, P. The Impact of Rheology of Human Fibronectin-Fibrinogen Solutions on Fibre Extrusion for Tissue Engineering. *Chemical Engineering Science* 57 (2002) 913-920

Barry, F.P., Boynton, R.E., Haynesworth, S., Murphy, J.M., Zaia, J. The Monoclonal Antibody SH-2, Raised Against Human Mesenchymal Stem Cells, Recognizes an Epitope on Endoglin (CD105). *Biochemical and Biophysical Research Communications* 265 (1999) 134-139

Batt, D.B. and Roberts, T.M. Cell Density Modulates Protein-Tyrosine Phosphorylation. *The Journal of Biological Chemistry* 273:6 (1998) 3408-3418

Biowhittaker Product Catalogue. Formulation for Dulbecco's Modified Eagle Medium. (2001) 73-74

Blue, S.R., Singh, V.R., Saubolle, M.A. Bacillus Licheniformis Bacteremia: Five Cases Associated with Indwelling Central Venous Catheters. *Clinical Infectious Diseases* 20:3 (1995) 629-633

Bourassa, M.G., Enjalbert, M., Campeau, L., Lesperance, J. Progression of Atherosclerosis in Coronary Arteries and Bypass Grafts: Ten Years Later. *The American Journal of Cardiology* 53:12 (1984) 102C-107C

Brittberg, M., Lindahl, A., Nilsson, A., Ohlsson, C., Isaksson, O., Peterson, L. Treatment of Deep Cartilage Defects in the Knee with Autologous Chondrocyte Transplantation. *The New England Journal of Medicine* 331:14 (1994) 889-895

Bruder, S.P., Jaiswal, N., Haynesworth, S.E. Growth Kinetics, Self-Renewal, and the Osteogenic Potential of Purified Human Mesenchymal Stem Cells During Extensive Subcultivation and Following Cryopreservation. *Journal of Cellular Biochemistry* 64 (1997) 278-294

Butler, M. *Animal Cell Culture & Technology*. Abingdon, UK: Garland Science/BIOS Scientific Publishers, 2004

Campbell, J.H. and Campbell, G.R. Endothelial Cell Influences on Vascular Smooth Muscle Phenotype. *Annual Review of Physiology* 48 (1986) 295-306

Caplan, A.I. and Bruder, S.P. Mesenchymal Stem Cells: Building Blocks for Molecular Medicine in the 21st Century. *TRENDS in Molecular Medicine* 7 (2001) 259-264

Caldamone, A.A. and Diamond, D.A. Long-Term Results of the Endoscopic Correction of Vesicoureteric Reflux in Children Using Autologous Chondrocytes. *The Journal of Urology* 165 (2001) 2224-2227

Carmeliet, P. One Cell, Two Fates. *Nature* 408 (2000) 43-44

Carmeliet, P. and Jain, R.K. Angiogenesis in Cancer and Other Diseases. *Nature* 407 (2000) 249-257

Carrier, R.L., Papadaki, M., Rupick, M., Schoen, F.J., Bursac, N., Langer, R., Freed, L.E., Vunjak-Novakovic, G. Cardiac Tissue Engineering: Cell Seeding, Cultivation Parameters, and Tissue Construct Characterization. *Biotechnology and Bioengineering* 64 (1999) 580 – 589

Chandy, T., Rao, G.H., Wilson, R.F., Das, G.S. The Development of Porous Alginate/Elastin/PEG Composite Matrix for Cardiovascular Engineering. *Journal of Biomaterials Applications* 17:4 (2003) 287-301

Charbord, P., Remy-Martin, J.P., Tamayo, E., Bernard, G., Keating, A., Peault, B. Analysis of the Microenvironment Necessary for Engraftment: Role of the Vascular Smooth Muscle-Like Stromal Cells. *Journal of Hematotherapy and Stem Cell Research* 9 (2000) 935-943

Chung, T.W., Lu, Y.F., Wang, S.S., Lin, Y.S., Chu, S.H. Growth of Human Endothelial Cells on Photochemically Grafted Gly-Arg-Gly-Asp (GRGD) Chitosans. *Biomaterials* 23 (2002) 4803-4809

Ciapetti, G., Cenni, E., Pratelli, L. and Pizzoferrato, A. In Vitro Evaluation of Cell/Biomaterial Interaction by MTT Assay. *Biomaterials* 14 (5) (1993) 359-364.

Constantinidis, I., Rask, I., Long, R. C., Sambanis, A. Effects of Alginate Composition on the Metabolic, Secretory, and Growth Characteristics of Entrapped βTC3 Mouse Insulinoma Cells. *Biomaterials* 20 (1999) 2019-2027

Coulson, J.M. and Richardson, J.F. *Chemical Engineering Volume 1: Fluid Flow, Heat Transfer and Mass Transfer*, Fifth Edition, Butterworth-Heinemann, UK (1996) 52

D'Addario, S.F., Morgan, M., Talley, L., Smoller, B.R. h-Caldesmon as a Specific Marker of Smooth Muscle Cell Differentiation in Some Soft Tissue Tumors of the Skin. *Journal of Cutaneous Pathology* 29:7 (2002) 426-429

Dahl, S.L., Koh, J., Prabhakar, V., Niklason, L.E. Decellularized Native and Engineered Arterial Scaffolds for Transplantation. *Cell Transplant* 12:6 (2003) 659-666

Dar, A., Shachar, M, Leor, J., Cohen, S. Optimization of Cardiac Cell Seeding and Distribution in 3D Porous Alginate Scaffolds. *Biotechnology and Bioengineering* 80(3) (2002) 305-312

Davies, M.G. and Hagen, P.O. Pathophysiology of Vein Graft Failure: a Review. *European Journal of Vascular and Endovascular Surgery* 9 (1995) 7-18

Deans, R.J. and Moseley, A.B. Mesenchymal Stem Cells: Biology and Potential Clinical Uses. *Experimental Hematology* 28 (2000) 875-884

Deasy, B.M., Jankowski, R.J., Huard, J. Muscle-Derived Stem Cells: Characterization and Potential for Cell-Mediated Therapy. *Blood Cells, Molecules, and Diseases* 27:5 (2001) 924-933

Dennis, J.E. and Charbord, P. Origin and Differentiation of Human and Murine Stroma. *Stem Cells* 20:3 (2002) 205-214

Devine, S.M., Peter, S., Martin, B.J., Barry, F. McIntosh, K.R. Mesenchymal Stem Cells: Stealth and Suppression. *Cancer Journal* 7:Suppl 2 (2001) S76-82

DeVos, P., DeHaan, B.J., Wolters, G.H.J., Strubbe, J.H., VanSchilfgaarde, R. Improved Biocompatibility but Limited Graft Survival After Purification of Alginate for Microencapsulation of Pancreatic Islets. *Diabetologia* 40 (1997) 262-270

Deutsch, M., Meinhart, J., Fischlein, T., Presiss, P., Zilla, P. Clinical Autologous In Vitro Endothelialization of Infrainguinal ePTFE Grafts in 100 Patients: a 9-Year Experience. *Surgery* 126 (1999) 847-855

Doran, P.M. *Bioprocess Engineering Principles*, Academic Press Ltd. (1995) 262-265, 277-279

Dormont, D. Prion Diseases: Pathogenesis and Public Health Concerns. *Federation of European Biochemical Societies Letters* 529:1 (2002) 17-21

Doumeche, B., Kuppers, M., Stapf, S., Blumich, B., Hartmeier, W., Ansorge-Schumacher, M.B. New Approaches to the Visualization, Quantification and Explanation of Acid-Induced Water Loss from Ca-Alginate Hydrogel Beads. *Journal of Microencapsulation* 21:5 (2004) 565-73

Dvir-Ginzberg, M., Gamlieli-Bonshtein, I., Agbaria, R., Cohen, S. Liver Tissue Engineering Within Alginate Scaffolds: Effects of Cell-Seeding Density on Hepatocyte Viability, Morphology, and Function. *Tissue Engineering* 9:4 (2003) 757-766

Eid, K., Chen, E., Griffith, L., Glowacki, J. Effect of RGD Coating on Osteocompatibility of PLGA-Polymer Disks in a Rat Tibial Wound. *Journal of Biomedical Materials Research* 57:2 (2001) 224-231

Eiselt, P., Yeh, J., Latvala, R.K., Shea, L.D., Mooney, D.J. Porous Carriers for Biomedical Applications Based on Alginate Hydrogels. *Biomaterials* 21 (2000) 1921-1927

Ertel, S.I, Ratner, B.D., Horbett, T.A. Radiofrequency Plasm Deposition of Oxygen-Containing Films on Polystryrene and Poly(ethylene terephthalate) Substrates Improves Endothelial Cell Growth. *Journal of Biomedical Materials Research* 24:12 (1990) 1637-1659

Ferrari, M., Fornasiero, M.C., Isetta, A.M. MTT Colorimetric Assay for Testing Macrophage Cytotoxic Activity *In Vitro*. *Journal of Immunological Methods.* 131 (1990) 165-172

Ferrera, R., Larese, A., Berthod, F., Guidollet, J., Rodriquez, C., Dureau, G. and Dittmar, A. Quantitative Reduction of MTT by Heart Biopsies *In Vitro* is an Index of Viability. *Journal of Molecular and Cellular Cardiology* 25:9 (1993), 1091-1099

Francis, S.C., Raizada, M.K., Mangi, A.A., Melo, L.G., Dzau, V.J., Vale, P.R., Isner, J.M., Losordo, D.W., Chao, J., Katovich, M.J., Berecek, K.H. Genetic Targeting for Cardiovascular Therapeutics: Are We Near the Summit or Just Beginning the Climb? *Physiological Genomics* 7 (2001) 79-94

Freshney, R.I. *Culture of Animal Cells.* Wiley-Liss, Inc., New York, New York (1994)

Gallico, G.G., O'Connor, N.E., Compton, C.C., Kehinde, O., Green, H. Permanent Coverage of Large Burn Wounds with Autologous Cultured Human Epthelium. *New England Journal of Medicine* 311:7 (1984) 448-451

Galmiche, M.C., Koteliansky, V.E., Briere, J., Herve, P., Charbord, P. Stromal Cells from Human Long-Term Marrow Cultures Are Mesenchymal Cells That Differentiate

Following a Vascular Smooth Muscle Differentiation Pathway. *Blood* 82 :1 (1993) 66-76

Galotto, M., Berisso, G., Delfino, L., Podesta, M., Ottaggio, L., Dallorso, S., Dufour, C., Ferrara, G.B., Abbondandolo, A., Dini, G., Bacigalupo, A., Cancedda, R., Quarto, R. Stromal Damage as Consequence of High-Dose Chemo/Radiotherapy in Bone Marrow Transplant Recipients. *Experimental Hematology* 27 (1999) 1460-1466

Genes, N.G., Rowley, J.A., Mooney, D.J., Bonassar, L.J. Effect of Substrate Mechanics on Chondrocyte Adhesion to Modified Alginate Surfaces. *Archives of Biochemistry and Biophysics* 422 (2004) 161-167

Geppert T.D. and Lipsky P.E. Antigen Presentation by Interferon-γ-Treated Endothelial Cells and Fibroblasts: Differential Ability to Function as Antigen-Presenting Cells Despite Comparable Ia Expression. *The Journal of Immunology* 135:6 (1985) 3750-3762

Gepstein, L. Derivation and Potential Applications of Human Embryonic Stem Cells. *Circulation Research* 91:10 (2002) 866-876

Giannobile, W.V. Periodontal Tissue Engineering by Growth Factors. *Bone* 19:1 Suppl (1996) 23S-37S

Girton, T.S., Oegema, T.R., Grassl, E.D., Isenberg, B.C., Tranquillo, R.T. Mechanisms of Stiffening and Strengthening in Media-Equivalents Fabricated Using Glycation. *Journal of Biomechanical Engineering* 122 (3) (2000) 216-223

Gooch, K.J., Blunk, T., Vunjak-Novakovic, G., Langer, R., Freed, L.E. Mechanical Forces and Growth Factors Utilized in Tissue Engineering. In: *Frontiers in Tissue Engineering*, edited by Patrick, C.W., Mikos, A.G., and McIntire, L.V., Pergamon, Oxford (1998) 68-75

Goosen, M.F. Physico-Chemical and Mass Transfer Considerations in Microencapsulation. *Annuals of the New York Academy of Sciences* 875 (1999) 84-104

Green, L.M., Reade, J.L., Ware, C.F. Rapid Colorimetric Assay for Cell Viability: Application to the Quantification of Cytotoxic and Growth Inhibitory Lymphokines. *Journal of Immunological Methods* 70 (1984) 257-268

Griffith, L.G. and Naughton, G. Tissue Engineering – Current Challenges and Expanding Opportunities. *Science* 295 (2002) 1009-1014

Grodin, C.M., Campeau, L., Lesperance, J., Enjalbert, M., Bourassa, M.G. Comparison of Late Changes in Internal Mammary Artery and Saphenous Vein Grafts in Two Consecutive Series of Patients 10 Years after Operation. *Circulation* 70: 3 Pt 2 (1984) I208-I212

Gronthos, S. and Simmons, P.J. The Growth Factor Requirements of STRO-1-Positive Human Bone Marrow Stromal Precursors Under Serum-Deprived Conditions In Vitro. *Blood* 85:4 (1995) 929-940

Halberstadt, C., Austin, C., Rowley, J., Culberson, C., Loebsack, A., Wyatt, S., Coleman, S., Blacksten, L., Burg, K., Mooney, D., Holder, W. A Hydrogel for Plastic and Reconstructive Applications Injected into the Subcutaneous Space of a Sheep. *Tissue Engineering* 8 (2) (2002) 309-319

Harding, S.I., Underwood, S., Brown, R.A., Dunnill, P. Assessment of Cell Alignment by Fibronectin Multi-Fiber Cables Capable of Large Scale Production. *Bioprocess Engineering* 22 (2000) 159-164

Harding, S.I., Afoke, A., Brown, R.A., McLeod, A.J., Ayazi-Shamlou, P., Dunnill, P. Engineering and Cell Attachment Properties of Human Fibronectin-Fibrinogen Tubes Suitable as Scaffolds for the Preparation of Tissue Engineered Blood Vessels. *Bioprocess Biosystems Engineering* 25:1 (2002) 53-59

Harris, D.A. Light Spectroscopy. BIOS Scientific Publishers Ltd., Oxford, UK (1996)

Hasse, C., Klock, G., Schlosser, A., Zimmermann, U., Rothmund, M. Parathyroid Allotransplantation Without Immunosuppression. *Lancet* 350:9087 (1997) 1296-1297

Haug, A., Larsen, B., Smidsrod, O. The Degradation of Alginates at Different pH values. *Acta Orthopaedica Scandinavica* 17 (1963) 1466-1468

Hauselmann, H.J., Fernandes, R.J., Mok, S.S., Schmid, T.M., Block, J.A., Aydelotte, M.B., Kuettner, K.E., Thonar, E.J.-M.A. Phenotypic Stability of Bovine Articular Chondrocytes After Long-Term Culture in Alginate Beads. *Journal of Cell Science* 107 (1994) 17-27

Hayflick, L. The Limited *In Vitro* Lifetime of Human Diploid Cell Strains. *Experimental Cell Research* 37 (1965) 614-636

Haynesworth, S.E., Baber, M.A., Caplan, A.I. Cell Surface Antigens on Human Marrow-Derived Mesenchymal Cells Are Detected by Monoclonal Antibodies. *Bone* 13 (1992) 69-80

He, Q., Cahill, C.J., Spiro M.J. Suspension Culture of Differentiated Rat Heart Myocytes on Non-adhesive Surfaces. *Journal of Molecular and Cellular Cardiology* 28 (1996) 1177-1186

Heo, D.S., Park, J.G., Hata, K., Day, R., Herberman, R.B., Whiteside, T.L. Evaluation of Tetrasolium-based Semiautomatic Colormetric Assay for Measurement of Human Antitumor Cytotoxicity. *Cancer Research* 50 (1990) 3681-3690

Higgens, S.P., Solan, A.K., Niklason, L.E. Effects of Polyglycolic Acid on Porcine Smooth Muscle Cell Growth and Differentiation. *Journal of Biomedical Biomaterials Research* 67A (2003) 295-302

Hiles, M.C., Badylak, S.F., Lantz, G.C., Kokini, K., Geddes, L.A., Morff, R.J. Mechanical Properties of Xenogeneic Small-Intestinal Submucosa When Used as an Aortic Graft in the Dog. *Journal of Biomedical Materials Research* 29 (1995) 883-891

Hirai, J., Kanda, K., Oka, T., Matsuda, T. Highly Orientated, Tubular Hybrid Vascular Tissue for a Low Pressure Circulatory System. *Transactions of the American Society of Artifical Internal Organs* 40 (1994) M383-88

Howell, T.H., Fiorellini, J.P., Paquette, D.W., Offenbacher, S., Antoniades, H.N., Lynch, S.E. Evaluation of a Combination of Recombinant Human Platelet-Derived Growth Factor-BB and Recombinant Human Insulin-Like Growth Factor-I in Patients with Periodontal Disease. *Journal of Dental Research* 74 (1995) 253

Hubbell, J.A. Matrix Effects. In: *Principles of Tissue Engineering*, Second Edition, Lanza, R., Langer, R., Vacanti, J. editors, Academic Press (2000) 237-250

Hunt, J.P., Hunter, C.T., Brownstein, M., Hultman, C.S., deSerres, S., Bracey, L., Frelinger, J., Meyer, A.A. Host Priming, Not Target Antigen Type, Decides Rejection Rate in Mice Primed with MHC II "Knockout" Cultured Keratinocytes. *The Journal of Surgical Research* 76:1 (1998) 32-36

Huveners-Oorspong, M.B.M., Hoogenboom, L.A.P., Kuiper, H.A. The Use of the MTT Test for Determining the Cytotoxicity of Veterinary Drugs in Pig Hepatocytes. *Toxicology in Vitro* 11 (1997) 385-392

Huynh, T., Abraham, G., Murray, J., Brockbank, K., Hagen, P.O., Sullivan, S. Remodeling of an Acellular Collagen Graft into a Physiologically Responsive Neovessel. *Nature Biotechnology* 17 (1999) 1083-1086

Iannuccelli, V., Coppi, G., Bondi, M., Pinelli, M., Mingione, A., Cameroni, R. Biodegradable Intraoperative System for Bone Infection Treatment II. In Vivo Evaluation. *International Journal of Pharmaceutics* 143 (1996) 187-194

Inoue, Y., Anthony, J.P., Lleon, P., Young, D.M. Acellular Human Dermal Matrix as a Small Vessel Substititute. *Journal of Reconstructive Microsurgery* 12 (1996) 307-311

Ishiyama, M., Miyazono, Y., Sasamoto, K., Ohkura, Y., Ueno, K. A Highly Water-Soluble Disulfonated Tetrazolium Salt as a Chromogenic Indicator for NADH as well as Cell Viability. *Talanta* 44 (1997) 1299-1305

Jen, A.C., Wake, M.C., Mikos, A.G. Review: hydrogels for cell immobilization. *Biotechnology and Bioengineering* 50 (4) (1996) 357-364

Jiang, Y., Jahagirdar, B.N., Reinhardt, R.L., Schwartz, R.E., Keene, C.D., Ortiz-Gonzalez, X.R., Reyes, M., Lenvik, T., Lund, T., Blackstad, M., Du, J., Aldrich, S., Lisberg, A., Low, W.C., Largaespada, D.A., Verfaillie, C.M. Pluripotency of Mesenchymal Stem Cells Derived from Adult Marrow. *Nature* 418 (2002) 41-49

Llanes, F., Ryan, D.H., Marchessault, R.H. Magnetic Nanostructured Composites Using Alginates of Different M/G Ratios as Polymeric Matrix. *International Journal of Biological Macromolecules* 27 (2000) 35-40

Johnson, O.L., Cleland, J.L., Lee, H.J., Charnis, M., Duenas, E., Jaworowicz, W., Shepard, D., Shahzamani, A., Jones, A.J., Putney, S.D. A Month-Long Effect from a Single Injection of Microencapsulated Human Growth Hormone. *Nature Medicine* 2 (7) (1996) 795-799

Joki, T., Machluf, M., Atala, A., Zhu., J., Seyfried, N.T., Dunn, I.F., Abe, T., Carroll, R.S., Black, P.McL. Continuous Release of Endostatin From Microencapsulated Engineered Cells for Tumor Therapy. *Nature Biotechnology* 19 (2001) 35-39

Jones, L.J., Gray, M., Yue, S.T., Haugland, R.P., Singer, V.L. Sensitive Determination of Cell Number Using the CyQuant® Proliferation Assay. *Journal of Immunological Methods* 254 (2001) 85-98

Junqueira, L.C., Carneiro, J., Kelley, R.O. The Circulatory System. In: *Basic Histology,* 9th Edition, Lange Medical Books/McGraw-Hill (1998) 202-217

Kadner, A., Hoerstrup, S.P., Zund, G., Eid, K., Maurus, C., Melnitchouk, S., Grunenfelder, J., Turina, M.I. A New Source for Cardiovascular Tissue Engineering: Human Bone Marrow Stromal Cells. *European Journal of Cardio-thoracic Surgery* 21 (2002) 1055-1060

Kamil, S.H., Vacanti, M.P., Aminuddin, B.S., Jackson, M.J., Vacanti, C.A., Eavey, R.D. Tissue Engineering of a Human Sized and Shaped Auricle Using a Mold. *Laryngoscope* 114 (2004) 867-870

Katz, A., Alimova, A., Xu, M., Gottlieb, P., Rudolph, E., Steiner, J.C., Alfano, R.R. In Situ Determination of Refractive Index and Size of Bacillus Spores by Light Transmission. *Optics Letters* 30:6 (2005) 589-591

Khot, U.N., Friedman, D.T., Pettersson, G., Smedira, N.G., Li, J., Ellis, S.G. Radial Artery Bypass Grafts Have an Increased Occurrence of Angiographically Severe Stenosis and Occlusion Compared With Left Internal Mammary Arteries and Saphenous Vein Grafts. *Circulation* 109 (2004) 2086-2091

Kilpatrick, T.J., Talman, P.S., Bartlett, P.F. The Differentiation and Survival of Murine Neurons *In Vitro* is Promoted by Soluble Factors Produced by an Astrocytic Cell Line. *The Journal of Neuroscience Research* 35:2 (1993) 147-161

Kimes, B. W. and Brandt, B. L. Characterization of Two Putative Smooth Muscle Cell Lines from Rat Thoracic Aorta. *Experimental Cell Research* 98 (1976) 349-366

Kinner, B., Zaleskas, J.M., Spector, M. Regulation of Smooth Muscle Actin Expression and Contraction in Adult Human Mesenchymal Stem Cells. *Experimental Cell Research* 278 (2002) 72-83

Klinkert, P., Post, P.N., Breslau, P.J., vanBockel, J.H. Saphenous Vein Versus PTFE for Above-Knee Femoropopliteal Bypass. A Review of the Literature. *European Journal of Vascular and Endovascular Surgery* 27:4 (2004) 357-62

Klock, G., Frank, H., Houben, R., Zekorn, T., Horcher, A., Siebers, U., Wohrle, M., Federlin, K., Zimmerman, U. Production of Purified Alginates Suitable for Use in Immunoisolated Transplantation. *Applied Microbiology and Biotechnology* 40 (1994) 638-643

Koc, O.N. and Lazarus, H.M. Mesenchymal Stem Cells: Heading into the Clinic. *Bone Marrow Transplantation* 27 (2001) 235-239

Kong, H.J., Smith, M.K., Mooney, D.J. Designing Alginate Hydrogels to Maintain Viability of Immobilized Cells. *Biomaterials* 24 (2003) 4023-4029

Kukreti, S., Konstantopoulos, K., McIntire, L.V. Cell-Cell Interactions. In: *Frontiers in Tissue Engineering*, edited by Patrick, C.W., Mikos, A.G., and McIntire, L.V., Pergamon, Oxford (1998) 29-37

Kuznetsov, S.A., Mankani, M.H., Gronthos, S., Satomura, K., Bianco, P., Robey, P.G. Circulating Skeletal Stem Cells. *The Journal of Cell Biology* 153:5 (2001) 1133-1139

Laham, R.J., Sellke, F.W., Edelman, E.R., Pearlman, J.D., Ware, J.A., Brown, D.L., Gold, J.P., Simons, M. Local Perivascular Delivery of Basic Fibroblast Growth Factor in Patients Undergoing Coronary Bypass Surgery: Results of a Phase I Randomized, Double-blind, Placebo-Controlled Trial. *Circulation* 100:8 (1999) 1865-1871

Lee, D.A., Reisler, T., Bader, D.L. Expansion of Chondrocytes for Tissue Engineering in Alginate Beads Enhances Chondrocytic Phenotype Compared to Conventional Monolayer Techniques. *Acta Orthopaedica Scandinavica* 74:1 (2003) 6-15

Lee, J.H., Kim, W.G., Kim, S.S. Lee, J.H., Lee, H.B. Development and Characterization of an Alginate Impregnated Polyester Vascular Graft. *Journal of Biomedical Materials Research* 36 (1997) 200-208

Leo, W.J., McLoughlin, A.J., Malone, D.M. Effects of Sterilization Treatments on Some Properties of Alginate Solutions and Gels. *Biotechnology Progress* 6:1 (1990) 51-53

Leor, J., Aboulafia-Etzion, S., Dar, A., Shapiro, L., Barbash, I.M., Battler, A., Granot, Y., Cohen, S. Bioengineered Cardiac Grafts A New Approach to Repair the Infarcted Myocardium? *Circulation* 102: Suppl III (2000) 56-61

L'Heureux, N., Paquet, S., Labbe, R., Germain, L., Auger, F.A. A Completely Biological Tissue-Engineered Human Blood Vessel. *The Federation of American Societies for Experimental Biology (FASEB) Journal* 12 (1998) 47-56

L'Heureux, N., Stoclet, J.C., Auger, F.A., Lagaud, G.J.L., Germain, L., Andriantsitohaina, R. A Human Tissue-Engineered Vascular Media: A New Model for Pharmacological Studies of Contractile Responses. *The Federation of American Societies for Experimental Biology (FASEB) Journal* 15 (2001) 515-524

Lindsay, D., Mosupye, F.M., Brozel, V.S., Von-Holy, A. Cytotoxicity of Alkaline-Tolerant Dairy-Associated Bacillus Spp. *Letters in Applied Microbiology* 30:5 (2000) 364-369

Lombarts, A.J., deKieviet, W., Franck, P.F., Baars, J.D. Recognition and Prevention of Two Cases of Erroneous Haemocytometry Counts Due to Platelet and White Blood Cell Aggregation. The Use of Acid Citrate Dextrose as an Auxiliary Anticoagulant. *European Journal of Clinical Chemistry and Clinical Biochemistry* 30:7 (1992) 429-432

Loop, F.D., Lytle, B.W., Cosgrove, D.M., Stewart, R.W., Goormastic, M., Williams, G.W., Golding, L.A., Gill, C.C., Taylor, P.C., Sheldon, W.C., Proudfit, W.L. Influence of the Internal-Mammary-Artery Graft on 10-Year Survival and Other Cardiac Events. *The New England Journal of Medicine* 314 (1986) 1-6

Louet, S. Reagent Safety Issues Surface For Cell/Tissue Therapies. *Nature Biotechnology* 22:3 (2004) 253-254

Lysaght, M.J. and Hazlehurst, A.L. Tissue Engineering: The End of the Beginning. *Tissue Engineering* 10:1/2 (2004) 309-320

Ma, H.-L. Hung, S.-C. Lin, S.-Y., Chen, Y.-L., Lo, W.-H. Chondrogenesis of Human Mesenchymal Stem Cells Encapsulated in Alginate Beads. *Journal of Biomedical Materials Research* 64A (2003) 273-281

Mann, B.K., Gobin, A.S., Tsai, A.T., Schmedlen, R.H., West, J.L. Smooth Muscle Cell Growth in Photopolymerized Hydrogels With Cell Adhesive and Proteolytically Degradable Domains: Synthetic ECM Analogs for Tissue Engineering. *Biomaterials* 22: 22 (2001) 3045-3051

Mann, B.K. and West, J.L. Cell Adhesion Peptides Alter Smooth Muscle Cell Adhesion, Proliferation, Migration, and Matrix Protein Synthesis on Modified Surfaces and in Polymer Scaffolds. *Journal of Biomedical Materials Research* 60 (2002) 86-93

Martinsen, A., Skjak-Braek, G., Smidsrod, O. Alginate as Immobilization Material: I. Correlation between Chemical and Physical Properties of Alginate Gel Beads. *Biotechnology and Bioengineering* 33 (1989) 79-89

Martinsen, A., Storro, I., Skjak-Braek, G. Alginate as Immobilization Material: III. Diffusional Properties. *Biotechnology and Bioengineering* 39 (1992) 186-194

Mason, C. Tissue Engineering. *Biotechnology Investment Today* 2:1 (2003a) 20-27

Mason, C. Automated Tissue Engineering: A Major Paradigm Shift in Health Care. *Medical Device Technology* 14 (2003b) 16-18.

Mason, C. Studies to Allow the Consistent Fabrication of Many Units of Engineered Tissue. University College London, UK, Doctor of Philosophy Thesis (2005)

Mason, C. and Town, M.A. Methods for forming harden sheets and tubes. Patent #WO 02/077336 (Geneva World Intellectual Property Organization) (2002)

Matsumura, G., Hibino, N., Ikada, Y., Kurosawa, H., Shin'oka, T. Successful Application of Tissue Engineered Vascular Autografts: Clinical Experience. *Biomaterials* 24 (2003a) 2303-2308

Matsumura, G., Miyagawa-Tomita, S., Shin'oka, T., Ikada, Y., Kurosawa, H. First Evidence that Bone Marrow Cells Contribute to the Construction of Tissue-Engineered Vascular Autografts in Vivo. *Circulation* 108 (2003b) 1729-1734

Matthew, I.R., Browne, R.M., Frame, J.W., Millar, B.G. Subperiosteal Behaviour of Alginate and Cellulose Wound Dressing Materials. *Biomaterials* 16 (1995) 265-274

Mavromatis, K., Fukai, T., Tate, M., Chesler, N., Ku, D.N., Galis, Z.S. Early Effects of Arterial Hemodynamic Conditions on Human Saphenous Veins Perfused Ex Vivo. *Arteriosclerosis, Thrombosis and Vascular Biology* 20:8 (2000) 1889-1895

Mayhew, T.A., Williams, G.R., Senica, M.A., Kuniholm, G., Du Moulin, G.C. Validation of a Quality Assurance Program for Autologous Cultured Chondrocyte Implantation. *Tissue Engineering* 4:3 (1998) 325-334

McKee, J.A., Banki, S.S., Boyer, M.J., Hamad, N.M., Lawson, J.H., Niklason, L.E., Counter, C.M. Human Arteries Engineered In Vitro. *European Molecular Biology Organization Reports* 4:6 (2003) 633-638

Menasche, P. Skeletal Muscle Satellite Cell Transplantation. *Cardiovascular Research* 58 (2003) 351-357

Michel, M., Germain, L., Auger, F.A. Anchored Skin Equivalent Cultured in Vitro: a New Tool for Percutaneous Absorption Studies. *In Vitro Cell Development Biology* 29A (1993) 834-837

Mitchell, S.L. and Niklason, L.E. Requirements for Growing Tissue-Engineered Vascular Grafts. *Cardiovascular Pathology* 12:2 (2003) 59-64

Moghaddam, M. J. and Matsuda, T. Development of a 3-D Artificial Extracellular Matrix Design Concept and Artificial Vascular Media. *Transactions of the American Society of Artificial Internal Organs* 37 (1991) M437-438

Molloy, C.J., Pawlowski, J.E., Taylor, D.S., Turner, C.E., Weber, H., Peluso, M., Seiler, S.M. Thrombin Receptor Activation Elicits Rapid Protein Tyrosine Phosphorylation and Stimulation of the Raf-1/MAP Kinase Pathway Preceding Delayed Mitogenesis in Cultured Rat Aortic Smooth Muscle Cells. *The Journal of Clinical Investigation* 97 (1996) 1173-1183

Mooney, D.J. and Mikos, A.G. Growing New Organs. *Scientific American Presents* (1997) 10-15

Mosmann, T. Rapid Colorimetric Assay for Cellular Growth and Survival: Application to Proliferation and Cytotoxicity Assays. *Journal of Immunological Methods*, 65 (1983) 55-63

Muguruma, Y., Reyes, M., Nakamura, Y., Sato, T., Matsuzawa, H., Miyatake, H., Akatsuka, A., Itoh, J., Yahata, T., Ando, K., Kato, S., Hotta, T. In Vivo and In Vitro Differentiation of Myocytes From Human Bone Marrow-Derived Multipotent Progenitor Cells. *Experimental Hematology* 31 (2003) 1323-1330

Mullen Y., Maruyama, M. Smith, C.V. Current Progress and Perspectives in Islet Transplantation. *Journal of Hepato-Biliary-Pancreatic Surgery* 7 (2000) 347-357

Naughton, G. From Lab Bench to Market. Critical Issues in Tissue Engineering. *Annals of the New York Academy of Sciences* 961 (2002) 372-385

Nerem, R.M. Tissue Engineering a Blood Vessel Substitute: The Role of Biomechanics. *Yonsei Medical Journal* 41:6 (2000) 735-739

Nerem, R. M. and Seliktar D. Vascular Tissue Engineering. *Annual Review of Biomedical Engineering* 3 (2001) 225-43

Niklason, L. E., Gao, J., Abbott, W. M., Hirschi, K. K., Houser, S., Marini, R., Langer, R. Functional Arteries Grown in Vitro. *Science* 284 (1999) 489-493

Niklason, L.E. and Langer, R. Prospects for Organ and Tissue Replacement. *The Journal of the American Medical Association* 285:5 (2001) 573-576

Orive, G., Ponce, S., Hernandez, R.M., Gascon, A.R., Igartua, M., Pedraz, J.L. Biocompatibility of Microcapsules for Cell Immobilization Elaborated with Different Type of Alginates. *Biomaterials* 23 (2002) 3825-3831

Owens, G.K. Regulation of Differentiation of Vascular Smooth Muscle Cells. *Physiological Reviews* 75:3 (1995) 487-517

Ozturk, S.S., Thrift, J.C., Blackie, J.D., Naveh, D. Real Time Monitoring and Control of Glucose and Lactate Concentrations in Mammalian Cell Perfusion Reactor. *Biotechnology and Bioengineering* 53 (4) (1997) 372-378

Pawlowski, J.E., Taylor, D.S., Valentine, M., Hail, M.E., Ferrer, P., Kowala, M.C., Molloy, C.J. Stimulation of Activin A Expression in Rat Aortic Smooth Muscle Cells

by Thrombin and Angiotensin II Correlates with Neointimal Formation *in Vivo*. *The Journal of Clinical Investigation* 100 (1997) 639-648

Pangarkar, N. and Hutmacher, D.W. Invention and Business Performance in the Tissue Engineering Industry. *Tissue Engineering* 9:6 (2003) 1313-1322

Papadimitriou, E. and Lelkes, P.I. Measurement of Cell Numbers in Microtiter Culture Plates using the Fluorescent Dye Hoeschst 33258. *Journal of Immunological Methods* 162:1 (1993) 41-45

Parham, P., Editor. Genomic Organization of the MHC: Structure, Origin and Function. *Immunological Reviews* 167 (1999) 5-379

Pedersen, R.A. Embryonic Stem Cells for Medicine. *Scientific American Presents* (1997) 18-23

Perets, A., Baruch, Y., Weisbuch, F., Shoshany, G., Neufeld, G., Cohen, S. Enhancing the Vascularization of Three-Dimensional Porous Alginate Scaffolds by Incorporating Controlled Release Basic Fibroblast Growth Factor Microspheres. *Journal of Biomaterials Research* 65A (2003) 489-497

Perry, T.E., Kaushal, S., Sutherland, F.W.H., Guleserian, K.J., Bischoff, J., Sacks, M., Mayer, J.E. Bone Marrow as a Cell Source for Tissue Engineering Heart Valves. *Annals of Thoracic Surgery* 75 (2003) 761-767

Persidis, A. Tissue Engineering (Industry Trends). *Nature Biotechnology* 17 (1999) 508-510

Peterson, L., Minas, T., Brittberg, M., Nilsson, A., Siogren-Jansson, E., Lindahl, A. Two- to 9-Year Outcome After Autologous Chondrocyte Transplantation of the Knees. *Clinical Orthopaedics and Related Research* 374 (2000) 212-234

Phinney, D.G., Kopen, G., Righter, W., Webster, S., Tremain, N., Prockop D.J. Donor Variation in the Growth Properties and Osteogenic Potential of Human Marrow Stromal Cells. *Journal of Cellular Biochemistry* 75 (1999) 424-436

Piscaglia, A.C., Di Campli, C., Gasbarrini, G., Gasbarrini, A. Stem Cells: New Tools in Gastroenterology and Hepatology. *Digestive and Liver Disease* 35 (2003) 507-514

Pittenger, M.F., Mackay, A.M., Beck, S.C., Jaiswal, R.K., Douglas, R., Mosca, J.D., Moorman, M.A., Simonetti, D.W., Craig, S., Marshak, D.R. Multilineage Potential of Adult Human Mesenchymal Stem Cells. *Science* 284 (1999) 143-147

Prockop, D.J. Marrow Stromal Cells as Stem Cells for Nonhematopoietic Tissues. *Science* 276 (1997) 71-74

Rangappa, S., Entwistle, J.W.C., Wechsler, A.S., Kresh, J.Y. Cardiomyocyte-Mediated Contact Programs Human Mesenchymal Stem Cells to Express Cardiogenic Phenotype. *The Journal of Thoracic and Cardiovascular Surgery* 126 (2003) 124-132

Rasmussen, H.S., Rasmussen, C.S., Macko, J., Yonehiro, G. Angiogenic Gene Therapy Strategies for the Treatment of Cardiovascular Disease. *Current Opinion in Molecular Therapeutics* 4:5 (2002) 476-481

Ratcliffe, A. Tissue Engineering of Vascular Grafts. *Matrix Biology* 19 (2000) 353-357

Read, T.A., Stensvaag, V., Vindenes, H., Ulvestad, E., Bjerkvig, R., Thorsen, F. Cells Encapsulated in Alginate: A Potential System for Delivery of Recombinant Proteins to Malignant Brain Tumours. *International Journal of Developmental Neuroscience* 17:5-6 (1999) 653-663

Read, T.A., Sorensen, D.R., Mahesparan, R., Enger, P., Timpl, R., Olsen, B.R., Hjelstuen, M.H.B., Haraldseth, O., Bjerkvig, R. Local Endostatin Treatment of Gliomas Administered by Micro-Encapsulated Producer Cells. *Nature Biotechnology* 19 (2001) 29-39

Reinecke, H., Poppa, V., Murry, C.E. Skeletal Muscle Stem Cells Do Not Transdifferentiate Into Cardiomyocytes After Cardiac Grafting. *Journal of Molecular and Cellular Cardiology* 34 (2002) 241-249

Remy-Martin, J.P., Marandin, A., Challier, B., Bernard, G., Deschaseaux, M., Herve, P., Wei, Y., Tsuji, T., Auerbach, R., Dennis, J.E., Moore, K.A., Greenberger, J.S., Charbord, P. Vascular Smooth Muscle Differentiation of Murine Stroma: A Sequential Model. *Experimental Hematology* 27 (1999) 1782-1795

Reyes, M., Lund, T., Lenvik, T., Aguiar, D., Koodie, L., Verfaillie, C.M. Purification and Ex Vivo Expansion of Postnatal Human Marrow Mesodermal Progenitor Cells. *Blood* 98:9 (2001) 2615-2625

Richardson, T.P., Peters, M.C., Ennett, A.B., Mooney, D.J. Polymeric System for Dual Growth Factor Delivery. *Nature Biotechnology* 19 (2001) 1029-1034.

Roeder, R., Wolfe, J., Lianakis, N., Hinson, T., Geddes, L.A., Obermiller, J. Compliance, Elastic Modulus, and Burst Pressure of Small-Intestine Submucosa (SIS), Small Diameter Vascular Grafts. *Journal of Biomedical Materials Research* 47 (1999) 65-70

Roskelley, C.D., Sebrow, A., Bissell, M.J. A Hierarchy of ECM-Mediated Signaling Regulates Tissue-Specific Gene Expression. *Current Opinion Cell Biology* 7 (1995) 736-747

Ross, J.M. Cell-Extracellular Matrix Interactions. In: *Frontiers in Tissue Engineering*, edited by Patrick, C.W., Mikos, A.G., and McIntire, L.V., Pergamon, Oxford (1998) 15-27

Ross, R. The Pathogenesis of Atherosclerosis – An Update. *New England Journal of Medicine* 314 (1986) 488-500

Rowley, J. A., Madlambayan, G., Mooney, D. J. Alginate Hydrogels as Synthetic Extracellular Matrix Materials. *Biomaterials* 20 (1999) 45-53

Rowley, J. A. and Mooney, D. J. Alginate Type and RGD Density Control Myoblast Phenotype. *Journal of Biomedical Materials Research* 60 (2002) 217-223

Ruckert, A., Ronimus, R.S., Morgan, H.W. A RAPD-Based Survey of Thermophilic Bacilli in Milk Powders from Different Countries. *International Journal of Food Microbiology* 96:3 (2004) 263-272.

Rutherford, R.B., Moalli, M., Franceschi, R.T., Wang, D., Gu, K., Krebsbach, P.H. Bone Morphogenetic Protein-Transduced Human Fibroblasts Convert to Osteoblasts and Form Bone In Vivo. *Tissue Engineering* 8:3 (2002) 441-452

Salacinski, H. J., Tai, N. R., Punshon, G., Giudiceandrea, A., Hamilton, G., Seifalian, A. M. Optimal Endothelialisation of a New Compliant Poly(Carbonate-Urea)Urethane Vascular Graft with Effect of Physiological Shear Stress. *European Journal of Vascular and Endovascular Surgery* 20 (2000) 342-352

Saltzman, W.M. Cell Interactions with Polymers. In: *Principles of Tissue Engineering*, Second Edition, Lanza, R., Langer, R., Vacanti, J. editors, Academic Press (2000) 221-235

Sato, M. and Ohshima, N. Flow-Induced Changes in Shape and Cytoskeletal Structure of Vascular Endothelial Cells. *Biorheology* 31:2 (1994) 143-153

Sawhney, A.S. and Drumheller, P.D. Polymer Synthesis. In: *Frontiers in Tissue Engineering*, edited by Patrick, C.W., Mikos, A.G., and McIntire, L.V., Pergamon, Oxford (1998) 142-145

Schmedlen, R.H., Masters, K.S., West, J.L. Photocrosslinkable Polyvinyl Alcohol Hydrogels That Can Be Modified With Cell Adhesion Peptides For Use in Tissue Engineering. *Biomaterials* 23 (2002) 4325-4332

Schneider, S., Feilen, P.J., Kraus, O., Haase, T., Sagban, T.A., Lehr, H.A., Beyer, J., Pommersheim, R., Weber, M.M. Biocompatibility of Alginates for Grafting: Impact of Alginate Molecular Weight. *Artificial Cells, Blood Substitutes, and Immobilization Biotechnology* 31:4 (2003) 383-394

Schob, O.M., Schmid, R.A., Morimoto, A.K., Largiader, F., Zucker, K.A. Laparoscopic Roux-en-Y Choledochojejunostomy. *American Journal of Surgery* 173:4 (1997) 312-319

Schumacker, P.T. and Samsel, R.W. Analysis of Oxygen Delivery and Uptake Relationships in the Krogh Tissue Model. *Journal of Applied Physiology* 67:3 (1989) 1234-1244

Schwartz, R.E., Reyes, M., Koodie, L., Jiang, Y., Blackstad, M., Lund, T., Lenvik, T., Johnson, S., Hu, W.S., Verfaillie, C.M. Multipotent Adult Progenitor Cells from

Bone Marrow Differentiate into Functional Hepatocyte-Like Cells. *The Journal of Clinical Investigation* 109:10 (2002) 1291-1302

Schwartz, S.M., Campbell, G.R., Campbell, J.H. Replication of Smooth Muscle Cells in Vascular Disease. *Circulation Research* 58 (1986) 427-444

Schwartz, S.M., Gajdusek, C.M., Selden, S.C. Vascular Wall Growth Control: The Role of the Endothelium. *Arteriosclerosis* 1 (1981) 107-161

Selden, C., Roberts, E., Stamp, G., Parker, K., Winlove, P., Ryder, T., Platt, H., Hodgson, H. Comparison of Three Solid Phase Supports for Promoting Three-Dimensional Growth and Function of Human Liver Cell Lines. *Artificial Organs* 22:4 (1998) 308-319.

Seliktar, D., Black, R.A., Vito, R.P., Nerem, R.M. Dynamic Mechanical Conditioning of Collagen-Gel Blood Vessel Constructs Induces Remodeling In Vitro. *Annals of Biomedical Engineering* 28 (2000) 351-362

Serp, D., Von-Stockar, U., Marison, I.W. Immobilized Bacterial Spores for Use as Bioindicators in the Validation of Thermal Sterilization Processes. *Journal of Food Protection* 65:7 (2002) 1134-1141

Seruya, M., Shah, A., Pedrotty, D., du-Laney, T., Melgiri, R., McKee, J.A., Young, H.E., Niklason, L.E. Clonal Population of Adult Stem Cells: Life Span and Differentiation Potential. *Cell Transplantation* 13:2 (2004) 93-101

Shin'oka, T., Imai, Y., Ikada, Y. Transplantation of a Tissue-Engineered Pulmonary Artery. *The New England Journal of Medicine* 344:7 (2001) 532-533

Simmons, C.A., Alsberg, E., Hsiong, S., Kim, W.J., Mooney, D.J. Dual Growth Factor Delivery and Controlled Degradation Enhance In Vivo Bone Formation by Transplanted Bone Marrow Stromal Cells. *Bone* 35:2 (2004) 562-569

Simper, D., Stalboerger, P.G., Panetta, C.J., Wang, S., Caplice, N.M. Smooth Muscle Progenitor Cells in Human Blood. *Circulation* 106 (2002) 1199-1204

Simpson, J.A., Smith, S.E., Dean, R.T. Alginate May Accumulate in Cystic Fibrosis Lung Because the Enzymatic and Free Radical Capacities of Phagocytic Cells Are Inadequate For Its Degradation. *Biochemistry and Molecular Biology International* 30:6 (1993) 1021-1034

Skjak-Braek, G., Murano, E., Paoletti, S. Alginate as Immobilization Material. II: Determination of Polyphenol Contaminants by Fluorescence Spectroscopy, and Evaluation for Their Removal. *Biotechnology and Bioengineering* 33 (1989) 90-94

Smidsrod, O. and Haug, A. Properties of Poly(1,4hexuronates) in the Gel State II. Comparison of Gels of Different Chemical Composition. *Acta Chemica Scandinavica* 26 (1972) 79-88

Solan, A., Mitchell, S., Moses, M., and Niklason, L. Effect of Pulse Rate on Collagen Deposition in the Tissue-Engineered Blood Vessel. *Tissue Engineering* 9:4 (2003) 579-586

Stabler, C.L., Sambanis, A., Constantinidis, I. Effects of Alginate Composition on the Growth and Overall Metabolic Activity of βTC3 Cells. *Annals of New York Academy of Sciences* 961 (2002) 103-133

Stecklow, S. Hazardous Trade – Britain's Feed Exports Extended the Risks of 'Mad Cow' Disease. *Wall Street Journal*, 23 Jan 2001

Steinert A., Weber, M., Dimmler, A., Julius, C., Schütze, N., Nöth, U., Cramer, H., Eulert, J., Zimmermann, U., Hendrich, C. Chondrogenic Differentiation of Mesenchymal Progenitor Cells Encapsulated in Ultrahigh-Viscosity Alginate. *Journal of Orthopaedic Research* 21 (2003) 1090-1097

Stone, A. FDA Issues Felled Advanced Tissue Sciences. *Genetic Engineering News* 23:11 (2003) 25-28

Storb, R. Allogeneic Hematopoietic Stem Cell Transplantation – Yesterday, Today, and Tomorrow. *Experimental Hematology* 31 (2003)1-10

Tai, N. R., Salacinski, H. J., Edwards, A., Hamilton, G., Seifalian, A. M. Compliance Properties of Conduits Used in Vascular Reconstruction. *British Journal of Surgery* 87 (2000) 1516-1524

Takahashi, K. and Okada, T.S. An Analysis of the Effect of Conditioned Medium Upon the Cell Culture at Low Density. *Development, Growth and Differentiation* 12:2 (1970) 65-77

Takigawa, M., Takano, T., Shirai, E., Suzuki, F. Cytoskeleton and Differentiation: Effects of Cytochalasin B and Colchicine on Expression of the Differentiated Phenotype of Rabbit Costal Chondrocytes in Culture. *Cell Differentiation* 14 (1984) 197-204

Taylor, D.S., Cheng, X., Pawlowski, J.E., Wallace, A.R., Ferrer, P., Molloy, C.J. Epiregulin is a Potent Vascular Smooth Muscle Cell-Derived Mitogen Induced by Angiotensin II, Endothelin-1, and Thrombin. *Proceedings of the National Academy of Sciences of the United States of America* 96:4 (1999) 1633-1638

Teebken, O.E. and Haverich, A. Tissue Engineering of Small Diameter Vascular Grafts. *European Journal of Vascular and Endovascular Surgery* 23 (2002) 475-485

Terada, N., Hamazaki, T., Oka, M., Hoki, M., Mastalerz, D.M., Nakano, Y., Meyer, E.M., Morel, L., Peterson, B.E., Scott, E.W. Bone Marrow Cells Adopt the Phenotype of Other Cells by Spontaneous Cell Fusion. *Nature* 416 (2002) 542-545

Terskikh, V.V. and Vasiliev, A.V. Cultivation and Transplantation of Epidermal Keratinocytes. *International Review of Cytology* 188 (1999) 41-72

Thomas, S. Alginate Dressings in Surgery and Wound Management – Part 1. *Journal of Wound Care* 9:2 (2000) 56-60

Thompson, C.A., Colon-Hernandez, P., Pomerantseva, I., MacNeil, B.D., Nasseri, B., Vacanti, J.P., Oesterle, S.N. A Novel Pulsatile, Laminar Flow Bioreactor for the Development of Tissue-Engineered Vascular Structures. *Tissue Engineering* 8:6 (2002) 1083-1088

Thomson, J.A., Itskovitz-Eldor, J., Shapiro, S.S., Waknitz, M.A., Swiergiel, J.J., Marshall, V.S., Jones, J.M. Embryonic Stem Cell Lines Derived From Human Blastocytes. *Science* 282:5391 (1998) 1145-1147

Thoumine, O., Ziegler, T., Girard, P.R., Nerem, R.M. Elongation of Confluent Endothelial Cells in Culture: The Importance of Fields of Force in the Associated Alterations of Their Cytoskeletal Structure. *Experimental Cell Research* 219 (1995) 427-441

Tiwari, A., Salacinski, H. J., Punshon, G., Hamilton, G., Seifalian, A. M. Development of a Hybrid Cardiovascular Graft Using a Tissue Engineering Approach. *The Federation of American Societies for Experimental Biology (FASEB) Journal* 16 (2002a) 791-796

Tiwari, A., Salacinski, H., Seifalian, A.M., Hamilton, G. New Prostheses For Use in Bypass Grafts with Special Emphasis on Polyurethanes. *Cardiovascular Surgery* 10:3 (2002b) 191-197

Tobias, C.A., Dhoot, N.O., Wheatley, M.A., Tessler, A., Murray, M., Fischer, I. Grafting of Encapsulated BDNF-Producing Fibroblasts into the Injured Spinal Cord Without Immune Suppression in Adult Rats. *Journal of Neurotrauma* 18:3 (2001) 287-301

Toma, C., Pittenger, M.F., Cahill, K.S., Byrne, B.J., Kessler, P.D. Human Mesenchymal Stem Cells Differentiate to a Cardiomyocyte Phenotype in the Adult Murine Heart. *Circulation* 105:1 (2002) 93-98

Tranquillo, R.T. Self-Organization of Tissue-Equivalents: The Nature and Role of Contact Guidance. *Biochemical Society Symposium* 65 (1999) 27-42

Uchida, N., Buck, D.W., He, D., Reitsma, M.J., Masek, M., Phan, T.V., Tsukamoto, A.S., Gage, F.H., Weissman, I.L. Direct Isolation of Human Central Nervous System Stem Cells. *Proceedings of the National Academy of Sciences of the United States of America* 97:26 (2000) 14720-14725

Underwood, S., Afoke, A., Brown, R.A., MacLeod, A.J., Dunnill, P. The Physical Properties of a Fibrillar Fibronectin-Fibrinogen Material With Potential Use in Tissue Engineering. *Bioprocess Engineering* 20 (1999) 239-248

Underwood, S., Afoke, A., Brown, R.A., MacLeod, A.J., Ayazi Shamlou, P., Dunnill, P. Wet Extrusion of Fibronectin-Fibrinogen For Application in Tissue Engineering, *Biotechnology and Bioengineering* 73 (2001) 295-305

Vacanti, J.P. and Langer, R. Tissue Engineering: The Design and Fabrication of Living Replacement Devices for Surgical Reconstruction and Transplantation. *The Lancet* 354: Suppl 1 (1999) 32-34

Vandenbossche, G.M.R. and Remon, J.P. Influence of the Sterilization Process on Alginate Dispersions. *The Journal of Pharmacy and Pharmacology* 45:5 (1993) 484-486

VanHoogmoed, C.G., Busscher, H.J., deVos, P. Fourier Transform Infrared Spectroscopy Studies of Alginate-PLL Capsules with Varying Compositions. *Journal of Biomedical Materials Research* 67A:1 (2003) 172-178

Vernon, S.M., Campos, M.J., Haystead, T., Thompson, M.M., DiCorleto, P.E., Owens, G.K. Endothelial Cell-Conditioned Medium Downregulates Smooth Muscle Contractile Protein Expression. *The American Journal of Physiology* 272: 2Pt1 (1997) C582-591

Vian, L., Yusuf, A., Guyomard, C., Cano, J.P. The Liverbeads as a Tool for the Comet Assay. *Mutation Research* 519 (2002) 163-170

Volkin, D.B. and Klibanov, A.M. Alterations in the Structure of Proteins that Cause Their Irreversible Inactivation. *Developments in Biological Standardization* 74 (1992) 73-80

Wakitani, S., Saito, T., Caplan, A.J. Myogenic Cells Derived From Rat Bone Marrow Mesenchymal Stem Cells Exposed to 5-Azacytidine. *Muscle Nerve* 18 (1995) 1417-1426

Wan, H., Williams, R., Doherty, P., Williams, D.F. A Study of the Reproducibility of the MTT Test. *Journal of Material Science: Materials in Medicine* 5 (1994) 154-159

Wang, D., Williams, C.G., Li, Q., Sharma, B., Elisseeff, J.H. Synthesis and Characterization of a Novel Degradable Phosphate-Containing Hydrogel. *Biomaterials* 24 (2003) 3969-3980

Wang, D., Park, J.S., Chu, J.S., Krakowski, A., Luo, K., Chen, D.J., Li, S. Proteomic Profiling of Bone Marrow Mesenchymal Stem Cells upon Transforming Growth Factor β1 Stimulation. *The Journal of Biological Chemistry* 279:42 (2004) 43725-43734

Wang, L., Shelton, R.M., Cooper, P.R., Lawson, M., Triffitt, J.T., Barralet, J.E. Evaluation of Sodium Alginate for Bone Marrow Cell Tissue Engineering. *Biomaterials* 24, (2003) 3475-3481

Wang, X., Willenbring, H., Akkari, Y., Torimaru, Y., Foster, M., Al-Dhallmy, M., Lagasse, E., Finegold, M., Olson, S., Grompe, M. Cell Fusion is the Principal Source of Bone-Marrow-Derived Hepatocytes. *Nature* 422 (2003) 897-901

Weinberg, C.B., and Bell, E. A Blood Vessel Model Constructed From Collagen and Cultured Vascular Cells. *Science* 231 (1986) 397-400

Wilkins, L.M., Watson, S.R., Prosky, S.J., Meunier, S.F., Parenteau, N.L. Development of a Bilayered Living Skin Construct for Clinical Applications. *Biotechnology and Bioengineering* 43:8 (1994) 747-756

Wong, M., Siegrist, M., Wang, X., Hunziker, E. Development of Mechanically Stable Alginate/Chondrocyte Constructs: Effects of Guluronic Acid Content and Matrix Synthesis. *Journal of Orthopaedic Research* 19 (2001) 493-499

Wong, W. and Wood, K.J. Transplantation Tolerance by Donor MHC Gene Transfer. *Current Gene Therapy* 4:3 (2004) 329-336

Wright, V.J., Peng, H., Huard, J. Muscle-Based Gene Therapy and Tissue Engineering for the Musculoskeletal System. *Drug Discovery Today* 6:14 (2001) 728-733

Wu, S., Suzuki, Y., Tanihara, M., Ohnishi, K., Endo, K., Nishimura, Y. Repair of Facial Nerve With Alginate Sponge Without Suturing: An Experimental Study in Cats. *Scandinavian Journal of Plastic and Reconstructive Surgery and Hand Surgery* 36:3 (2002) 135-140

Wu, S.L., Leung, D., Tretyakov, L., Hu, J., Guzzetta, A., Wang, Y.J. The Formation and Mechanism of Multimerization in a Freeze-Dried Peptide. *International Journal of Pharmaceutics* 200:1 (2000) 1-16

www.apligraf.com
www.biotissue-tec.com
www.carticel.com
www.curis.com
www.cytograft.com
www.dentigenix.com
www.dermagraft.com
www.edwardslifesciences.com (porcine valve)
www.fao.org
www.lifecell.com (alloderm)
www.mattek.com (epiderm, epiairway, epiocular)
www.mercksource.com (bypass photo)
www.medtronics.com (porcine valve)
www.obi.com
www.osiristx.com
www.stemcellsinc.com
http://wound.smith-nephew.com

Xia, W., Coa, Y., Shang, Q. An Experimental Study of Tissue Engineered Autologous Cartilage by Using an Injectable Polymer. *Chinese Journal of Plastic Surgery* 17:5 (2001) 302-205

Xu, C., Inokuma, M.S., Denham, J., Golds, K., Kundu, P., Gold, J.D., Carpenter, M.K. Feeder-Free Growth of Undifferentiated Human Embryonic Stem Cells. *Nature Biotechnology* 19:10 (2001) 971-974

Xu, W., Zhang, X., Qian, H., Zhu, W., Sun, X., Hu, J., Zhou, H., Chen, Y. Mesenchymal Stem Cells from Adult Human Bone Marrow Differentiate into a Cardiomyocyte Phenotype *In Vitro*. *Experimental Biology and Medicine* 229 (2004) 623-631

Yamashita, J., Itoh, H., Hirashima, M., Ogawa, M., Nishikawa, S., Yurugi, T., Naito, M., Nakoa, K., Nishikawa, S.-I. Flk1-Positive Cells Derived From Embryonic Stem Cells Serve As Vascular Progenitors. *Nature* 408:6808 (2000) 92-96

Yan, L., Boyd, K.G., Adams, D.R., Burgess, J.G. Biofilm-Specific Cross-Species Induction of Antimicrobial Compounds in Bacilli. *Applied and Environmental Microbiology* 69:7 (2003) 3719-3727

Yang, L., Korom, S., Welti, M., Hoerstrup, S.P., Zund, G., Jung, F.J., Neuenschwander, P., Weder, W. Tissue Engineered Cartilage Generated From Human Trachea Using DegraPol Scaffold. *European Journal of Cardio-thoracic Surgery* 24 (2003) 201-207.

Yang, X.B., Roach, H.I., Clarke, N.M., Howdle, S.M., Quirk, R., Shakesheff, K.M., Oreffo, R.O. Human Osteoprogenitor Growth and Differentiation on Synthetic Biodegradable Structures After Surface Modification. *Bone* 29:6 (2001) 523-531

Young, J.H., Teumer, J., Kemp, P.D., Parenteau, N.L. Approaches to Transplanting Engineered Cells and Tissues, In: *Principals of Tissue Engineering*. Lanza, R.P., Langer, R., and Chick, W.L. editors, R.G. Landes Company, Austin, TX (1997) 301-304

YSI 2700 Select Biochemistry Analyzer User's Manual, YSI (UK) Ltd., Analytical Technologies, Farnborough, UK (June 2001)

Yu, X. and Bellamkonda, R.V. Tissue-Engineered Scaffolds are Effective Alternatives to Autografts for Bridging Peripheral Nerve Gaps. *Tissue Engineering* 9:3 (2003) 421-430

Zacharias, A., Habib, R.H., Schwann, T.A., Riordan, C.J., Durham, S.J., Shah, A. Improved Survival With Radial Artery Versus Vein Conduits in Coronary Bypass Surgery With Left Internal Thoracic Artery to Left Anterior Descending Artery Grafting. *Circulation* 109 (2004) 1489-1496

Zandstra, P.W. and Nagy. A. Stem Cell Bioengineering. *Annual Review of Biomedical Engineering* 3 (2001) 275-305

Zheng, S., Xiao, Z.X., Pan, Y.L, Han, M.Y., Dong, Q. Continuous release of interleukin 12 from microencapsulated engineered cells for colon cancer therapy. *World Journal of Gastroenterology* 9 (2003) 951-955

Zimmermann, U., Mimietz, S., Zimmermann, H., Hillgartner, M., Schneider, H., Ludwig, J., Hasse, C., Haase, A., Rothmund, M., Fuhr, G. Hydrogel-Based Non-Autologous Cell and Tissue Therapy. *BioTechniques* 29:3 (2000) 564-581

Zimmermann, U., Thurmer, F., Jork, A., Weber, M., Mimietz, S., Hillgartner, M., Brunnenmeier, F., Zimmermann, H., Westphal, I., Fuhr, G., Noth, U., Haase, A., Steinert, A., Hendrich, C. A Novel Class of Amitogenic Alginate Microcapsules for Long-Term Immunoisolated Transplantation. *Annals of the New York Academy of Sciences* 944 (2001) 199-215

Zimmermann, W.H. and Eschenhagen, T. Cardiac Tissue Engineering for Replacement Therapy. *Heart Failure Reviews* 8:3 (2003) 259-269

Zmora, S., Glicklis, R., Cohen, S. Tailoring the Pore Architecture in 3-D Alginate Scaffolds by Controlling the Freezing Regime During Fabrication. *Biomaterials* 23 (2002) 4087-4094

Zoro, B. Automated Bioprocessing of Mammalian Cells for Tissue Engineering and Cell Therapies. University College London, UK, Doctor of Engineering Thesis (2005)

Zund, G., Ye, Q., Hoerstrup, S.P., Schoeberlein, A., Schmid, A.C., Grunenfelder, J., Vogt, P., Turnia, M. Tissue Engineering in Cardiovascular Surgery: MTT, a Rapid and Reliable Quantitative Method to Assess the Optimal Human Cell Seeding on Polymeric Meshes. *European Journal of Cardio-thoracic Surgery* 15 (1999) 519-524.